THE UNIVERSITY
of EDINBURGH

Genomic analysis of secondary metabolism in *Ramularia collo-cygni*, causative agent of Ramularia leaf spot disease of barley

François Mathieu Didier Dussart

Thesis submitted to the University of Edinburgh for the degree of Doctor of Philosophy

THE UNIVERSITY *of* EDINBURGH

March 2017

Declaration

I hereby declare that this thesis has been composed by me and that the work is my own, except as acknowledged by means of references. This thesis has not been submitted for any other degree or professional qualification except as specified.

François Mathieu Didier DUSSART

Table of contents

List of Figures ..... **v**
List of Tables ..... **ix**
List of abbreviations ..... **xi**
Acknowledgment ..... **xiv**
Abstract ..... **xv**
Lay summary ..... **xvii**
Chapter 1: General introduction **1**
1.1. Crop fungal diseases in history 2
1.2. Barley: a resilient crop 3
1.2.1. History of barley 3
1.2.2. Barley production 4
1.2.3. Main uses of barley 5
1.2.4. Threats to barley production 6
1.2.4.1. Abiotic stresses 6
1.2.4.2. Biotic stresses 7
1.3. Ramularia leaf spot: an emerging leaf disease of barley 9
1.3.1. Taxonomy of Ramularia leaf spot 9
1.3.2. Distribution of *Ramularia collo-cygni* 10
1.3.3. Ramularia leaf spot symptoms 11
1.3.4. Host range of *Ramularia collo-cygni* 13
1.3.5. Consequences of Ramularia leaf spot 14
1.3.6. Life cycle of *Ramularia collo-cygni* 14
1.3.7. Control methods for Ramularia leaf spot 16
1.3.7.1. Seed treatment 16
1.3.7.2. Varietal resistance 16
1.3.7.3. Fungicide treatments 17
1.4. Fungal secondary metabolites 18
1.4.1. Secondary metabolites 18
1.4.2. History of fungal secondary metabolites 19
1.4.3. Importance of fungal secondary metabolites 20
1.4.3.1. Pharmaceutical products 20
1.4.3.2. Harmful secondary metabolites 21
1.4.4. Role of secondary metabolites in fungal biology 22
1.4.5. Rubellins: secondary metabolites produced by *Ramularia collo-cygni* 23
1.5. Aims and objectives 27

Chapter 2: Identification and characterisation of secondary metabolite gene clusters in *Ramularia collo-cygni* 28

2.1. Biosynthesis of fungal secondary metabolites 29

2.1.1. The polyketide pathway 32

2.1.1.1. Mechanism of polyketide biosynthesis 32
2.1.1.2. Classification of fungal polyketide synthases 34
2.1.1.3. Specific domains from non-reducing polyketide synthetases 35
2.1.1.4. Release of the polyketide from the core enzyme 35

2.1.2. The non-ribosomal peptide pathway 36

2.1.2.1. Non-ribosomal peptide elongation mechanism 36
2.1.2.2. Classification of NRPS 37
2.1.2.3. Peptide modification 38

2.1.3. The hybrid PKS/NRPS pathway 39

2.1.4. The role of secondary metabolism in plant pathogenic fungi 40

2.1.5. Objectives 41

2.2. Materials and Methods 42

2.2.1. *Ramularia collo-cygni* genome data 42

2.2.2. Identification of core genes 42

2.2.2.1. Identification of putative core genes in *Ramularia collo-cygni* 42
2.2.2.2. Secondary metabolites core gene domain analysis 44
2.2.2.3. Localisation of secondary metabolites core genes in the genome 44

2.2.3. Identification of putative secondary metabolism gene clusters 44

2.2.4. Detailed investigation of selected secondary metabolite-related gene clusters 45

2.2.5. Phylogenetic study of secondary metabolites core genes 45

2.3. Results 47

2.3.1. Identification of secondary metabolism core genes in *Ramularia collo-cygni* 47

2.3.1.1. Identification of putative polyketide synthases and non-ribosomal peptide synthetases 47
2.3.1.2. Identification of putative functional core genes 51

2.3.2. Identification of putative secondary metabolism gene clusters 57

2.3.3. Characterisation of putative secondary metabolites clusters 65

2.3.3.1. Phylogenetic study 65
2.3.3.2. Detailed study of selected clusters 74

2.4. Discussion 115

Chapter 3: Expression of *Ramularia collo-cygni* secondary metabolism-related core genes during the development of Ramularia leaf spot on barley seedling 123

3.1. Secondary metabolites and disease development 124

3.1.1. Phytotoxins in disease development 124

3.1.1.1. Role of host specific toxins 124
3.1.1.2. Role of non-host specific toxins 125

3.1.2. Alternative role of secondary metabolites in plant-pathogen interactions 127

3.1.3. SM-related gene expression in disease development 128
3.1.4. Regulation of secondary metabolism-related genes 130
3.1.4.1. Regulation of secondary metabolism within cluster 130
3.1.4.2. Master regulators of fungal secondary metabolism 131
3.1.4.3. Environmental regulation of fungal secondary metabolism 132
3.1.5. Objectives 134
3.2. Materials and Methods 135
3.2.1. Plant material 135
3.2.2. Barley seedling inoculation with *Ramularia collo-cygni* 135
3.2.3. Assessment of Ramularia leaf spot development on barley seedlings 136
3.2.3.1. Visual assessment of Ramularia leaf spot 136
3.2.3.2. Microscopic assessment of *Ramularia collo-cygni* colonisation 136
3.2.3.3. *Ramularia collo-cygni* DNA quantification 137
3.2.4. Gene expression analysis 137
3.2.4.1. Expression profiling of secondary metabolite core genes in artificially inoculated seedlings 137
3.2.4.2. Gene expression analysis from naturally inoculated barley leaves 138
3.2.5. Co-regulation of secondary metabolite-related genes 139
3.2.6. Fungal competition assay 139
3.3. Results 141
3.3.1. Inoculation assay 141
3.3.1.1. Visual assessment 141
3.3.1.2. Fungal development during infection 142
3.3.2. Expression profiling of *Ramularia collo-cygni* secondary metabolism core genes 144
3.3.3. Co-regulation of secondary metabolism gene clusters in *Ramularia collo-cygni* 150
3.3.3.1. Expression profiling of environmental regulators of secondary metabolism 150
3.3.3.2. Pathway-specific regulation 152
3.3.4. Fungal competition assays 157
3.4. Discussion 160
Chapter 4: Determining the *in planta* mode of action of rubellin D, a phytotoxin produced by *Ramularia collo-cygni*. 171
4.1. Introduction 172
4.1.1. Rubellins: toxins produced by *Ramularia collo-cygni* 172
4.1.2. Role of known anthraquinone toxins in plant pathogenic fungi 172
4.1.3. Role of photosensitisers in plant pathogenic fungi 174
4.1.4. Salicylic acid in plant defence mechanism 175
4.1.4.1. Salicylic acid biosynthesis in higher plants 176
4.1.4.2. Salicylic acid in plant immunity 176
4.1.4.3. Salicylic acid regulates cell death during the immune response 180
4.1.5. Objectives 181

4.2. Material and methods 182
4.2.1. Infiltration solutions used in this study 182
4.2.2. Plant materials used in this study 183
4.2.2.1. Barley plant materials used in this study 183
4.2.2.2. *Arabidopsis thaliana* plant materials used in this study 184
4.2.3. Chemical infiltration of barley and *Arabidopsis thaliana* leaves to determine the *in planta* effect of rubellin D 185
4.2.3.1. Infiltration of barley leaves with rubellin D 185
4.2.3.2. Infiltrations of *Arabidopsis thaliana* leaves with rubellin D 186
4.2.4. Electrolyte leakage assay 187
4.3. Results 188
4.3.1. Relationship between rubellin D-induced necrosis and Ramularia leaf spot development in barley 188
4.3.2. Analysis of the *in planta* mode of action of rubellin D 191
4.3.2.1. Assessing the suitability of *A. thaliana* as a model for studying the in planta mode of action of rubellin D 191
4.3.2.2. Role of the salicylic acid pathway in rubellin D-induced cell death 193
4.3.2.3. Role of the proteasome in rubellin D induced cell death 199
4.4. Discussion 201
Chapter 5: General discussion 210
References 230
Thesis outputs 270
Appendix 271

List of Figures

Figure 1.1: Swan-neck shaped conidiophore of *Ramularia collo-cygni*. 10

Figure 1.2: Map showing the year of the first identification of *Ramularia collo-cygni*. 11

Figure 1.3: Ramularia leaf spot and physiological leaf spot symptoms on barley. ... 12

Figure 1.4: Life cycle of *Ramularia collo-cygni*. 15

Figure 1.5: Chemical structure of several relevant secondary metabolites. 26

Figure 2.1: Secondary metabolism gene cluster involved in the production of two known fungal toxins. 31

Figure 2.2: Mechanism of polyketide elongation. 33

Figure 2.3: Typical domain organisation of highly- partially- and non-reducing polyketide synthase. 34

Figure 2.4: Typical domain organisation of a non-ribosomal peptide synthetase. 37

Figure 2.5: Typical domain organisation of fungal hybrids PKS/NRPS. 40

Figure 2.6: Domain organisation of predicted polyketide synthases in *Ramularia collo-cygni*. 54

Figure 2.7: Domain organisation of predicted non-ribosomal peptide synthetases in *Ramularia collo-cygni*. 55

Figure 2.8: Domain organisation of hybrids PKS/NRPS in *Ramularia collo-cygni*. 56

Figure 2.9: Organisation of putative secondary metabolism clusters surrounding polyketide synthase core genes in *Ramularia collo-cygni*. 59

Figure 2.10: Organisation of open reading frames at genetic loci that contains a polyketide synthase which are not enriched in secondary metabolites genes. ... 60

Figure 2.11: Organisation of putative secondary metabolism clusters surrounding hybrid polyketide synthase/non-ribosomal peptide synthetase core gene in *Ramularia collo-cygni*. 62

Figure 2.12: Organisation of putative secondary metabolism clusters surrounding non-ribosomal peptide synthetase core genes in *Ramularia collo-cygni.* 63

Figure 2.13: Phylogenetic analysis of polyketide synthases in *Ramularia collo-cygni*. 68

Figure 2.14: Phylogenetic analysis of hybrids polyketide synthase/non-ribosomal peptide synthetase in *Ramularia collo-cygni*. 70

Figure 2.15: Phylogenetic analysis of non-ribosomal peptide synthetases in Ramularia collo-cygni. 73

Figure 2.16: Relationship between putative *Ramularia collo-cygni* secondary metabolism cluster PKSm24 and secondary metabolism clusters in *Bipolaris victoriae* and *Aspergillus nidulans*..... 75

Figure 2.17: Relationship between putative *Ramularia collo-cygni* secondary metabolism cluster PKS118 and secondary metabolism cluster in *Zymoseptoria tritici*..... 77

Figure 2.18: Relationship between putative *Ramularia collo-cygni* secondary metabolism cluster PKS30 and secondary metabolism clusters in *Phoma betae* and *Zymoseptoria tritici*..... 81

Figure 2.19: Relationship between putative *Ramularia collo-cygni* secondary metabolism cluster PKS58 and secondary metabolism cluster in *Scedosporium apiospermum*..... 83

Figure 2.20: Relationship between putative *Ramularia collo-cygni* secondary metabolism cluster PKS282 and secondary metabolism clusters in *Neofusicoccum parvum* and *Macrophomina phaseolina*..... 85

Figure 2.21: Relationship between putative *Ramularia collo-cygni* secondary metabolism cluster HPS1 and secondary metabolism cluster in *Sphaerulina musiva*..... 88

Figure 2.22: Relationship between putative *Ramularia collo-cygni* secondary metabolism cluster HPS14 and the chaetoglobosin A cluster in *Penicillium expansum*..... 90

Figure 2.23: Relationship between putative *Ramularia collo-cygni* secondary metabolism cluster HPS38 and secondary metabolism cluster in *Podospora anserina*..... 92

Figure 2.24: Relationship between putative *Ramularia collo-cygni* secondary metabolism cluster NRPS246-1 and secondary metabolism clusters in *Rosellinia necatrix* and *Aspergillus udagawae*..... 95

Figure 2.25: Relationship between putative *Ramularia collo-cygni* secondary metabolism cluster NRPS246-2 and the gliotoxin biosynthetic cluster in *Aspergillus fumigatus*..... 97

Figure 2.26: Relationship between putative *Ramularia collo-cygni* secondary metabolism cluster NRPS51 and the secondary metabolite cluster in *Pseudocercospora fijiensis*..... 101

Figure 2.27: Relationship between putative *Ramularia collo-cygni* secondary metabolism cluster NRPS245 and the secondary metabolite cluster in *Zymoseptoria tritici*..... 102

Figure 2.28: Relationship between putative *Ramularia collo-cygni* secondary metabolism cluster NRPS207 and the secondary metabolite cluster in *Pseudogymnoascus pannorum* var. *pannorum*..... 104

Figure 2.29: Relationship between putative *Ramularia collo-cygni* secondary metabolism cluster NRPS134 and the secondary metabolite clusters in *Schizosaccharomyces pombe*, *Cladosporium fulvum* and *Dothistroma septosporum*..... 107

Figure 2.30: Relationship between putative *Ramularia collo-cygni* secondary metabolism cluster NRPS301 and the secondary metabolite cluster in *Bipolaris sorokiniana*. 109

Figure 2.31: Identification of a putative secondary metabolite cluster with no core gene on *Ramularia collo-cygni* contig 247. 112

Figure 2.32: Identification of a putative secondary metabolite cluster with no core gene on *Ramularia collo-cygni* contig 113. 113

Figure 3.1: Development of Ramularia leaf spot symptoms and green leaf area retention on barley cv. Century. 142

Figure 3.2: Microscopic assessment of Ramularia leaf spot development. 143

Figure 3.3: Expression profile of selected *Ramularia collo-cygni* polyketide synthases during disease development in artificially inoculated barley seedlings. 145

Figure 3.4: Expression profile of selected *Ramularia collo-cygni* PKS/NRPS hybrids during disease development in artificially inoculated barley seedlings. 146

Figure 3.5: Expression profile of selected *Ramularia collo-cygni* non-ribosomal peptide synthetases during disease development in artificially inoculated barley seedlings. 147

Figure 3.6: Expression profile of a *Ramularia collo-cygni* catalase gene during disease development in artificially inoculated barley seedlings. 148

Figure 3.7: *Ramularia collo-cygni* DNA levels during disease development in artificially inoculated barley seedlings. 149

Figure 3.8: Expression profile of *Ramularia collo-cygni* environmental-dependent master regulators of secondary metabolism during disease development in artificially inoculated barley seedlings. 151

Figure 3.9: Expression profile of genes involved in the velvet complex in *Ramularia collo-cygni* during disease development in artificially inoculated barley seedlings. 152

Figure 3.10: Expression profile of aflatoxin-regulatory gene homologs in *Ramularia collo-cygni* during disease development in artificially inoculated barley seedlings. 153

Figure 3.11: Antagonistic effect of *Ramularia collo-cygni* on common fungal barley pathogens. 158

Figure 3.12: Red coloration observed on *Ramularia collo-cygni* cultures. 159

Figure 4.1: Role of salicylic acid in immunity in unchallenged and challenged cells. 179

Figure 4.2: Rubellin D-induced lesions in barley cultivar Concerto. 189

Figure 4.3: Lesion size observed in barley leaves following a rubellin D infiltration treatment. 190

Figure 4.4: Rubellin D infiltration in *mlo* mutants of barley and *A. thaliana*. 192

Figure 4.5: Lesions induced by rubellin D infiltrations in *A. thaliana* mutants impaired in the salicylic acid pathway. 194

Figure 4.6: Effect of co-infiltration of salicylic acid or benzothiadiazole-S-methylester in rubellin D-induced lesion formation in *A. thaliana* plants impaired in the SA pathway. 196

Figure 4.7: Rubellin D-induced lesions and cell death after infiltrations in the *npr1-2* mutant..... 198

Figure 4.8: Proteasome inhibition increases lesion size and cell death induced by rubellin D in *A. thaliana* Col-0. 200

Figure 4.9: Proposed model of how SA, NPR1 and the proteasome affect rubellin D-induced programmed cell death in A. *thaliana*. 206

Figure 5.1: Comparison of the domain organisation of fungal non-reducing polyketide synthases involved in the biosynthesis of anthraquinone- and perylenequinone-derived secondary metabolites and putative NR-PKSs identified in *Ramularia collo-cygni*. 220

Figure 5.2: Proposed model presenting the putative roles of secondary metabolites in the interactions between *Ramularia collo-cygni* and its environment. 226

List of Tables

Table 2.1: Fungal proteins used as query sequences for the identification of core genes in *Ramularia collo-cygni*. 43

Table 2.2: Number of BLASTp hits in *Ramularia collo-cygni* for each query fungal polyketide synthase and non-ribosomal peptide synthetase gene. 47

Table 2.3: List of putative *Ramularia collo-cygni* polyketide synthases. 49

Table 2.4: List of putative *Ramularia collo-cygni* non-ribosomal peptide synthetases. 50

Table 2.5: Protein BLAST hit table for the genes identified in cluster PKSm24. 76

Table 2.6: Protein BLAST hit table for the genes identified in PKS118 cluster. 78

Table 2.7: Protein BLAST hit table for the genes identified in PKS30. 82

Table 2.8: Protein BLAST hit table for the genes identified in PKS58. 84

Table 2.9: Protein BLAST hit table for the genes identified in PKS282. 86

Table 2.10: Protein BLAST hit table of the genes identified in HPS1. 89

Table 2.11: Protein BLAST hit table for the genes identified in cluster HPS14. 91

Table 2.12: Protein BLAST hit table for the eight genes identified in cluster HPS38. 93

Table 2.13: Protein BLAST hit table for the genes identified in cluster NRPS246-1. 96

Table 2.14: Protein BLAST hit table for the genes identified in cluster NRPS246-2. 98

Table 2.15: Protein BLAST hits table for the genes identified in cluster NRPS245. 103

Table 2.16: Protein BLAST hits table for the genes identified in cluster NRPS207. 105

Table 2.17: Protein BLAST hit table for the genes identified in NRPS134. 108

Table 2.18: Protein BLAST hit table for the genes identified in NRPS301. 110

Table 2.19: Comparison of the number of core genes between *Ramularia collo-cygni* and other fungi. 116

Table 3.1: Protein BLAST hits in *Ramularia collo-cygni* of known regulators of secondary metabolism. 150

Table 3.2: Gene expression and number of *AflR* binding site identified in the promoter region of the genes located in the putative secondary metabolism cluster found on contig 17. 155

Table 3.3: Number of *AflR* binding site identified in the promoter region of the genes located in the putative secondary metabolism cluster PKSm24. 156

Table 4.1: Ramularia leaf spot resistance status of the barley plant materials used in this study. 184

List of abbreviations

A: Adenylation
AA: Amino acids
ABC: ATP-binding cassette
ACV: δ-(L-α-aminoadipyl)-L-cysteine-D-valine
AEA: Alkyl ester agar
ACP: Acyl carrier protein
AntiSMASH: Antibiotics & secondary metabolite analysis shell
AT: Acyl transferase
AUDPC: Area under disease progress curve
BA2H: Benzoic acid-2-hydroxylase
BLAST: Basic local alignment search tool
BLASTp: Protein basic local alignment search tool
Bp: Base pair
BTH : Benzothiadiazole S methylester
bZIP : Basic leucine zipper
C: Condensation
CUL3 : Cullin 3
DH: Dehydratase
DHN: Dihydroxynaphtalene
DMATS: Dimethylallyl tryptophan synthase
DMI: Sterol demethylation inhibitors
DNA: Desoxyribonucleic acid
DON: Deoxynivalenol
dpi: Days post inoculation
EFα: Elongation factor α
ER: Enoyl reductase
ER: Endoplasmic reticulum
ERAD: Endoplasmic reticulum-associated degradation
eSDR: Extended short chain dehydrogenase
ETP: Epipolythiodioxopiperazine
FAD: Flavin adenine dinucleotide
FAS: Fatty acid synthase
GA: Gibberellic acid
GAPDH: Glyceraldehyde-3-phosphate dehydrogenase
GLM: General linear model
GS: Growth stage
HGT: Horizontal gene transfer
hpi: Hours post infiltration
HPS: Hybrid polyketide synthase/non-ribosomal peptide synthetase
HR: hypersensitive response
HR-PKS: Highly reducing polyketide synthase
HST: Host-specific toxin
ICS: Isochorismate synthase
INA: 2,6-dichloroisonictinic acid

IRE1: inositol-requiring enzyme 1
IUPAC: International union of pure and applied chemistry
JA: Jasmonic acid
kb: Kilo base
KO: Knockout
KR: Keto-reductase
KS: Keto-synthase
MDP: Monodictyphenone
MFS: Major facilitator superfamily
MLO/mlo: Mildew resistance locus O wild-type/Mildew resistance locus O mutant
MM: Minimum medium
MPA: Mycophenolic acid
mt: Million tonnes
MT: Methyl transferase
NAD: Nicotinamide adenine dinucleotide
NADP: Nicotinamide adenine dinucleotide phosphate
NB-LRR: nucleotide-binding leucine rich repeat
NPR1: Nonexpresser of PR 1
nr: Non-redundant
NRP: Non-ribosomal peptide
NR-PKS: Non-reducing polyketide synthase
NRPS: Non-ribosomal peptide synthetase
ORF: Open reading frame
PAL: Phenylalanine ammonia lyase
PAMP: pathogen associated molecular pattern
PDA: Potato dextrose agar
PDB: Potato dextrose broth
PCD: Programmed cell death
PCP: Peptidyl carrier protein
PHI: Pathogen-host interaction
PKS: Polyketide synthase
PR: Pathogenesis related
PR-PKS: Partially reducing polyketide synthase
PT: Product template
QoI: Quinone outside inhibitors
qRT-PCR: Quantitative reverse transcription PCR
R: Reductase
RAxML: Randomized a(x)ccelerated maximum likelyhood
Rcc: *Ramularia collo-cygni*
REML: Restricted maximum likelihood
RLS: Ramularia leaf spot
ROS: Reactive oxygen species
SA: Salicylic acid
SAR: Systemic acquired resistance
SAT: Starter unit: acyl carrier protein transacylase
SDHI: Succinate dehydrogenase inhibitors
SM: Secondary metabolite
SMRT: Single molecule real time

SUMO: Small ubiquitin-like modifiers
TC: Terpene cyclase
TE: Thiolesterase
TF: Transcription factor
TGA: TGACG cis-element-binding protein
TRX: Thioredoxin
TS: Terpene synthase
UPR: Unfolded protein response

Acknowledgment

First of all, I would like to thank my supervisors: Dr. Peter Hoebe, Dr. Steven Spoel and Dr. Graham McGrann for their advice and the continuous support they have provided throughout the entire course of this project. Thank you Steven for your help and expertise when my project ventured into the scary world of Arabidopsis and Peter for your help throughout the PhD, in revising this thesis and also for being an amazing recipient during though times. Massive thanks go to the awesome Graham without whom this project would not have been the same, thank you for your invaluable help and advice, revision and constant questioning which helped me make this project possible.

I would like to thank my fellow PhD student, the technical team and the researchers. I also thank Ryan Douglas and Lindsey Williams for their help and for providing me with my first supervision experience

Thank you to all my friends for their support and for all the good times we had for the last four years. Although naming them all would be too long, some special thanks must go to Marta, Davide and his flatmate Julie, Alberto, Coline, Steven, Elise, Nikolaos as well as my fellow "phyte club" member: Maree.

Finally, I most specially thank my two officemates Paloma and Anna, my flatmate Irene and my family. Thank you Paloma for sharing all your dodgy career plans that always made me laugh so much; Anna for the extensive chatting / tea / chocolate sessions in the office and Irene for being the best flatmate. Most importantly, thank you to my family, Cecile, Alain, Benoit, Silvia, Aline and Gautier for their support throughout the PhD.

Abstract

In the past two decades a new barley threat has emerged as the disease Ramularia leaf spot (RLS) became more prevalent in temperate regions worldwide. This disease, first identified in the late 19th century, is caused by the filamentous fungus *Ramularia collo-cygni* (Rcc) and can cause substantial yield losses as well as reduce grain quality. RLS typically occurs late in the growing season and characteristic disease symptoms are usually seen after the crop has flowered. Expression of RLS lesions is thought to be associated with the action of fungal secondary metabolism products. The one group of secondary metabolites (SMs) characterised to date from Rcc, the anthraquinone toxins rubellins, are known to cause necrosis to plant tissues in a non-host specific manner. Therefore, it appears that fungal secondary metabolism might be a key component in understanding the interaction between Rcc and its host.

In this study, more than 23 core genes involved in the biosynthesis of SMs belonging to the polyketide and non-ribosomal peptide pathways were identified in the genome of Rcc. Putative clusters containing genes with a predicted function relating to secondary metabolism were identified by *in silico* genome walking in the genetic loci adjacent to Rcc SM core genes. Two gene clusters containing no SM core gene were also identified. Five of the putative SM clusters exhibited similarity to the known fungal SM biochemical pathways involved in gliotoxin, monodictyphenone, ferricrocin, betaenone and chaetoglobosins biosynthesis. Several gene clusters exhibited similarity to SM clusters from fungal species where the SM pathway is uncharacterised.

Changes in transcript abundance of selected SM core genes during RLS development in artificially inoculated barley seedlings were tested. Transcript levels were found to be the highest at an early stage of disease development, typically during the asymptomatic and early lesions formation stages and declined over time, suggesting that the associated SMs in Rcc, may not necessarily be involved in symptoms appearance.

The *in planta* mode of action of the non-host specific photoactivated toxin rubellin D was studied in the model plant *Arabidopsis thaliana*. Rubellin-induced cell death appeared phenotypically reminiscent of programmed cell death (PCD). Full expression of rubellin D-induced cell death required the host salicylic acid (SA) pathway and the host proteasome supporting the PCD response to this fungal SM. However, a clear correlation between toxin sensitivity and disease susceptibility could not be found, suggesting a potential alternative role for rubellin in disease symptom development.

Lay summary

Ramularia leaf spot (RLS) is an important disease of barley (*Hordeum vulgare*) occurring in all the temperate regions of the world and causing yield losses estimated to be in the range of 5-20% although these can be as high as 70%. Importantly this disease can also affect the quality of the grain increasing the proportion of smaller grains called screening which reduces the value of the crop. The disease is caused by the filamentous fungus *Ramularia collo-cygni* (Rcc) and has been gaining in importance over the past few decades. Despite being first identified over a century ago, the causative agent of RLS has only recently attracted scientific attention. Over the past two decades major advances were made in understanding the life cycle of Rcc and some aspects affecting disease development *in planta* started to appear. However, the interactions between the host and the fungus remained largely unexplored. The aim of this study was to investigate, at a genomic and molecular level, several components of the secondary metabolism of Rcc. Secondary metabolism results in the biosynthesis of accessory compounds such as toxins and pigments that are not essential for Rcc to live but these compounds mediate the interactions the fungus has with its environment including its host plants. This study focussed on polyketide and non-ribosomal peptide secondary metabolites (SMs), two major classes of fungal SMs, in Rcc.

Analysis of the Rcc genome revealed that this fungus possesses the genetic ability to produce several SMs derived from polyketide and non-ribosomal peptide pathways. Based on this study, it appears that Rcc contains at least 23 core polyketide synthase (PKS), non-ribosomal peptide synthetase (NRPS) and hybrid PKS/NRPS genes potentially involved in the biosynthesis of SMs. In addition, several clusters of genes with predicted functions in SM biosynthesis were identified at specific genetic loci, further supporting the hypothesis that Rcc can produce a wide range of SMs. Expression of several SM core genes identified in the genome of Rcc was followed during disease development in barley seedlings. The majority of the SM core genes tested appeared to be most highly expressed during the earliest

stages of disease development which coincided with the asymptomatic and early lesion formation stages that happened just before the leaves started to senesce.

The mode of action of a previously identified polyketide phytotoxin produced by Rcc was studied. Rubellin D, is a phytotoxic compound which is known to induce necrosis in barley leaves upon light activation. Development of RLS lesions was thought to be linked with the deployment of phytotoxic compounds such as rubellin D in the host tissue. Although the mode of action of this toxin remains unknown, this study provides evidence that the plant defense mechanism appear to mediate sensitivity to this toxin. However, rubellin D-induced lesions do not appear similar to typical RLS lesions suggesting that the link between RLS and rubellin is more complex than previously thought and calls for more in depth study of the barley/Rcc pathosystem at the molecular level.

Chapter 1:

General introduction

1.1. Crop fungal diseases in history

Since the start of agriculture more than 10,000 years ago, mankind has struggled to protect crops from a multitude of parasites and pathogens. Fungal diseases have always been of particular concern, so much that the Romans worshiped Robigus, the Corn God who protected grain fields from disease (McIntosh *et al.*, 1995). As agriculture evolved through history, disease control methods were developed including the appearance of the first natural antifungal agents such as copper and sulphur. Both copper and sulphur were used extensively on vineyards to control powdery and downy mildew diseases. However early plant protection methods sometimes failed to efficiently control fungal pathogens and epidemics resulted in humanitarian catastrophes. The Great Famine in Ireland during the European Subsistence Crisis in 1845-1850, caused the death of approximately one million people and was largely caused by the oomycete *Phytophtora infestans*, the agent responsible for potato late blight disease (Vanhaute *et al.*, 2006). The discovery and mass production of synthetic fungicides in the 1960s has helped to control fungal diseases in plants. However, less than 20 years after their introduction, some fungicides have been rendered ineffective due to the development of fungal isolates insensitive to their chemistry (Milaire, 1982). Furthermore, combined with the appearance of fungicide insensitivity, new and emerging disease threats have surfaced across the globe. Diseases deemed secondary in the past became more prevalent and as their economic importance grew they started to attract scientific attention. Stem rust caused by *Puccinia graminis* f. sp. *tritici* became a major threat of wheat (*Triticum aestivum*) when the recently evolved Ug99 isolate identified in Uganda in 1999 was found to be virulent in 70% of the cultivated wheat varieties (Newton *et al.*, 2011). However, recent discovery of a resistance gene (*Sr33*) in *Aegilops tauchii* and subsequent introgression in wheat conferred resistance to the Ug99 isolates (Periyannan *et al.*, 2013). The development of modern science has helped us understand crop diseases through better detection which has improved our knowledge of the biology of these organisms. This in turn helped farmers to protect their crops in more sustainable ways. For instance, understanding the life cycle of the hemibiotropohic fungus *Rhynchosporium commune* provided evidence that

agronomic practices such as ploughing helped to control outbreaks of barley leaf scald (Avrova & Knogge, 2012). More recently, the development of molecular biology provided deeper insights into understanding the interactions between plants and pathogens at the cellular level. This combined with genomic resources has helped researchers identify fungal genes involved in different aspects of fungal interactions with plants, including disease. One area of particular interest to the scientific community is the complex arsenal of secondary metabolites produced by fungi that aid exploitation of various ecological niches. Be it through toxic properties or by conferring ecological advantage over other species, secondary metabolites, although not required for an organism to live, are often crucial for the organism to thrive in its local environment. Many plant diseases have been linked with the production and *in planta* release of secondary metabolites produced by fungi. The dothistromin toxin produced by the Dothideomycete *Dothistroma septosporum*, the agent responsible for the Dothistroma needle blight of pine trees, is a virulence factor known to mediate disease severity (Kabir *et al.*, 2015). Therefore, studying the secondary metabolism of a fungus may provide insight into its biology which in the case of plant pathogens may be used to help control disease development. This thesis focuses on the secondary metabolism of the newly important pathogen of barley *Ramularia collo-cygni*.

1.2. Barley: a resilient crop

1.2.1. History of barley

Barley (*Hordeum vulgare*) is one of the oldest cultivated cereals in the world and one of the first domesticated crops. The origins of cultivated barley are found in the Fertile Crescent around 8,000 B.C (Zohary & Hopf, 2000) when humans started selecting for grain and straw quality from wild barley (*Hordeum vulgare* ssp. *spontaneum*). Molecular analysis based on amplified fragment length polymorphism narrowed down the domestication cradle to the Israel-Jordan region (Badr *et al.*, 2000). The wild barley population found in this part of the Fertile Crescent presented more similarities to cultivated barley than any other *H. vulgare* ssp. *spontaneum*

(Badr *et al.*, 2000). The ability to quickly adapt to changing environmental conditions as well as relatively high levels of resistance against pests, including virus vectoring aphids, turned *H. vulgare* ssp. *spontaneum* into a good source for cultivated barley improvement (Nevo *et al.*, 2012). Even though cultivated and wild barley are rather phenotypically similar, domestication was accompanied by some minor morphological changes. Zohary & Hopf (2000) observed that *H. vulgare* presented broader leaves, larger grain and shorter stems than *H. vulgare* ssp. *spontaneum*. These features remain present in modern commercial barley varieties and are still used as selection criteria in the breeding industry because of their direct involvement in yield, be it through photosynthesis efficiency by increased leaf area or reduced susceptibility to lodging by shortening stem length.

1.2.2. Barley production

There are two different types of cultivated barley: spring and winter barley. Spring barley is sown in spring and is less resistant to low temperature than winter barley which is sown before winter. Furthermore, spring varieties do not require a vernalisation period at low temperature to initiate flowering unlike winter varieties. Throughout this thesis, unless stated otherwise, barley will refer to both spring and winter varieties.

Barley has the widest geographic range of all cereal crops and is grown throughout the world (Hayes *et al.*, 2003). The total area of global barley production is a little under 50 million hectares based on data collected between 2009 and 2013 (FAOSTAT, 2014). Being particularly tolerant to extreme climates and offering less variation in yield and quality under poor environmental conditions, barley is often cultivated as a source of staple food in developing countries and grown in marginal areas offering soil and climatic conditions less favourable to grow other cereals. Thus barley is cultivated in extremely fertile regions such as the Beauce region in France and Saxony-Anhalt in Germany as well as in region with less favourable conditions such as the slopes of the Andes and the particularly arid regions of the Middle East (Akar *et al.*, 1999).

In terms of tonnage barley is the fourth most important cereal crops in the world after maize, wheat and rice. The main producers of barley are the Russian Federation producing 14.3 million tonnes (mt), France (10.8 mt), Germany (10.5 mt) and Ukraine (9.1 mt). Average yields worldwide are approximately 2.7 tonnes ha^{-1} (t ha^{-1}) but behind this figure lay vast inequalities in regional barley production. The lowest yields reported are about 0.5 t ha^{-1} in countries such as Libya or Ecuador while the highest yields vary between 8 and 9 t ha^{-1} in Belgium and Ireland (average between 2009-2013) (FAOSTAT, 2014).

1.2.3. Main uses of barley

Although barley was historically one of the main cereals in human diets over the world, its uses in food recipes are now limited to either traditional use such as soups and bread in Morocco (Amri *et al.*, 1994) or as a more secure food supply in developing countries. Being more resistant than wheat to adverse growing condition, barley is used as a more robust food source in many less developed countries. In more developed countries, barley is mainly used for animal feed. In the USA alone, cattle feed represents more than 65% of the total barley usage (Newman and Newman, 2006). Even though the most common use is to grow barley to produce grain, some marginal uses can be found for instance in Northern Africa where barley can be grazed by sheep (Fischbeck, 2002). Furthermore, the discovery of beneficial effects of β-glucan on cholesterol levels has paved the way to a larger use of barley in foodstuffs (Newman *et al.*, 1989). Naturally occurring β-glucans in barley have been shown to reduce low density lipoprotein and cholesterol concentration (Wang *et al.*, 1992). Considering that high cholesterol is a major health issue in developed countries, the importance of barley usage in human food and its economic value are expected to grow in the near future.

Barley is also used for malting. During that process, barley seeds are germinated to initiate degradation of starch to sugars used in subsequent fermentation processes (Greenwood & Thomson, 1959). Although the malting market only represents a small part of the world's barley production, malting is the first use of barley in terms of added value. Malt is used mostly in the production of alcoholic beverages in the

brewing and distilling industries but approximately 2% of malt production can also be used in a wide range of food applications such as the production of malted bread or malt vinegar (Newton *et al.*, 2011). Although it only represents 4% of the malt production, distilling has a considerable weight in barley's economic value because of its expensive end product: whisky. In terms of quantity, brewing is by far the largest malt consumer with 94% of its total production (Newton *et al.*, 2011). Boosted by growing markets such as Asia (+7.4% *per annum*) and Africa (+5.7% *p.a.*) the demand for barley malt is expected to increase in the coming years.

Being used all over the world in different food recipes and processes, barley is a crop of prime importance, therefore its protection from diseases and pests that negatively influence quality and yield is equally crucial.

1.2.4. Threats to barley production

1.2.4.1. Abiotic stresses

Abiotic stress can limit the potential of barley production resulting in lower yields and in extreme cases total crop loss. Abiotic stress can be caused by several factors. Mineral deficiency or toxicity largely depends on soil condition. Saline soils found in coastal and arid regions are generally associated with sodium toxicity which is estimated to limit cultivated crop potential by 15% (Munns & Tester, 2008). Environmental conditions can also result in abiotic stress to crops. It has been estimated that the difference between the potential of the crop and the average harvested yield can be explained by non-optimal environmental conditions such as drought, cold, heat or water logging (Atkinson & Urwin, 2012). One of the most common stress response observed on barley leaves is associated with a response to light. When light levels and intensity are high, barley exhibit spontaneous spotting known as physiological leaf spot. Due to its atypical leaf spotting, physiological leaf spot had long been thought to be linked with a disease. Based on phenotypical observation, the distinction between physiological spotting and the fungal disease Ramularia leaf spot is challenging to accurately determine. A study by Wu & von Tiedemann (2004) showed that physiological leaf spot development was linked to a

deficient antioxidant system in the plant. The antioxidant system comprises enzymes such as catalases, superoxide dismutase and ascorbate peroxidases involved in protecting the plant from oxidative stress, notably reactive oxygen species (ROS)-induced stress. Superoxide ($O_2^{\bullet-}$) was found to be involved in both physiological leaf spot and in the response to rubellin toxins produced by *Ramularia collo-cygni*, the causative agent of Ramularia leaf spot, further highlighting the similarity between these abiotic and biotic stresses (Heiser *et al.*, 2003; Wu & von Tiedemann, 2004).

1.2.4.2.Biotic stresses

Barley crops are attacked by many different biotic organisms including pests, such as insects and nematodes, pathogenic fungi, bacteria and viruses which can all be important causes of yield losses. However, this thesis will only focus on fungal plant pathogens and how they affect barley.

Fungal diseases can affect all parts of the barley plant. Seedling blight is one of the major diseases affecting the stem at an early stage of plant development and is caused by *Fusarium* species including *F. graminearum* (syn. *Gibberella zeae*), *F. poae* and *F. avenaceum* (syn. *Gibberella avenacea*) (Khan *et al.*, 2006). The damage caused on seedling can lead to a reduction of plant density in the field thus negatively impacting yield. Stem rust, also known as black rust, caused by the biotrophic fungus *Puccinia graminis* f. sp. *tritici*, is a growing concern. Although not present yet in Europe, stem rust is a serious threat because the Ug99 isolates have been shown to be virulent on more than 90% of cultivated barley varieties in the world (Newton *et al.*, 2011). In addition to an increased virulence, Ug99 isolates have also been shown to be thriving in cooler temperatures than more common stem rust races thus expanding its climatic range (Rouse & Jin, 2009).

Barley leaf scald caused by the hemibiotrophic fungus *Rhynchosporium commune* is the main foliar disease of barley in Northern Europe. Even though *R. commune* emerged as a barley pathogen between 2,500 to 5,000 years ago (Brunner *et al.*, 2007) its management remains problematic as fungicides and agronomic practices lack efficiency (Zhan *et al.*, 2007). Powdery mildew caused by the fungus *Blumeria graminis* f. sp. *hordei* was also a recurrent problem in barley fields.

However, the discovery that mutations at the *Mildew resistance locus O* (*MLO*) resulting in a loss of function conferred resistance to powdery mildew largely abolished the problem (Piffanelli *et al.*, 2002). The *mlo*-mediated resistance against *B. graminis* f. sp. *hordei* has been used extensively in the breeding industry, the most commonly used *mlo-11* allele is now found in more than 70% of the cultivars used in Europe (Dreiseitl, 2012). Brown rust and yellow rust caused by the biotrophic fungi *Puccinia hordei* and *Puccinia striiformis* f. sp. *hordei* respectively, are among the major leaf diseases of barley. However, quantitative trait loci conferring partial resistance to both diseases have been used by plant breeding companies to improve modern barley cultivars (Chen *et al.*, 1994; Qi *et al.*, 1998).

Several diseases can also affect the ears and heads of barley plants including the seed-borne diseases rice blast caused by *Magnaporthe oryzae* and barley leaf scald caused by *R. commune*. However, Fusarium head blight caused by a fungal complex involving several species of *Fusarium* such as *F. graminearum*, *F. culmorum* and *Microdochium nivale* remains one of the major threats to barley ears (Bottalico & Perrone, 2002). In addition to yield losses, Fusarium head blight is often associated with grain contamination caused by mycotoxins such as deoxynivalenol (DON), produced by certain fungal species within the disease complex. Mycotoxins such as DON which is also known as vomitoxin, are known to be highly toxic to humans and animals and therefore present a serious threat to grains destined for use in human food products and animal feed (Pestka & Smolinski, 2005).

In recent years new threats have emerged such as that posed by *Magnaporthe oryzae,* a hemibiotrophic fungus responsible for rice blast. Blast has been reported on barley leaves and is particularly devastating on spring barley cultivars carrying mutant *mlo* alleles that confer resistance to powdery mildew disease (Jarosch *et al.*, 1999). Therefore, in regions where *mlo* varieties are used, farmers are faced with a trade-off between resistance to one disease and susceptibility to the other. Similarly, McGrann *et al.*, (2014) showed that barley lines carrying mutant *mlo* alleles were more susceptible to the emerging Ramularia leaf spot disease caused by *Ramularia collo-cygni* than wildtype *MLO* alleles suggesting that the emergence of new diseases such as Ramularia leaf spot may have resulted from an extensive use of the mildew *mlo*-mediated resistance in barley cultivars.

1.3. Ramularia leaf spot: an emerging leaf disease of barley

1.3.1. Taxonomy of Ramularia leaf spot

Ramularia leaf spot (RLS) is a disease of barley that has been known for over a century with the earliest report coming from northern Italy in the late 1800s (Cavara, 1893). The diagnosis and observation of the fungus on barley leaves led to the classification of the causal organism as *Ophiocladium hordei*. Since then, the name and classification of the pathogen was disputed. After a thorough comparison between *Ophiocladium* and *Ovularia* species, Sprague (1946) introduced the name of *Ovularia hordei* instead of *Ophiocladium hordei*. Later, based on a comparative description of conidia and conidiophores from *Ovularia* and *Ramularia* species, Sutton & Waller (1988) proposed to reclassify *Ovularia hordei* into the *Ramularia* genus. They introduced the current name *Ramularia collo-cygni* (Rcc) to account for the shape of the conidiophores, which are curved resembling a swan neck (from the latin: collum meaning neck and cygnus- swan) (Figure 1.1). The taxonomy of Rcc has since been confirmed by phylogenetic analysis based on internal transcribed spacer regions ITS-1, ITS-2 and 5.8S of ribosomal RNA of 46 *Mycosphaerella* species including *Ramularia* anamorphs (Crous *et al.*, 2000). Rcc has finally been classified within the Dothideomycetes class in the order of the Capnodiales and in the Mycosphaerellacae family. Recently, Rcc was found to be a sister species to the wheat pathogen *Zymoseptoria tritici* (syn. *Mycosphaerella graminicola*) and was also found to be closely related to the pine pathogen *Dothistroma septosporum* (syn. *Mycosphaerella pini*) and its sister species *Cladosporium fulvum* (syn. *Passalora fulva*) as well as to the banana pathogen *Pseudocercospora fijiensis* (syn. *Mycosphaerella fijiensis*) (McGrann *et al.*, 2016).

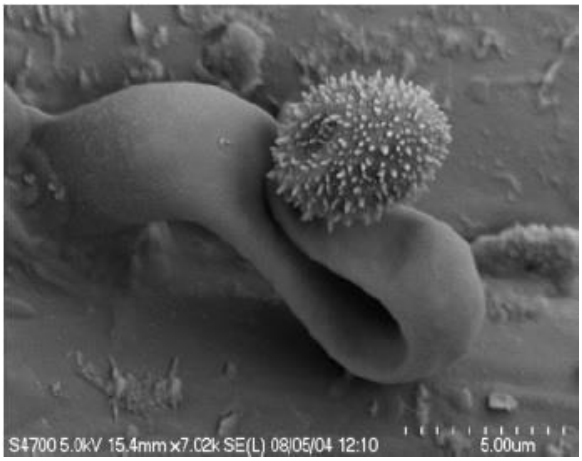

Figure 1.1: Swan-neck shaped conidiophore of *Ramularia collo-cygni*.
Extracted from Walters *et al.* (2008).

1.3.2. Distribution of *Ramularia collo-cygni*

Following the discovery of Rcc in Italy the disease has been observed throughout Europe with reports coming from Germany (Sachs *et al.*, 1998), Switzerland (Frei & Gindrat, 2000), Norway (Salamati *et al.*, 2002), Denmark (Pinnschmidt *et al.*, 2006), Sweden (Djurle & Rasmussen, 2006), Great Britain (Havis *et al.*, 2002), Czech Republic (Minarikova *et al.*, 2002), France (Caron *et al.*, 2009), Hungary (Manninger *et al.*, 2009) and Ireland (O'Sullivan, 2002). More recently, Rcc has been also identified in fields in Russia, Estonia, Latvia, Iceland, Spain and Poland (Havis *et al.*, 2015). Outbreaks of RLS have also been reported outside Europe (Figure 1.2). Rcc was identified on the American continent (Argentina, Chile, Uruguay, Colombia, USA, Mexico) (Walters *et al.*, 2008; Clemente *et al.*, 2014), in Africa (Namibia, Israel) (Havis *et al.*, 2015) and in Oceania (New Zealand) (Harvey, 2002). The detection of Rcc DNA in barley seeds worldwide could explain these sporadic outbreaks of RLS in isolated countries (Havis *et al.*, 2015).

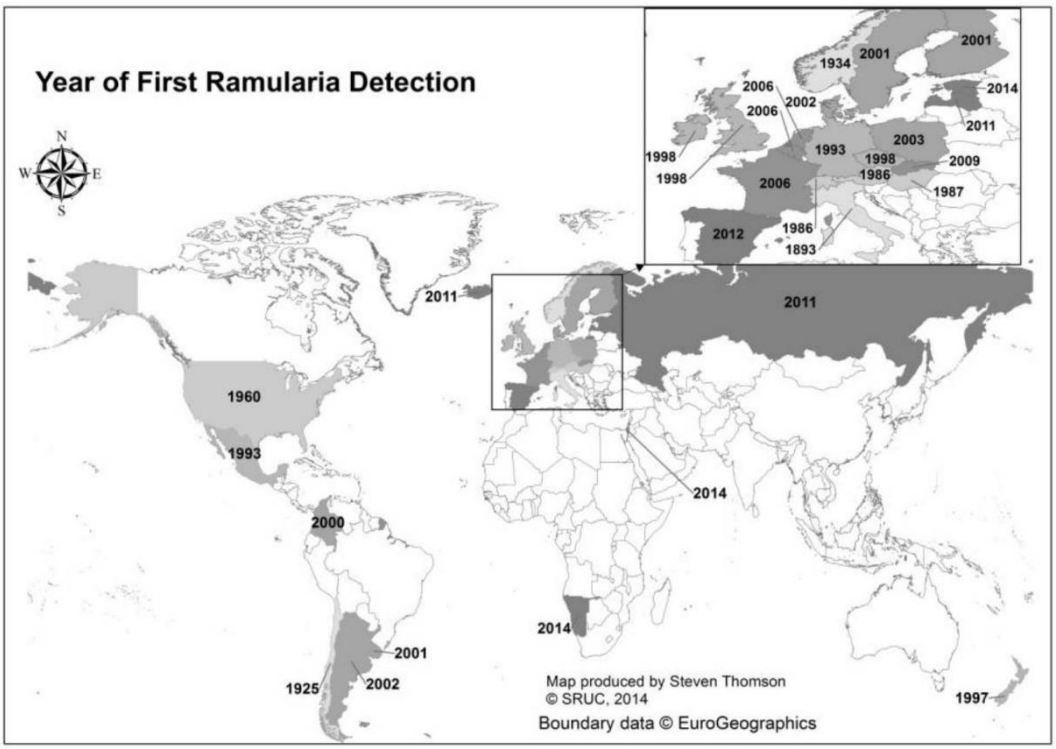

Figure 1.2: Map showing the year of the first identification of *Ramularia collo-cygni*. Extracted from Havis *et al.* (2015).

1.3.3. Ramularia leaf spot symptoms

The identification of RLS symptoms at an early stage of their development can be challenging. Disease lesions are first observed as small brown spots often called "pepper spots" located on the upper side of the leaves. These early symptoms can be confused with physiological leaf spot (Figure 1.3.C). The similarity between early RLS and physiological spotting symptoms could explain the delay between the first description of RLS by Cavara and later reports in Europe almost 100 years after. Makepeace *et al.*, (2008) confirmed that Rcc fulfilled Koch's postulates proving the causal link between Rcc and RLS. Furthermore the development of molecular techniques has considerably improved the identification of Rcc even at very early stages of infection, allowing rapid distinction of RLS from physiological leaf spot and other fungal diseases (Havis *et al.*, 2006, 2014; Frei *et al.*, 2007; Taylor *et al.*, 2010; Clemente *et al.*, 2014). As the fungus develops, the "pepper spot" symptoms evolve into typical RLS lesions. These are described as small rectangular reddish-

brown necrotic lesions, approximately 1-2 mm long and 0.5 mm wide, sharply delineated by leaf veins and usually surrounded by a chlorotic halo (Figure 1.3.A) (Huss, 2002). Unlike many other fungal diseases, RLS symptoms are characteristically visible on both sides of the leaf. Lesions can expand and merge resulting in chlorosis of the leaf and eventually in necrosis (Walters *et al.*, 2008). Although spotting is mostly observed on leaves, in high disease pressure conditions symptoms can also be seen on leaf sheath as well as on the stem (Figure 1.3.B) and awns (Harvey, 2002; Sachs, 2002; Walters *et al.*, 2008). As the disease progresses, conidiophores bearing single conidia can be seen emerging in caespituli, where several conidiophores are grouped together, through necrotic stomata on the lower side of the leaf and form lines of small white dots visible by the naked eye. This can also be seen more rarely on necrotic tissue located on the adaxial side of the leaf (Stabentheiner *et al.*, 2009; Kaczmarek *et al.*, 2017).

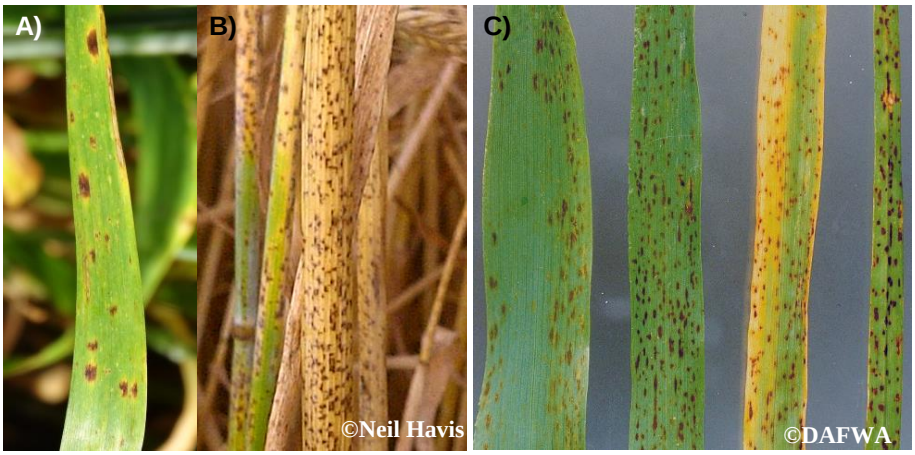

Figure 1.3: Ramularia leaf spot and physiological leaf spot symptoms on barley.
A) Typical RLS symptoms on barley leaf cv. Optic, B) RLS symptoms on stems of barley cv. Optic, C) Physiological leaf spot symptoms on barley cv. Vlamingh.

Although symptoms can occasionally be observed on senescing lower leaves early in the season, typical ramularia leaf spot symptoms are usually seen after the crop has flowered (growth stage GS 61; Zadoks *et al.*, 1974) which led to the classification of Rcc as a late season pathogen. The spotting which generally develops after anthesis has been proposed to be linked with the *in planta* release by

Rcc of phytotoxic secondary metabolites called rubellins (Makepeace *et al.*, 2008). The role and biochemistry of rubellins will be discussed later in this thesis (section 1.4.5). What causes Rcc to switch from asymptomatic to symptomatic growth is still unknown. It is thought that ontogenic changes such as the degradation of the antioxidant system occurring during flowering could act as a signal triggering necrotrophic growth of Rcc (Schützendübel *et al.*, 2008). Observations that plants grown in a stressful environment such as high light intensity prior to inoculation, exhibited more symptoms compared to plants grown in normal conditions supports this hypothesis (Makepeace *et al.*, 2008; Peraldi *et al.*, 2014). Furthermore, recent studies highlighted the relationship between RLS development and plant stress responses, showing that genes involved in drought resistance or maintaining redox homeostasis in barley affect the expression of RLS symptoms (McGrann *et al.*, 2015a,b).

1.3.4. Host range of *Ramularia collo-cygni*

Although barley crop is the main host of Rcc, this fungus is considered to have a broad host range. It has also been reported on other *Poaceae* such as winter wheat (*Triticum aestivum*) (Kaczmarek *et al.*, 2017), oat (*Avenae sativa*), rye (*Secale cereale*), maize (*Zea maydis*) (Huss, 2002) and triticale (*Triticum secalum*) (Sutton & Waller 1988). Rcc is also frequently reported on wild grasses such as false barley (*Hordeum murinum*) and to a lesser extent on false oat (*Arrhenatherum elatius*) (Huss, 2002), king's fescue (*Festuca kingii*), Italian ryegrass (*Lolium multiflorum*) (Sprague, 1946), couch grass (*Agropyron repens*), wind grass (*Apera spic-venti*) (Frei & Gindro, 2015) and black grass (*Alopecurus myosuroides*) (Kaczmarek *et al.*, 2017). Rcc is also able to infect the model grass *Brachypodium distachyon* (purple false brome) (Peraldi *et al.*, 2014) and cannabis plants (*Cannabis sativa*) (Huss, 2002). Whether these alternative hosts are important to the biology of RLS remains to be determined.

1.3.5. Consequences of Ramularia leaf spot

Development of RLS symptoms leads to yield reduction due to a loss of green leaf area resulting in a decrease in photosynthetic ability. This has two consequences, firstly it affects the grain filling stage and secondly due to leaf senescence, early ripening is often observed (Greif, 2002). The average yield loss due to Rcc in the UK in 2008 was estimated between 0.2 and 0.6 t ha^{-1} for spring barley (Oxley *et al.*, 2008). However yield losses have been reported worldwide and vary greatly. For instance Huss *et al.* (1987) reported losses of about 10% in Austria, while it reached more than 35% in New Zealand (Cromey *et al.*, 2002) and up to 70% in south America (Havis *et al.*, 2015).

Ramularia leaf spot also has an impact on grain quality. Rcc infection leads to a decrease in thousand grain weight directly impacting the specific weight of the crop (Leistrumaite & Liatukas, 2006). Furthermore, due to grain size reduction, RLS can result in increased grain screenings, one criteria used by the malting industry to assess grain quality in a batch, by up to 4%. Increased screenings can result in grain being downgraded from suitable for the malting market to feed barley which decreases the value of the crop (Cromey *et al.*, 2002).

1.3.6. Life cycle of *Ramularia collo-cygni*

Although recent studies have provided novel insights in to the biology of Rcc, gaps remain in our understanding of its complex life cycle. *Ramularia collo-cygni* has recently been identified as a seed-borne pathogen (Havis *et al.*, 2014). DNA of Rcc was detected in the lemma and to a lower extent in the pericarp and embryo of barley grain (Matusinsky *et al.*, 2011). Adult plants grown from Rcc infected seeds were found to be heavily colonised by Rcc mycelium in the absence of external inoculation confirming seed infection as an important source of inoculum (Havis *et al.*, 2014). Fungal mycelium spreads asymptomatically from the seed in barley seedlings as it develops. At this stage Rcc behaves as an endophyte and its presence can only be observed using molecular diagnostics (Havis *et al.*, 2015).

Air-borne inoculum from spores is potentially important for Rcc infection of spring barley crops. Frei *et al.*, (2007) showed that Rcc infection in spring barley occurred after the fungus has sporulated on winter crops. Rcc is able to survive on winter barley crops over the winter period as a saprophyte living on dead leaves or on straw (Frei *et al.*, 2007). Following Rcc spore dispersal, the infection process begins with the germination of the conidia on the leaf surface. Fungal hyphae quickly develop to form a dense network on the leaf surface before penetrating the leaf through open stomata (Stabentheiner *et al.*, 2009). Stomatal and subsequent mesophyll colonisation occurs within 24h and is facilitated by the formation of stomatopodia (Sutton & Waller, 1988; Kaczmarek *et al.*, 2017). At this stage the fungus grows intercellularly, without causing cellular damage, in the middle lamella most probably as an endophyte (Stabentheiner *et al.*, 2009; Kaczmarek *et al.*, 2017). Later in the season, as a response to unknown complex changes in the growing environment of the fungus (section 1.3.3.), Rcc becomes necrotrophic and typical RLS symptoms are seen on leaves and awns (Havis *et al.*, 2015). The life cycle of Rcc is presented in Figure 1.4.

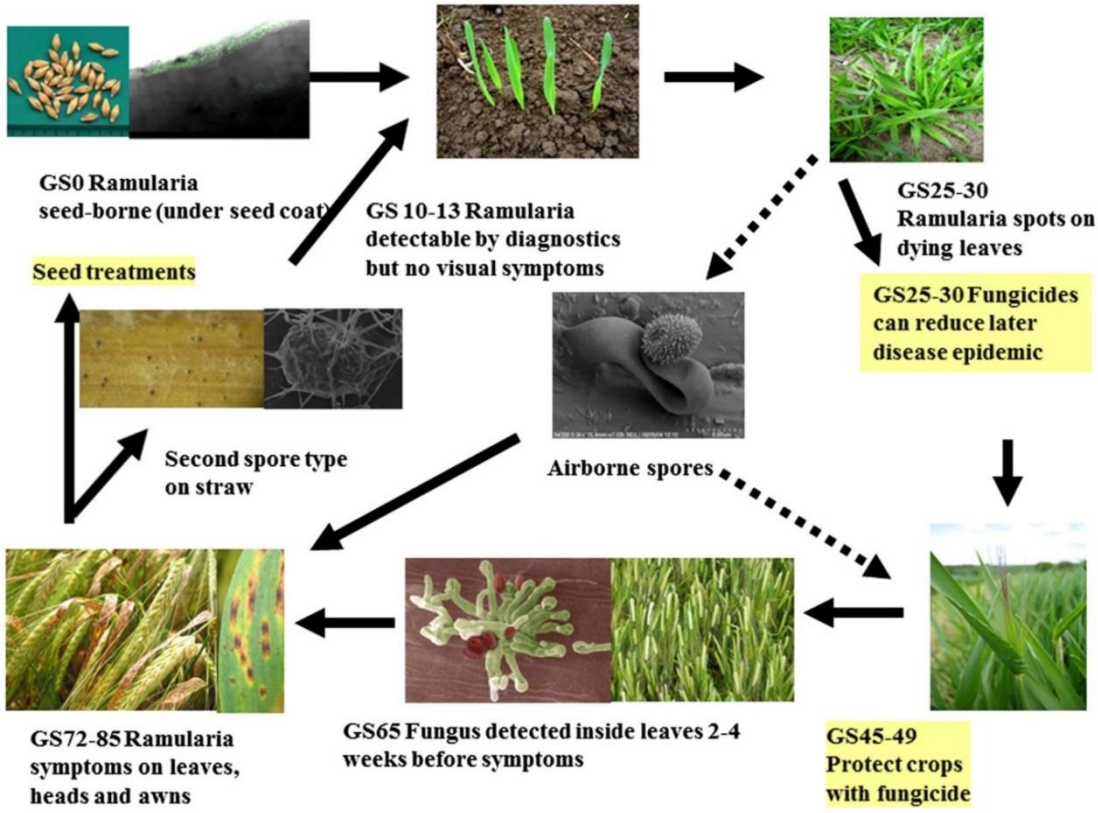

Figure 1.4: Life cycle of *Ramularia collo-cygni*.
Extracted from Havis *et al.* (2015).

1.3.7. Control methods for Ramularia leaf spot

1.3.7.1.Seed treatment

At present no seed treatments have been shown to control RLS efficiently. Fungicide treatments carried out with triazoxide and tebuconazole gave inconsistent results over several season (Havis *et al.*, 2010). The use of succinate-dehydrogenase inhibitors (SDHI) combined with triticonazole as seed treatment managed to lower the amount of fungal DNA present in both seeds and seedlings (Havis *et al.*, 2015). However the effect of this treatment has not been investigated further and more evidence is required to link the efficacy of these chemicals with reduced RLS severity. Physical seed treatments such as steam or hot water treatments can be effective. For instance, hot water treatment reduced Rcc DNA levels in infected grains; however, these types of seed treatments are not applicable as they also negatively affect seed viability (Havis *et al.*, 2015).

1.3.7.2.Varietal resistance

Spring barley varieties carrying mutant allele of the *Mildew resistance locus O* (*MLO*) which confers complete resistance to powdery mildew (*B. graminis* f. sp. *hordei*) exhibit higher susceptibility to RLS (Bistrich *et al.*, 2006; McGrann *et al.*, 2014). Due to the very destructive nature of powdery mildew, this *mlo*-mediated resistance is now used widely in spring barley breeding with approximately 70% of elite European commercial varieties carrying *mlo* thus potentially increasing the risk of RLS outbreaks. No spring or winter barley varieties currently have complete resistance to Rcc although some cultivars exhibit moderate resistance to RLS (Minarikova *et al.*, 2002; Pinnschmidt *et al.*, 2006). Disease resistance ratings in the UK recommended list for spring barley for 2016 confirm that even the latest varieties fail to achieve complete resistance to RLS (https://cereals.ahdb.org.uk). The observation of partial resistance to RLS in different geographical regions of Europe and on different cultivars (Leistrumaite & Liatukas, 2006; Oxley *et al.*, 2008) suggest

that resistance to RLS is quantitative and is potentially influenced by environmental effects. Therefore, the control of RLS relies predominantly on foliar fungicide applications.

1.3.7.3.Fungicide treatments

At present barley protection against RLS relies on three families of fungicides: the chloronitriles, the SDHI and the triazole sterol demethylation inhibitors (DMI) (Jorgensen *et al.*, 2006; Oxley *et al.*, 2006). However, DMI efficacy is starting to decline as isolates from 2015 showed lower sensitivity than that of isolates from 2010 to 2013 (Piotrowska *et al.*, 2016b) and although only few field isolates with reduced sensitivity to SDHI have been reported yet (Piotrowska *et al.*, 2016b), a recent study showed that several single amino acid mutations were sufficient to confer resistance to SDHI in lab-derived Rcc mutants (Piotrowska *et al.*, 2016a). Therefore, the risk of seeing the emergence of SDHI-resistant isolates is serious. The quinone outside inhibitors (QoI), also known as strobilurins, have now been overcome by the pathogen and the mutation conferring QoI resistance is found in almost the whole Rcc population in the UK (Fountaine & Fraaije, 2009; FRAG, 2013). Similarly, a study of the Rcc population in Czech Republic in 2009 showed that 47% of Rcc population had acquired the mutation providing QoI resistance (Matusinsky *et al.*, 2010). For maximum efficacy, a combination of two or more fungicides with a different mode of action is recommended (HGCA, 2013). To achieve optimal RLS control, fungicides must be applied prior to symptom appearance at an appropriate timing. Jorgensen *et al.*, (2006) showed that in spring barley fungicides applied between booting and heading at around GS 45-51 gave the most efficient protection against RLS. However, earlier application at GS 37-39 also gave moderate control (Balz *et al.*, 2006). Most spray programs are now based on two treatments and a more accurate timing showed maximum control for application at the stem elongation stage (GS 30) and first awns visible (GS 49) (Havis *et al.*, 2015). However, fungicides application should not be done routinely and spray programs need to be modulated depending on disease severity in the field. A forecast model including risk factors such as leaf wetness duration and occurrence was

created to help farmers by advising them when fungicides should be applied to the crop to obtain optimal RLS control (Oxley & Havis, 2010).

Our understanding of Rcc biology has considerably improved over the past 20 years; however, the interactions between Rcc and barley at a genetic, molecular and biochemical level remain largely unknown. Particularly the role played by Rcc secondary metabolism in disease development has not yet been investigated.

1.4. Fungal secondary metabolites

1.4.1. Secondary metabolites

Metabolism can be separated into two main types, primary and secondary. Primary metabolism relates to all the metabolic processes required for an organism to grow and reproduce. Therefore primary metabolism aims to produce energy and synthesise vital molecules such as carbohydrates, lipids, nucleic acids and proteins. Because of their involvement in crucial processes many primary metabolites are shared by all living organisms.

Secondary metabolism involves processes that are not necessary for an organism to survive such as the biosynthesis of antibiotics or iron-chelating compounds, known as siderophores. The products of secondary metabolism are called secondary metabolites (SMs) and unlike primary metabolites, SMs are typically unique to a particular species, a genus or a family and reflect the individuality of that species. Secondary metabolites are often low molecular-weight compounds and represent a large group of very diverse metabolic products. Bérdy (2005) reported that over one million SMs were characterised although only 25% of these had medicinal properties. Among these products the antibiotics, antitumor and enzyme inhibitors are widely researched by pharmaceutical companies because of their potential as new medicinal drugs. Approximately half of these bioactive SM compounds come from higher plants; the others are produced by microbes, algae, protozoa, invertebrates, lichens and some animals. Considering that only 1% of the microbes in the world have been cultivated *in vitro* and these have already provided an important number of bioactive molecules, the spectrum for new drug discovery is rather large (Kaeberlein

et al., 2002). Fungal species account for approximately 5% of the total production of bioactive compounds. Fungi are the most important producers of antibiotics as they are responsible for the biosynthesis of approximately 50% of known antibiotics (Bérdy, 2005). Fungal species are also producers of other important SMs, some of which are harmful such as mycotoxins which pose a serious threat to human and livestock health when they contaminate food sources.

In plant pathogenic fungi several SMs are important determinant of disease development as some define the ability of a given fungus to infect plants while others mediate disease severity. The production of victorin toxin by the oat pathogen *Bipolaris victoriae* has been linked with the development of Victoria blight symptoms (Navarre & Wolpert, 1999). Similarly, the cercosporin toxin produced by Cercospora spp. is a known virulence factor that modulates disease severity (Upchurch *et al.*, 1991; Daub & Chung, 2007). Previous analysis of the Rcc genome revealed the presence in this fungus of putative paralogues of genes involved in the biosynthesis of pathogenicity and virulence factors such as cercosporin, HC-toxin or dothistromin (McGrann *et al.*, 2016). An in depth analysis of the SM-related gene complement in Rcc may provide usefull insight into the infection biology of this fungus.

1.4.2. History of fungal secondary metabolites

Fungal SMs have been used for food production or preservation for thousands of years, although the underlying process was not understood. Cultures of *Penicillium roquefortii* were already used 4,000 years ago for the conservation of cheeses. Fungal cultures were also used in non-alimentary processes with SMs such as those from *Monascus purpureus* used as pigments in Chinese medicine in 800 AD (Ma *et al.*, 2000). However, it is only since the discovery of penicillin by Alexander Fleming in 1928 that fungal fermentation and SMs became studied and started to play an important role in the development of medicine. However, the very first antibiotic discovered was mycophenolic acid isolated by Bartolomeo Gosio in 1893 from spoiled corn (Bentley, 2001). Gosio isolated the fungus that later became known as *Penicillium brevicompactum* and harvested crystals of a compound that

inhibited the growth of *Bacillus anthracis*. This was the first report of a pure compound having antibiotic activity. Due to the development of modern genome sequencing, molecular biology and biochemical technologies the number of SMs discovered over recent years is rapidly increasing. In 1940, only a few (~10-20) antibiotics were known but by the 1970's approximately 2,500 had been discovered and in 2000 more than 20,000 antibiotic compounds were identified (Bérdy, 2005).

1.4.3. Importance of fungal secondary metabolites

1.4.3.1.Pharmaceutical products

Fungal SMs are a major source of pharmaceutical products such as antibiotics, hypocholesterolemic compounds or immunosuppressive and anticancer drugs (Bérdy, 2005). Antibiotics are arguably the most important SMs in terms of number and economic value with the market for antibiotics in 2009 estimated to be worth $42 billion (Hamad, 2010). Antibiotics are extremely diverse in their chemical structure and their mode of action. The major class of antibiotics in terms of medical use are the beta-lactams such as penicillins and cephalosporins. This group is defined by the presence of a cyclic amide, or lactam ring, and act by inhibiting bacterial cell wall biosynthesis (Suarez & Gudiol, 2009). Other important antibiotics include the quinolones, sulphonamides and aminoglycosides which act by inhibiting DNA replication, nucleic acid biosynthesis and protein synthesis, respectively (Henry, 1943; Mingeot-Leclercq *et al.*, 1999; Andriole, 2005).

Some fungal SMs are used as anti-cancer drugs because of their ability to interfere with cell division processes such as microtubules breakdown, resulting in mitosis inhibition (Kumaran *et al.*, 2012). Taxol is the most important anti-cancer SM and was isolated from *Taxomyces andreanae*, an ascomycete endophyte of the pacific yew tree (*Taxus brevifolia*) (Stierle *et al.*, 1993). Statins represent a group of fungal SMs with important pharmaceutical properties in regards to cholesterol regulation in bloodstream. All statins share a common backbone that consists of a naphthalene ring and a hydroxy-lactone ring in the beta position. Statins act as hypolipidemic drugs by inhibiting the first enzyme involved in cholesterol

biosynthesis, 3-hydroxy-3-methylglutaryl-CoA reductase, (Manzoni & Rollini, 2002). The first statin was identified from *Penicillium citrinum* in 1976 and named mevastatin but also known as compactin (Endo *et al.*, 1977). Since their discovery statins became important molecules for pharmaceutical research.

Immunosuppressive drugs are widely used in medicine to avoid rejection after organ transplants and to control auto-immune diseases. The first identified immunosuppressive compounds was cyclosporin A, a fungal SM isolated from *Tolypocladium nivenum* (Borel *et al.*, 1976). Cyclosporins act by indirectly inhibiting calcineurin which normally triggers the immune response via activation of the transcription of interleukin-2. Since its introduction in the pharmaceutical world its usage became more prevalent such that nowadays the cyclosporin market is estimated to be around $2 billion per year (Demain, 2014).

Fungal SMs are an important source for new drugs discovery and have a multitude of medicinal uses. Probing for SM in fungal genomes has identified new SM and diversified the arsenal of medicinal drugs however, not all fungal SMs are beneficial.

1.4.3.2.Harmful secondary metabolites

Harmful SMs produced by filamentous fungi are called mycotoxins. Mycotoxins can be found in foodstuffs and induce poisoning when ingested by animals. Being stable compounds, the processes involved in food production such as milling, brewing or baking only partially reduces mycotoxin concentrations in the end product (Bullerman & Bianchini, 2007). Although mycotoxins were identified in recent history, most notably during the 19th century, their effects have been known for centuries. One of the most recognisable symptoms of mycotoxicosis was ergotism such as St Anthony's fire which was particularly prevalent during the Middle-Age. Consumption of food contaminated by lysergic acid, a toxic SM derivative of lysergic acid diethylamide known for its psychedelic and gangrene-inducing effects, produced by the rye ergot fungus *Claviceps purpurea* caused large epidemics. In 994 AD an epidemic of St Anthony's fire resulted in the deaths of approximately 40,000 people in France (Pfohl-Leszkowicz, 1999). The difference

between a toxic compound and a beneficial pharmaceutical drug often relies on small chemical differences such as the presence or absence of an alcohol function. Lysergic acid is obtained by hydrolisation of ergotamine, a SM extracted from *C. purpurea* and used during the 16th century as a drug to induce abortion by promoting uterine contraction (Bove, 1970).

Other mycotoxins have been discovered more recently and numerous other mycotoxin-producing fungi have been identified. Among the most important toxins are the deoxynivalenol (DON), zearalanone and fumonisins produced by some *Fusarium* species, notably *F. graminearum* and *F. culmorum*. With the aflatoxins produced by the *Aspergilli* section *flavi* fungi, fumonisins are amongst the most potent carcinogenic compounds known to date (Norred *et al.*, 1992; Wild & Turner, 2002). Zearalenone and DON have been shown to exert high cytotoxic activities resulting in hepatotoxicity, genotoxicity and heamatotoxicity (Abid-Essefi *et al.*, 2004; Pestka & Smolinski, 2005). Recent studies showed that these mycotoxins were detected on more than 50% of the feed ingredients found in Europe raising major concern for human and animal health (Binder *et al.*, 2007; Richard, 2007). As a result, a legislation relating to mycotoxin levels in unprocessed foodstuffs was enforced to assess whether or not agricultural products can be used for specific markets such as human consumption or animal feed (European Commission, 2006). Therefore, extensive studies have been carried out for decades to understand the role and biosynthesis of such toxins.

1.4.4. Role of secondary metabolites in fungal biology

The role of most of the currently identified SMs in fungal biology remains unclear. However, the biological function has been characterised for a handful of SMs. Production of SMs can confer an advantage to a given fungus by increasing its adaptability to a specific environment thereby allowing the organisms to exploit various ecological niches.

Some SMs act as anti-competition agents. This type of SM aims at protecting the fungus and/or its host against other biotic threats such as insect pests, or other fungi. This anti-competition function for SM to protect the SM-producing fungus is

particularly highlited in *LaeA* mutants of *Aspergillus nidulans*, which are impaired in the production of some SMs, as these mutants are predated upon more by the fungivorous arthropod *Folsomia candida* than the wild-type strains (Rohlfs *et al.*, 2007). The host protection by anti-competition SMs is generally found in endophytic fungi such as *Epichloë* and *Chaetomium* species, which produce the insect antifeedant peramine and the antifungal chaetoglobosins, respectively that protects their plant hosts from predation (Tanaka *et al.*, 2005; Zhang *et al.*, 2013).

Secondary metabolites can also have a role in protection against abiotic stresses. The cladofulvin pigment produced by the tomato pathogen *Cladosporium fulvum* is involved in protecting conidia against UV radiation as well as low temperatures (Griffiths *et al.*, 2017). Similarly, the black pigment melanin produced by the pear pathogen *Alternaria alternata* is involved in tolerance to UV radiation as the *brm2* mutant impaired in melanin production exhibited increased susceptibility to UV light than the wild type strain (Takano *et al.*, 1997).

Many fungal SMs in pathogenic species are involved in the development of the disease. When necessary for infection to occur and cause disease a SM can be defined as a pathogenicity factor whereas if the SM only mediates disease severity it is termed a virulence factor. Host-specific toxins (HSTs) have targets that are specific to host cells which results in a narrow spectrum of sensitive plants to these toxins, and considering that toxins are often involved in disease development, HSTs are generally pathogenicity factor. In contrast, non-HSTs exert their activity through widely conserved targets or mechanisms therefore inducing toxicity in diverse type of cells and organisms. As a result, non-HSTs are more likely to be virulence factors (Stergiopoulos *et al.*, 2013).

Because of the involvement of SM in diverse aspects of fungal biology, the number and type of SMs produced by a given fungus often correlates with its lifestyle by conferring to the fungus the ability to colonise diverse ecological niches.

1.4.5. Rubellins: secondary metabolites produced by *Ramularia collo-cygni*

Knowledge of the arsenal of SMs produced by Rcc might give useful insights into its biology. At present, only one SM family has been characterised in Rcc.

Sutton & Waller (1988) hypothesised that a phytotoxin was associated with RLS symptoms based on the observation of cell death away from the fungal hyphae. Later a series of SM, characterised as rubellins, were identified from *in vitro* Rcc cultures (Heiser *et al.*, 2004; Miethbauer *et al.*, 2006) and also from infected leaves (Miethbauer *et al.*, 2003). Rubellins were first identified in *Mycosphaerella rubella*, the agent responsible for necrotic leaf spot in *Angelica silvestris* (Arnone *et al.*, 1986). Six derivatives of rubellin have been extracted from Rcc cultures and named alphabetically from rubellin A to rubellin E plus 14-dehydro rubellin D (Miethbauer *et al.*, 2008). Rubellins, as part of the anthraquinone family (IUPAC: dioxoanthracene) have an aromatic backbone with formula $C_{14}H_8O_2$. Anthraquinones are predicted to be synthesised via a polyketide-derived biosynthetic pathway (Gill, 2001). The recently elucidated biosynthetic pathways of the fungal anthraquinones aflatoxins (Figure 1.5.E), dothistromin (Figure 1.5.F) and cladofulvin (Figure 1.5.G), which are structurally related to rubellins, confirmed the involvement of polyketide-derived pathway in the production of these SMs (Yu *et al.*, 2004; de Wit *et al.*, 2012; Griffiths *et al.*, 2016). The biosynthesis of fungal SMs including polyketides will be reviewed in Chapter 2. Rubellins are predicted to be synthesised by dimerization of the anthraquinone backbone to yield the intermediates uredinorubellins (Figure 1.5.B) and caeruleoramularin (Figure 1.5.D). Rubellins A, B, E and F are likely to be obtained via Baeyer-Villiger oxidation of uredinorubellins in which the oxidation of a cyclic ketone yields a cyclic ester also known as lactone (Miethbauer *et al.*, 2008). Rubellins C and D (Figure 1.5.C) are thought to be obtained *in vivo* by conversion of rubellins A and B (Figure 1.5.A), respectively, via an unknown reaction (Miethbauer *et al.*, 2006).

Rubellins are photodynamic biologically active molecules. Detached barley leaves exposed to rubellin B and D showed necrosis only when incubated in the light (Heiser *et al.*, 2003). If rubellin is important for RLS symptom development then the link between light-activation of rubellin-mediated necrosis is supported by the effects of increased light intensity on the expression of disease symptoms as reported by Peraldi *et al.*, (2014) and Makepeace *et al.*, (2008) showing a link between light regime and RLS symptoms appearance *in planta*. However, the light-dependent activity of rubellins is non-host specific (Heiser *et al.*, 2004) indicating that these

toxins may not necessarily be specifically involved in disease symptom expression in barley. The mode of action of rubellins has been studied *in vitro* and rubellin D was shown to induce fatty acid peroxidation via the production of ROS, predominantly singlet oxygen ($^1O_2$) and to a lesser extent superoxide ($O_2^{\bullet -}$) (Heiser *et al.*, 2003, 2004). However, the biology of rubellin-induced cell death *in planta* is still unclear. Rubellins have been reported to exert antibacterial activity against three Gram positive bacteria, *Bacillus subtilis*, *Staphylococcus aureus* and *Enterococcus faecalis*, as well as having cytotoxic effects on rabbit, murine and human cells (Miethbauer *et al.*, 2008). Rubellins also exhibit light-independent activities. Antiproliferative and cytotoxic activities have been reported on human cells including umbilical vein endothelium, myeloid leukemia and HeLa cancerous cells (Miethbauer *et al.*, 2008). These data imply a possible antimicrobial function of rubellin; however, the precise function of this phytotoxic SM remains to be determined.

A)

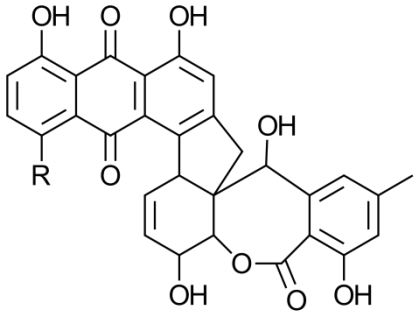

R=H Rubellin A
R=OH Rubellin B

B)

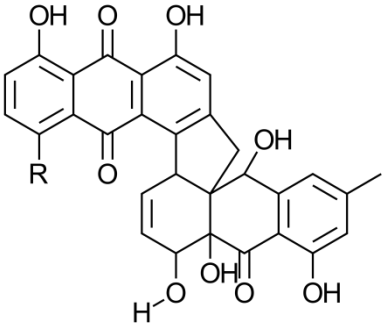

R=OH Uredinorubellin I
R=H Uredinorubellin II

C)

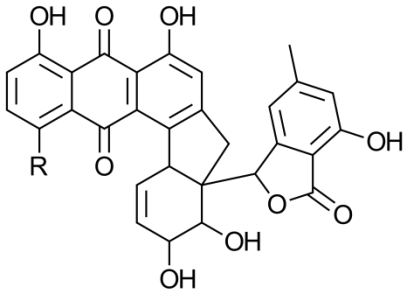

R=H Rubellin C
R=OH Rubellin D

D)

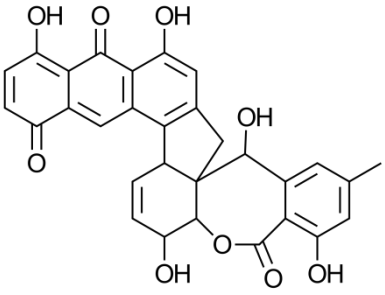

Caeruleoramularin

E)

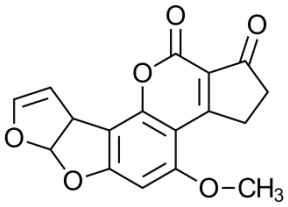

Aflatoxin B1

F)

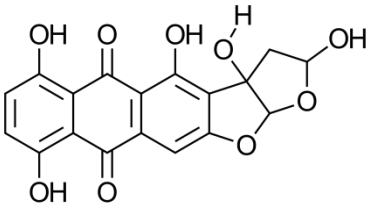

Dothistromin

G)

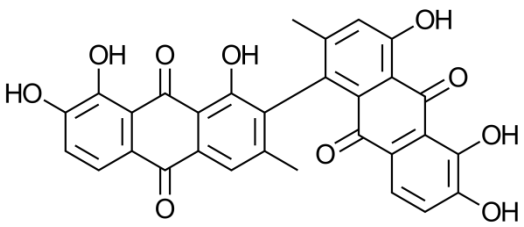

Cladofulvin

Figure 1.5: Chemical structure of several relevant secondary metabolites.
Adapted from Bradshaw & Zhang (2006); Miethbauer *et al.* (2008); Griffiths *et al.* (2016).

1.5. Aims and objectives

This study aimed at identifying and characterising genes with predicted roles in secondary metabolite production in the fungus *Ramularia collo-cygni*. Expression of secondary metabolism-related genes was profiled during the development of RLS to associate changes in transcript levels with the expression of disease symptoms. Finally the mode of action of the known Rcc phytotoxin, rubellin D, was investigated *in planta* to provide further insights into how this phytotoxin interacts with the plant.

Chapter 2:
Identification and characterisation of secondary metabolite gene clusters in *Ramularia collo-cygni*

2.1. Biosynthesis of fungal secondary metabolites

Microbial secondary metabolites (SMs), also often called natural products are an important source of new pharmaceutical drugs and also of potentially toxic compounds such as food contaminants. Fungal species are among the most important producers of SMs as half of the antibiotics known to date are produced by fungi (Bérdy, 2005). SMs are also involved in the development of numerous diseases in animals and plants alike. For instance, the Dothideomycete *Bipolaris zeicola* (syn. *Cochliobolus carbonum*) a pathogen of maize, produces a toxic SM known as HC-toxin which was found to be involved in disease development (Walton, 2006). In spite of the large diversity of SMs, the biochemical pathways leading to their production are relatively similar and conserved across living organisms. Genes involved in SMs biosynthesis are typically grouped in clusters (Keller & Hohn, 1997). A gene cluster is defined as a set of two or more genes involved in the same biosynthetic pathway resulting in co-regulation of these genes within the organism's genome. A given pathway can be either composed of one or several clusters. The anthraquinone toxins aflatoxin and dothistromin produced by *Aspergillus* species and *Dothistroma septosporum* (syn. *Mycosphaerella pini*) respectively are synthesised through biochemical pathways that typically illustrate this diversity. Aflatoxin biosynthesis is governed by 25 genes grouped in a single cluster of approximately 70 kb (Figure 2.1.A) (Yu *et al.*, 2004). The dothistromin pathway comprises 20 genes, 19 of them being orthologous to genes in the aflatoxin pathway, arranged in six different clusters scattered over chromosome XII (1.26 Mb) plus a single gene on chromosome XI (Figure 2.1.B) (Chettri *et al.*, 2013). Secondary metabolite pathways are usually organised around one specific gene called a core gene which is involved in the biosynthesis of the backbone of the SM product. As a result a core gene is often the gene responsible for the production of the first intermediate compound in the biosynthetic pathway.

The nature of the enzyme encoded by the core gene defines the type of biosynthetic pathway and resulting SM. There are four main biosynthetic pathways involved in the production of fungal SMs: the polyketide synthase (PKS), the non-ribosomal peptide synthetase (NRPS), the dimethylallyl tryptophan synthase

(DMATS) and the terpene cyclase (TC), also known as terpene synthase (TS) pathways (Keller *et al.*, 2005). A study by McGrann *et al.*, (2016) showed, based on sequence similarity, that the genome of Rcc did not contain any DMATS and only four TCs were identified. The number of PKSs and NRPSs however, was substantially higher with 19 and 14 putative genes respectively identified. Although important fungal metabolites involved in plant-pathogen interactions are derived from all four pathways including ergotamine from DMATS (Correia *et al.*, 2003) and deoxynivalenol and T2-toxin for the TC pathway (Desjardins & Proctor, 2007) this thesis will only focus on the PKS and NRPS pathways.

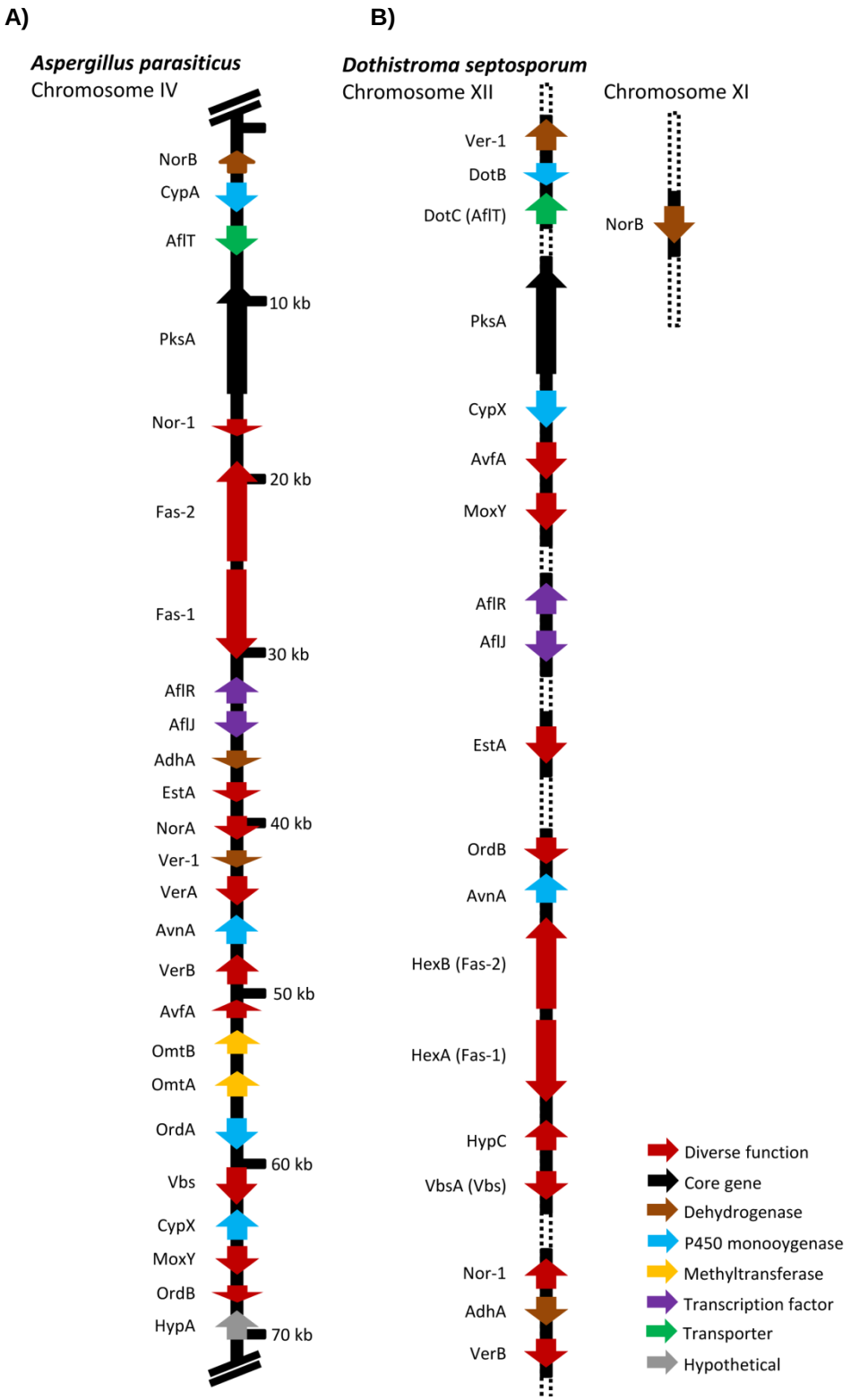

Figure 2.1: Secondary metabolism gene cluster involved in the production of two known fungal toxins.
(A) The production of aflatoxins in *A. parasiticus* is regulated by a single 70 kb-gene cluster on chromosome IV. (B) The phytotoxin dothistromin produced by *D. septosporum* is synthesised by six mini clusters spread across the 1.26 Mb-chromosome XII (dotted line) and a single gene on chromosome XI. Adapted from Yu *et al.* (2004); Chettri *et al.* (2013).

2.1.1. The polyketide pathway

Polyketides are polymers presenting a long, complex often aromatic carbon skeleton. These polymers are diverse including polyphenols, polyenes, polyesters, macrolides (macrocylic esters) and enediynes. The core genes in the polyketide pathway are polyketide synthases (PKSs) which are large multi-domain enzymes that catalyse the synthesis of polyketides from derivatives of acyl-CoA. Polyketides are synthesised through Claisen condensation with the formation of a carbon-carbon bond between an α-carboxyacyl-CoA and a carbonyl yielding a β-diketone and carbon dioxide (Rawlings, 1998). To perform the condensation, the PKS requires three specific domains: a keto-synthase (KS), acyl transferase (AT) and acyl carrier protein (ACP) domain.

2.1.1.1.Mechanism of polyketide biosynthesis

Polyketides are synthesised by condensation of an extender unit, which is usually the conjugated base of an α-carboxyacyl-CoA such as malonyl-CoA or acetyl-CoA, to a carbonyl group (Hopwood, 1997). During polyketide synthesis the extender unit is activated by removal of the coenzyme A and binding of the carboxyacyl to the AT domain of the PKS (Figure 2.2.i). The ACP domain acting like a swinging arm (Figure 2.2.ii) physically transfers the activated carboxyacyl from the AT domain to the KS domain. During Claisen condensation, decarboxylation occurs on the carboxyacyl (Figure 2.2.iii) yielding an intermediate carbanion-enolate stabilised by mesomerism (Figure 2.2.iv) (Jez *et al.*, 2000). The carbanion acts as a nucleophile to attack the thiolester group of the growing polyketide extending the carbonated chain of the polyketide by two carbons (Figure 2.2.v). The newly extended polyketide can either be used in a new round of elongation (Figure 2.2.vi) or processed by β-keto processing domains resulting in chain modification. β-keto processing domains found in PKSs are as diverse as dehydratase (DH), enoyl reductase (ER), keto-reductase (KR). These domains are involved in adding chemical group functions such as alcohol or enoyl on the β carbon of the growing polyketide product during chain elongation (Hertweck, 2009).

Despite being involved in the methylation of the α carbon, the methyltransferase (MT) domain is considered to be part of the β-keto processing domains. These domains work as a cascade to modify the newly synthesised polyketide. The KR domain catalyses the reduction of the β-ketone into a secondary alcohol. Subsequent dehydration by the DH domain yields an enoyl group which upon reduction by the ER domain, is converted into an alkane (Hertweck, 2009). Therefore, the type of domains recruited dictates the nature of the resulting functions of the protein. Depending on their domain organisation, PKSs are classified into three distinct types.

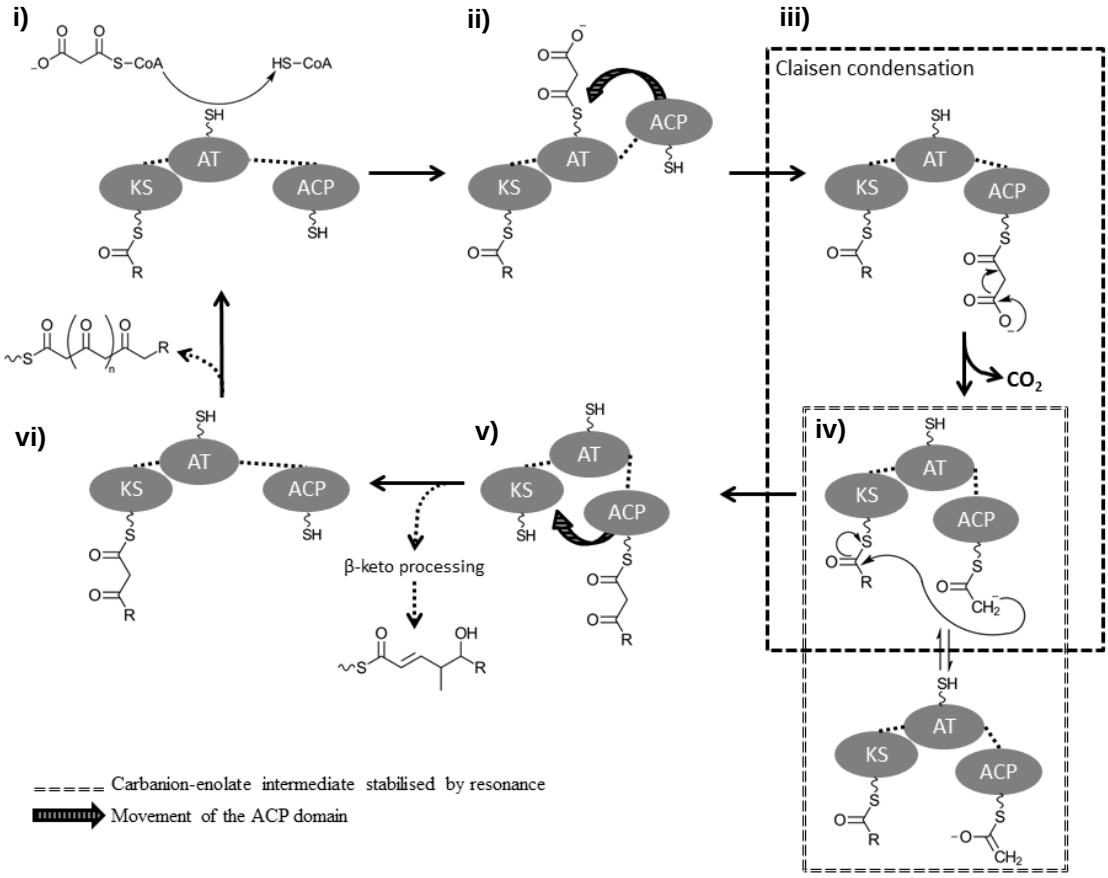

Figure 2.2: Mechanism of polyketide elongation.
The extender malonate-CoA unit is activated by the AT domain (i). The ACP domain carries the activated extender unit (ii) which is used in the decarboxylative Claisen condensation (iii) via the formation of a carbanion intermediate (iv). After condensation, the extended polyketide (v) can be processed or used in a new round of elongation (vi). Adapted from Jez *et al.* (2000); Hertweck (2009); Khosla (2009); Dunn *et al.* (2013).

2.1.1.2.Classification of fungal polyketide synthases

PKSs are classified based on the presence or absence of specific processing domains. Non-reducing PKSs (NR-PKSs) possess none of the reducing DH, ER or KR domains. Most partially reducing PKSs (PR-PKSs) are defined by the domain sequence KS-AT-DH-KR-ACP (Cox, 2007). However, a recent study identified alternative domain organisation for PR-PKSs in *Aspergilli* spp. that lacked the DH domain and where the KR domain was replaced by MT (Bhetariya *et al.*, 2016). Highly reducing PKSs (HR-PKSs) contain a DH domain followed by MT and in most cases by ER. The terminal processing domain in HR-PKSs is always KR (Figure 2.3). In the few HR-PKSs cases where the ER domain is absent an amino acid sequence of equivalent length and no known function replaces it (Cox, 2007). The chemical nature of a polyketide partially depends on the type of PKS involved in its biosynthesis. Non-reducing PKSs are typically responsible for the synthesis of aromatic polyketides. Contrastingly PR-PKSs and HR-PKSs are involved in the production of aliphatic compounds. Therefore polyketide diversity partly arises from the optional recruitment of processing domains during post-condensation modifications (Hertweck, 2009).

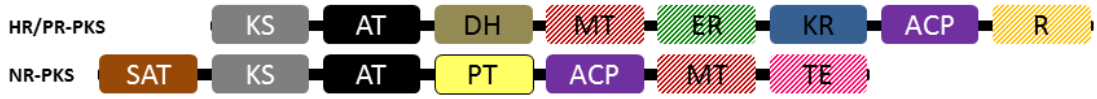

Figure 2.3: Typical domain organisation of highly-(HR) partially-(PR) and non-reducing (NR) polyketide synthase (PKS).
The three essential domains, keto-synthase (KS), acyl transferase (AT) and acyl carrier protein (ACP) involved in polyketide biosynthesis are present in all PKSs. HR- and PR-PKSs often contain several β-keto processing domains such as dehydratase (DH), enoyl reductase (ER) and keto-reductase (KR) that modify the carbonated chain of the polyketide. NR-PKSs usually have a starter unit: acyl carrier protein transacylase (SAT) domain preceding the KS domain at the N-terminus and a product template (PT) domain that follows the AT domain. All PKSs may contain a methyltransferase (MT) domain involved in the methylation of the α carbon of the polyketide. The release of the polyketide from the enzyme can be mediated by a reductase (R) or a thiolesterase (TE) domain. Optional domains are shaded in diagonal lines.

2.1.1.3.Specific domains from non-reducing polyketide synthases

Two types of domains are specific to NR-PKSs. Starter unit: acyl carrier protein transacylase (SAT) domains are located at the N-terminus of NR-PKSs and are involved in accepting the starter unit, be it a carboxyacyl-coA or a fatty acid (Crawford & Townsend, 2010). In the aflatoxin biosynthesis pathway, the starting unit is a hexanoyl-CoA produced by the fatty acid synthases *HexA* and *HexB* (Watanabe *et al.*, 1996). Crawford *et al.* (2006) showed that the SAT domain of *PksA* in *Aspergilli* spp. exhibited higher affinity for hexanoyl-CoA than any other carboxyacyl-CoA suggesting that the recognition of the hexanoyl-CoA as a starter unit by this enzyme is assured by the SAT domain. Contrastingly acyl-coA is used as a starter unit by the SAT domain-containing NR-PKSs *EncA*, *MdpG* or *ClaG* involved in the production of endocrocin, monodictyphenone and cladofulvin respectively (Chiang *et al.*, 2010; Lim *et al.*, 2012; Griffiths *et al.*, 2016).

Product template (PT) domains act as chaperones directing the newly elongated carbonated chain of the polyketide towards β-keto processing domains resulting in chemical modifications depending on the recruited domains (Hertweck 2009). PT domains are also involved in the cyclisation of polyketide intermediates which stabilises these intermediates and reduces potential reactivity with cell components (Crawford *et al.*, 2008).

2.1.1.4.Release of the polyketide from the core enzyme

Although not essential for polyketide synthesis, thiolesterase (TE) domains whose protein sequence is similar to that of α/β-hydrolases are involved in the release of the polyketide from the PKS enzyme. After the last round of polyketide elongation and once the carbonated chain has reached its final length, the newly synthesised polyketide is transferred from the ACP domain to the TE domain. Final release from the TE domain can occur either via hydrolysis if an external nucleophilic compound such as water is involved in attacking the carbon of the carbonyl bound to the serine residue of the TE domain, or via macrocyclisation if the

nucleophile involved is a chemical group such as NH_2 or OH from the polyketide (Du & Lou, 2010). Hydrolysis typically yields non cyclic products whereas, macrocyclisation generally yields lactam or lactone rings. Therefore, TE domains play an important role in polyketide cyclisation (Ma *et al.*, 2008). In addition, TE domains are also involved in shortening the carbonated chain when required (Cox, 2007).

Reductase (R) domains demonstrate protein sequence similarity with short chain dehydrogenases/reductases and are also involved in polyketide release. R domain-mediated release occurs via reductive release when the redox potential of $NAD(P)H+H^+$ is used to reduce the thiolester of the polyketide bound to the ACP domain to yield an aldehyde (Bailey *et al.*, 2007).

2.1.2. The non-ribosomal peptide pathway

Unlike the polyketide pathway, which is based on carboxylic acid building blocks, the non-ribosomal peptide (NRP) pathway uses primarily amino acids (AA) to construct SM products. The NRP pathway is found in bacteria and fungi and is responsible for the production of small peptides, usually smaller than 15 AA. The NRP pathway is dedicated to secondary metabolism which contrasts with the ribosomal peptide pathway which is generally orientated towards primary metabolism (Mootz *et al.*, 2002). NRP are more diverse than ribosomal peptides. Increased NRP diversity arises from the capacity of the non-ribosomal peptide synthetases (NRPSs), the core enzymes in this pathway, to process a larger number of substrates ranging from the proteinogenic AA to unnatural AA, including modified AA such as N-methyl valine and non proteinogenic AA such as L-α-amino butyric acid (Caboche *et al.*, 2008) as well as amines (Marahiel *et al.*, 1997).

2.1.2.1.Non-ribosomal peptide elongation mechanism

Non-ribosomal peptide synthetases are organised in domains. Three domains are required for NRP synthesis: adenylation domains (A), condensation domains (C) and peptidyl carrier protein domains (PCP) also termed thiolation domains (Figure 2.4).

Together these domains form an elongation unit or module (C-A-PCP). The initiation of peptide formation is carried out by an initiation module composed of only A-PCP. The NRPS domains can be compared to the three essential domains found in PKSs. The A domain, like the AT domain in PKSs, is responsible for the selection and activation of the extender unit, in other terms, the A domains are specific to certain AA (Finking & Marahiel, 2004). The condensation domain of NRPS enzymes is involved in the formation of the peptide bound between the extender AA and the growing peptide, a functionally analogous role to that of the KS domain in PKSs. The PCP domain, like the ACP domain in PKSs, is responsible for carrying the growing peptide chain and moving it forward towards a new elongation unit (Finking & Marahiel, 2004). The domain organisation of the NRPSs defines three different types of enzymes.

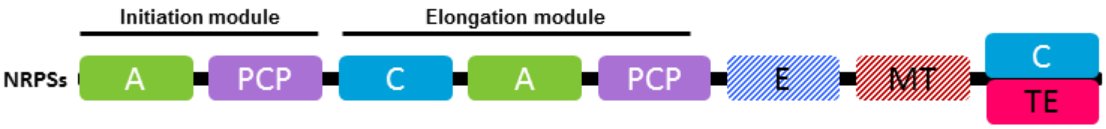

Figure 2.4: Typical domain organisation of a non-ribosomal peptide synthetase (NRPS).
The three essential domains, adenylation (A), condensation (C) and peptidyl carrier protein (PCP) are present in all NRPSs. The initiation module (A-PCP) initiates non-ribosomal peptide formation continued by successive elongation modules (C-A-PCP). Non-ribosomal peptide release is carried out either by a C-terminal thiolesterase (TE) domain or a condensation domain. Epimerisation (E) and methyltransferase (MT) domains may be involved in peptide modification. Optional domains are shaded in diagonal lines.

2.1.2.2.Classification of NRPS

NRPSs can be classified based on the architecture of catalytic domains or on functionality. Based on the domain organisation, NRPSs are classified as three different types. Linear NRPSs, also called type A NRPSs, are composed of an initiation module followed by a succession of elongation modules. Each elongation module is responsible for one round of elongation resulting in a peptide chain containing potentially diverse AA. The iterative NRPSs (type B NRPSs) can utilise the same module for several rounds of elongation. As a result, because each A domain is substrate specific, peptides formed by iterative NRPSs exhibit generally a

symmetrical chemical structure (Mootz *et al.*, 2002). Nonlinear NRPSs (type C NRPSs) are the most complex NRPSs because their organisation differs from the typical module (C-A-PCP) organisation. In type C NRPSs, stand-alone domains can be recruited to work alongside typical modules or other stand-alone domains either in an iterative or non-iterative way (Finking & Marahiel, 2004). The most studied example of type C NRPS is that of the bacterial siderophore enterobactin in *E. coli* where a stand-alone A domain encoded by the *EntE* gene works alongside the isochorismate lyase gene *EntB* to produce 2,3-dihydroxybenzoate subsequently used by the single NRPS module C-A-PCP-TE encoded by *EntF* (Weissman, 2015). The three genes work iteratively three times to yield enterobactin.

In addition to this structural classification, Bushley & Turgeon (2010) proposed a functional classification based on the nature of the resulting product. This classification identified nine groups of fungal NRPSs including the siderophore synthetase, cyclosporin synthetase, the β-lactam-yielding δ-(L-α-aminoadipyl)-L-cysteine-D-valine (ACV) synthetase and Euascomycete-only synthetase groups as well as NRPS-related groups such as the adenylating enzymes belonging to the α-aminoadipate reductase family.

2.1.2.3.Peptide modification

Modifications of the non-ribosomal peptide are carried out by specific domains and are involved either in widening the range of product synthesised by a given NRPS or in protecting the peptide from reacting with cell components. Modifications can either occur before or after peptide synthesis. Epimerisation is a common modification that occurs prior to AA incorporation. It is carried out by a specific domain, termed an E domain, which converts an L-amino acid to its D-form or *vice versa* (Linne *et al.*, 2001). The E domains are also thought to be involved in the recognition of the product of one NRPS by the second NRPS to use as a starting unit when several NRPSs are involved in a given pathway (Linne *et al.*, 2003).

Methylation of amino acid residues in the peptide chain is carried out by methyltransferase (MT) domains that have been identified embedded within A domains of several NRPSs (Finking & Marahiel, 2004). Methylation is involved in

protecting the non-ribosomal peptide from proteolytic degradation. N-methylation was shown to occur on the activated AA bound to the PCP domain prior to its incorporation to the NRP whereas C-methylations occur on the α carbon after peptide bound formation (Walsh *et al.*, 2001).

Thiolesterase (TE) domains are involved in release of the final NRP product in a similar way to that observed for polyketide release from the PKS. TE domains either catalyse hydrolysis of the carbonyl of the NRP to release a linear product or if the nucleophile attack comes from within the NRPS macrocyclisation occurs and releases cyclic products (Du & Lou, 2010).

2.1.3. The hybrid PKS/NRPS pathway

Both PKSs and NRPSs appear to share several common features such as the elongation mechanism or the organisation in domains. Highlighting further this similitude is the existence of hybrid enzymes between PKSs and NRPSs. Hybrid PKS/NRPS (HPSs) are multi-modular enzymes that combine extending modules from both PKS and NRPS proteins. HPSs have been found in both bacteria and fungi but the architecture of HPSs between these organisms differs despite yielding chemically related products based on polyketides fused with amino acids (Fisch, 2013). Where bacterial HPSs are based on NRPS modules followed by a non-iterative PKS, fungal HPSs have a simple architecture consisting in an iterative PKS followed by a single NRPS module (Figure 2.5). The structure of all PKS domains observed in fungal HPSs resemble HR-PKSs with a domain organisation such as KS-AT-DH-MT-(ER)-KR-ACP. Based on protein sequence alignments, all ER domains in HPSs are thought to be non-functional. Enoyl reduction requires binding of NADPH to the ER domain which is normally achieved by a GGVG motif that all ER domains found in HPSs lack (Fisch, 2013). However, many HPS-derived products exhibit a fully reduced polyketide part as observed in tenellin and lovastatin (Fisch, 2013) which can only be explained by the action of second enzyme resulting in *in trans* reduction of the polyketide. The NRPS module involved in fungal HPSs has the structure of a typical NRPS module C-A-PCP. However, the affinity of the A domain for a given AA in HPSs is thought to be less specific than in NRPSs (Xu *et*

al., 2010). This relative lack of selectivity in HPSs determines how one pathway can lead to the production of several products. For instance the *ApdA* gene cluster involved in the production of the cytotoxic compound aspyridone from *Aspergillus nidulans* can lead to the production of eight different compounds (Wasil *et al.*, 2013).

Figure 2.5: Typical domain organisation of a fungal hybrid PKS/NRPS (HPS).
An iterative HR-PKS presenting a typical domain organisation keto-synthase (KS), acyl transferase (AT), dehydratase (DH), methyltransferase (MT), enoyl reductase (ER), keto-reductase (KR) and acyl carrier protein (ACP) is fused to a single NRPS module with typical condensation (C), adenylation (A) and peptidyl carrier protein (PCP) domain organisation. An optional C-terminal reductase (R) domain is involved in product release. Optional domains are shaded with diagonal lines. Superscript 0 marks non-functional domains.

2.1.4. The role of secondary metabolism in plant pathogenic fungi

Many fungal secondary metabolites are involved in plant disease. PKSs, NRPSs and HPSs play a major role in the interactions between plant and pathogen. For instance, several polyketide-derived metabolites such as dothistromin, cercosporin or elsinochrome produced by *Dothistroma septosporum*, *Cercospora nicotianae* and *Elsinoë fawcettii* respectively, are defined as virulence factors due to their ability to mediate disease severity (Choquer *et al.*, 2005; Liao & Chung, 2008a; Kabir *et al.*, 2015). Similarly, the NRP HC-toxin produced by *Bipolaris zeicola* was shown to be involved in pathogenicity as mutants impaired in HC-toxin production were unable to infect maize (Ahn & Walton, 1997). Therefore, understanding the potential arsenal of secondary metabolites produced by a pathogenic organism can provide insight into the biology of the infection.

2.1.5. Objectives

The objective of this chapter is to identify and characterise putative polyketide- and non-ribosomal peptide derived secondary metabolites gene clusters in the recently sequenced genome of *Ramularia collo-cygni* by:

- Identification of PKS, NRPS and HPS core genes in the genome of Rcc.
- *In silico* characterisation of the genomic regions surrounding PKS, NRPS and HPS core genes to detect the presence of putative SM biosynthesis genes clusters in Rcc.
- Determine phylogenetic relationships between Rcc PKS, NRPS and HPS proteins and these enzymes from other fungal species with known biological functions to provide insights in to the putative secondary metabolites produced by Rcc.

2.2. Materials and Methods

2.2.1. *Ramularia collo-cygni* genome data

The genome of Rcc isolate DK05 Rcc001 has recently been sequenced. DK05 was isolated from the susceptible spring barley cultivar Braemar in Denmark in 2005. The draft genome was estimated as 30.3 Mb with 90x coverage and 11,617 gene models predicted (McGrann *et al.*, 2016). RNAseq data were generated from total RNA extracted from mycelium of DK05 grown *in vitro* on potato dextrose agar (PDA) plates for 10-12 days and confirmed the expression under these conditions of 8,514 of the predicted 11,617 genes.

2.2.2. Identification of core genes

2.2.2.1. Identification of putative core genes in *Ramularia collo-cygni*

A database containing the 11,617 Rcc protein models was created in GeneiousR9 software (Biomatters Ltd, Auckland, NZ). Protein sequences of known PKSs and NRPSs involved in the synthesis of products considered as model fungal SMs such as gliotoxin or cercosporin for which the chemical structure, biosynthetic pathway and mode of action are fully described in other fungal species were downloaded from the NCBI gene bank database (www.ncbi.nlm.nih.gov). These sequences were used to interrogate the Rcc genome using protein BLAST (BLASTp) (Altschul *et al.*, 1990) searching in Rcc protein model database using a protein query to identify putative paralogues in Rcc (Table 2.1). Significant matched hits in Rcc were retained if the BLASTp search with at least one of the fungal proteins used as a query had an e-value lower than $1.e^{-10}$. The FASTA format of the protein sequence of the corresponding Rcc gene models was used for further analysis.

Table 2.1: Fungal proteins used as query sequences for the identification of core genes in *Ramularia collo-cygni*.

Gene name	Accession number	Pathway	Organism	Metabolite	Role
PksA	EME39092.1	PKS	*Dothistroma septosporum*	Dothistromin	Phytotoxin (virulence factor)
PksA	AAS90093.1	PKS	*Aspergillus flavus*	Aflatoxin	Mycotoxin (virulence factor)
PKS4	ABB90283.1	PKS	*Fusarium graminearum*	Zearalenone	Mycotoxin
Pks1	AAB08104.3	PKS	*Bipolaris maydis*	T-toxin	Phytotoxin (virulence factor)
LovF	Q9Y7D5.1	PKS	*Aspergillus terreus*	Lovastatin	Competition agent
CTB1	AAT69682.1	PKS	*Cercospora nicotianae*	Cercosporin	Phytotoxin (virulence factor)
GliP	XP_750855.1	NRPS	*Aspergillus fumigatus*	Gliotoxin	Mycotoxin (virulence factor, competitive agent)
GliP	XP_002380016.1	NRPS	*Aspergillus flavus*	Gliotoxin	Mycotoxin (virulence factor, competitive agent)
SidC	XP_753088.1	NRPS	*Aspergillus fumigatus*	Siderophore	Iron uptake
HTS1	AAA33023.2	NRPS	*Bipolaris zeicola*	HC-toxin	Phytotoxin (pathogenicity factor)

2.2.2.2.Secondary metabolites core gene domain analysis

Domain analysis was carried out on the selected Rcc proteins to verify the presence of domains conserved in PKS and NRPS core genes. Domains were identified using InterproScan (www.ebi.ac.uk) and the PKS/NRPS analysis website (http://nrps.igs.umaryland.edu). Results of the two websites were aggregated and proteins that did not contain at least one of the domains typical to either PKS or NRPS proteins were not investigated further.

2.2.2.3.Localisation of secondary metabolites core genes in the genome

Sequences of Rcc proteins that contained at least one core gene domain were used to perform a tBLASTn (using a protein query to interrogate a DNA database) against the Rcc contig or scaffold containing the corresponding Rcc gene model in order to locate its start and stop codons. Localisation of the core gene was confirmed by translating the Rcc nucleotide sequence from the genomic sequence using ExPASy (Swiss Institute of Bioinformatics, Lausanne, Switzerland) (http://web.expasy.org) and using the translated sequence in a BLASTp analysis against the Rcc protein models to confirm that the correct gene had been identified on the contig/scaffold.

2.2.3. Identification of putative secondary metabolism gene clusters

Putative SMs gene clusters were identified by *in silico* genome walking upstream and downstream along Rcc contigs/scaffolds where each core gene was reported. Identification of open reading frames (ORFs) along each contig/scaffold was done using the Java version of StarOrf (http://star.mit.edu/orf) (Massachusetts Institute of Technology, MA, USA) with a minimal ORF size of 120 bp. Sequences of proteins predicted in the genetic space surrounding each putative core gene were used to perform BLASTp against the NCBI non-redundant (nr) protein database with an e-value cut-off lower than $1.e^{-10}$. The protein sequence of the fungal BLAST hit

with the lowest e-value was downloaded from the NCBI gene bank and used to interrogate the Rcc protein models by BLASTp. The corresponding gene model was located as described in section 2.2.2. The borders of a gene cluster were delineated by a 5 kb region of non-coding DNA or when three consecutive genes with no predicted function associated with SM production were identified.

2.2.4. Detailed investigation of selected secondary metabolite-related gene clusters

Detailed examination of identified SM gene clusters was carried out by assessing the putative function of each gene present in the Rcc clusters. This was done using BLASTp to interrogate each Rcc protein identified at locus against the NCBI nr database. The putative function of each Rcc gene was based on the predicted consensus function determined across all BLAST hits obtained with the Rcc protein. Similarity between Rcc SM gene clusters and clusters found in other fungal species was identified using the Antibiotics & Secondary Metabolite Analysis Shell (antiSMASH) website (http://antismash.secondarymetabolites.org) (Blin *et al.*, 2013). Sequence similarity between fungal proteins identified by antiSMASH and Rcc sequences was confirmed by performing tBLASTn using antiSMASH identified proteins to interrogate the Rcc gene model database. For each match between Rcc and the antiSMASH predicted fungal gene the BLAST hit from the corresponding organism is presented. When the best match in Rcc did not correspond to the antiSMASH predicted organism the best BLAST hit is presented.

2.2.5. Phylogenetic study of secondary metabolites core genes

Protein sequences of known fungal PKSs, NRPSs and HPSs involved in the biosynthesis of characterised SMs used in previous phylogenetic studies (Fisch, 2013; Collemare *et al.*, 2014) as well as sequences from species related to Rcc showing sequence similarity to known SMs core genes were downloaded from the gene bank database (Appendix 1). Full length sequences of PKSs and HPSs were aligned using MAFFT (http://www.ebi.ac.uk) and manually edited in GeneiousR9 to

remove poorly aligned sequences. NRPS proteins were aligned using the same procedure except that only the adenylation domains of these proteins were used in the alignment (Collemare *et al.*, 2014; Chang *et al.*, 2016). Phylogenetic trees were built based on the Randomized A(x)ccelerated Maximum Likelihood (RAxML) model (Stamatakis *et al.*, 2005) using the RAxML (version 7.2.8) plug-in in GeniousR9 with the bootstrapping algorithm and protein model GAMMA BLOSSUM62 (Henikoff & Henikoff, 1992). Consensus trees were built in GeneiousR9 from 100 bootstrap trees with a support threshold of 70%.

2.3. Results

2.3.1. Identification of secondary metabolism core genes in *Ramularia collo-cygni*

2.3.1.1. Identification of putative polyketide synthases and non-ribosomal peptide synthetases

BLASTp analysis using known fungal core genes to interrogate the Rcc genome identified between 20 and 28 putative PKSs and 24 to 39 putative NRPSs depending on the query sequence used. The number of BLASTp hits for each gene is given in Table 2.2 and the list of BLASTp hits for each BLAST enquiry is given in Appendix 2. Gene models with BLASTp hits in both PKSs and NRPSs were set aside as putative HPSs. A final number of 30 putative PKSs, 38 NRPSs and two HPSs was obtained through this *in silico* analysis. A list detailing the Rcc gene models that correspond to the putative PKSs and NRPSs in Rcc is given in Table 2.3 and Table 2.4 respectively.

Table 2.2: Number of BLASTp hits in *Ramularia collo-cygni* for each query fungal polyketide synthase and non-ribosomal peptide synthetase gene.

Gene	Organism	Number of putative paralogues in Rcc
PksA	*D. septosporum*	21
PksA	*A. flavus*	21
PKS4	*F. graminearum*	28
Pks1	*B. maydis*	27
LovF	*A. terreus*	26
CTB1	*C. nicotiniae*	20
GliP	*A. fumigatus*	39
GliP	*A. flavus*	33
SidC	*A. fumigatus*	27
HTS1	*B. zeicola*	24

For clarity in this thesis the following nomenclature will be used to abbreviate the name of each Rcc core gene: type of core gene italicised with only the first letter capitalised (*Pks*, *Hps* or *Nps*) followed by the Rcc contig number where the gene model was located and the gene number (*e.g. Pks17-1.203*, *Hps1-2.140, Npsm40-0.149*). Putative SM clusters will be named after the type of core gene fully capitalised followed by the contig number and a cluster number if several clusters are located on the same contig (e.g. PKS17-1, HPS1 or NRPSm40).

Table 2.3: List of putative *Ramularia collo-cygni* polyketide synthases.

Putative Rcc gene models paralogues to reference PKSs	
augustus_masked-contig_14-processed-gene-0.66-mRNA-1	snap_masked-contig_118-processed-gene-3.158-mRNA-1
augustus_masked-contig_280-processed-gene-0.23-mRNA-1	maker-contig_1-fgenesh-gene-2.140-mRNA-1
fgenesh_masked-contig_30-processed-gene-1.114-mRNA-1	maker-contig_118-augustus-gene-3.254-mRNA-1
genemark-contig_58-processed-gene-0.40-mRNA-1	maker-contig_220-fgenesh-gene-0.9-mRNA-1
maker-contig_17-augustus-gene-1.203-mRNA-1	augustus_masked-contig_5-processed-gene-0.137-mRNA-1
maker-contig_38-fgenesh-gene-0.269-mRNA-1	maker-contig_51-augustus-gene-4.195-mRNA-1
maker-contig_60-snap-gene-2.193-mRNA-1*****	fgenesh_masked-contig_112-processed-gene-1.91-mRNA-1
maker-contig_282-snap-gene-0.161-mRNA-1	maker-contig_137-fgenesh-gene-2.388-mRNA-1
maker-contig_301-snap-gene-0.98-mRNA-1	fgenesh_masked-contig_27-processed-gene-0.105-mRNA-1
snap_masked-contig_187-processed-gene-0.130-mRNA-1*****	augustus_masked-contig_1-processed-gene-3.280-mRNA-1
augustus_masked-contig_233-processed-gene-0.136-mRNA-1	maker-contig_61-snap-gene-2.323-mRNA-1
snap_masked-contig_60-processed-gene-2.105-mRNA-1*****	maker-contig_146-augustus-gene-0.150-mRNA-1
maker-contig_220-fgenesh-gene-0.8-mRNA-1	genemark-contig_17-processed-gene-1.45-mRNA-1
maker-scaffold_m46-fgenesh-gene-0.119-mRNA-1	maker-contig_147-fgenesh-gene-0.136-mRNA-1
augustus_masked-scaffold_m24-processed-gene-1.219-mRNA-1	maker-scaffold_m17-fgenesh-gene-0.247-mRNA-1
maker-contig_187-snap-gene-0.262-mRNA-1*****	maker-contig_330-augustus-gene-0.55-mRNA-1

Putative hybrids PKS/NRPS are highlighted in bold. ***** Annotation errors where one gene was designated as two distinct gene models in the draft genome assembly (McGrann *et al.*, 2016) were identified and corrected in further analysis.

Table 2.4: List of putative *Ramularia collo-cygni* non-ribosomal peptide synthetases.

Putative Rcc gene models paralogues to reference NRPSs	
maker-scaffold_m40-fgenesh-gene-0.149-mRNA-1	snap_masked-contig_100-processed-gene-0.53-mRNA-1*****
snap_masked-contig_245-processed-gene-0.164-mRNA-1	snap_masked-contig_100-processed-gene-0.54-mRNA-1*****
maker-contig_301-fgenesh-gene-0.83-mRNA-1	augustus_masked-scaffold_m29-processed-gene-0.249-mRNA-1
fgenesh_masked-contig_175-processed-gene-0.41-mRNA-1	augustus_masked-contig_20-processed-gene-0.252-mRNA-1
augustus_masked-scaffold_m42-processed-gene-0.88-mRNA-1	augustus_masked-contig_207-processed-gene-0.46-mRNA-1
fgenesh_masked-contig_301-processed-gene-0.34-mRNA-1	fgenesh_masked-contig_113-processed-gene-2.65-mRNA-1
maker-contig_246-snap-gene-0.414-mRNA-1	fgenesh_masked-contig_84-processed-gene-2.87-mRNA-1
maker-contig_58-snap-gene-0.220-mRNA-1	fgenesh_masked-contig_37-processed-gene-10.84-mRNA-1
augustus_masked-contig_113-processed-gene-0.134-mRNA-1	maker-contig_30-snap-gene-0.203-mRNA-1
fgenesh_masked-contig_280-processed-gene-0.11-mRNA-1	maker-contig_151-fgenesh-gene-1.190-mRNA-1
augustus_masked-contig_245-processed-gene-0.245-mRNA-1	maker-scaffold_m42-fgenesh-gene-5.203-mRNA-1
fgenesh_masked-contig_246-processed-gene-0.103-mRNA-1	maker-scaffold_m42-fgenesh-gene-0.99-mRNA-1
genemark-contig_55-processed-gene-3.77-mRNA-1	maker-contig_187-fgenesh-gene-0.193-mRNA-1
snap_masked-contig_100-processed-gene-0.55-mRNA-1*****	genemark-contig_117-processed-gene-0.13-mRNA-1
augustus_masked-contig_51-processed-gene-1.140-mRNA-1	maker-contig_150-fgenesh-gene-0.150-mRNA-1
maker-contig_134-snap-gene-0.394-mRNA-1	maker-contig_13-fgenesh-gene-0.366-mRNA-1
augustus_masked-contig_166-processed-gene-1.135-mRNA-1	fgenesh_masked-contig_246-processed-gene-0.159-mRNA-1
augustus_masked-contig_163-processed-gene-0.152-mRNA-1	maker-scaffold_m17-fgenesh-gene-0.238-mRNA-1
genemark-contig_207-processed-gene-0.9-mRNA-1	**augustus_masked-contig_14-processed-gene-0.66-mRNA-1**
maker-scaffold_m42-snap-gene-0.127-mRNA-1	**maker-contig_38-fgenesh-gene-0.269-mRNA-1**

Putative hybrids PKS/NRPS are highlighted in bold. ***** Annotation errors where one gene was designated as two distinct gene models in the draft genome assembly (McGrann *et al.*, 2016) were identified and corrected in further analysis.

2.3.1.2.Identification of putative functional core genes

From the Rcc 30 gene models with BLASTp hits to PKSs, 19 contained at least one typical PKS domain. Furthermore, one gene model encoding for a protein exhibiting a typical NRPS module fused to a HR-PKS was reclassified as HPS after domain analysis. Of the 18 putative PKSs identified in Rcc, ten were predicted to be functional as they possessed the three essential PKSs domains, KS, AT and ACP (Figure 2.6). Three PKSs, *Pks118-3.254*, *Pksm46-0.119* and *Pksm24-1.219*, exhibited the organisation of NR-PKSs and could potentially be involved in the biosynthesis of aromatic compounds. However, the *Pks118-3.254* differed from the typical NR-PKS domain organisation (SAT-KS-AT-PT-ACP-(TE)) as this PKS does not possess a PT domain but rather has a MT domain after the ACP domain giving the atypical organisation SAT-KS-AT-ACP-MT-TE. Atypical domain organisations have been reported in other fungi such as the citrinin synthase in the non-pathogenic Eurotiomycete *Monascus purpureus* whose domain organisation is similar to that of *Pks118-3.254* (Shimizu *et al.*, 2005). Two of the NR-PKSs, *Pks118-3.254* and *Pksm46-0.119*, contained a C-terminal TE domain potentially involved in the release of the newly synthesised polyketide from the PKS (Du & Lou, 2010). The absence of the TE domain in *Pksm24-1.219* suggests another release mechanism may be operating in this PKS. A similar domain organisation has been reported in other PKSs such as *EncA* in *Aspergillus fumigatus* responsible for endocrocin biosynthesis where a β-lactamase is coupled to and acting *in trans* with the PKS to release the polyketide (Lim *et al.*, 2012).

Seven Rcc PKSs showed the domain organisation typical of highly- and partially-reducing PKS proteins (KS-AT-DH-(MT)-(ER)-KR-ACP). Two of these PKSs, *Pks17-1.203* and *Pks282-0.161*, lacked the MT domain whereas *Pks30-1.114* lacked the ER domain. Four PKSs, *Pks280-0.23*, *Pks58-0.40*, *Pks233-0.136* and *Pks60-2.105+2.193* hereafter called *Pks60* presented all four β-keto processing domains. From the HR/PR-PKSs, only *Pks30-1.114* possessed a reductase domain specialised in polyketide release. The polyketides synthesised by the other HR- and PR-PKSs are likely to be released via other mechanisms. Domain organisation of HR- and PR-PKSs suggests that Rcc has the potential to produce several polyketides

exhibiting different degrees of reduction. Similar observations were made in *Fusarium* species, for instance *F. graminearum* (syn. *Gibberella zeae*) which is able to produce fully reduced polyketides, such as fumonisins, as well as partially reduced polyketides, such as aurofusarin (Hansen *et al.*, 2012).

Of the 38 Rcc gene models showing BLASTp hits to NRPSs only 21 contained at least one domain typical of NRPSs (Figure 2.7). Functional NRPSs have been predicted to have an initiation module A-PCP at the N-terminus and at the C-terminus either a condensation domain or a TE domain involved in peptide release (Finking & Marahiel, 2004; Du & Lou, 2010). In the Rcc genome, only ten NRPSs have all three of these domains. However, assessing the functionality of NRPSs based on domain analysis can be difficult. Unlike PKSs, the domain organisation of some NRPSs, and in particular type C NRPSs, may vary greatly without affecting the functionality of the gene. Out of the ten NRPSs exhibiting both an initiation module and terminal C or TE domain, three were mono-modular (*Nps245-0.245*, *Npsm29-0.249* and *Npsm40-0.149*), two bi-modular (*Npsm42-0.88* and *Nps301-0.34*) and five were multi-modular (*Nps246-0.103, Nps51-1.140*, *Nps134-0.394*, *Nps55-3.77* and *Nps100-0.53+0.54+0.55* hereafter called *Nps100*). *Nps245-0.164*, *Nps207-0.46* and *Nps301-0.83* all contained a stand-alone A domains which could be involved in the organisation of a type C NRPS as described in section 2.1.2.2. However, because the domain organisation of such NRPSs differs from that of typical successive C-A-PCP modules, based solely on domain analysis the accurate identification of type C NRPSs is difficult and therefore the stand-alone domains will not be discussed further.

Three HPSs were identified in the genome of Rcc, *Hps1-2.140*, *Hps14-0.66* and *Hps38-0.269*. Their domain organisation is typical from fungal HPSs with the reducing PKS domains KS-AT-DH-MT-KR-ACP at the N-terminus followed by a single NRPS module C-A-PCP (Figure 2.8). None of the identified HPS contained an ER domain which differs from other fungal HPSs. However, the ER domain in fungal HPSs identified to date appear to be non-functional (Fisch, 2013). This difference could arise from the fact that the method used in this study to identify domain is based on the recognition of important sites for domain functionality. Considering that most fungal ER domains in HPSs were found to be non-functional

because they lacked a GGVG motif required for NADPH binding (Fisch, 2013) it is likely that non-functional ER domains in Rcc HPSs would not have been identified. Only one HPS, *Hps1-2.140*, contained a reductase domain involved in product release suggesting that the release of the two other HPS products occurs by another mechanism. However, both *Hps14-0.66* and *Hps38-0.269* exhibited a nicotinamide adenine dinucleotide (NADH)-binding motif containing C-terminal sequence resembling that of extended short chain dehydrogenase (eSDR). eSDR have only been found in multidomain enzymes such as PKSs, NRPSs or fatty acid synthases and exhibit diverse nature such as, dehydratases, epimerases, or oxidoreductases (Kallberg *et al.*, 2002).

The identification of putative PKSs, NRPSs and HPSs in the Rcc genome demonstrated that this fungus possesses several core genes potentially involved in secondary metabolism. Whether these core genes are located in putative SM-related gene clusters in the Rcc genome may provide further insights into the potential functions of SMs in this organism and highlight how SMs relates to the biology of Rcc.

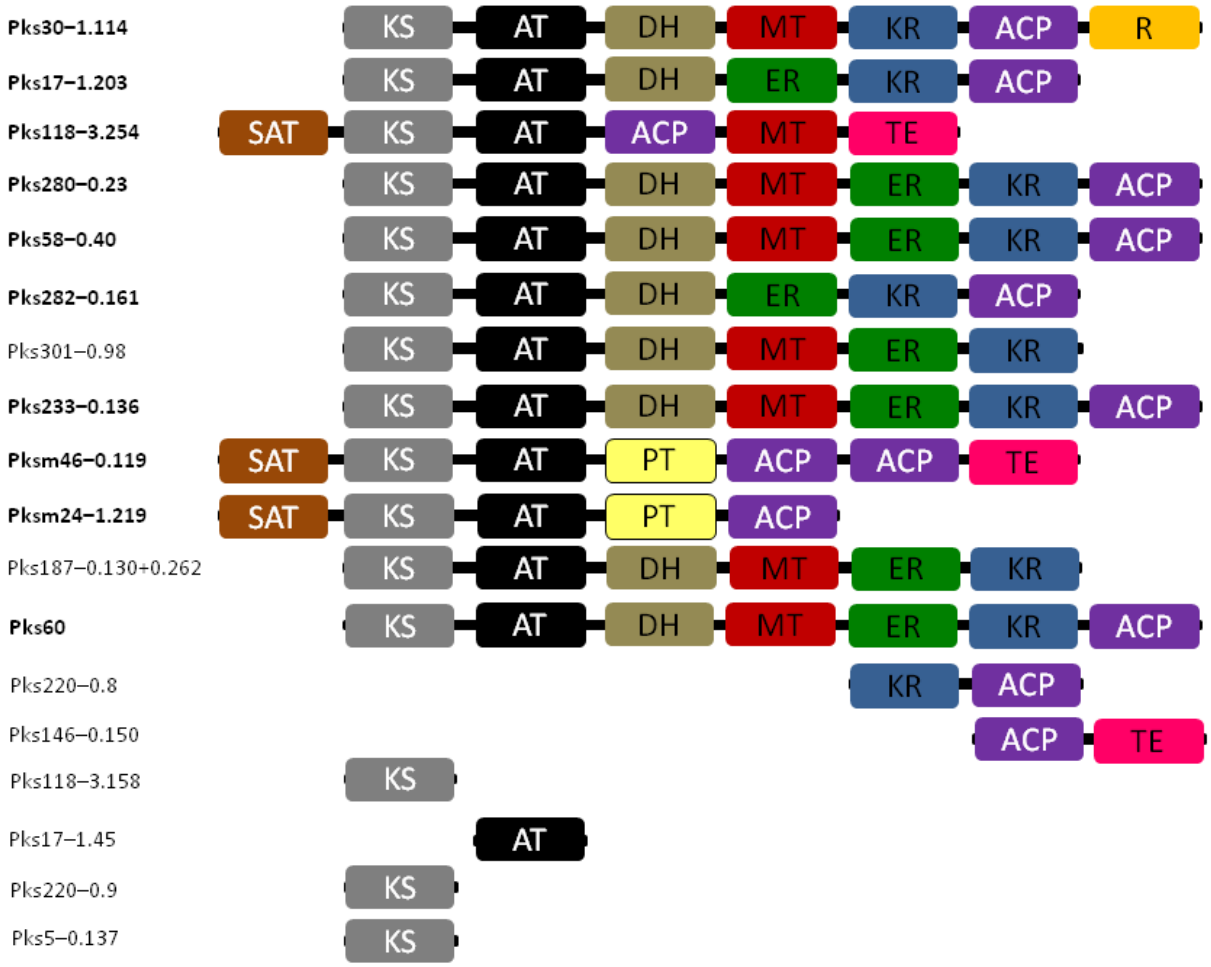

Figure 2.6: Domain organisation of predicted polyketide synthases (PKSs) in *Ramularia collo-cygni*.
Putative functional PKSs are highlighted in bold. From the N-terminus to the C-terminus domain modules are: SAT (starter unit: acyl carrier protein transacylase), KS (keto-synthase), AT (acyl transferase), PT (product template), DH (dehydratase), MT (methyltransferase), ER (enoyl reductase), KR (keto-reductase), ACP (acyl carrier protein), TE (thiolesterase), R (reductase).

Figure 2.7: Domain organisation of predicted non-ribosomal peptide synthetases (NRPSs) in *Ramularia collo-cygni*. Putative functional type A and B NRPS genes are highlighted in bold. Typical NRPS domains are labelled; A (adenylation), C (condensation), PCP (peptidyl carrier protein) and TE (thiolesterase).

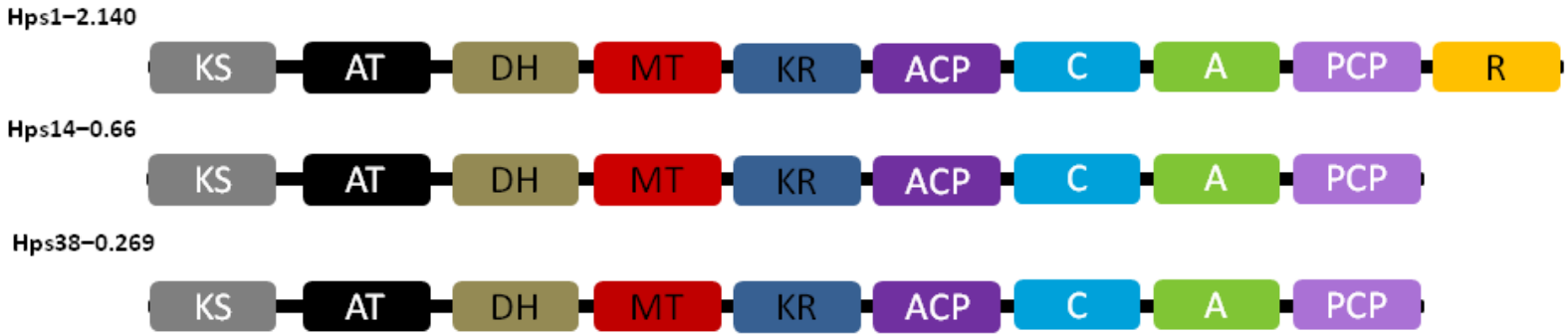

Figure 2.8: Domain organisation of hybrids PKS/NRPS (HPSs) in *Ramularia collo-cygni*.
The reducing PKS domains keto-synthase (KS), acyl transferase (AT), dehydratase (DH), methyltransferase (MT), keto-reductase (KR) and acyl carrier protein (ACP) are followed by a single NRPS module made of condensation (C), Adenylation (A) and peptidyl carrier protein (PCP) domains. When present, a reductase (R) domain is thought to be involved in product release.

2.3.2. Identification of putative secondary metabolism gene clusters

Putative SM gene clusters are genetic loci encoding a number of genes with known SM-related predicted functions such as reductases, cytochrome P450 monooxygenases, transporters and dehydrogenases. Identification of putative SM gene clusters in Rcc was carried out for all the core genes described in section 2.3.1.1, whether they were predicted to be functional or not. This was done to broaden the search for SM gene clusters, as a core gene predicted to be non-functional maybe due to a sequencing error or a naturally occurring mutation, might still be part of an SM cluster.

Eight clusters containing putative SM-related genes were identified for the PKSs described in section 2.3.1.1 (Figure 2.9). All eight clusters were located in the vicinity of putative functional PKSs. Two putative functional PKSs, *Pks233-0.136* and *Pksm46-0.119*, and all non-functional PKSs did not appear to be part of SM clusters (Figure 2.10). However, as both *Pks233-0.136* and *Pksm46-0.119* are located at an end of their respective contig/scaffold there is a possibility that SM-related genes are present near these core genes but these regions were not assembled at these loci in the draft genome assembly. The largest cluster, located on contig 58, was spread over 45.2 kb and contained 16 putative SM-related genes and two hypothetical genes which are genes currently without evidence of *in vivo* expression based on RNAseq data (McGrann *et al.*, 2016). The shortest cluster spanned 17 kb on contig 282 and contained five SM-related ORFs including the core gene. Out of the eight putative SM clusters located around PKSs, half appeared to have more than one predicted core gene present within the cluster. The cluster on contig 118 contained two ORFs with predicted PKSs domains, *Pks118-3.254* and *Pks118-3.158*, while two other clusters, PKS280 and PKS58, contained both predicted PKSs and NRPSs. A third type of core gene present alongside a PKS in the cluster on contig 282 was identified as one of the four Rcc terpene cyclases previously identified in the Rcc genome (McGrann *et al.*, 2016). The presence of several different types of core gene in a single cluster suggests a potentially high degree of chemical complexity of the resulting compound, if it is indeed produced. For instance, the chemical structure of several meroterpenoids which are hybrids polyketide-terpenes, exhibited a highly

oxygenated structure with halogenic compounds found alongside lactone rings and epoxide within the same molecule (Kaysser *et al.*, 2012; Li *et al.*, 2016). Five of the eight clusters, PKS30, PKS280, PKS58, PKSm24 and PKS60, possessed at least one ORF with a predicted function associated with cellular transport from either the major facilitator superfamily (MFS) or ATP-binding cassette family (ABC). This could indicate that the SM, if produced, might be either secreted or moved within fungal hyphae to be stored in vesicles. Analysis of the published Rcc secretome (McGrann *et al.*, 2016) showed that the protein encoded by *Pks118-3.254* was predicted to be secreted. Another potential role for transporters involves self-protection from the potential SM. It was shown that a *Leptosphaeria maculans* (syn. *Phoma lingam*) mutant lacking a functional *SirA* gene that encodes an ABC transporter was more sensitive to its own sirodesmin than the wild-type (Gardiner *et al.*, 2005a). Two clusters, PKSm24 and PKS118, contained predicted transcription factors such as $Zn(II)_2Cys_6$ DNA binding domains (also known as GAL4 domains) suggesting local transcriptional regulation of the cluster.

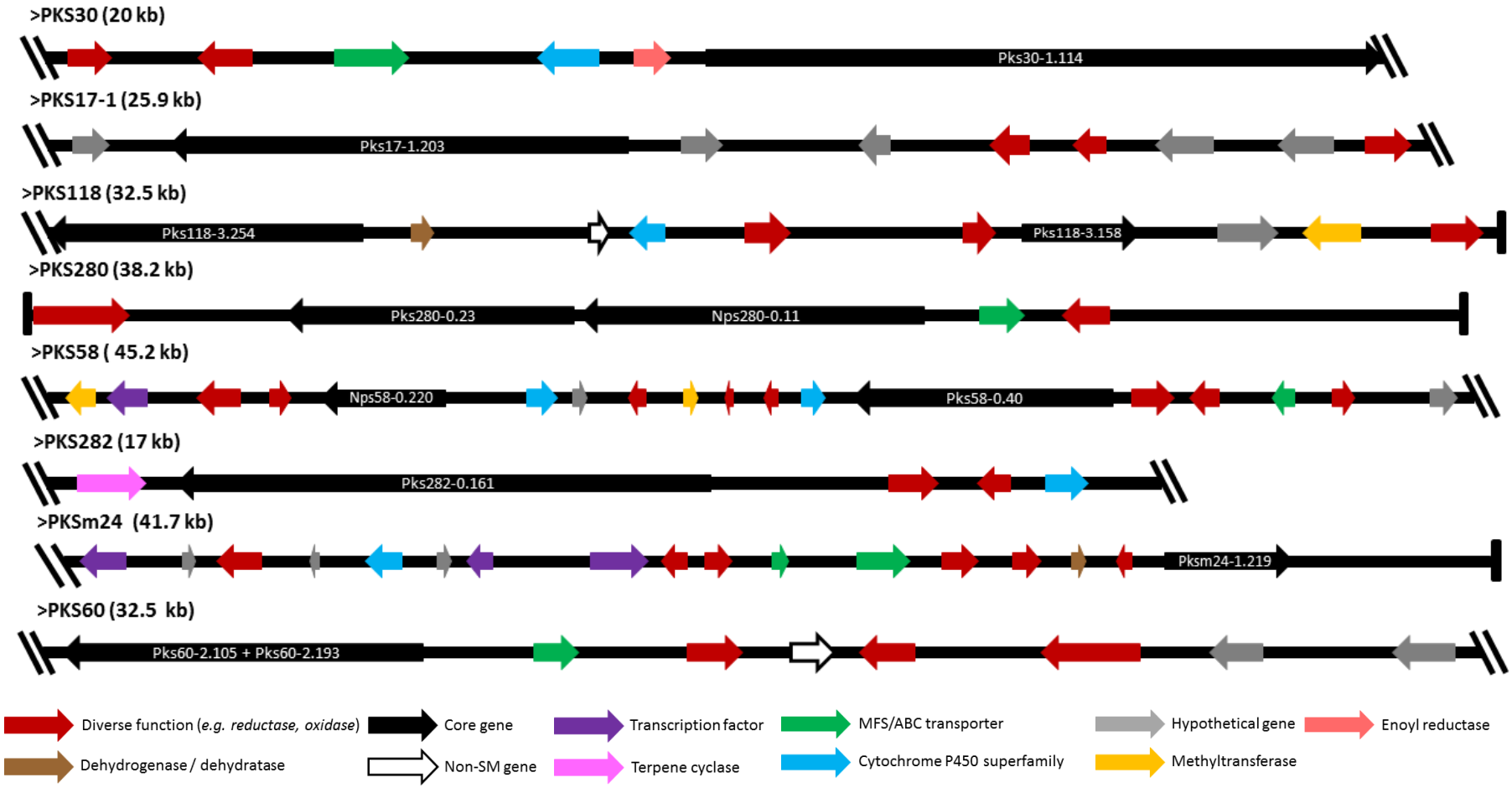

Figure 2.9: Organisation of putative secondary metabolism clusters surrounding polyketide synthase (PKS) core genes in *Ramularia collo-cygni*.
Arrow heads indicate ORFs predicted transcription direction. The end of a cluster is marked by a double oblique bars and the end of a contig/scaffold is marked by a single vertical bar. Cluster size is indicated in brackets after the clusters name. Each individual cluster is drawn to scale.

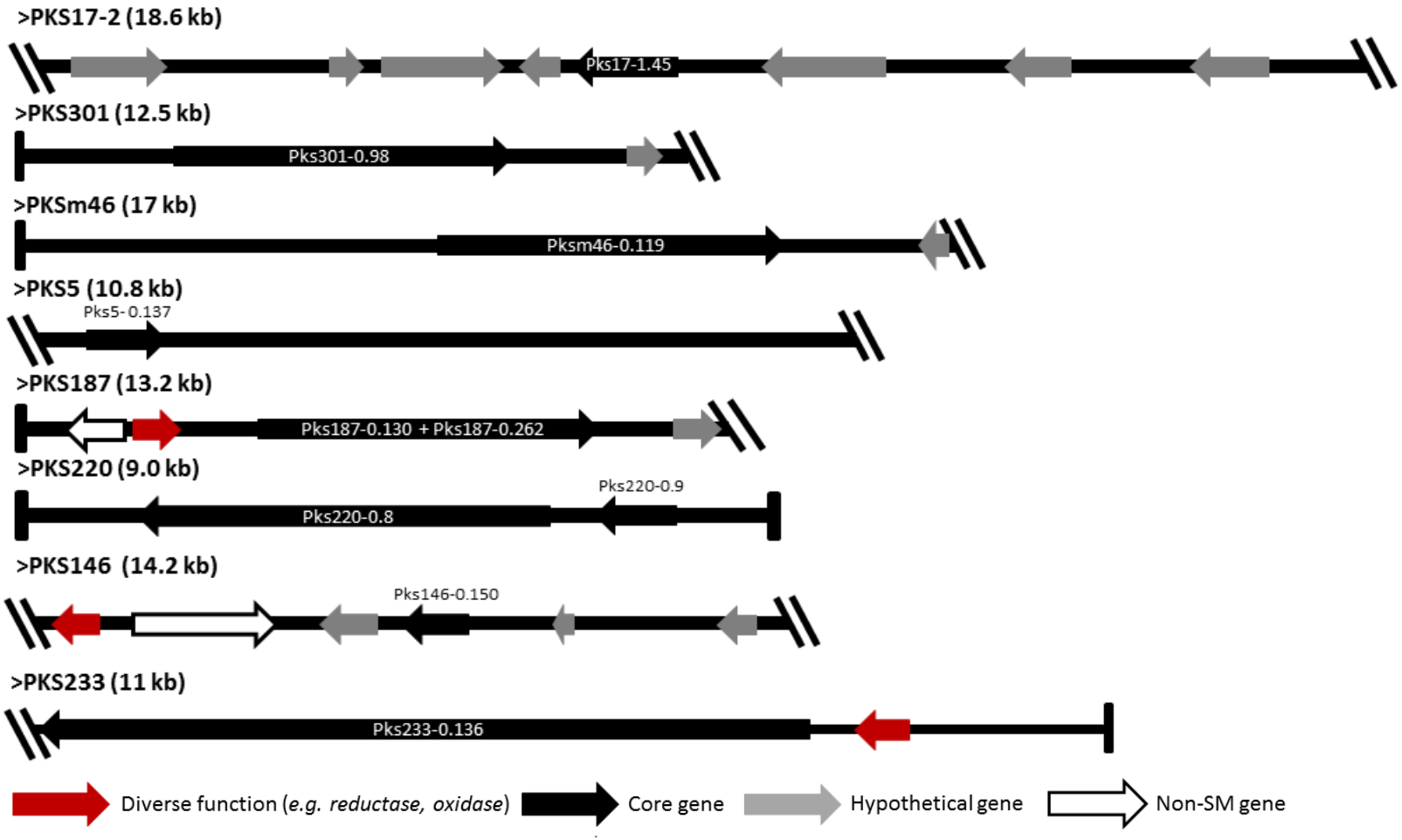

Figure 2.10: Organisation of open reading frames at genetic loci that contains a polyketide synthase (PKS) which are not enriched in secondary metabolites genes.
Arrow heads indicate ORFs predicted transcription direction. The end of a cluster is marked by a double oblique bars and the end of a contig/scaffold is marked by a single vertical bar. Each individual cluster is drawn to scale.

All three HPSs were found to be part of a putative SM cluster (Figure 2.11). The largest cluster (HPS1) spanned over 43.4 kb and comprised twelve ORFs including two hypothetical proteins and two proteins with a predicted function not related to secondary metabolism. Within this cluster one gene encoding for an ABC multidrug transporter and two transcription factors were identified. Cluster HPS14 contained nine genes over 32.2 kb. All nine proteins on HSP14 had predicted functions related to secondary metabolism. Two transcription factors and one transporter were predicted to be among the genes identified on HPS14. The HPS38 cluster was found to span over 34.5 kb and contained eight ORFs, of which three encoded hypothetical proteins.

Twenty of the putative NRPS genes identified in the genome of Rcc appeared to be located in an SM-related gene-enriched regions of DNA (Figure 2.12). The average size for SM clusters organised around NRPSs was 33.8 kb with a maximum of 59.8 kb for a cluster containing 26 genes on contig 246 (NRPS246-2). A total of 17 SM-related clusters containing NRPSs were identified amongst which five contained more than one core gene. Two of these clusters contained one PKS and one NRPS, PKS58 and PKS280, have already been described in this section. The three remaining clusters NRPS301, NRPS207 and NRPS245, were each found to contain two NRPSs. In all three cases one of the two NRPS is a stand alone A domain while the other NRPS exhibit a more typical domain organisation. Although more than half of the NRPS clusters identified contained at least one ORF encoding for a transporter, only *Npsm29-0.249* was present in the predicted secretome of Rcc (McGrann *et al.*, 2016), suggesting that the other NRPSs may not be secreted and NRP synthesis may occur in the fungal hyphae prior to an eventual secretion of the product. Out of the 17 NRPS clusters, eight contained putative transcription factors potentially involved in cluster specific regulation. *Nps113-0.134* and *Npsm42-0.88* were not located in putative SM-clusters.

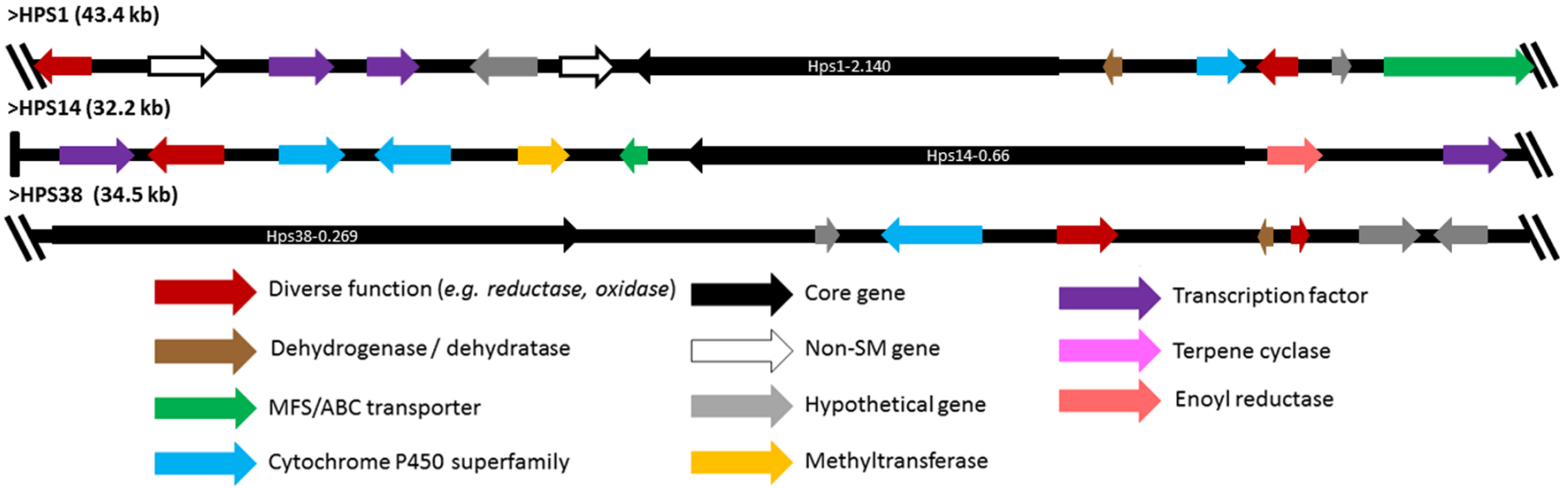

Figure 2.11: Organisation of putative secondary metabolism clusters surrounding hybrid polyketide synthase/ non-ribosomal peptide synthetase (HPS) core genes in *Ramularia collo-cygni*.
Arrow heads indicate ORFs predicted transcription direction. The end of a cluster is marked by double oblique bars and the end of a contig/scaffold is marked by a single vertical bar. Each individual cluster is drawn to scale.

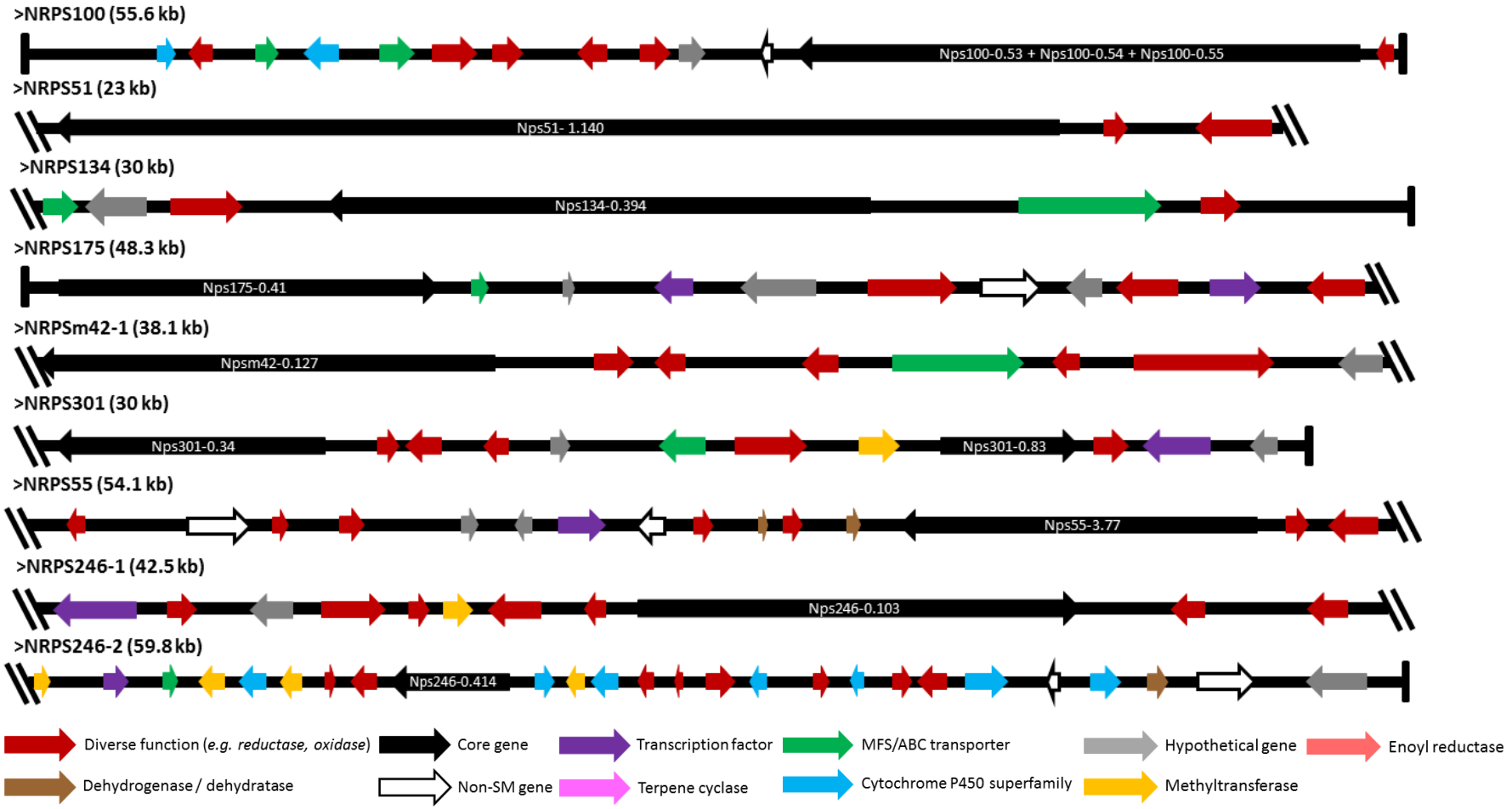

Figure 2.12: Organisation of putative secondary metabolism clusters surrounding non-ribosomal peptide synthetase (NRPS) core genes in *Ramularia collo-cygni*.
Arrow heads indicate ORFs predicted transcription direction. The end of a cluster is marked by double oblique bars and the end of a contig/scaffold is marked by a single vertical bar. Each individual cluster is drawn to scale.

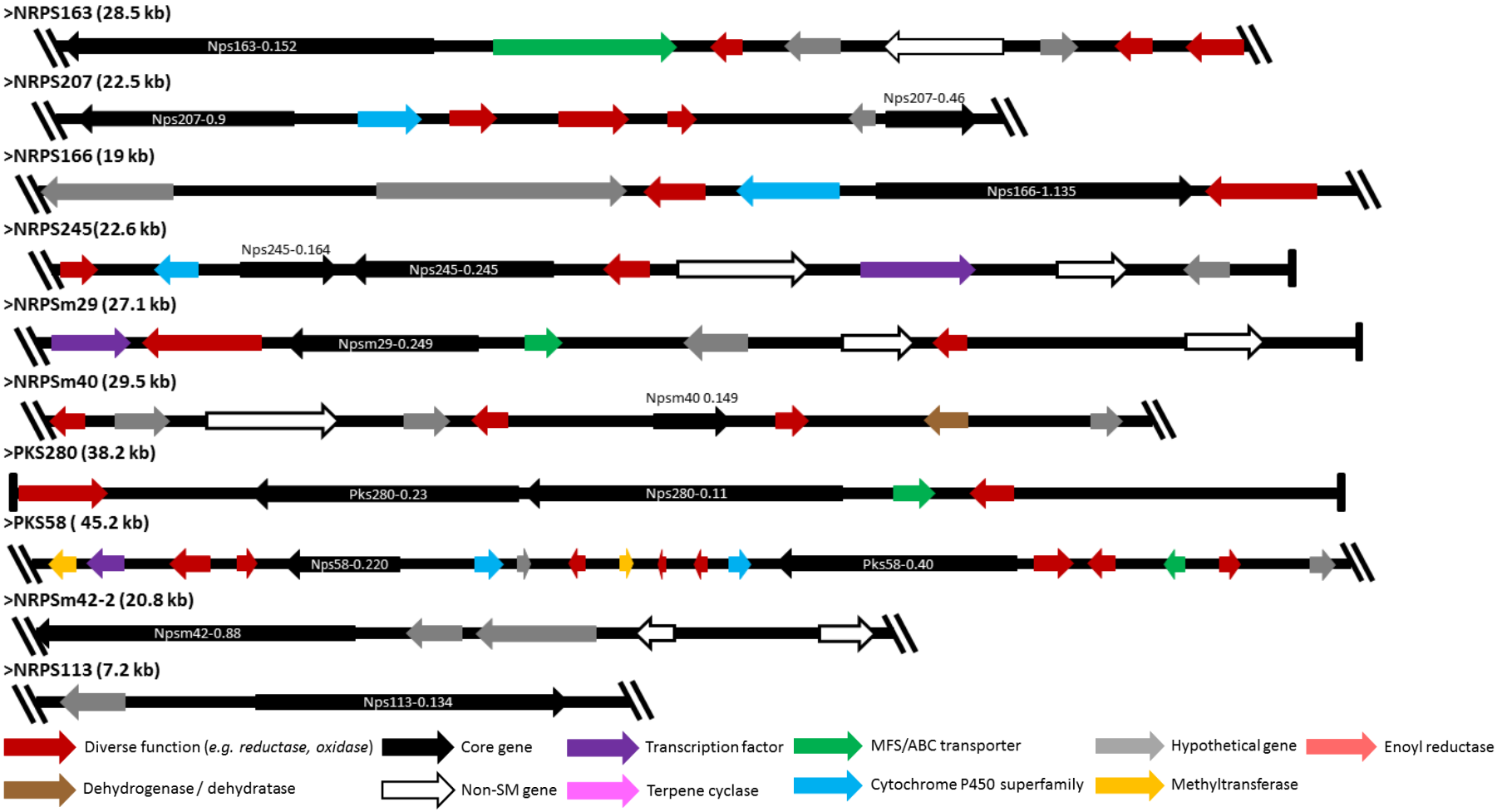

Figure 2.12 (continued): Organisation of putative secondary metabolism clusters surrounding non-ribosomal peptide synthetase (NRPS) core genes in *Ramularia collo-cygni.*

Arrow heads indicate ORFs predicted transcription direction. The end of a cluster is marked by double oblique bars and the end of a contig/scaffold is marked by a single vertical bar. Each individual cluster is drawn to scale.

The identification of putative SM clusters in Rcc revealed that this fungus has the genetic potential to produce a wide range of polyketide and non-ribosomal peptide-derived SMs. A more in depth study of Rcc core genes and clusters might help characterise some SMs potentially produced by Rcc.

2.3.3. Characterisation of putative secondary metabolites clusters

2.3.3.1.Phylogenetic study

A phylogenetic study was carried out for the proteins encoded by the core genes present in Rcc to characterise the relationship between Rcc genes and those core genes from other fungi with known SM products. Phylogenetic relationships between core genes and those present in fungi with known SM products may provide insights into the chemical family of the backbone of the putative resulting SM. Only putatively functional PKS and HPS proteins were used in the phylogenetic study. Due to the difficulty of assessing NRPSs functionality based on domain analysis, all putative NRPSs identified in Rcc have been used for the following study.

Pks118-3.254, *Pksm46-0.119* and *Pksm24-1.219* grouped within the NR-PKSs, while all other Rcc PKSs grouped with HR-PKSs (Figure 2.13) supporting the domain analysis predictions. *Pks118-3.254* was closely related to the *Penicillium brevicompactum* mycophenolic acid (MPA) synthase gene *MpaC*. However, the domain organisation of the enzyme encoded by *MpaC* (SAT-KS-AT-PT-ACP-MT-TE) appears to be different from that of the protein encoded by *Pks118-3.254* and the organisation of the MPA cluster differs from that of PKS118, suggesting that Rcc is unlikely to produce MPA but may synthesise a methylated aromatic compound. The PT domain, often found after the AT domain in NR-PKSs, is thought to have derived from a DH domain in PR-PKSs (Crawford & Townsend, 2010). The 3D structure of PT domains from NR-PKSs was shown to be similar to that of DH domains from reducing PKSs and fatty acid synthases (Crawford *et al.*, 2009). This is supported by the relationship between MpaC and the asperfuranone synthase AN1034 in *Aspergillus nidulans* whose domain organisation is SAT-KS-AT-DH-ACP-MT-TE. Furthermore, these proteins were found to be the closest relatives to the PR-PKSs.

Pksm24-1.219 was positioned within a clade that comprised the proteins encoded by the *Acas*, *MdpG*, *EncA* and *ClaG* genes found respectively in *Aspergillus terreus*, *A. nidulans*, *A. fumigatus* and *Cladosporium fulvum* (syn. *Passalora fulva*). All of these PKSs have the same domain organisation SAT-KS-AT-PT-ACP. They have been shown to be involved in the production of the anthraquinones atrochrysone carboxylic acid, monodictyphenone and emodin, endocrocin and cladofulvin respectively (Awakawa *et al.*, 2009; Chiang *et al.*, 2010; Lim *et al.*, 2012; Griffiths *et al.*, 2016). Remarkably, none of these genes encode proteins that possess a domain involved in polyketide release, but they have all been found to be coupled to a β-lactamase thought to act as release mechanism (Du & Lou, 2010; Li *et al.*, 2011). In Rcc, *Pksm24-1.219* was also found to be coupled to a β-lactamase.

The third NR-PKS in Rcc, encoded by *Pksm46-0.119*, appeared to be closely related to an unknown PKS in *Zymoseptoria tritici* (syn. *Mycosphaerella graminicola*), the sister species of Rcc (McGrann *et al.*, 2016). In this clade, an unknown PKS from *Pseudocercospora fijiensis* (syn. *Mycosphaerella fijiensis*) is also found as well as the elsinochrome and phleichrome synthases encoded by *Pks1* and *CpPks1* in the Dothideomycetes *Elsinoë fawcettii* and *Cladosporium phlei*. Elsinochromes and phleichromes are red-coloured perylenequinones exhibiting light-dependant phytotoxic activities (Liao & Chung, 2008b; So *et al.*, 2015) which is reminiscent of the properties reported for the rubellins produced by Rcc (Heiser *et al.*, 2003). These results are supported by previous observations reporting that light intensity increased disease severity caused by *Z. tritici*, *P. fijiensis* and Rcc (Keon *et al.*, 2007; Makepeace *et al.*, 2008; Brown & Makepeace, 2009; Cruz-Cruz *et al.*, 2011; Peraldi *et al.*, 2014). Furthermore, the domain organisation of *Pksm46-0.119* is consistent with that of other known PKSs involved in phytotoxin production such as cercosporin or dothistromin with SAT-KS-AT-PT-$(ACP)_n$-TE (n=2 in the cercosporin synthase *CTB1* as well as in *Pksm46-0.119* whereas n=3 in *PksA* in dothistromin biosynthesis).

For the HR-PKSs, one Rcc PKS was found to be very different from the others. *Pks30-1.114* was found at the base of the tree along with a PKS of unknown function in *Z. tritici*. *Pks280-0.23* was related to *Bipolaris maydis* (syn. *Cochliobolus*

heterostrophus) *Pks2*. *Pks2* is only present in race T of *B. maydis* and is involved in the production of the host-specific fully reduced T-toxin. *B. maydis Pks2* functions alongside *Pks1*, to produce T-toxin (Baker *et al.*, 2006). This second *B. maydis* PKS, did not appear to be related to any Rcc PKS. Therefore, it is unlikely that Rcc produces T-toxin or if it does this would occur through a different biochemical process than reported in *B. maydis*. The PKS on contig 233 encoded by *Pks233-0.136* appeared to be closely related to the protein encoded by the *Fum1* gene involved in fumonisin biosynthesis in *Fusarium oxysporum* (Desjardins & Proctor, 2007). Taken together these results suggest that the putative compounds produced by *Pks233-0.136* and *Pks280-0.23* might have a fully reduced aliphatic backbone. *Pks58-0.40* was found to be related to a PKS yielding an unknown SM from *Zymoseptoria brevis*. Both PKSs were part of a subclade containing the lovastatin synthase *LovF* of *Scedosporium apiospermum* (syn. *Pseudallescheria boydii*). This subclade was grouped within a larger clade that contained proteins encoded by genes involved in statin related compound biosynthesis such as *MlcB*, *LDKS* and *Mkb* responsible for mevastatin, lovastatin and monacolin biosynthesis respectively in *Penicillium expansum*, *Aspergillus terreus* and *Monascus purpureus*. *Pks282-0.161* appeared related to a PKS yielding an unknown SM in the Dothideomycete *Macrophomina phaseolina*. These two PKSs were found in a clade that contained the proteins encoded by *Dep5* and *Pks9* involved in depudecin and botcinic acid biosynthesis respectively in *Alternaria brassicicola* and *Botrytis cinerea* (syn. *Botryotinia fuckeliana*) (Wight *et al.*, 2009; Dalmais *et al.*, 2011). Both depudecin and botcinic acid are cyclic ethers. Depudecin exhibits two oxirane rings (formula $(CH_2)_2O$) and botcinic acid present a tetrahydrofuran ring (formula $(CH_2)_4O$). This suggests that the compound produced by *Pks282-0.161* might have a cyclic ether backbone. The PKS located on contig 60 appeared to be related to a PKS yielding an unknown SM from *Aspergillus nominus*. Similarly, *Pks17-1.203* was found to be related to two PKSs involved in an unknown biochemical pathway in the Dothideomycete *Setosphaeria turcica* (syn. *Helminthosporium turcicum*) and the Sordariomycete *Podospora anserina*. *S. turcica* is the agent responsible for northern leaf blight in corn for which symptoms have been linked with the action of the polyketide-derived phytotoxin monocerin (Cuq *et al.*, 1993; Axford *et al.*, 2004).

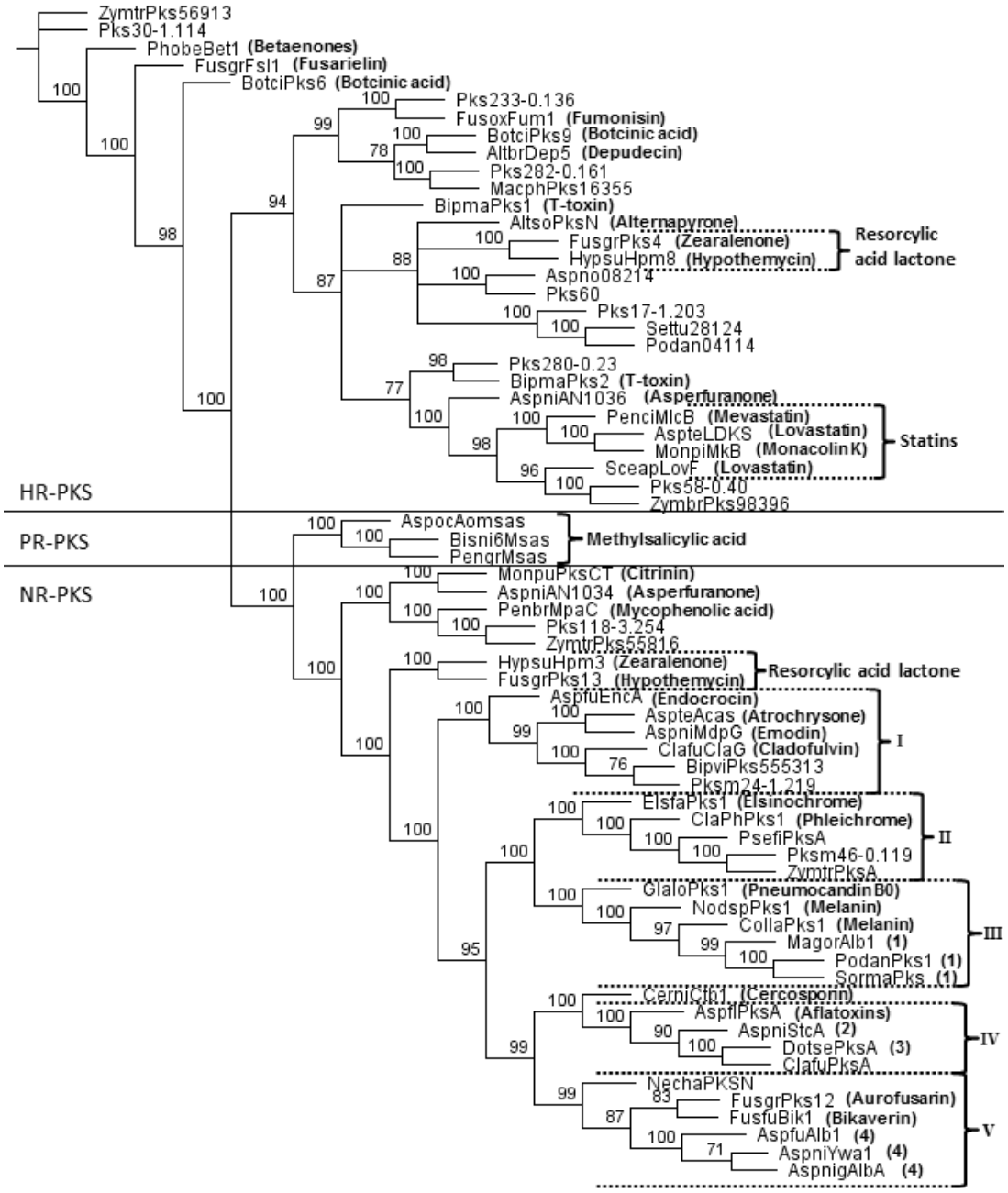

Figure 2.13: Phylogenetic analysis of polyketide synthases in *Ramularia collo-cygni*. The tree was built on full length PKS protein sequences using maximum likelihood with 100 replications. A supporting bootstrap cut-off value of 70% was chosen. Highly-reducing PKSs (HR-PKS) are clustering near the base of the tree. Partially-reducing PKSs (PR-PKS) are located in the centre and the non-reducing PKSs (NR-PKS) are shown at the top of the tree. Species names and accession numbers of the protein used in this analysis are given in Appendix 1. Known secondary metabolites are shown in brackets. (1): melanin, (2): sterigmatocystin, (3): dothistromin, (4): naphtopyrone. Chemical family for the corresponding SM is also indicated I: anthraquinone (tri- and tetra-hydroxyanthraquinone), II: elsinochrome derivative, III: naphthalene (tetra- and di-hydroxynaphtalene), IV: anthraquinone derivative, V: pigments (naphtoquinone, naphtopyrone).

Phylogenetic analysis of the three HPSs identified in Rcc (Figure 2.14) showed that *Hps38-0.269* was closely related to an unknown HPS found to be part of an uncharacterised SM cluster located on chromosome V of *Podospora anserina* (described in section 2.3.3.2). Therefore no prediction can be made regarding the chemical nature of the backbone of the putative SM produced by *Hps38-0.269*.

Hps14-0.66 was found to be part of a clade that comprised the hybrid PKS/NRPS involved in chaetoglobosin synthesis encoded by *CheA* in *Penicillium expansum* (Andersen *et al.*, 2004). Chaetoglobosins are part of the cytochalasans which are alkaloids containing a isoindoline backbone (heterocyclic compound with formula C_8H_9N) fused to a macrocyclic ring (Scherlach *et al.*, 2010). HPSs involved in cytochalasan synthesis utilise a specific range of amino acids. Chaetoglobosins are synthesised from tryptophan, cytochalasins from phenylalanine, alachalasins from alanine, scoparasins from tyrosine and aspochalasins from leucine (Scherlach *et al.*, 2010). AntiSMASH analysis, based on NRPSpredictor2 (Röttig *et al.*, 2011), using Stachelhaus and Minowa algorithms for NRP prediction (Stachelhaus *et al.*, 1999; Minowa *et al.*, 2007) showed that *Hps14-0.66* A-domain is likely to incorporate leucine, tryptophan or alanine respectively (Appendix 3). These results imply that the product of *Hps14-0.66* could be a cytochalasan, potentially belonging to the chaetoglobosin, aspochalasin or alachalasin family. However, in contrast to the protein encoded by *CheA*, the HPS in Rcc did not contain a reductase domain suggesting that the release of the compound if it occurs might be achieved through a different mechanism.

Hps1-2.140 was found to belong to a clade containing proteins encoded by genes involved in the production of the alkaloid cyclopiazonic acid (*CpaA*) in both *Aspergillus flavus* and *Aspergillus oryzae* as well as pyridone derived and cytochalasan SM. All three types of SMs exhibit a heterocyclic structure (carbon, hydrogen and nitrogen) suggesting that the compound produced by *Hps1-2.140* might also be heterocyclic.

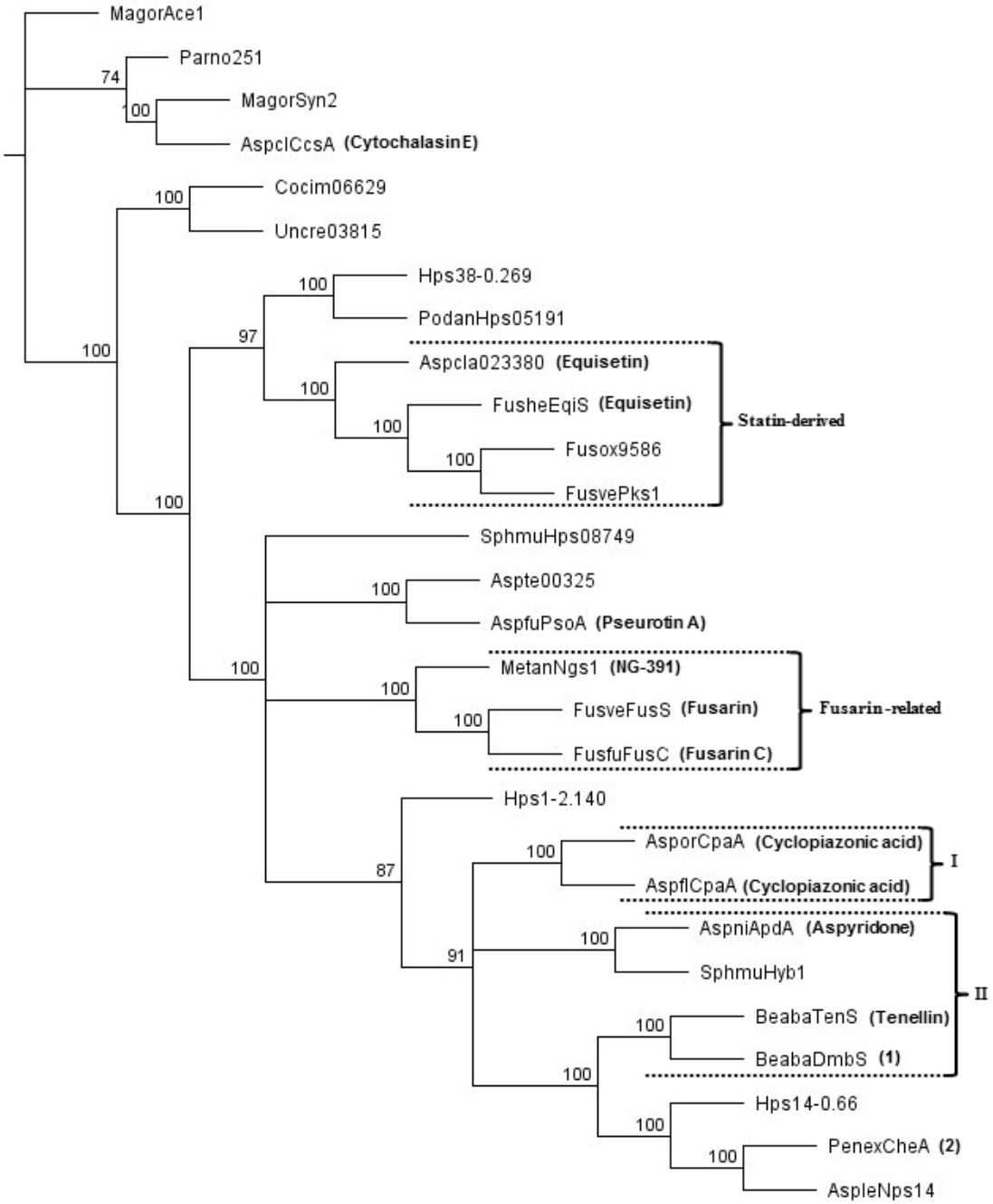

Figure 2.14: Phylogenetic analysis of hybrids polyketide synthase/non-ribosomal peptide synthetase in *Ramularia collo-cygni*.
The full sequences of HPSs were used to build maximum likelihood tree with bootstrap cut-off value set at 70%. Sequences were aligned using MAFFT and poorly aligned sequences were removed from the analysis. Species name and accession number of the protein used in this analysis is given in Appendix 1. Known secondary metabolites are shown in brackets. (1): desmethylbassianin, (2): chaetoglobosin A. Chemical family for the corresponding SM is also described I: tryptophan-derived alkaloids, II: tyrosine-derived pyridones.

Initial phylogenetic analyses for all the NRPSs identified in Rcc yielded largely unresolved trees (Appendix 4). The Rcc NRPSs *Nps100*, *Nps55-3.77*, *Npsm29-0.249*, *Nps51-1.140*, *Npsm42-0.88* and *Nps113-0.134* appeared to be very different from the rest of the sequences used in this analysis and from each other. For clarity these sequences were removed from the analysis and a more resolved tree was generated (Figure 2.15).

The A-domains of Rcc NRPSs *Nps280-0.11* and *Nps175-0.41* were closely related to the A-domains of an NRPS yielding an unknown SM in *Parastagonospora nodorum* (syn. *Phaeosphaeria nodorum*). *Nps175-0.41* seemed more closely related to the *P. nodorum* NRPS as all of it's A-domains were found to be related to the equivalent domains in *P. nodorum*. The third A domain present in *Nps175-0.41* and the *P. nodorum* NRPS appeared to be absent in *Nps280-0.11*. Furthermore, the domain organisation of both *Nps175-0.41* and its related NRPS in *P. nodorum* was found to be identical (C-A-PCP-C-C-C-A-PCP-C-A-PCP-C). This domain organisation suggest that the genes encoding for these proteins might have been truncated as they are lacking the initiation module A-PCP, which might result in a non-functional protein.

The A domains of *Nps246-0.103* were found to be related to the equivalent A domains in *Aspergillus udagawae* (syn. *Neosartorya udagawae*) *Nps8* and in an NRPS acting in an unknown biochemical pathway in *Rosellinia necatrix* (syn. *Dematophore necatrix*), the causative agent of white root rot of several fruit trees including, apple, pear and avocado trees (Eguchi *et al.*, 2009; Granum *et al.*, 2015). The three proteins exhibited the same domain organisation that consisted in an initiation module A-PCP followed by three elongation modules C-A-PCP and a terminal C domain. The compounds produced by both *Nps8* in *A. udagawae* and the NRPS in *R. necatrix* are still unknown, therefore no prediction can be made regarding the chemical nature of the backbone of the potential SM produced by *Nps246-0.103*.

Two Rcc NRPSs, *Nps134-0.394* and *Npsm42-0.127*, appeared phylogenetically related to NRPSs involved in the biosynthesis of siderophores. *Nps134-0.394* A domains appeared to be most closely related to the A domains of an NRPS yielding an unknown SM in the related fungus *Dothistroma septosporum*. *Nps134-*

0.394 was found to be part of a larger clade containing the A domains of ferricrocin synthetases from *Bipolaris maydis* and *Magnaporthe oryzae* (syn. *Pyricularia grisea*). However, the domain organisation of *Nps134-0.934* was distinct from that of all the other three NRPSs in this clade. The domains of *Nps134-0.394* were organised as A-PCP-C-A-PCP-C-PCP-C-A-PCP-C-PCP-C, while the other ferricrocin synthases contained an additional PCP-C repeat at the C-terminal end. The first A domain identified in *Npsm42-0.127* was found to be related to the second A domain of *SidC*, *Fer3* and *Fso1* ferrichrome synthetases in *Aspergillus fumigatus*, *Ustilago maydis* and *Omphalotus olearius* respectively. Similarly, the second A domain in *Npsm42-0.127* appeared related to the third A domain in the three ferrichrome synthetases. The domains of the ferrichrome synthetases and *Npsm42-0.127* are organised in an initiaion module A-PCP followed by two consecutive elongation modules C-A-PCP followed by PCP-C repeated twice. *Npsm42-0.127* exhibited the same organisation except that it lacked both the A- and PCP-domain at the N-terminus. Taken together these results suggest that *Npsm42-0.127* is related to the ferrichrome synthetase, however, the gene appeared to be truncated. Therefore Rcc is unlikely to produce a siderophore of the ferrichrome type, but could potentially produce a ferricrocin type one.

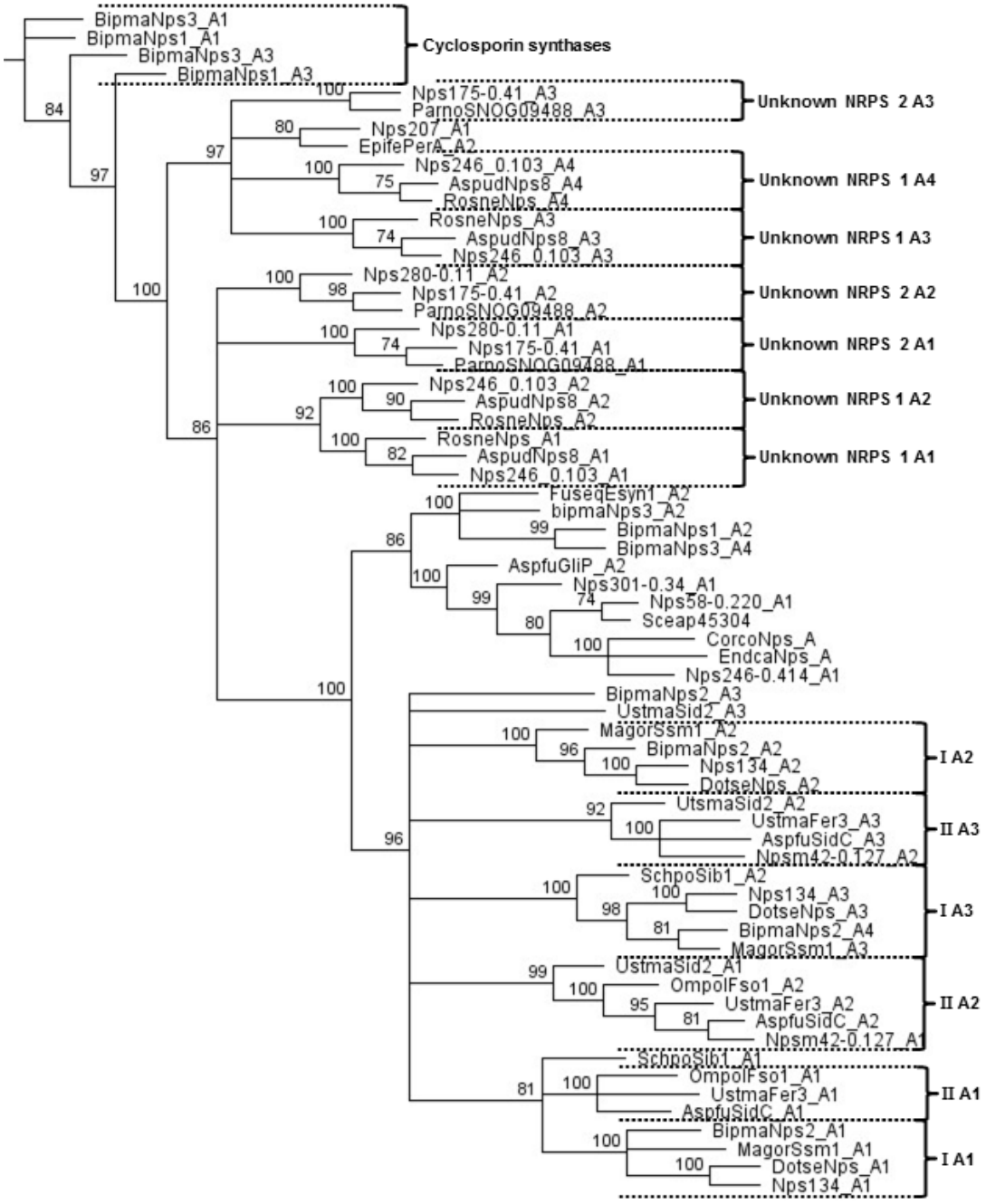

Figure 2.15: Phylogenetic analysis of non-ribosomal peptide synthetases in *Ramularia collo-cygni*.

Maximum likelihood tree (consensus of 100 repetitions) of NRPSs A-domains using a supporting bootstrap cut-off value set at 70%. Sequences were aligned using MAFFT and poorly aligned sequences were removed from the analysis. The cyclosporin synthetases are grouped together at the base of the tree and the siderophore synthetases at the top. I: ferricrocin, II: ferrichrome.

2.3.3.2.Detailed study of selected clusters

To further investigate what SMs could potentially be produced by Rcc a detailed study of all the putative SM clusters identified in section 2.3.2 was carried out. Out of the 27 core gene-based clusters found in Rcc, fifteen were highly similar to SM clusters found in other fungal species. However, only seven of the Rcc SM clusters were similar to SM clusters where the actual produced fungal metabolite is known.

The two NR-PKSs-based clusters were similar to SM clusters found in other fungal species. Cluster PKSm24 showed similarity to the monodictyphenone (MDP) biosynthesis cluster in *Aspergillus nidulans* and to an unknown SM cluster in *Bipolaris victoriae* (syn. *Cochliobolus victoriae*) (Figure 2.16, Table 2.5). In both the *A. nidulans* and the *B. victoriae* clusters the NR-PKS lacking the TE domain was coupled with a divergently transcribed metallo-β-lactamase which has been shown in other fungi to be involved as a polyketide release mechanism (Awakawa *et al.*, 2009; Li *et al.*, 2011; Lim *et al.*, 2012). Similarly, in PKSm24 the NR-PKS, *Pksm24-1.219*, that lacks the TE domain appeared to be coupled to a divergently transcribed metallo-β-lactamase. However, only four out of the twelve genes that compose the *A. nidulans* MDP cluster were found to have putative paralogues in PKSm24 whereas 40% of the genes in this cluster were similar to those genes in the *B. victoriae* cluster. Together these data suggest that Rcc is unlikely to produce MPD and because the *B. victoriae* cluster has not been characterised yet, no further hypotheses can be made regarding the potential nature of the polyketide produced by PKSm24.

The cluster PKS118 was found to be 70% similar at the gene level to an unknown SM gene cluster located on chromosome II of *Z. tritici* (Figure 2.17, Table 2.6). That cluster comprised 12 genes, two of which are PKSs. The *Z. tritici* PKSs have both been shown to be putative paralogues of the Rcc PKSs *Pks118-3.254* and *Pks118-3.158*. Gene organisation between the Rcc and *Z. tritici* clusters appeared to be conserved between the two species with five putative paralogues located in a region of strong synteny between the two PKSs in both species.

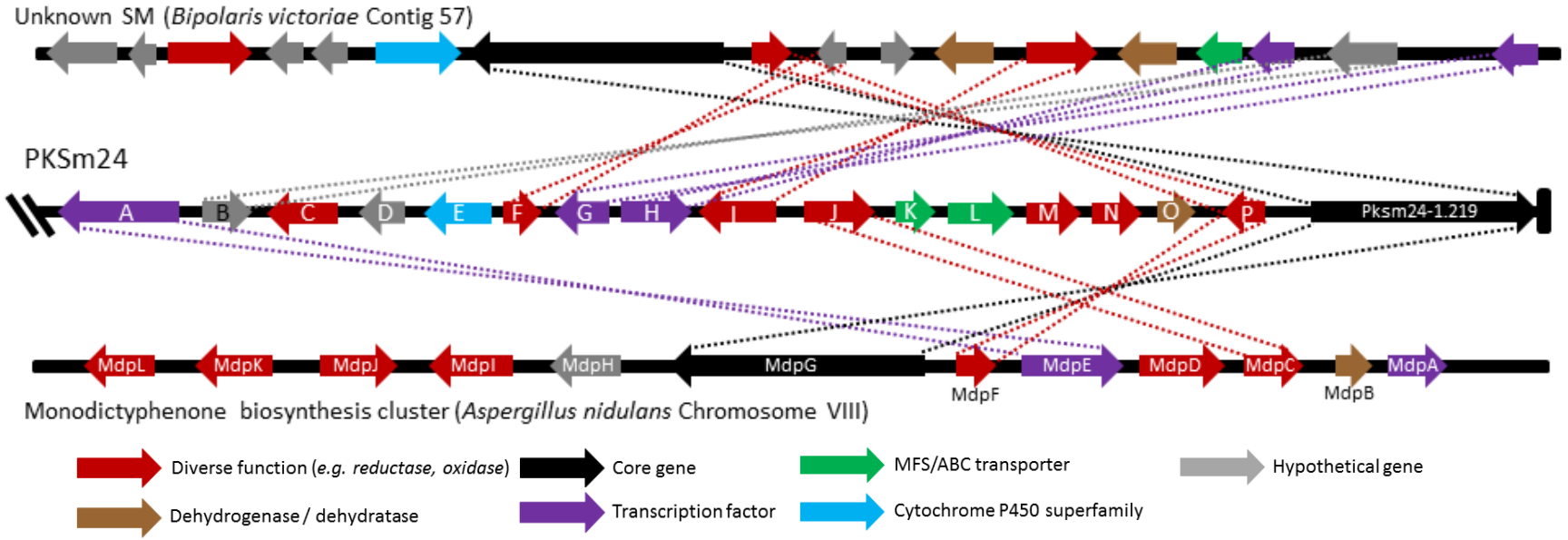

Figure 2.16: Relationship between putative *Ramularia collo-cygni* secondary metabolism cluster PKSm24 and secondary metabolism clusters in *Bipolaris victoriae* and *Aspergillus nidulans*.
PKSm24 showed similarity to the MDP biosynthesis cluster in *Aspergillus nidulans* (28% gene similarity) and to an unknown SM cluster in *Bipolaris victoriae* (41% gene similarity). The core gene *Pksm24-1.219* showed similarity to the core gene in each of the two secondary metabolism clusters. The divergently transcribed metallo-β-lactamase (gene code P in Table 2.5) was also found to be similar to divergently transcribed metallo-β-lactamase genes in *B. victoriae* and *A. nidulans*. The oxidase identified as a putative StcQ (gene code I) only had a similar gene in *B. victoriae*. The versicolorin reductase (gene code J) was only similar to a gene in the *A. nidulans* MDP cluster. The two transcription factors coded G and H were found to be similar to the two transcription factors found on the *B. victoriae* cluster while the transcription factor coded A was found to be similar to *A. nidulans MdpE*. The putative anthrone oxidase (gene code F) and the hypothetical gene B were similar to two hypothetical genes on the *B. victoriae* cluster. The *B. victoriae* and *A. nidulans* clusters are drawn based on AntiSMASH data. Clusters are not drawn to scale. The putative function of the genes present in PKSm24 is given in Table 2.5.

Table 2.5: Protein BLAST hit table for the genes identified in cluster PKSm24.

Gene code	Putative function of Rcc gene model [1]	Organism [2]	Accession number	E-value	Query cover	Identity
A	AflR-like protein	*Aspergillus nidulans*	XP_657752.1	6e-29	92%	27%
B	Hypothetical	*Bipolaris victoriae*	XP_014555318.1	7e-57	87%	71%
C	Monooxygenase	*Setosphaeria turcica*	XP_008023479.1	4e-176	95%	60%
D	Hypothetical	*Pyrenophora tritici-repentis*	XP_001933044.1	2e-22	94%	46%
E	Cytochrome P450 oxidoreductase	*Beauveria bassiana*	XP_008596070.1	2e-160	97%	66%
F	Anthrone oxidase-like protein	*Bipolaris victoriae*	XP_014555315.1	1e-36	96%	48%
G	Toxin biosynthesis regulatory AflJ	*Bipolaris victoriae*	XP_014555319.1	9e-28	71%	39%
H	Fungal transcription factor	*Bipolaris victoriae*	XP_014555317.1	1e-14	46%	29%
I	StcQ-like protein	*Bipolaris victoriae*	XP_014555316.1	5e-146	100%	75%
J	Versicolorin reductase	*Aspergillus nidulans*	XP_657750.1	5e-142	99%	73%
K	ABC transporter	*Beauveria bassiana*	XP_008596064.1	1e-50	85%	57%
L	ABC transporter	*Aerobasidium pullulans*	KEQ83331.1	0.0	99%	60%
M	Oxidoreductase	*Colletotrichum orbiculare*	ENH76218.1	5e-103	99%	45%
N	Short chain dehydrogenase	*Dothistroma septosporum*	EME43185.1	2e-105	97%	53%
O	Scytalone dehydratase	*Cladophialophora ygresii*	XP_007754619.1	1e-50	97%	67%
P	Metallo-β lactamase	*Bipolaris victoriae* *Aspergillus nidulans*	XP_014555314.1 XP_657753.1	3e-25 2e-26	45% 45%	66% 67%
Pksm24-1.219	Polyketide synthase	*Bipolaris victoriae* *Aspergillus nidulans*	XP_014555313.1 XP_657754.1	0.0 0.0	97% 97%	58% 56%

[1] The putative function of Rcc gene models is based on a consensus across all BLAST hits in the NCBI non-redundant database. [2] BLASTp analyses were carried out in the *A. nidulans* (taxid: 162425) and *B. victoriae* F13 (taxid: 930091) databases for Rcc genes with matches to the *A. nidulans* or *B. victoriae* secondary metabolism cluster. The best BLAST hit in the nr database is presented for Rcc genes which had no match to the *A. nidulans* or *B. victoriae* cluster.

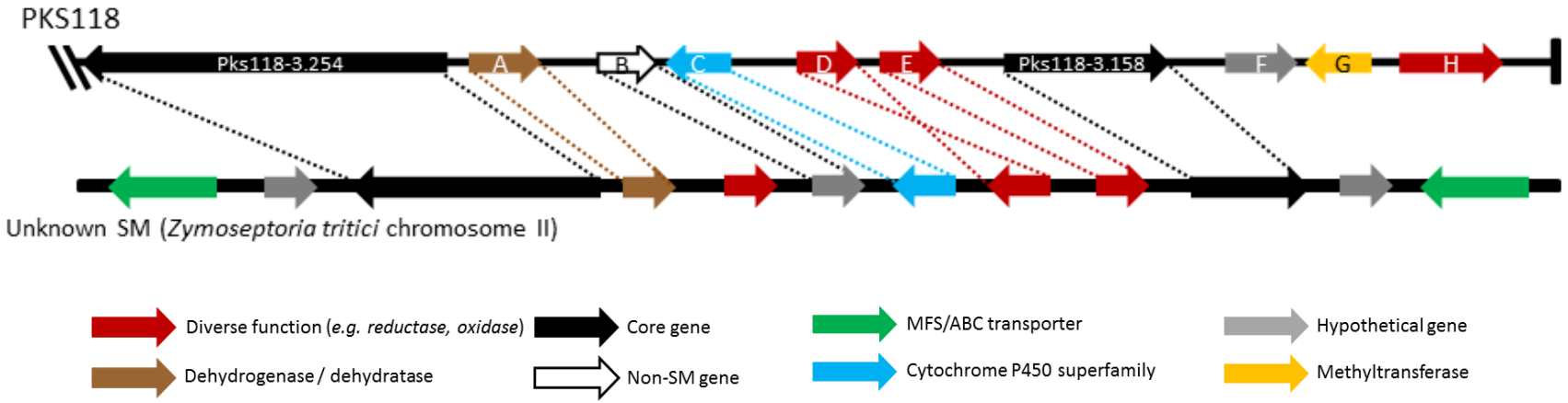

Figure 2.17: Relationship between putative *Ramularia collo-cygni* secondary metabolism cluster PKS118 and secondary metabolism cluster in *Zymoseptoria tritici*.
The core genes *Pks118-3.254* and *Pks118-3.158* showed similarity to the core genes in the *Z. tritici* cluster. The scytalone dehydratase (gene code A in Table 2.6), the cytochrome P450 monooxygenase (gene code C), and the two oxidases (gene code D and E) had a similar gene in *Z. tritici*. The peroxisomal membrane protein encoding gene (gene code B) showed similarity to a hypothetical gene in *Z. tritici*. The *Z. tritici* cluster is drawn based on AntiSMASH data. Clusters are not drawn to scale. The putative function of the genes present in PKS118 is given in Table 2.6.

Table 2.6: Protein BLAST hit table for the genes identified in PKS118 cluster.

Gene code	Putative function of Rcc gene model [1]	Organism [2]	Accession number	E-value	Query cover	Identity
Pks118-3.254	Polyketide synthase	*Zymoseptoria tritici*	XP_003855816.1	0.0	95%	69%
A	Scytalone dehydratase	*Zymoseptoria tritici*	XP_003854701.1	1e-72	100%	65%
B	Peroxisomal membrane protein	*Zymoseptoria tritici*	XP_003854703.1	2e-97	98%	70%
C	Putative P450 monooxygenase	*Zymoseptoria tritici*	XP_003855815.1	3e-41	66%	72%
D	Multicopper oxidase	*Zymoseptoria tritici*	XP_003855814.1	5e-153	100%	75%
E	Oxidase (laccase)	*Zymoseptoria tritici*	XP_003854704.1	5e-120	87%	82%
Pks118-3.158	Polyketide synthase	*Zymoseptoria tritici*	XP_003855813.1	0.0	34%	87%
F	Hypothetical protein	*Zymoseptoria brevis*	KJX93617.1	3e-157	68%	72%
G	O-methyltransferase	*Zymoseptoria brevis*	KJX92106.1	5e-150	100%	83%
H	Aldo-keto-reductase	*Zymoseptoria brevis*	KJX93186.1	0.0	92%	84%

[1] Putative function of Rcc gene models is based on a consensus across all BLAST hits in the NCBI non-redundant database. [2] BLASTp analyses were carried out in the *Z. tritici* IPO323 (taxid: 336722) database for Rcc genes with matches to the *Z. tritici* secondary metabolism cluster. The best BLAST hit in the nr database is presented for Rcc genes which had no match to the *Z. tritici* cluster.

Half of the HR-PKSs identified in putative SM clusters in Rcc were found to show similarity to SM clusters in other species. Cluster PKS30 exhibited similarity to the betaenone biosynthesis cluster (Figure 2.18). Betaenones are phytotoxic compounds first isolated from the oilseed rape pathogen *Phoma betae* (syn. *Pleospora betae*). The *P. betae* betaenone cluster comprises four genes, the HR-PKS *bet1* is located at the 5' end of the cluster and the domain organisation of the protein encoded by *bet1* resembles that of *Pks30-1.114* (KS-AT-DH-MT-KR-ACP-R). A cytochrome P450 monooxygenase (*bet2*), an enoyl reductase (*bet3*) and a short chain dehydrogenase (*bet4*) located upstream from *bet1* complete the cluster (Ugai *et al.*, 2015). *P. betae bet3* is thought to functionally replace the non-functional ER domain in *bet1*. Considering that *Pks30-1.114* was not predicted to possess an ER domain the enoyl reductase (gene code E in Table 2.7) might be acting *in trans* to reduce the growing polyketide. Predicted Rcc genes located in PKS30 showed similarity to the four betaenone biosynthesis genes. The Rcc genes were also found to be similar to genes found in an unknown SM cluster located on chromosome I in Rcc sister species *Z. tritici*. In addition, the MFS transporter found in *Z. tritici* appeared to have a paralogue in PKS30.

PKS58 was found to be similar to a gliotoxin-like cluster in the Sordariomycete *Scedosporium apiospermum*. However, both PKS58 and the *S. apiospermum* clusters that contain two core genes, a PKS and a *GliP*-like NRPS, differ from the typical gliotoxin cluster that contains only one NRPS named *GliP*. Half of the genes present in PKS58 were similar to one of the genes in the *S. apiospermum* cluster (Figure 2.19). In addition to the *GliP*-like NRPS, five putative gliotoxin biosynthesis-like genes from *S. apiospermum* were similar to genes in PKS58. The two *GliC*- and *GliF*-like cytochrome P450 monooxygenases (gene code E and K in Table 2.8), the *GliM*-like O-methyltransferase (gene code H), the *GliT*-like thioredoxin reductase (gene code C) and a putative *GliK*-like (gene code J) were similar to genes in *S. apiospermum*. The second core gene *Pks58-0.40*, as well as a gene of hypothetical function (gene code F) also had putative paralogues in *S. apiospermum*. Taken together these suggest that the potential SM produced by this cluster is unlikely to be gliotoxin but might be related to it.

The cluster located on contig 282 exhibited high similarity with clusters found in the two Dothideomycete fungi *Neofusicoccum parvum* and *Macrophonia phaseolina*. All but one of the genes present in Rcc cluster PKS282 had putative paralogues in both *N. parvum* and *M. phaseolina* clusters (Figure 2.20, Table 2.9). The two SMs produced by the *N. parvum* and *M. phaseolina* clusters are uncharacterised and therefore no predictions can be made regarding the potential SM produced by PKS282.

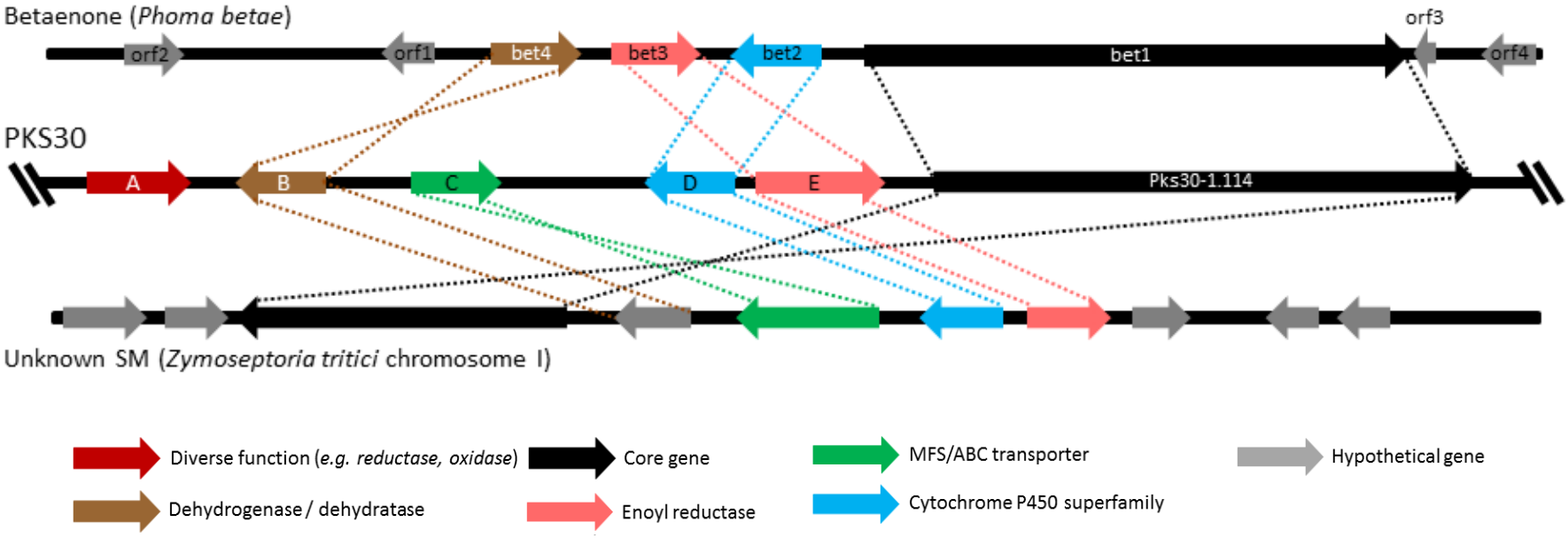

Figure 2.18: Relationship between putative *Ramularia collo-cygni* secondary metabolism cluster PKS30 and secondary metabolism clusters in *Phoma betae* and *Zymoseptoria tritici*.
PKS30 was similar to the betaenone biosynthesis cluster in *Phoma betae* and to an unknown SM cluster in *Zymoseptoria tritici*. The core gene *Pks30-1.114* showed similarity to the core gene in each of the two secondary metabolism clusters. The enoyl reductase (gene code E in Table 2.7) and cytochrome P450 monooxygenase (gene code D) showed similarity to enoyl reductases and cytochrome P450 monooxygenases in *P. betae* and *Z. tritici*. The short chain dehydrogenase (gene code B) was shown to be similar to *bet4* and a hypothetical gene in *P. betae* and Z. tritici respectively. The MFS transporter (gene code C) had a similar gene in the *Z. tritici* cluster. The *P. betae* and *Z. tritici* clusters are drawn based on AntiSMASH data. The clusters are not drawn to scale. The putative function of the genes present in PKS30 is given in Table 2.7.

Table 2.7: Protein BLAST hit table for the genes identified in PKS30.

Gene code	Putative function of Rcc gene model [1]	Organism [2]	Accession number	E-value	Query cover	Identity
A	Kinase	*Aspergillus ochraceoroseus*	KKK24110.1	8e-68	96%	49%
B	Short chain dehydrogenase (bet4)	*Zymoseptoria tritici* *Phoma betae*	XP_003856912.1 BAQ25463.1	7e-120 1e-76	98% 98%	63% 43%
C	MFS superfamily	*Zymoseptoria tritici*	XP_003856911.1	4e-107	67%	59%
D	Cytochrome P450 monooxygenase (bet2)	*Zymoseptoria tritici* *Phoma betae*	XP_003856910.1 BAQ25465.1	4e-137 2e-76	82% 85%	72% 41%
E	Enoylreductase (bet3)	*Zymoseptoria tritici* *Phoma betae*	XP_003856767.1 BAQ25464.1	6e-85 2e-67	96% 89%	74% 55%
Pks30-1.114	Polyketide synthase (bet1)	*Zymoseptoria tritici* *Phoma betae*	XP_003856913.1 BAQ25466.1	0.0 0.0	99% 99%	66% 46%

[1] The putative function of Rcc gene models is based on a consensus across all BLAST hits in the NCBI nr database. [2] BLASTp analyses were carried out in the *P. betae* (taxid: 137527) and *Z. tritici* IPO323 (taxid: 336722) databases for Rcc genes with matches to the *P. betae* or *Z. tritici* secondary metabolism cluster. The best BLAST hit in the nr database is presented for Rcc genes which had no match to the *P. betae* or *Z. tritici* cluster.

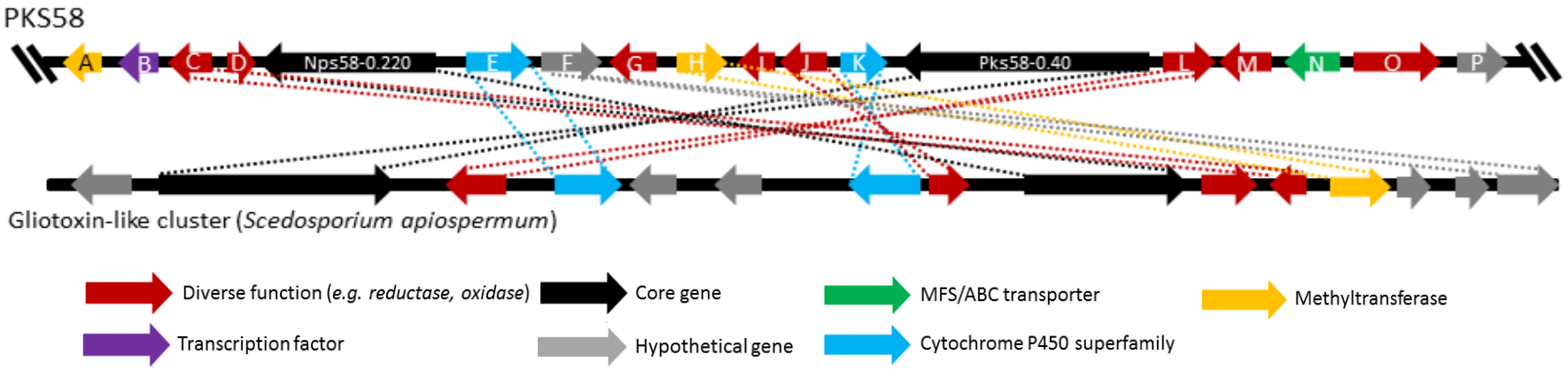

Figure 2.19: Relationship between putative *Ramularia collo-cygni* secondary metabolism cluster PKS58 and secondary metabolism cluster in *Scedosporium apiospermum*.
PKS58 showed similarity to a gliotoxin-like cluster in *S. apiospermum*. The two core genes identified in *S. apiospermum* were conserved in Rcc (*Nps58-0.220* and *Pks58-0.40*) as well as gliotoxin biosynthesis-like genes such as the cytochrome P450 monooxygenases *GliC* and *GliF* (genes E and K respectively in Rcc), the O-methyltransferase *GliM* (gene code H), the thioredoxin reductase *GliT* (genes code C) and *GliK* (gene code J). In addition, the hypothetical gene F in Rcc exhibited sequence similarity to a hypothetical gene in the *S. apiospermum* cluster. The putative function of the genes present in PKS58 is given in Table 2.8. The *S. apiospermum* cluster is drawn based on AntiSMASH data. The clusters are not drawn to scale. The putative function of the genes present in PKS58 is given in Table 2.8.

Table 2.8: Protein BLAST hit table for the genes identified in PKS58.

Gene code	Putative function of Rcc gene model [1]	Organism [2]	Accession number	E-value	Query cover	Identity
A	O-methyltransferase	*Trichoderma virens*	XP_013955926.1	4e-33	39%	56%
B	Fungal transcription factor	*Penicillium italicum*	KGO74479.1	1e-09	68%	25%
C	Thioredoxin reductase (GliT-like)	*Scedosporium apiospermum*	XP_016645306.1	2e-95	61%	55%
D	Aminotransferase (GliI-like)	*Aspergillus flavus*	XP_002380005.1	1e-58	92%	51%
Nps58-0.220	NRPS (GliP-like)	*Scedosporium apiospermum*	XP_016645304.1	6e-130	100%	43%
E	Acc synthase (GliC-like)	*Scedosporium apiospermum*	XP_016645299.1	1e-120	100%	52%
F	Hypothetical	*Scedosporium apiospermum*	XP_016645310.1	9e-23	68%	43%
G	Glutathion-S-transferase (GliG-like)	*Madurella mycetomatis*	KXX77986.1	2e-53	69%	66%
H	O-methyltransferase (GliM-like)	*Scedosporium apiospermum*	XP_016645307.1	6e-60	100%	59%
I	Dipeptidase (GliJ-like)	*Aspergillus flavus*	XP_002380015.1	6e-14	91%	47%
J	Gliotoxin biosynthesis (GliK-like)	*Scedosporium apiospermum*	XP_016645303.1	1e-29	71%	49%
K	P450 monooxygenase (GliF-like)	*Scedosporium apiospermum*	XP_016645302.1	2e-97	96%	60%
Pks58-0.40	PKS	*Scedosporium apiospermum*	XP_016645297.1	0.0	93%	41%
L	Toxin biosynthesis, Tri-7 like	*Scedosporium apiospermum*	XP_016645298.1	5e-104	78%	34%
M	Short chain dehydrogenase	*Zymoseptoria tritici*	XP_003855802.1	1e-136	94%	68%
N	MFS transporter (GliA_like)	*Aspergillus fumigatus*	XP_753059.2	4e-40	72%	47%
O	Thioredoxin reductase (GliT-like)	*Madurella mycetomatis*	KXX83234.1	2e-66	55%	77%
P	Hypothetical	*Zymoseptoria brevis*	KJX96050.1	7e-94	93%	56%

[1] The putative function of Rcc gene models is based on a consensus across all BLAST hits in the NCBI nr database. [2] BLASTp analyses were carried out in the *S. apiospermum* (taxid: 563466) database for Rcc genes with matches to the *S. apiospermum* secondary metabolism cluster. The best BLAST hit in the nr database is presented for Rcc genes which had no match to the *S. apiospermum* cluster.

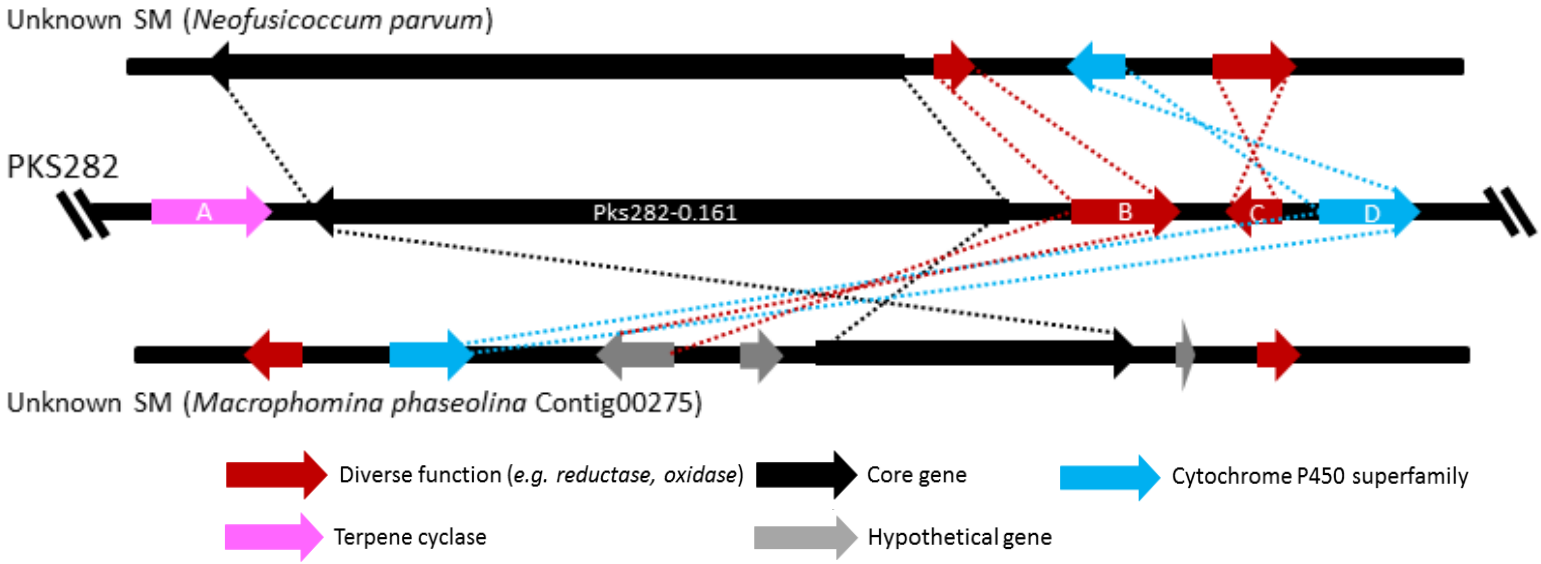

Figure 2.20: Relationship between putative *Ramularia collo-cygni* secondary metabolism cluster PKS282 and secondary metabolism clusters in *Neofusicoccum parvum* and *Macrophomina phaseolina*.
PKS282 was similar to two unknown SM clusters in *Neofusicoccum parvum* and *Macrophomina phaseolina*. The core gene *Pks282-0.161* showed similarity to the core gene in each of the two secondary metabolism clusters. The esterase lipase and the cytochrome P450 (gene code B and D respectively in Table 2.9) showed similarity to genes in both *N. parvum* and *M. phaseolina* clusters. The hydrolase (gene code C) only had a similar gene in the *N. parvum* cluster. The *N. parvum* and *M. phaseolina* clusters are drawn based on AntiSMASH data. The clusters are not drawn to scale. The putative function of the genes present in PKS282 is given in Table 2.9.

Table 2.9: Protein BLAST hit table for the genes identified in PKS282.

Gene code	Putative function of Rcc gene model [1]	Organism [2]	Accession number	E-value	Query cover	Identity
A	Terpene cyclase	*Leptosphaeria maculans*	XP_003845083.1	4e-152	97%	57%
Pks282-0.161	PKS	*Neofusicoccum parvum* *Macrophomina phaseolina*	XP_007581490.1 EKG16355.1	0.0 0.0	99% 90%	59% 62%
B	Esterase lipase	*Macrophomina phaseolina* *Neofusicoccum parvum*	EKG16353.1 XP_007581489.1	1e-143 1e-133	100% 98%	75% 70%
C	Hydrolase	*Neofusicoccum parvum*	XP_007581487.1	2e-40	97%	45%
D	Cytochrome P450	*Macrophomina phaseolina* *Neofusicoccum parvum*	EKG16352.1 XP_007581488.1	5e-53 8e-50	57% 57%	65% 63%

[1] The putative function of Rcc gene models is based on a consensus across all BLAST hits in the NCBI nr database. [2] BLASTp analyses were carried out in the *N. parvum* UCRNP2 (taxid: 1287680) and *M. phaseolina* MS6 (taxid: 1126212) databases for Rcc genes with matches to the *N. parvum* or *M. phaseolina* secondary metabolism cluster. The best BLAST hit in the nr database is presented for Rcc genes which had no match to the *N. parvum* or *M. phaseolina* cluster.

Conserved gene clusters present in other fungi were identified for all three HPSs located in Rcc with one of these being a cluster with a characterised SM product pathway. Half of the genes identified in HPS1 were found to have paralogues in an uncharacterised SM cluster in the Dothideomycete *Sphaerulina musiva* (syn. *Mycosphaerella populorum*) (Figure 2.21). The core gene *Hps1-2.140* and all the genes downstream from it were conserved in *S. musiva*. All but one of the conserved genes (gene code G in Table 2.10) exhibited the same direction of transcription in both species.

HPS14 was similar to the chaetoglobosin A biosynthesis cluster identified in the Eurotiomycete *Penicillium expansum*. The *P. expansum* cluster comprises seven genes with similarity to genes in HPS14 (Figure 2.22 and Table 2.11). The biosynthesis of chaetoglobosin A in *P. expansum* involves a HPS (*CheA*) and a divergently transcribed enoyl reductase (*CheB*). A transcription factor (CheC) is located upstream of *CheA* and *CheB*. Located downstream from *CheA*, are two cytochrome P450 monooxygenases (*CheD* and *CheG*), a flavin adenine dinucleotide (FAD)-dependant monooxygenase (*CheE*) and a transcription factor (*CheF*) (Schumann & Hertweck, 2007). The similarity between *Hps14-0.66* and *CheA* confirms the earlier phylogenetic observation indicating that the two genes are related. In addition to the putative paralogues of the chaetoglobosin cluster, two genes encoding a MFS transporter and O-methyltransferase were also identified directly upstream from *Hps14-0.66*. Taken together with the phylogenetic data, this confirms that the putative SM produced by *Hps14-0.66* might belong to the chaetoglobosin family.

The third HPS cluster was similar to an unknown SM cluster located on chromosome V of the coprophilous Sordariomycete *Podospora anserina*. Two thirds of the genes present in HPS38 had putative paralogues in *P. anserina*. The similarity between these SM clusters in Rcc and *P. anserina* was supported by the phylogenetic analysis that showed that *Hps38-0.269* was closely related to one HPS in *P. anserina* (accession number XP_001905191.1). However, it appeared that some rearrangement occurred as the organisation of the two clusters differs significantly (Figure 2.23 and Table 2.12).

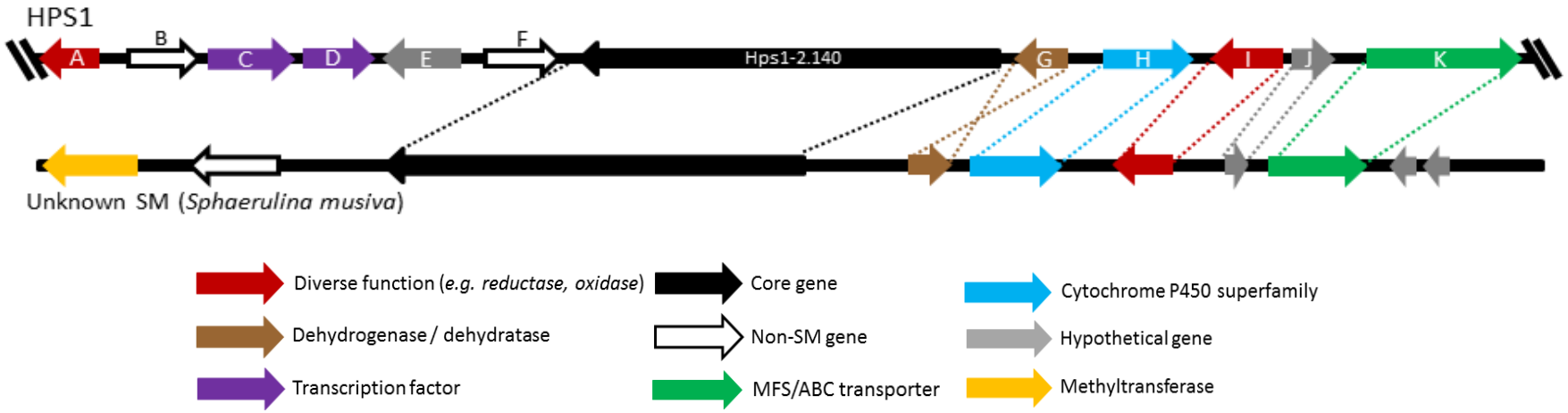

Figure 2.21: Relationship between putative *Ramularia collo-cygni* secondary metabolism cluster HPS1 and secondary metabolism cluster in *Sphaerulina musiva*.
HPS1 showed similarity to an unknown SM cluster in *Sphaerulina musiva*. The core gene *Hps1-2.140* showed similarity to the core gene in the *S. musiva* cluster. The two clusters exhibited high level of conservation downstream of the core genes as the alcohol dehydrogenase (gene code G in Table 2.10), the cytochrome P450 (gene code H), the amino transferase (gene code I), the hypothetical gene (gene code J) and the ABC transporter (gene code K) had similar genes in the *S. musiva* cluster. The *S. musiva* cluster is drawn based on AntiSMASH data. Clusters are not drawn to scale. The putative function of the genes present in HPS1 is given in Table 2.10.

Table 2.10: Protein BLAST hit table of the genes identified in HPS1.

Gene code	Putative function of Rcc gene model [1]	Organism [2]	Accession number	E-value	Query cover	Identity
A	2-polyprenyl-6-methoxyphenol hydroxylase	*Zymoseptoria brevis*	KJX98699.1	0.0	74%	70%
B	Glycoside hydrolase	*Zymoseptoria tritici*	XP_003854844.1	0.0	92%	83%
C	Fungal transcription factor	*Dothistroma septosporum*	EME48245.1	0.0	97%	65%
D	Putative fungal transcription factor	*Zymoseptoria tritici*	XP_003854843.1	0.0	96%	61%
E	Hypothetical	*Dothistroma septosporum*	EME47877.1	6e-53	63%	36%
F	Phosphatidylserine decarboxylase	*Zymoseptoria brevis*	KJY01223.1	0.0	97%	70%
Hps1-2.140	Hybrid PKS/NRPS	*Sphaerulina musiva*	EMF08749.1	0.0	99%	77%
G	Alcohol dehydrogenase	*Sphaerulina musiva*	EMF08748.1	1e-98	100%	76%
H	Cytochrome P450	*Sphaerulina musiva*	EMF08747.1	0.0	100%	69%
I	Branched chain aminotransferase	*Sphaerulina musiva*	EMF08746.1	0.0	98%	70%
J	Hypothetical	*Sphaerulina musiva*	EMF08745.1	1e-104	97%	76%
K	ABC transporter	*Sphaerulina musiva*	EMF08744.1	0.0	85%	56%

[1] The putative function of Rcc gene models is based on a consensus across all BLAST hits in the NCBI nr database. [2] BLASTp analyses were carried out in the *S. musiva* SO2202 (taxid: 692275) database for Rcc genes with matches to the *S. musiva* secondary metabolism cluster. The best BLAST hit in the nr database is presented for Rcc genes which had no match to the *S. musiva* cluster.

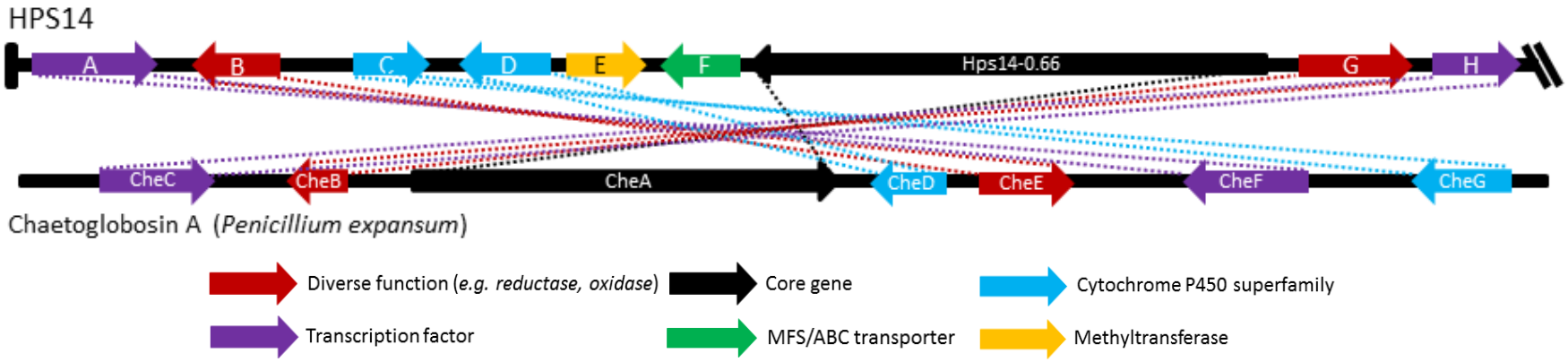

Figure 2.22: Relationship between putative *Ramularia collo-cygni* secondary metabolism cluster HPS14 and the chaetoglobosin A cluster in *Penicillium expansum*.
HPS14 showed similarity to the chaetoglobosin A biosynthesis cluster in *Penicillium expansum*. The two clusters exhibited high level of conservation with 78% of the genes being conserved. The core gene *Hps14-0.66* showed similarity to the *CheA core* gene in chaetoglobosin A biosynthesis. The divergently transcribed enoyl reductase (gene code G in Table 2.11) was found to be similar to the divergently transcribed enoyl reductase *CheB in P. expansum*. The two cytochrome P450 monooxygenases (gene code C and D) were similar to the *CheG* and *CheD* genes respectively and the two transcription factors (gene code A and H) showed similarity to the transcription factors *CheF and CheC* respectively. The monooxygenase (gene code E) exhibited similarity to a gene of equivalent function, *CheE*, in the chaetoglobosin cluster. The *P. expansum* cluster is drawn based on AntiSMASH data. Clusters are not drawn to scale. The putative function of the genes present in HPS14 is given in Table 2.11.

Table 2.11: Protein BLAST hit table for the genes identified in cluster HPS14.

Gene code	Putative function of Rcc gene model [1]	Organism [2]	Accession number	E-value	Query cover	Identity
A	Transcription factor (CheF)	*Penicillium expansum*	CAO91864.1	0.0	89%	61%
B	Monooxygenase (CheE)	*Penicillium expansum*	CAO91863.1	0.0	95%	53%
C	Cytochrome P450 monooxygenase (CheG)	*Penicillium expansum*	CAO91862.1	8e-99	100%	46%
D	Cytochrome P450 monooxygenase (CheD)	*Penicillium expansum*	CAO91865.1	6e-131	100%	81%
E	Putative methyltransferase	*Neofusicoccum parvum*	XP_007586820.1	5e-29	87%	29%
F	MFS transporter	*Penicillium roqueforti*	CDM32053.1	1e-84	93%	72%
Hps14-0.66	Hybrid PKS/NRPS (CheA)	*Penicillium expansum*	CAO91861.1	0.0	100%	59%
G	Enoyl reductase (CheB)	*Penicillium expansum*	CAO91860.1	3e-107	98%	51%
H	Transcription factor (CheC)	*Penicillium expansum*	CAO91859.1	9e-109	96%	46%

[1] The putative function of Rcc gene models is based on a consensus across all BLAST hits in the NCBI nr database. [2] BLASTp analyses were carried out in the *P. expansum* NRRL 62431 (taxid: 1208580) database for Rcc genes with matches to the *P.expansum* secondary metabolism cluster. The best BLAST hit in the nr database is presented for Rcc genes which had no match to the *P. expansum* cluster.

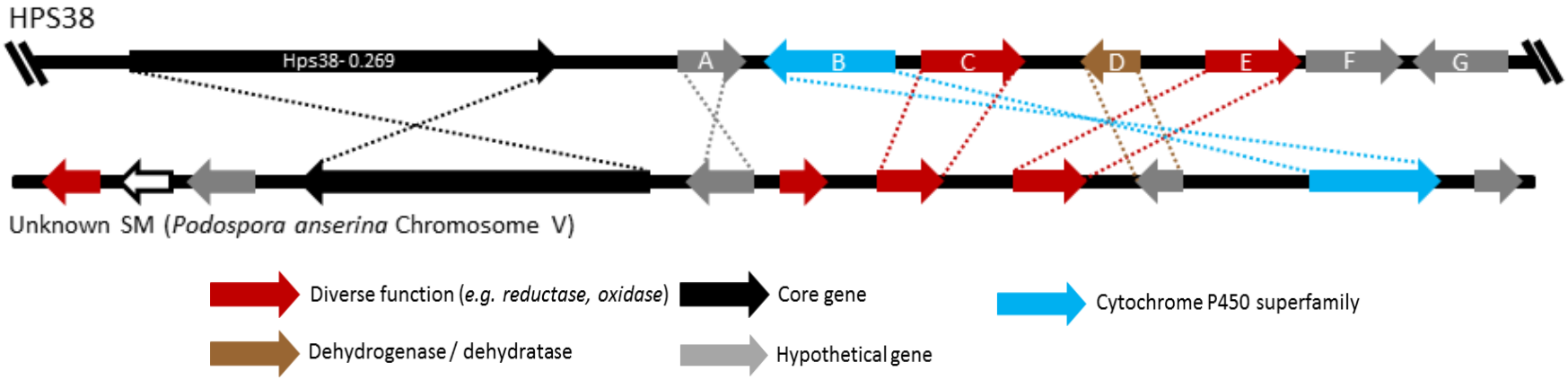

Figure 2.23: Relationship between putative *Ramularia collo-cygni* secondary metabolism cluster HPS38 and secondary metabolism cluster in *Podospora anserina*.
HPS38 showed similarity to an unknown SM cluster in *Podospora anserina.* The cluster in *P. anserina* and HPS38 exhibited high level of conservation with 75% of the genes between the two clusters being conserved. The core gene *Hps38-0.269* was found to be similar to the core gene in the *P. anserina* cluster. Similarly, the bifunctional P450/NADPH P450 reductase (gene code B in Table 2.12), the hydroxylase (gene code C) and the 2-oxoglutarate-Fe oxygenase (gene code E) were similar to genes in the *P. anserina* cluster. The alcohol dehydrogenase (gene code D) and the hypothetical gene A showed similarity to hypothetical genes in *P. anserina*. The *P. anserina* cluster is drawn based on AntiSMASH data. Clusters are not drawn to scale. The putative function of the genes present in HPS14 is given in Table 2.12.

Table 2.12: Protein BLAST hit table for the eight genes identified in cluster HPS38.

Gene code	Putative function of Rcc gene model [1]	Organism [2]	Accession number	E-value	Query cover	Identity
Hps38-0.269	Hybrid PKS/NRPS	*Podospora anserina*	XP_001905191.1	0.0	98%	66%
A	Hypothetical	*Podospora anserina*	XP_001905190.1	1e-29	68%	52%
B	Bifunctional P450/NADPH P450 reductase	*Podospora anserina*	XP_001905185.1	2e-129	89%	63%
C	Hydroxylase	*Podospora anserina*	XP_001905188.1	5e-127	68%	58%
D	Alcohol dehydrogenase	*Podospora anserina*	XP_001905186.1	6e-24	82%	58%
E	2-Oxoglutarate-Fe oxygenase	*Podospora anserina*	XP_001905187.1	1e-22	71%	51%
F	Hypothetical	*Zymoseptoria tritici*	XP_003855972.1	0.0	98%	80%
G	Hypothetical	*Diaporthe ampelina*	KKY29699.1	4e-134	99%	51%

[1] The putative function of Rcc gene models is based on a consensus across all BLAST hits in the NCBI nr database. [2] BLASTp analyses were carried out in the *P. anserina* S mat+ (taxid: 515849) database for Rcc genes with matches to the *P. anserina* secondary metabolism cluster. The best BLAST hit in the nr database is presented for Rcc genes which had no match to the *P. anserina.*

Out of the 17 NRPSs identified to be part of a putative SM cluster in Rcc, seven of these clusters were similar to a SM cluster in another fungal species but in only two cases the similar fungal SM cluster was recognised as producing a known SM.

The first putative SM cluster located on contig 246 (NRPS246-1) was similar to two SM clusters with no known SM product. One cluster was identified in the Sordariomycete *Rosellinia necatrix* and the other in the Eurotiomycete *Aspergillus udagawae*. Although the Rcc, *R. necatrix* and *A. udagawae* clusters seemed to differ quite significantly, the region located downstream of the core genes in *R. necatrix* and *A. udagawae* was syntenic to the region upstream of *Nps246-0.103* (Figure 2.24 and Table 2.13). Gene organisation of these regions appeared to be conserved in all three species except for the presence of a putative O-methyltransferase located in the middle of the Rcc cluster that is absent in the *R. necatrix* and *A. udagawae* clusters.

The second putative SM cluster located on contig 246 (NRPS246-2) was found to have putative paralogues of genes present in the gliotoxin biosynthesis cluster of *Aspergillus fumigatus*. Gliotoxin is an epipolythiodioxopiperazine (ETP) toxin acting as a virulence factor in *A. fumigatus*. It was shown to inhibit the growth of other fungi and to induce apoptosis in animal cells but its role *in vivo* remains unclear (Pardo *et al.*, 2006; Coleman *et al.*, 2011). The biosynthetic pathway leading to the production of gliotoxin in *A. fumigatus* consists of fourteen genes, thirteen of which are organised around the core NRPS gene *GliP* located on chromosome VI. An additional gene, *gtmA*, which is required for gliotoxin production in *A. fumigatus* is located on chromosome II (Dolan *et al.*, 2015). Six of the twelves genes found in the gliotoxin cluster were found to have potential paralogues in NRPS246-2. The O-methyltransferase *GliM*, cytochrome P450 monooxygenase *GliF*, thioredoxin reductase *GliT*, γ-glutamyl cyclotransferase *GliK* and the dipeptidase *GliJ* showed similarity to Rcc genes F, O, G, R and H respectively (Figure 2.25 and Table 2.14). The sequence of the core gene in NRPS246-2, *Nps246-0.414*, was similar to the *A. fumigatus GliP* sequence. However, as NRPS246-2 contains another 20 putative genes with a predicted function related to secondary metabolism, this suggests that cluster NRPS246-2 is unlikely to produce gliotoxin but could be involved in the synthesis of a gliotoxin-derived metabolite.

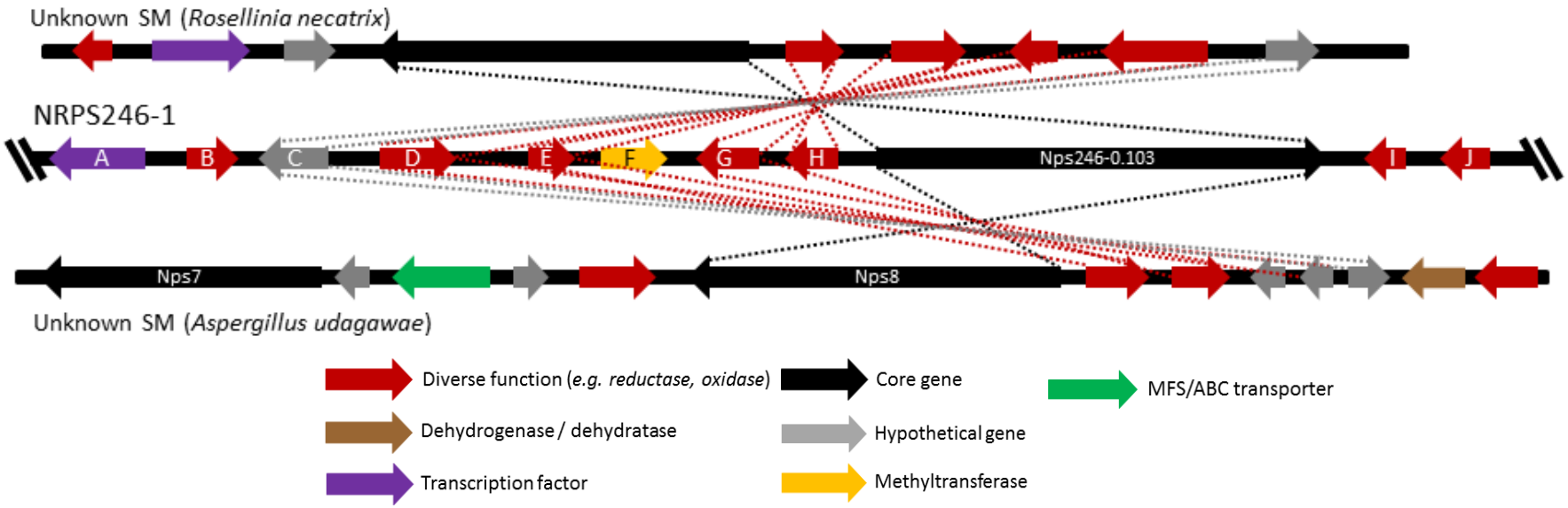

Figure 2.24: Relationship between putative *Ramularia collo-cygni* secondary metabolism cluster NRPS246-1 and secondary metabolism clusters in *Rosellinia necatrix* and *Aspergillus udagawae*.
NRPS246-1 showed high similarity to two putative secondary metabolite clusters in *Rosellinia necatrix* and *Aspergillus udagawae*. The core gene *Nps246-0.103* showed similarity with *Nps8* in *A. udagawae* and with an NRPS of unknown function in *R. necatrix*. The glycine amidinotransferase (gene code E in Table 2.13) and the cystathionine gamma synthase (gene code G) showed similarity to genes in both *A. udagawae* and *R. necatrix*. The phytanoyl dioxygenase (gene code D) exhibited similarity to a phytanoyl dioxygenase in *R. necatrix* and to a hypothetical gene in *A. udagawae.* Similarly, the hypothetical gene (gene code C) was found to be similar to hypothetical genes in both *A. udagawae and R. necatrix* clusters. The lysine amidinotransferase (gene code H) exhibited similarity to a gene of equivalent function in the *R. necatrix* cluster. The *R. necatrix* and *A. udagawae* clusters are drawn based on AntiSMASH data. Clusters are not drawn to scale. The putative function of the genes present in NRPS246-1 is given in Table 2.13.

Table 2.13: Protein BLAST hit table for the genes identified in cluster NRPS246-1.

Gene code	Putative function of Rcc gene model [1]	Organism [2]	Accession number	E-value	Query cover	Identity
A	Transcription factor TFIIB-like	*Zymoseptoria brevis*	JX92508.1	0.0	91%	62%
B	Aldolase	*Zymoseptoria brevis*	JX92509.1	2e-179	92%	93%
C	Hypothetical	*Aspergillus udagawae* *Rosellinia necatrix*	GAO84825.1 GAP90074.1	4e-136 1e-129	88% 88%	55% 55%
D	Phytanoyl dioxygenase	*Aspergillus udagawae* *Rosellinia necatrix*	GAO84824.1 GAP90073.1	2e-122 0.0	42% 99%	61% 48%
E	Glycine amidinotransferase	*Aspergillus udagawae* *Rosellinia necatrix*	GAO84821.1 GAP90072.1	2e-94 8e-85	99% 99%	64% 59%
F	O-methyltransferase	*Penicillium roqueforti*	CDM27894.1	2e-52	91%	39%
G	Cystathionine gamma synthase	*Aspergillus udagawae* *Rosellinia necatrix*	GAO84822.1 GAP90071.1	0.0 0.0	94% 99%	63% 61%
H	Lysine amidinotransferase	*Rosellinia necatrix*	GAP90070.1	6e-126	100%	70%
Nps246-0.103	NRPS	*Aspergillus udagawae* *Rosellinia necatrix*	GAO84820.1 GAP90069.1	0.0 0.0	99% 99%	54% 52%
I	Putative kinase	*Dothistroma septosporum*	EME41626.1	2e-168	98%	66%
J	β-ketoadipyl CoA thiolase	*Zymoseptoria tritici*	XP_003854356.1	0.0	100%	87%

[1] The putative function of Rcc gene models is based on a consensus across all BLAST hits in the NCBI nr database. [2] BLASTp analyses were carried out in the *Rosellinia necatrix* (taxid: 77044) and *Aspergillus udagawae* (taxid: 91492) databases for Rcc genes with matches to the *R. necatrix* or *A. udagawae* secondary metabolism cluster. The best BLAST hit in the nr database is presented for Rcc genes which had no match to the *R. necatrix* or *A. udagawae* cluster.

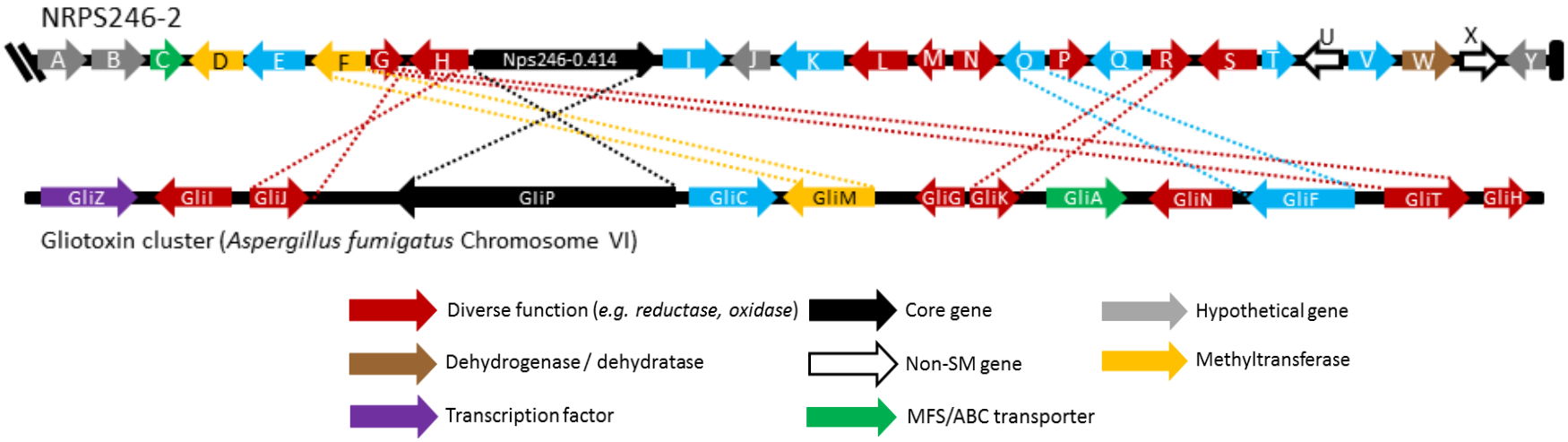

Figure 2.25: Relationship between putative *Ramularia collo-cygni* secondary metabolism cluster NRPS246-2 and the gliotoxin biosynthetic cluster in *Aspergillus fumigatus*.
NRPS246-2 showed similarity to the *Aspergillus fumigatus* gliotoxin cluster. The core gene *Nps246-0.414* exhibited similarity to the gliotoxin core gene *GliP*. The cytochrome P450 monooxygenase and the O-methyltransferase (gene code O and F respectively in Table 2.14) showed similarity to *GliF* and *GliM* respectively. The gliotoxin biosynthesis gene *GliK* was found to have a similar gene in the Rcc cluster (gene code R). The thioredoxin reductase and membrane dipeptidase (gene code G and H respectively) exhibited similarity to *GliT* and *GliJ*. The fourteenth gene in the gliotoxin cluster *gtmA* is not represented on this figure. No genes exhibiting similarity to *gtmA* were found in the Rcc genome with an e-value < e^{-5}. The *A. fumigatus* cluster is drawn based on AntiSMASH data. Clusters are not drawn to scale. The putative function of the genes present in NRPS246-2 is given in Table 2.14.

Table 2.14: Protein BLAST hit table for the genes identified in cluster NRPS246-2.

Gene code	Putative function of Rcc gene model [1]	Organism [2]	Accession number	E-value	Query cover	Identity
A	Hypothetical	*Fusarium langsethiae*	KPA39672.1	1e-30	100%	30%
B	Hypothetical	*Penicillium freii*	KUM59110.1	8e-21	89%	31%
C	MFS transporter	*Mycosphaerella emusae*	KXT06987.1	6e-67	98%	51%
D	O-methyltransferase	*Penicillium griseofulvum*	KXG50020.1	3e-95	94%	42%
E	Cytochrome P450	*Cordyceps confragosa*	OAA76648.1	6e-176	99%	60%
F	O-methyltransferase (GliM)	*Aspergillus flavus*	KOC07843.1	2e-121	100%	51%
G	Thioredoxin reductase (GliT)	*Aspergillus fumigatus*	XP_750863.1	5e-76	91%	49%
H	Membrane dipeptidase (GliJ)	*Aspergillus fumigatus*	XP_750854.2	1e-100	97%	48%
Nps246-0.414	NRPS (GliP)	*Aspergillus fumigatus*	XP_750855.1	4e-130	84%	31%
I	Cytochrome P450	*Cordyceps confragosa*	OAA76642.1	3e-111	97%	61%
J	Hypothetical	*Endocarpon pusillum*	XP_007801850.1	2e-15	88%	57%
K	Cytochrome P450 monooxygenase	*Cordyceps confragosa*	OAA76657.1	0.0	96%	61%
L	Thioredoxin reductase	*Aspergillus lentulus*	GAQ03180.1	8e-28	77%	37%
M	Glutathione-S-transferase (GliG-like)	*Cordyceps confragosa*	OAA76659.1	7e-42	98%	70%
N	Toxin biosynthesis, TRI7-like	*Cordyceps confragosa*	OAA76656.1	3e-177	98%	60%
O	Cytochrome P450 monooxygenase (GliF)	*Aspergillus fumigatus*	XP_750862.1	6e-79	99%	52%

Table 2.14 (continued): Protein BLAST hit table for the genes identified in cluster NRPS246-2.

Gene code	Putative function of Rcc gene model [1]	Organism [2]	Accession number	E-value	Query cover	Identity
P	1-aminocyclopropane-1-carboxylate synthase	*Penicillium nordicum*	KOS38165.1	6e-28	67%	42%
Q	Cytochrome P450	*Cordyceps confragosa*	OAA76640.1	7e-65	75%	65%
R	Gliotoxin biosynthesis (GliK)	*Aspergillus fumigatus*	XP_750859.2	1e-56	88%	38%
S	AMP-dependent synthetase / ligase	*Cordyceps confragosa*	OAA76643.1	6e-138	97%	50%
T	Cytochrome P450	*Cordyceps confragosa*	OAA76644.1	2e-69	97%	72%
U	HET domain containing protein	*Colletotrichum fioriniae*	XP_007590308.1	1e-31	83%	45%
V	Cytochrome P450	*Dothistroma septosporum*	EME46239.1	0.0	97%	68%
W	Acyl-CoA dehydrogenase	*Zymoseptoria brevis*	KJX94586.1	3e-164	100%	77%
X	RNA polymerase β subunit	*Zymoseptoria brevis*	KJX94590.1	0.0	96%	84%
Y	Hypothetical	*Zymoseptoria tritici*	XP_003852914.1	0.0	98%	63%

[1] The putative function of Rcc gene models is based on a consensus across all BLAST hits in the NCBI nr database. [2] BLASTp analyses were carried out in the *Aspergillus fumigatus* Af293 (taxid: 330879) database for Rcc genes with matches to the *A. fumigatus* secondary metabolism cluster. The best BLAST hit in the nr database is presented for Rcc genes which had no match to the *A. fumigatus* cluster.

A detailed study of the Rcc cluster located on contig 51 (NRPS51) showed that two out of the three genes present in that cluster had putative paralogues in a SM cluster in the related Dothideomycete *Pseudocercospora fijiensis*. No characterised SM product has been reported for the *P. fijiensis* cluster. The organisation of the cluster did not appear to have been conserved as the two genes are transcribed in a convergent manner in *P. fijiensis* but divergently in Rcc (Figure 2.26).

Four of the nine genes identified in the cluster NRPS245 were found to have putative paralogues in a SM cluster located on chromosome VI of *Z. tritici* which has no known SM product reported to date. The sequences of the proteins encoded by the two core genes identified in the Rcc cluster, *Nps245-0.164* and *Nps245-0.245*, were found to be similar to that of the two NRPSs identified in *Z. tritici*. A cytochrome P450 monooxygenase and a carboxylesterase located upstream from the core genes showed co-linearity with two genes in *Z. tritici* whose predicted function and location in the cluster is similar to that in Rcc (Figure 2.27 and Table 2.15). Although this region of the two clusters appeared to be conserved, it comprises less than half of the genes in both clusters which suggest that the SMs produced by these two clusters might differ significantly.

The cluster NRPS207 was similar to an unknown SM cluster in the Eurotiomycete *Pseudogymnoascus pannorum* var. *pannorum* as 85% of the genes in Rcc had putative paralogues in *P. pannorum*. The organisation of the two clusters differs significantly suggesting that some gene rearrangement might have occurred (Figure 2.28). For example, the two core genes in NRPS207, *Nps207-0.9* and *Nps207-0.46*, are located at both end of the cluster while in *P. pannorum* they are found in the central region. Similarly, the direction of transcription of all but the NRPS *Nps207-0.46* and the putative oxidase (gene code D in Table 2.16) was found to be different between Rcc and *P. pannorum*.

A)

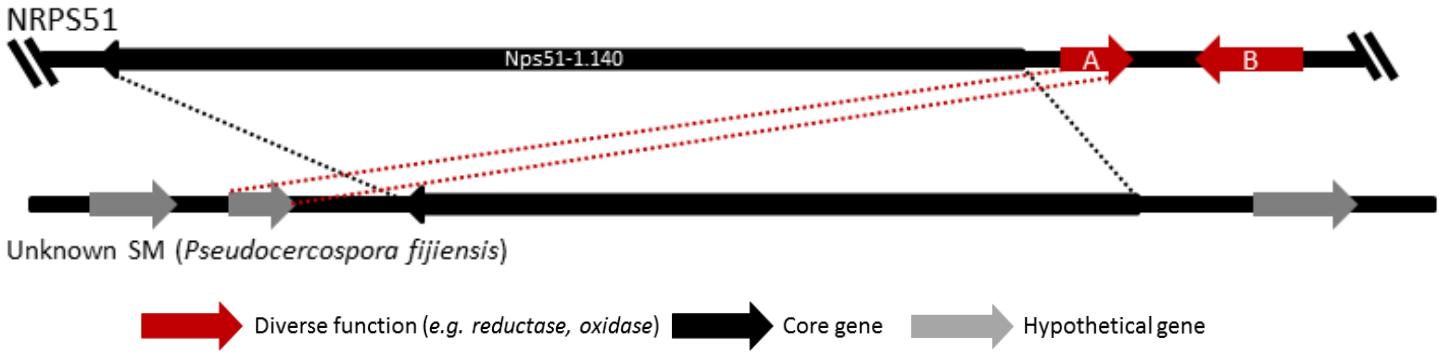

B)

Gene code	Putative function of Rcc gene model [1]	Organism [2]	Accession number	E-value	Query cover	Identity
Nps51-1.140	NRPS	*Pseudocercospora fijiensis*	XP_007922073.1	0.0	99%	44%
A	Oxidoreductase / dioxygenase	*Pseudocercospora fijiensis*	XP_007922072.1	1e-20	65%	58%
B	Proton-dependent oligopeptide transporter	*Pseudocercospora fijiensis*	XP_007920193.1	7e-19	72%	31%

Figure 2.26: Relationship between putative *Ramularia collo-cygni* secondary metabolism cluster NRPS51 and the secondary metabolite cluster in *Pseudocercospora fijiensis*.
A) Schematic representation of the similarity between NRPS51 and the SM cluster in *P. fijiensis*. The core gene *Nps51-1.140* exhibited similarity with the core gene in the *P. fijiensis* cluster. NRPS51 also exhibited similarity between a putative oxidase (gene code A) and a gene encoding for a hypothetical protein in *P. fijiensis*. The *P. fijiensis* cluster is drawn based on AntiSMASH data. Clusters are not drawn to scale. B) Protein BLAST hits table for the genes identified in NRPS51. [1] The putative function of Rcc gene models is based on a consensus across all BLAST hits in the NCBI nr database. [2] BLASTp analyses were carried out in the *Pseudocercospora fijiensis* CIRAD86 (taxid: 383855) database for Rcc genes with matches to the P. *fijiensis* secondary metabolism cluster. The best BLAST hit in the nr database is presented for Rcc genes which had no match to the P. *fijiensis* cluster.

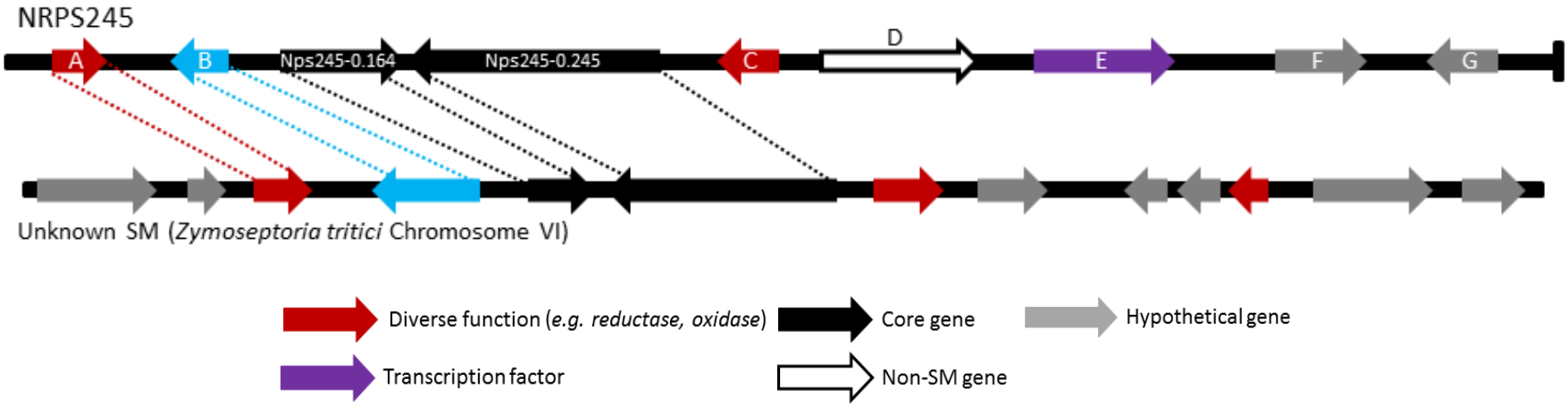

Figure 2.27: Relationship between putative *Ramularia collo-cygni* secondary metabolism cluster NRPS245 and the secondary metabolite cluster in *Zymoseptoria tritici*.
NRPS245 showed similarity to an unknown SM cluster in *Zymoseptoria tritici*. The two core genes *Nps245-0.164* and *Nps245-0.245* exhibited similarity to two NRPSs in the *Z. tritici* cluster. Similarly, the carboxylesterase and the P450 monooxygenase identified in cluster NRPS245 (gene code A and B respectively in Table 2.15) exhibited similarity to genes of similar function found in the *Z. tritici* cluster. The *Z. tritici* cluster is drawn based on AntiSMASH data. Clusters are not drawn to scale. The putative function of the genes present in NRPS245 is given in Table 2.15.

Table 2.15: Protein BLAST hits table for the genes identified in cluster NRPS245.

Gene code	Putative function of Rcc gene model [1]	Organism [2]	Accession number	E-value	Query cover	Identity
A	Carboxylesterase	*Zymoseptoria tritici*	XP_003851565.1	3e-41	79%	66%
B	P450 monooxygenase	*Zymoseptoria tritici*	XP_003851778.1	3e-127	95%	71%
Nps245-0.164	NRPS	*Zymoseptoria tritici*	XP_003851566.1	3e-140	45%	64%
Nps245-0.245	NRPS	*Zymoseptoria tritici*	XP_003851777.1	0.0	91%	64%
C	Glutathione-S-transferase	*Mycosphaerella emusae*	KXS98879.1	7e-145	83%	82%
D	Helicase	*Zymoseptoria tritici*	XP_003854148.1	0.0	79%	71%
E	Transcription factor	*Pseudocercospora musae*	KXT08923.1	0.0	96%	55%
F	Hypothetical	*Zymoseptoria brevis*	KJX97354.1	0.0	76%	71%
G	Hypothetical	*Zymoseptoria tritici*	XP_003849410.1	3e-170	98%	70%

[1] The putative function of Rcc gene models is based on a consensus across all BLAST hits in the NCBI nr database. [2] BLASTp analyses were carried out in the *Z. tritici* IPO323 (taxid: 336722) database for Rcc genes with matches to the Z. *tritici* secondary metabolism cluster. The best BLAST hit in the nr database is presented for Rcc genes which had no match to the Z. *tritici* cluster.

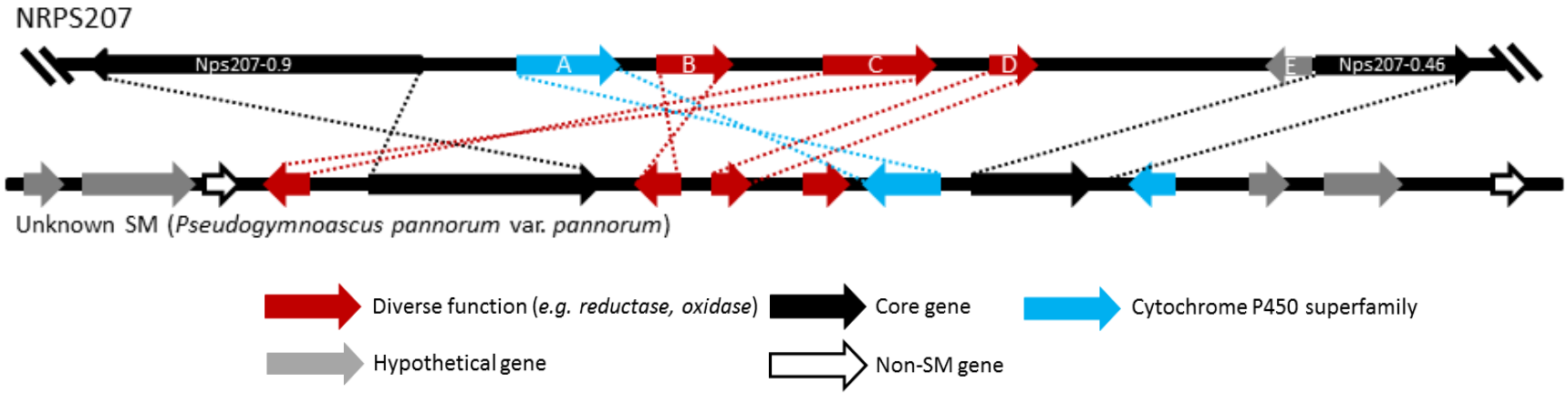

Figure 2.28: Relationship between putative *Ramularia collo-cygni* secondary metabolism cluster NRPS207 and the secondary metabolite cluster in *Pseudogymnoascus pannorum* var. *pannorum*.
NRPS207 showed similarity to an unknown SM cluster in *Pseudogymnoascus pannorum.* The cluster in *P. pannorum* and NRPS207 were highly similar with 85% of the genes between the two clusters being conserved. The two core genes *Nps207-0.9* and *Nps207-0.46* exhibited similarity to two core genes present in the *P. pannorum* cluster. Similarly, the cytochrome P450 monooxygenase (gene code A in Table 2.16) showed similarity to a cytochrome P450 monooxygenase in *P. pannorum*. The aminotransferase, carbamoyltransferase and oxidase (gene code B, C and D respectively) identified in the NRPS207 cluster exhibited similarity to genes found in the *P. pannorum* cluster. The *P. pannorum* cluster is drawn based on AntiSMASH data. Clusters are not drawn to scale. The putative function of the genes present in NRPS207 is given in Table 2.16.

Table 2.16: Protein BLAST hits table for the genes identified in cluster NRPS207.

Gene code	Putative function of Rcc gene model [1]	Organism [2]	Accession number	E-value	Query cover	Identity
Nps207-0.9	NRPS	*Pseudogymnoascus pannorum*	KFY60100.1	0.0	98%	81%
A	Cytochrome P450 monooxygenase	*Pseudogymnoascus pannorum*	KFY60096.1	1e-178	94%	54%
B	Aminotransferase	*Pseudogymnoascus pannorum*	KFY60097.1	3e-136	76%	64%
C	Carbamoyltransferase	*Pseudogymnoascus pannorum*	KFY60101.1	0.0	99%	90%
D	Oxidase	*Pseudogymnoascus pannorum*	KFY60098.1	6e-156	100%	90%
E	Hypothetical	*Acidomyces richmondensis*	KYG41239.1	6e-38	82%	44%
Nps207-0.46	NRPS	*Pseudogymnoascus pannorum*	FY60095.1	0.0	99%	82%

[1] The putative function of Rcc gene models is based on a consensus across all BLAST hits in the NCBI nr database. [2] BLASTp analyses were carried out in the *Pseudogymnoascus pannorum* var. *pannorum* F-4520 (FW-2644) (taxid: 1420915) database for Rcc genes with matches to the P*. pannorum* secondary metabolism cluster. The best BLAST hit in the nr database is presented for Rcc genes which had no match to the P*. pannorum* cluster.

Genes identified in the NRPS134 cluster exhibited similarity to the ferricrocin cluster in *Schizosaccharomyces pombe* as well as to a ferricrocin-like cluster in *Cladosporium fulvum* and its sister species *Dothistroma septosporum* (Figure 2.29 and Table 2.17). The ferricrocin cluster in *S. pombe* comprises two genes, the NRPS *Sib1* and a divergently transcribed L-ornithine N5-oxygenase (Schwecke *et al.*, 2006). These two genes have putative paralogues in NRPS134. This result supports the phylogenetic relationship between *Nps134-0.394* and *S. pombe Sib1*. However, in Rcc the cluster differs from that in *S. pombe*. In cluster NRPS134 a putative ABC transporter-encoding gene was inserted between the two ferricrocin genes. This organisation has been reported in a ferricrocin-like cluster in *C. fulvum* (Collemare *et al.*, 2014). These three genes in the *C. fulvum* cluster were similar to *Nps134-0.394*, gene D and E in cluster NRPS134. The same genes in NRPS134 demonstrated co-linearity with genes located at the *D. septosporum Nps2* locus. The organisation of this cluster appeared to be conserved in the three Dothideomycetes. Taken together with the phylogenetic study, this suggests that Rcc might produce a siderophore of the ferricrocin type.

A detailed study of the genes located at the NRPS301 locus indicated that cluster NRPS301 was similar to a SM cluster located in scaffold 20 of *Bipolaris sorokiniana* (syn. *Cochliobolus sativus*) with no known SM product characterised to date. Ten of the twelve genes identified in NRPS301 were found to have putative paralogues in *B. sorokiniana* (Figure 2.30 and Table 2.18). Both clusters revealed the presence of two NRPSs. The organisation of the genes located at the *Nps301-0.34* locus was conserved in both species, despite some rearrangement at the *Nps301-0.83* locus. A putative MFS transporter located in the centre of the NRPS301 cluster was similar to a MFS gene located 5970 bp downstream of the cluster in *B. sorokiniana*. How this gene evolved in Rcc or *B. sorokiniana* is unknown. Considering that the *B. sorokiniana* cluster comprises double the number of genes identified in Rcc NRPS301, the two resulting putative SM might exhibit very different chemical structures and properties.

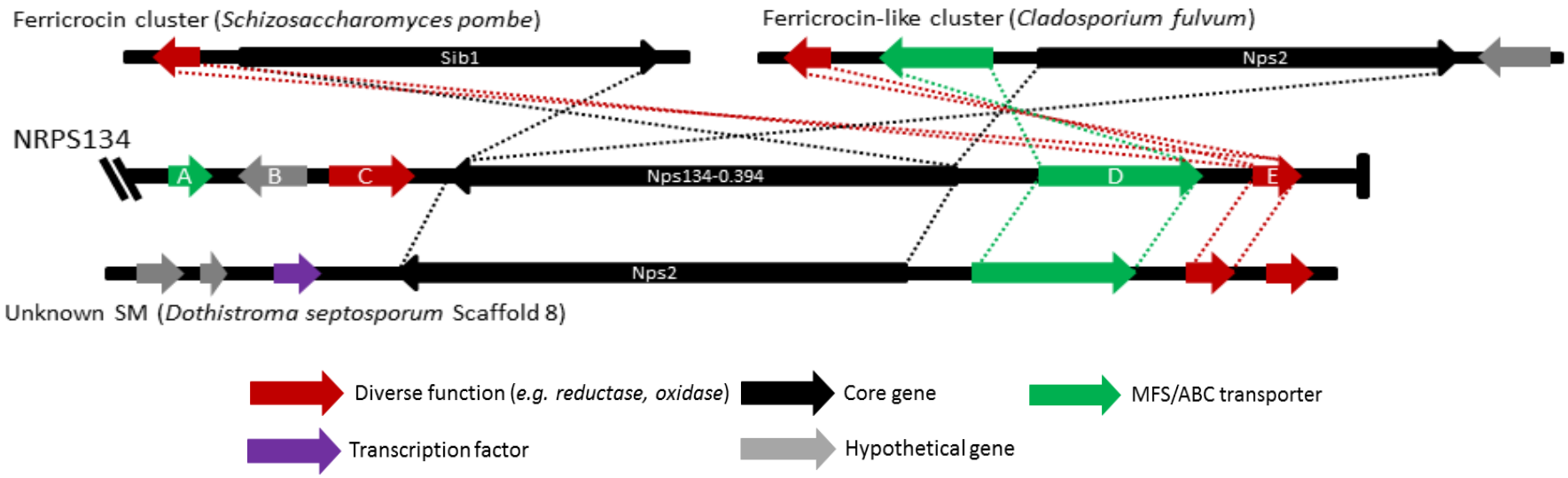

Figure 2.29: Relationship between putative *Ramularia collo-cygni* secondary metabolism cluster NRPS134 and the secondary metabolite clusters in *Schizosaccharomyces pombe*, *Cladosporium fulvum* and *Dothistroma septosporum*.
NRPS134 showed similarity to the ferricrocin biosynthesis cluster in *Schizosaccharomyces pombe* as well as a ferricrocin-like cluster in *Cladosporium fulvum* and its sister species *Dothistroma septosporum*. The core gene *Nps134-0.394* exhibited similarity to the core gene *Sib1* in *S. pombe* as well as to the *Nps2* core genes in both *C. fulvum* and *D. septosporum*. The L-ornithine N5 oxygenase (gene code E in Table 2.17) was similar to that found in *S. pombe*, *C. fulvum* and *D. septosporum*. An ABC transporter (gene code D) inserted between *Nps134-0.394* and the L-ornithine N5 oxygenase in NRPS134 showed similarity to genes encoding for ABC transporters located between the core gene and the L-ornithine N5 oxygenase in both the *C. fulvum* and *D. septosporum* clusters. The *S. pombe* and *D. septosporum* clusters are drawn based on AntiSMASH data. The *C. fulvum* cluster is drawn based on Collemare *et al.* (2014). Clusters are not drawn to scale. The putative function of the genes present in NRPS134 is given in Table 2.17.

Table 2.17: Protein BLAST hit table for the genes identified in NRPS134.

Gene code	Putative function of Rcc gene model [1]	Organism [2]	Accession number	E-value	Query cover	Identity
A	MFS transporter	*Pseudocercospora musae*	KXT09413.1	4e-164	100%	78%
B	Hypothetical	*Zymoseptoria tritici*	KJY00519.1	0.0	100%	78%
C	α/β hydrolase	*Aspergillus flavus*	KOC18179.1	3e-42	87%	51%
Nps134-0.394	NRPS (Sib1)	*Dothistroma septosporum* *Schizosaccharomyces pombe* *Cladosporium fulvum*	EME41700.1 NP_593102.1 Protein ID [3] 193954	0.0 0.0 0.0	99% 93% 173%	57% 29% 45%
D	ABC transporter	*Dothistroma septosporum* *Cladosporium fulvum*	EME41701.1 Protein ID [3] 193953	0.0 0.0	80% 100%	74% 66%
E	L-ornithine N5-oxygenase	*Dothistroma septosporum* *Schizosaccharomyces pombe* *Cladosporium fulvum*	EME41702.1 NP_593103.1 Protein ID [3] 193952	8e-153 4e-50 1e-135	100% 84% 51%	71% 40% 73%

[1] The putative function of Rcc gene models is based on a consensus across all BLAST hits in the NCBI nr database. [2] BLASTp analyses were carried out in the *D. septosporum* NZ10 (taxid: 675120) and *S. pombe* 972h- (taxid: 284812) databases for Rcc genes with matches to the S*. pombe* or *D. septosporum* secondary metabolism cluster. The best BLAST hit in the nr database is presented for Rcc genes which had no match to the S*. pombe* or *D. septosporum* secondary metabolism cluster. [3] BLASTp analyses were performed in the JGI genome portal (http://genome.jgi.doe.gov) for *C. fulvum*.

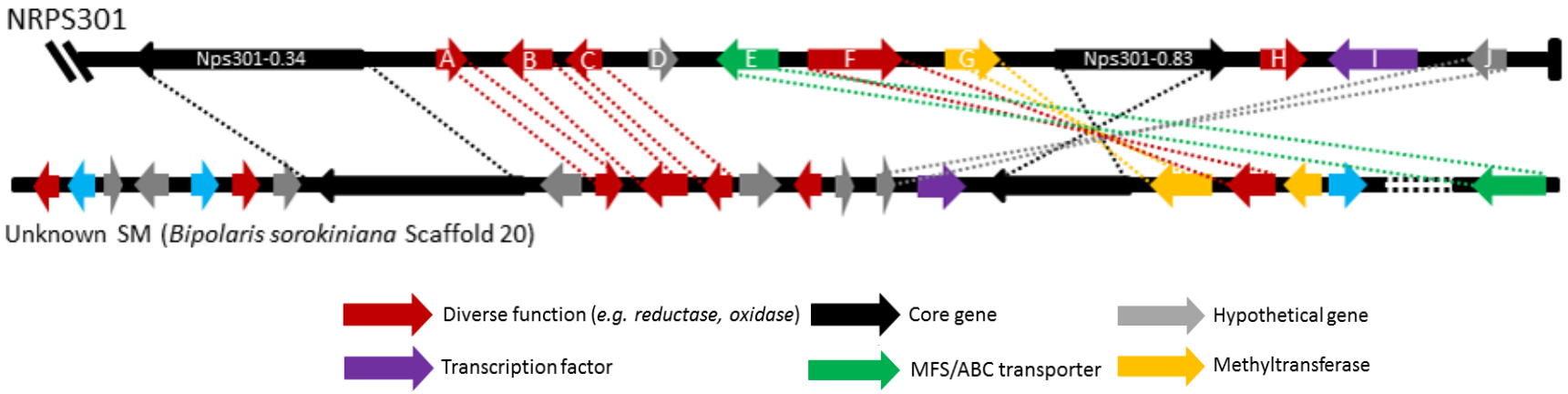

Figure 2.30: Relationship between putative *Ramularia collo-cygni* secondary metabolism cluster NRPS301 and the secondary metabolite cluster in *Bipolaris sorokiniana.*

NRPS301 showed similarity to an unknown SM cluster in *Bipolaris sorokiniana.* The cluster in B. *sorokiniana* and NRPS207 exhibited high level of conservation with 75% of the genes found in NRPS301 and in the *B. sorokiniana* clusters being conserved. The two core genes *Nps301-0.34* and *Nps301-0.83* were found to be similar to the two core genes located in the *B. sorokiniana* cluster. The aminotransferase, γ-glutamyl cyclotransferase and thioredoxin reductase (gene code A, B and C respectively in Table 2.18) were co-linear with genes of similar function in *B. sorokiniana*. Similarly, the O-methyltransferase and nucleoside transporter (gene code G and F respectively) showed similarity to genes in *B. sorokiniana*. The hypothetical gene J showed similarity to a hypothetical gene in the *B. sorokiniana* cluster. Inserted in the middle of the NRPS301 cluster, a MFS transporter exhibited similarity to a transporter encoding gene in *B. sorokiniana* found at another locus on scaffold 20. The *B. sorokiniana* cluster is drawn based on AntiSMASH data. Clusters are not drawn to scale. The putative function of the genes present in NRPS301 is given in Table 2.18.

Table 2.18: Protein BLAST hit table for the genes identified in NRPS301.

Gene code	Putative function of Rcc gene model [1]	Organism [2]	Accession number	E-value	Query cover	Identity
Nps301-0.34	NRPS	*Bipolaris sorokiniana*	XP_007705863.1	0.0	98%	53%
A	Aminotransferase	*Bipolaris sorokiniana*	XP_007705865.1	2e-52	93%	57%
B	Gamma-glutamyl cyclotransferase	*Bipolaris sorokiniana*	XP_007705866.1	2e-115	96%	63%
C	Thioredoxin reductase	*Bipolaris sorokiniana*	XP_007705867.1	1e-64	66%	74%
D	Hypothetical	*Macrophomina phaseolina*	EKG10411.1	1e-11	93%	31%
E	MFS transporter	*Bipolaris sorokiniana*	XP_007705877.1	2e-138	96%	57%
F	NCS1 transporter (nucleoside transport)	*Bipolaris sorokiniana*	XP_007705873.1	0.0	91%	65%
G	O-methyltransferase	*Bipolaris sorokiniana*	XP_007705872.1	9e-149	98%	69%
Nps301-0.83	NRPS	*Bipolaris sorokiniana*	XP_007705806.1	1e-170	45%	56%
H	Kinase	*Cenococcum geophilum*	OCK90170.1	3e-108	93%	61%
I	ZnIICys6 transcription factor	*Parastagonospora nodorum*	XP_001801523.1	7e-21	28%	35%
J	Hypothetical	*Bipolaris sorokiniana*	XP_007705871.1	8e-13	77%	30%

[1] The putative function of Rcc gene models is based on a consensus across all BLAST hits in the NCBI nr database. [2] BLASTp analyses were carried out in the *Bipolaris sorokiniana* ND90Pr (taxid: 665912) database for Rcc genes with matches to the *B. sorokiniana* secondary metabolism cluster. The best BLAST hit in the nr database is presented for Rcc genes which had no match to the *B. sorokiniana* cluster.

In addition to the clusters described above two other clusters with no core genes were identified in Rcc. One cluster, located on contig 247, contained putative paralogues to the aflatoxin fatty acid synthases (FASs) *HexA* and *HexB* (formerly *AflA* and *AflB*) (Figure 2.31). *HexA* and *HexB* are involved early in the aflatoxin biosynthetic pathway and their homologs in *D. septosporum* (also named *HexA* and *HexB*) play a similar role in dothistromin biosynthesis (Yu *et al.*, 2004; Chettri *et al.*, 2013; Kabir *et al.*, 2015). *HexA* and *HexB* are involved in the biosynthesis of a fatty acid subsequently used by the non-reducing PKS *PksA* to produce the backbone of aflatoxin and dothistromin. In Rcc, the fatty acid subunit α and β located on contig 247 appeared to be the only FASs present in the genome. Furthermore, in both *D. septosporum* and *Aspergillus* spp. the expression of *HexA* and *HexB* is under the regulation of a cluster-specific transcription factor encoded by *AflR* (Woloshuk *et al.*, 1994; Ehrlich *et al.*, 1999; Chettri *et al.*, 2013). AflR protein, which is a zinc cluster protein, regulates the expression of aflatoxin and dothistromin biosynthetic genes upon binding specific motifs in the promoter region of the regulated genes (Fernandes *et al.*, 1998; Ehrlich *et al.*, 1999; Zhang *et al.*, 2007). The identification, *in silico*, of an *AflR* binding motif 5'-TCG(N_{11})CGR-3' (Zhang *et al.*, 2007) located in the promoter region of both paralogues of *HexA* and *HexB* in Rcc support the similarity between these FASs in Rcc and the ones involved in the aflatoxin intermediate sterigmatocystin and dothistromin biosynthesis which also exhibited *AflR* binding motifs (Fernandes *et al.*, 1998; Chettri *et al.*, 2013).

The second SM cluster with no core gene identified in this study was located on contig 113 and contained a putative paralogue of the *MoxY* gene (formerly *AflW*) in aflatoxin biosynthesis (Figure 2.32). *MoxY* encodes a monooygenase involved in the biosynthesis of versicolorin A, an intermediate in aflatoxins biosynthesis (Chang *et al.*, 2007). Similarly to what was found on contig 247, the promoter region of the *MoxY* paralogue in Rcc contained one *AflR* binding motif 5'TCG(N_{10})TCG-3' (Fernandes *et al.*, 1998) which is reminiscent to the results observed in dothistromin and sterigmatocystin biosynthesis (Fernandes *et al.*, 1998; Chettri *et al.*, 2013).

A)

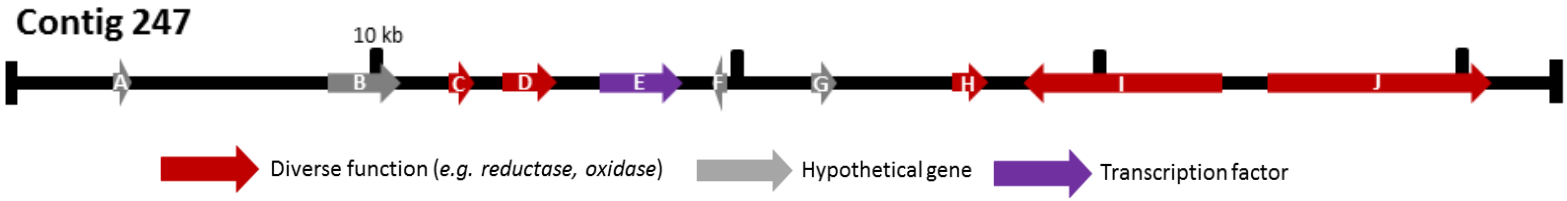

B)

Gene code	Putative function[1]	Organism[2]	Accession number	E-value	Query cover	Identity
A	Hypothetical	*Pseudocercospora musae*	KXS97409.1	4e-60	100%	56%
B	Hypothetical	*Zymoseptoria tritici*	XP_003854635.1	0.0	95%	46%
C	Monooxygenase	*Dothistroma septosporum*	EME48372.1	5e-77	92%	55%
D	Aldo/Keto-reductase	*Sphaerulina musiva*	XP_016759519.1	0.0	96%	82%
E	C2H2 transcription factor	*Sphaerulina musiva*	XP_016759520.1	0.0	99%	62%
F	Hypothetical	*Zymoseptoria tritici*	XP_003853645.1	4e-12	81%	43%
G	Hypothetical	*Sphaerulina musiva*	XP_016759390.1	3e-61	99%	54%
H	Arginino-succinate synthase	*Zymoseptoria brevis*	KJY01670.1	0.0	96%	87%
I	Fatty acid synthase α-subunit (*HexA*)	*Zymoseptoria tritici*	XP_003854656.1	0.0	99%	90%
J	Fatty acid synthase β-subunit (*HexB*)	*Zymoseptoria tritici*	XP_003853632.1	0.0	96%	90%

Figure 2.31: Identification of a putative secondary metabolite cluster with no core gene on *Ramularia collo-cygni* contig 247.
A) Schematic representation of the SM-related cluster located on contig 247. Arrows indicates ORF putative transcription direction. B) Protein BLAST hit table for the genes identified in the cluster on contig 247.[1] The putative function of Rcc gene models is based on a consensus across all BLAST hits in the NCBI nr database. [2] The best BLAST hits in the nr database are presented.

A)

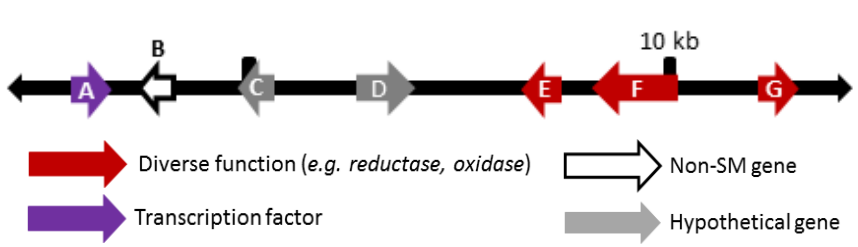

B)

Gene code	Putative function[1]	Organism[2]	Accession number	E-value	Query cover	Identity
A	Eukaryotic translation initiation factor 3 subunit	*Zymoseptoria brevis*	KJX97504.1	1e-106	91%	80%
B	ATP phospho-ribosyltransferase	*Pseudocercospora fijiensis*	XP_007928772.1	1e-112	90%	82%
C	Hypothetical	*Dothistroma septosporum*	EME39606.1	3e-34	88%	41%
D	Hypothetical (putative transcription factor)	*Pseudocercospora musae*	KXT13065.1	6e-85	44%	72%
E	Sterigmatocystin biosynthesis monooxygenase *StcW*-like (*MoxY*)	*Zymoseptoria brevis*	KJX97020.1	8e-116	95%	66%
F	Hydrolase	*Zymoseptoria brevis*	KJX97019.1	0.0	99%	61%
G	Hydrolase	*Baudoinia panamericana*	XP_007681689.1	7e-48	95%	50%

Figure 2.32: Identification of a putative secondary metabolite cluster with no core gene on *Ramularia collo-cygni* contig 113.
A) Schematic representation of the SM-related cluster located on contig 113. Arrows indicates ORF putative transcription direction. B) Protein BLAST hit table for the genes identified in the cluster on contig 113.[1] The putative function of Rcc gene models is based on a consensus across all BLAST hits in the NCBI nr database. [2] The best BLAST hits in the nr database are presented.

The present study suggests that Rcc possesses the genetic capacity to produce a wide range of SMs. Based on antiSMASH predictions Rcc appeared to have clusters with differing degrees of similarity to five clusters that produce known SMs, namely betaenone, monodictyphenone, gliotoxin, ferricrocin and chaetoglobosin, as well as an uncharacterised gliotoxin-like cluster. The detailed study of Rcc SM putative clusters also showed similarity to many unknown SM clusters identified in other fungal species. On several occurrences, similarity was found between Rcc and *Z. tritici* SM clusters further highlighting the close relationship between the two sister species (McGrann *et al.*, 2016). Some putative Rcc SM clusters were not found in Dothideomycetes but in other fungi of the Ascomycota phylum. This result suggests that SM clusters are shared and conserved between fungi. This was supported by the phylogenetic analysis carried out on the protein encoded by the core genes found in these clusters.

2.4. Discussion

The genomes of filamentous ascomycetes and specifically of Dothideomycetes possess a large number of SM-related genes which often result in the ability to produce a wide range of chemical compounds (Kroken *et al.*, 2003; Bushley & Turgeon, 2010). Previous analysis of the Rcc genome revealed the presence of 19 PKSs, fourteen NRPSs and four TCs. No DMATS nor HPS were identified in the draft genome assembly (McGrann *et al.*, 2016). The present analysis gave contrasting results as ten putatively functional PKSs, three hybrids PKS/NRPS and a total of 22 NRPS domain-containing proteins were identified. However, considering that the domain organisation in NRPSs does not necessarily impact functionality, assessing *in silico* the functionality of this type of protein is difficult. Based on current knowledge of the required domains essential for functional type A and type B NRPSs, namely the initiation module A-PCP and termination C or TE domain, and assuming that no sequencing error occurred in the sequences of the genes encoding these Rcc proteins, ten putative NRPSs are predicted to be functional. The other twelve Rcc NRPSs identified may still be functional but are unlikely to belong to the type A or type B NRPSs. The discrepancy observed between the result of this study and that of McGrann *et al.* (2016) could be explained by the difference in methods used to identify putative core genes. McGrann *et al.* (2016) used Blast2GO analyses to identify SM core genes whereas the present study interrogated at a nucleotide level the genome of Rcc. Furthermore, this study also investigated putative core gene domain organisation. When compared to other members of the Dothideomycetes, Rcc has similar numbers of PKSs as most of the hemibiotrophic fungi which was on average nine (Ohm *et al.*, 2012). The number of NRPSs identified in Rcc is closer to that observed in necrotrophic Dothideomycete fungi of the order Pleosporales which have on average twelve (Table 2.19). Rcc has been classified as an endophyte with a necrotrophic phase (Salamati & Reitan, 2006). The observation that Rcc possesses substantially more PKSs and NRPSs than other endophytes in the Dothideomycetes such as *Aureobasidium pullulans* spp. (Gostincar *et al.*, 2014) supports this hypothesis. The genome of Rcc appeared to contain more HPSs than many other hemibiotrophic Dothideomycetes. However, this discrepancy could arise from the

fact that different methods have been used to identify core genes in previously published studies (de Wit *et al.*, 2012; Rudd *et al.*, 2015; Noar & Daub, 2016a).

Table 2.19: Comparison of the number of core genes between *Ramularia collo-cygni* and other fungi.

Class	Species	PKS	NRPS	HPS	Lifestyle
Dothideomycete	*Ramularia collo-cygni*	10	10	3	Endophyte/necrotroph
Dothideomycete[g]	*Aureobasidium pullulans var. melanogenum*	5	2	0	Endophyte
Dothideomycete[g]	*Aureobasidium pullulans var. pullulans*	1	3	0	Endophyte
Dothideomycete[g]	*Aureobasidium pullulans var. subglaciae*	6	2	3	Endophyte
Dothideomycete[b]	*Zymoseptoria tritici*	11	6	2	Hemibiotroph
Dothideomycete[c]	*Pseudocercospora fijiensis*	7	8	2	Hemibiotroph
Dothideomycete[a]	*Sphaerulina musiva*	9	7	2	Hemibiotroph
Dothideomycete[b]	*Dothistroma septosporum*	5	3	2	Hemibiotroph
Dothideomycete[a]	*Leptosphaeria maculans*	10	5	0	Hemibiotroph
Dothideomycete[d]	*Cladosporium fulvum*	8	5	1	Biotroph
Dothideomycete[a]	*Bipolaris sorokiniana*	13	11	0	Hemibiotroph
Dothideomycete[a]	*Bipolaris maydis C4*	19	10	1	Necrotroph
Dothideomycete[a]	*Bipolaris maydis C5*	19	9	0	Necrotroph
Dothideomycete[a]	*Setosphaeria turcica*	23	10	1	Necrotroph
Dothideomycete[b]	*Parastagonospora nodorum*	22	10	2	Necrotroph
Dothideomycete[a]	*Bipolaris victoriae*	14	8	2	Necrotroph
Dothideomycete[a]	*Macrophomina phaseolina*	20	13	3	Necrotroph
Dothideomycete[a]	*Neofusicoccum parvum*	16	10	3	Necrotroph
Dothideomycete[a]	*Pyrenophora teres f. teres*	17	24	1	Necrotroph
Dothideomycete[a]	*Pyrenophora tritici-repentis*	14	10	1	Necrotroph
Dothideomycete[a]	*Hysterium pulicare*	21	5	2	Saprotroph
Dothideomycete[a]	*Rhytidhysteron rufulum*	28	11	5	Saprotroph
Dothideomycete[e]	*Baudoinia compniacensis*	2	2	0	Saprotroph/extremophile
Sordariomycete[a]	*Colletotrichum graminicola*	33	4	4	Hemibiotroph
Sordariomycete[f]	*Fusarium graminearum*	15	19	1	Necrotroph
Eurotiomycete[a]	*Penicillium expansum*	25	15	6	Necrotroph
Eurotiomycete[b]	*Aspergillus nidulans*	26	10	2	Saprotroph
Leotiomycete[a]	*Marssonina brunnea f sp. multigermtubi*	6	2	1	Hemibiotroph
Leotiomycete[a]	*Botrytis cinerea*	13	7	1	Necrotroph

[a] data obtained on the jgi website (http://genome.jgi.doe.gov) (October 2016)
[b,c,d,e,f,g] data from de Wit *et al.* (2012); Chang *et al.* (2016); Collemare *et al.* (2014); Ohm *et al*, (2012); Hansen *et al.* (2012); Gostincar *et al.* (2014), respectively.

In the present study, 26 gene clusters containing SM core genes were identified in the Rcc genome. Few of the gene clusters appeared to be complete, containing putative paralogues of each gene necessary to result in the production of a known SM. PKS30 and HPS14 a betaenone-like cluster and a chaetoglobosin-like cluster respectively, are arguably the most relevant examples as they both contained

paralogues of all the genes found in the original betaenone and chaetoglobosin clusters. The HPS14 cluster contained the seven genes involved in the biosynthesis of chaetoglobosin A in *Penicillium expansum* and two additional genes, a putative O-methyltransferase and a MFS transporter. Chaetoglobosins are known to have cytotoxic properties (Ohtsubo *et al.*, 1978) and to exhibit antifungal effect (Zhang *et al.*, 2013). Considering that Rcc develops as an endophyte one possible hypothesis for chaetoglobosins, if produced, could be in protecting the host from other fungal infection therefore protecting Rcc habitat. Rcc being a slow growing fungus (Salamati *et al.*, 2002; Walters *et al.*, 2008), another possible role for chaetoglobosin could be to eliminate potential competing fungi from the leaf surface prior to penetration or sporulation which is known to occur primarily through the stomata (Stabentheiner *et al.*, 2009). Similarly, the PKS30 cluster contained paralogues to all the genes involved in betaenone biosynthesis in *P. betae*. Betaenones are phytotoxin associated with leaf spot disease of sugar beet as the toxin was shown to induce leaf chlorosis (Ichihara *et al.*, 1983). To date Rcc is known to produce only one family of non-host specific toxins called rubellins that have been associated with disease expression, however, if betaenones are also synthesised by Rcc, it is possible that the fungus is releasing several phytotoxins during the necrotrophic stage of disease development. Notwithstanding the fact that the genome of Rcc appears to contain numerous genes encoding proteins involved in SMs production, based on related organisms is it not likely that Rcc will produce multiple SMs during necrotrophic development. Although many SM core genes are highly expressed during the necrotic stage of disease development in the closely related species *D. septosporum*, only one phytotoxin, dothistromin, has been isolated from lesions to date (Bradshaw *et al.*, 2016).

The analysis of the Rcc genome carried out in this study may provide insights into the biosynthetic pathway resulting in rubellin production. Rubellins are structurally related to previously characterised anthraquinone SMs such as cladofulvin, endocrocin or emodin that are synthesised by *C.fulvum*, *A. fumigatus* and *A. nidulans* via the polyketide pathway through the action of the NR-PKSs *ClaG*, *EncA* and, *Acas* and *MdpG*, respectively (Chiang *et al.*, 2010; Lim *et al.*, 2012;

Griffiths *et al.*, 2016). Of the three NR-PKSs identified in the Rcc genome, *Pksm24-1.219* appears to be a strong candidate for rubellin biosynthesis. The SAT-KS-AT-PT-ACP domain organisation of *Pksm24-1.219*, resembles that of *ClaG*, *EncA* and *MdpG*. Further supporting this result, the protein encoded by *Pksm24-1.219* is related to the above mentioned NR-PKSs as it belongs to the same clade as the proteins encoded by *ClaG*, *EncA*, Acas and *MdpG* (Figure 2.13). Finally, *Pksm24-1.219* is located in a cluster containing putative paralogues of genes present in the monodictyphenone biosynthetic cluster in *A. nidulans* which is known to yield emodin and emodin analogues including chrysophanol (Chiang *et al.*, 2010; Simpson, 2012). As the chemical structure of rubellin resembles that of a dimer of chrysophanol, these results suggest that the PKSm24 cluster may be a strong candidate for rubellin biosynthesis.

However, based on the data presented in this study, *Pksm46-0.119* may also be involved in rubellin biosynthesis. The protein encoded by *Pksm46-0.119* exhibits a domain organisation found in NR-PKSs involved in anthraquinone biosynthesis and was also located in a clade that comprise several PKSs involved in anthraquinone synthesis such as *PksA* from *D. septosporum*. However, the protein encoded by *Pksm46-0.119* also exhibits the same domain organisation and appeared to be related to enzymes involved in perylenequinone biosynthesis such as the elsinochrome synthase *Pks1* from *E. fawcetii* (Liao & Chung, 2008a). *E. fawcetii Pks1* is also related to the conidial pigment dihydroxynaphtalene (DHN) melanin synthetic gene *PKS18* from *B. maydis* (Liao & Chung, 2008a), therefore, including additional sequences in the phylogenetic, study such as those of proteins involved in DHN melanin biosynthesis, may help to further support *Pksm24-1.219* as the best NR-PKS candidate for rubellin biosynthesis in Rcc. Functional analysis of *Pksm24-1.219* and *Pksm46-0.119* may provide further evidence for the roles of these two PKSs is rubellin biosynthesis in Rcc. Genetic transformation of Rcc is possible (Thirugnanasambandam et al., 2011) and using targeted gene knock outs of *Pksm24-1.219* and *Pksm46-0.119* followed by biochemical analysis of fungal metabolites produced by the transformed isolates under rubellin inductive conditions (Heiser et al., 2003; 2004) should confirm whether or not these two PKSs are important in the biosynthesis of rubellin in Rcc.

In addition to the findings of McGrann *et al.* (2016) who identified on contig 17 a 40 kb SM-related cluster containing putative paralogues of the aflatoxin *AflR* and *OrdB* (formerly *AflX*) genes but did not contain any core gene, the present study identified two gene clusters with no core gene that contained putative paralogues of genes involved in aflatoxin and dothistromin biosynthesis. Taken together these results confirm that of McGrann *et al.* (2016) suggesting that the organisation of Rcc metabolic clusters is fragmented. Rcc paralogues of a SM biosynthesis pathway such as aflatoxin or dothistromin appeared to be distributed across different contigs/scaffolds in the Rcc genome and located within distinct clusters. Gene cluster fragmentation has also been reported for other Dothideomycetes. The genes responsible for dothistromin biosynthesis are present across six clusters scattered on chromosome XII plus a single gene found on chromosome XI in *D. septosporum* (Chettri *et al.*, 2013). This pathway is even more fragmented in *C. fulvum*, the sister species of *D. septosporum* (de Wit *et al.*, 2012). However, this fragmentation does not appear to affect functionality of the pathway in *D. septosporum* which is able to produce dothistromin. Whether a given pathway is functional seems to rely mostly on the functionality of key genes involved in that pathway. Key genes such as SM core genes are generally involved early in the pathway and their expression results in the biosynthesis of the backbone of the SM. Mutants of *D. septosporum* lacking the functional core gene *PksA*, the third gene involved in the dothistromin biosynthesis pathway, were unable to produce dothistromin (Bradshaw *et al.*, 2006). Similarly, two genes involved at an early stage in the same pathway, *HexA* and *Nor1*, in *C. fulvum* contain non-sense mutations resulting in a non-functional pathway (Chettri *et al.*, 2013).

Therefore, locating putative non-core gene containing SM clusters and studying their homology with other fungal clusters might help identify SM pathways present in Rcc. A study of the functionality of the key genes involved in these pathways might give better insight into the complete arsenal of SM potentially produced by Rcc. Furthermore, considering that some of the core genes identified in Rcc were located at the end of their contig or scaffold such as *Pksm46-0.119* and *Nps100*, re-sequencing the genome using a technology yielding longer reads such as single

molecule real time (SMRT) sequencing might help identify new SM-related clusters or complete already identified ones (Faino *et al.*, 2015).

The detailed study of the clusters identified in Rcc revealed that more than half (15 out of 28 clusters) showed similarity to other clusters in different species. A potential explanation could be that these clusters may have been present in the common ancestor of all these fungal species and due to different evolution pathways undergone by these species some clusters may have been lost in certain species and conserved in others. Another possible hypothesis to explain the similarity between gene clusters across several fungal families could be the effect of horizontal gene transfer (HGT) at an ancestral level. Horizontal gene transfer in contrast to vertical gene transfer, from parents to offspring, is the exchange and integration of genetic information between species (Doolittle, 1999). Therefore, several species can share common loci. As a result, several taxonomically unrelated fungi might share SM clusters and a given SM may be produced by a wide range of species.

In this study seven out of the 15 examined clusters showed similarity only to a putative SM cluster from a Dothideomycete. Five of them were found in very closely related species with three in *Z. tritici*, one in *D. septosporum* and one in *P. fijiensis* suggesting that the putative SM or their derivatives could be shared across species in this phylogenetic clade. Six clusters showed similarity only to clusters found in fungi from a different class of which three were similar to Eurotiomycete clusters, two Sordariomycete clusters and one Rcc SM cluster was most similar to a SM cluster found in both Eurotiomycetes and Sordariomycetes. The identification of syntenic or co-linear blocks of genetic material such as gene clusters in unrelated fungal species and absent in related ones is generally considered as evidence of HGT (Fitzpatrick, 2012). HGT has been shown to occur frequently in fungi and plays a crucial role in fungal genome evolution (Marcet-Houben & Gabaldón, 2010). A complete, functional and highly conserved sterigmatocystin cluster from the Sordariomycete *Podospora anserina* was shown to have been horizontally transferred from a Eurotiomycete *Aspergillus* species (Slot & Rokas, 2011). HGT was shown to occur particularly often in the Pezizomycotina, the clade that comprises amongst other classes the Eurotiomycetes, Leotiomycetes, Sordariomycetes and Dothideomycetes (Marcet-Houben & Gabaldón, 2010). The results in this study support a possible role

for HGT between Rcc and other fungi and could explain how a given SM cluster might be shared by several unrelated or distantly related fungi. Although most of the clusters identified in Rcc only showed similarity of few genes with other clusters, it has been shown that clusters involved in a given pathway in different fungi can differ partially in terms of gene number and ontology (Ohm *et al.*, 2012). The chaetoglobosin A cluster in the Sordariomycete *Chaetomium globosum* comprises nine genes while this cluster in the Eurotiomycete *P. expansum* only comprises seven genes (Schumann & Hertweck, 2007; Ishiuchi *et al.*, 2013). Therefore, the chaetoglobosin-like cluster identified in Rcc, HPS14, might be involved in the production of this specific SM even though it contains a methyltransferase and a MFS transporter not found in the chaetoglobosin A cluster in other fungi. The same reasoning can be applied to other Rcc clusters such as the betaenone-like SM cluster identified on contig 30. However, considering that many clusters in Rcc appeared to be fragmented, more work is required to assess whether Rcc possesses more paralogues to known clusters. For instance mining the genome for paralogues of the genes involved in a given pathway may reveal the presence of other SM-related clusters. Further investigation of the clusters identified in this study such as locating transposable elements or repetitive DNA may also give insight into the evolution and transcription dynamics of SM-related clusters. Characterisation of new SMs produced by Rcc may also provide insights into the functionality of some clusters identified in this study.

Although the present study suggests that Rcc has the genetic potential to produce a large variety of SM, it is unlikely that all the putative clusters identified will result in a functional pathway. The presence of numerous non-functional pathways is recurrent in fungal genomes. Analysis of the *Fusarium graminearum* genome revealed the presence of 15 PKSs, 19 NRPSs, one HPS and eight TCs, suggesting that this fungus has the genetic potential to produce as many as 40 different families of SM. However, only eight SM families have been reported to be synthesised by *F. graminearum* confirming that many pathways are non-functional or maintained cryptic. The number of predicted SM in *F. graminearum* is similar to that predicted for the entire *Fusarium* genus (Ma *et al.*, 2013). Similarly, the recently sequenced

genome of *P. fijiensis* revealed the presence of seven PKS-based SM clusters but only one showed high homology to a cluster involved in melanin biosynthesis (Noar & Daub, 2016a). This raises the question of knowing whether these pathways are cryptic and only expressed in very specific conditions or if they are non-functional, and if non-functional why are these pathways retained over time? A possible explanation for retaining non-functional gene clusters could be the redundancy of some genes present in such clusters. For instance, a loss of function mutation of the PKS found in the endocrocin cluster, *EncA*, in *A. fumigatus* did not abolish endocrocin production. This was only achieved when the PKS found in the trypacidin cluster, *TpcC*, was also mutated, suggesting that both NR-PKSs *EncA* and *TpcC* can result in the production of the same SM (Throckmorton *et al.*, 2016). Although both trypacidin and endocrocin pathways are functional in *A. fumigatus* it is possible that some non-functional gene clusters may be retained if they contain genes exhibiting redundant function with other genes found in functional pathways.

This chapter focussed on the identification and characterisation *in silico* of SM clusters in Rcc. Considering that many fungal SMs are involved in disease expression in plants, for instance as virulence factors such as dothistromin (Kabir *et al.*, 2015) or as pathogenicity factor such as HC-toxin (Cheng *et al.*, 1999), the next chapter will investigate the expression of SM core genes during RLS development. This could provide insight into the role played by the putative SMs produced by Rcc during the infection process

Chapter 3:

Expression of *Ramularia collo-cygni* secondary metabolism-related core genes during the development of Ramularia leaf spot on barley seedling

3.1. Secondary metabolites and disease development

It is widely understood that the arsenal of secondary metabolites (SMs) produced by a given fungal plant pathogen is related to its lifestyle. Biotrophic fungi produce effector proteins and SMs that manipulate the host to facilitate pathogen colonisation through inactivation of the host defence response. In contrast, necrotrophs have a secretome enriched in toxic SMs such as phytotoxins that trigger plant cell death to induce the release of nutrient to provide the fungus with a source of energy (Horbach *et al.*, 2011). However, this distinction becomes less clear for fungi like Rcc that develop with both an endophytic and necrotrophic phase. Investigating the expression of SM-related core genes during disease development in Rcc might provide valuable insights into the potential role played by SMs in the expression of RLS in barley.

3.1.1. Phytotoxins in disease development

Many phytotoxins are SMs produced by fungal pathogens that are often involved in plant-pathogen interactions by inducing host cell death via diverse mechanisms (Stergiopoulos *et al.*, 2013). These SMs can modulate the severity of disease symptoms, in the case of virulence factors such as dothistromin, a toxin produced by the pine needle pathogen *Dothistroma septosporum* (syn. *Mycosphaerella pini*) (Kabir *et al.*, 2015), or in some cases define the ability of the producing fungus to cause disease which is typical of pathogenicity factors such as the perylenequinone toxin cercosporin produced by *Cercospora kikuchii* (Upchurch *et al.*, 1991). Dothideomycetes, the class of fungi to which Rcc belongs, are known to produce different types of phytotoxins, some are host specific toxins (HSTs) whereas others do not demonstrate host specificity and are termed, non-HSTs (Berestetskiy, 2008).

3.1.1.1.Role of host specific toxins

Host specific toxins induce cell death only in a restrictive group of plant species and sometimes only on specific plant cultivars. The victorin toxin produced by

Bipolaris victoriae (syn. *Cochliobolus victoriae*), the fungus responsible of the Victoria blight on oats (*Avena sativa*), has been shown to induce cell death only on cultivars carrying the *Pc-2* gene conferring resistance to the crown rust fungus *Puccinia coronata* f. sp. *avenae* (Navarre & Wolpert, 1999). Victorin induces programmed cell death (PCD), a genetically determined process resulting in organised cell destruction, by interacting with a nucleotide-binding site leucine-rich-repeat (NB-LRR) membrane receptor which results in ions fluxes, notably Ca^{2+} influx that serves as a signal to initiate defence mechanisms including PCD (Tada *et al.*, 2005; Sweat & Wolpert, 2007). The specificity of HSTs for a given host target often dictates both the success or failure of disease development and consequently the host range of the fungus. Some HSTs such as victorin toxin act as pathogenicity factors. Only the Victorin-sensitive oat cultivars were shown to be susceptible to Victoria blight (Lorang *et al.*, 2004). Almost all HSTs known to date are produced by Dothideomycetes (Stergiopoulos *et al.*, 2013). HC-toxin and T-toxin produced by *Bipolaris zeicola* (syn. *Cochliobolus carbonum*) and *Bipolaris maydis* (syn. *Cochliobolus hetersotrophus*), respectively, have been particularly well studied because of their role in northern corn leaf spot and southern corn leaf blight. Both of these well studied toxins are considered models in this research field in terms of mode of action and role of HSTs (Baker *et al.*, 2006; Walton, 2006).

3.1.1.2.Role of non-host specific toxins

In contrast to HSTs, non-HSTs exhibit biological activity on a wide range of cell types in organisms belonging to different taxa (Berestetskiy, 2008). This lack of specificity arises from the fact that many targets of non-HSTs are widely conserved molecules or pathways across taxonomic kingdoms. Many non-HSTs induce cell death by triggering the production of toxic reactive oxygen species (ROS) such as hydrogen peroxide (H_2O_2), superoxide ($O_2^{\bullet-}$), singlet oxygen ($^1O_2$) or hydroxyl radicals ($OH^{\bullet}$). This mode of action is particularly common in photoactivated toxins belonging to the perylenequinones family (Daub *et al.*, 2005). Perylenequinones are polyketide-derived photosensitisers with a chemical structure based on a penta-cyclic chromophore core and generally exhibiting axial symmetry (Daub & Chung, 2007).

Photosensitisers are molecules that are able to convert light energy into chemical energy through the production of highly energetic ROS (Valenzeno & Pooler, 1987). Cercosporin, a perylenequinone toxin produced by *Cercospora* species, was shown to induce cell death in different cell types such as animal cells or bacteria via singlet oxygen-mediated lipid peroxidation (Cavallini *et al.*, 1979). Although cercosporin is a non-HST, it has been shown to play an important role in disease development in *Cercospora nicotianae* (Choquer *et al.*, 2005). Despite belonging to a different chemical family, the anthraquinone rubellins produced by Rcc were found to share a similar mode of action with the perylenequinones, as rubellins are also light-activated and thought to induce singlet oxygen- and superoxide-mediated fatty acid peroxidation (Heiser *et al.*, 2004).

The epipolythiodioxopiperazines (ETPs) are NRP-derived, non-HSTs toxins produced only by fungi and exhibiting an intramolecular disulphide bridge. The toxicity of ETPs was imputed to the presence of this highly reactive disulphide bridge (Mullbacher *et al.*, 1986). The mode of action of ETPs involves both ROS formation and protein inactivation (Gardiner *et al.*, 2005b). Gliotoxin produced by *Aspergilli* species, notably *Aspergillus fumigatus* has been shown to target a transcription factor involved in the immune response in animal cells (Pahl *et al.*, 1996) as well as mitochondrial proteins (Salvi *et al.*, 2004) and proteasome-mediated protein degradation (Kroll *et al.*, 1999). The effect of gliotoxin on mitochondria is thought to be responsible for gliotoxin-induced PCD (Pardo *et al.*, 2006). PCD is a widely conserved mechanism in which a cell undergoes organised death. This process is involved in many aspects of both plants and animals development and plays a key role in the immune response (Danon *et al.*, 2000). Some ETPs have been identified in plant pathogens belonging to the Dothideomycetes such as sirodesmin PL produced by *Leptosphaeria maculans* (syn. *Phoma lingam*), the agent responsible of the blackleg disease on oilseed rape (*Brassica napus*). Sirodesmin was shown to induce necrosis in oilseed rape as well as in non-hosts plants. The phytotoxic activity of sirodesmin was later attributed to its ability to interfere with conserved metallo-proteins, specifically zinc-containing enzymes such as RNA polymerases (Rouxel *et al.*, 1988), and supported the theory that sirodesmin was involved in disease development. However, mutants of *L. maculans* impaired in sirodesmin production

were able to cause disease although lesions appeared to be smaller than that observed with a wild-type isolate (Sock & Hoppe, 1999). Furthermore, sirodesmin-induced necrosis was found to be phenotypically different from disease lesions (Rouxel *et al.*, 1988). In addition to a potential role in virulence, some authors hypothesised that sirodesmin might also be involved in a different biological process such as competition against other micro-organisms (Gardiner *et al.*, 2005b).

3.1.2. Alternative role of secondary metabolites in plant-pathogen interactions

The role of fungal SMs in disease expression is not limited to merely that of phytotoxins. Some SMs such as those belonging to the melanin pigment family are often involved in host penetration. The *alb*$^{-}$ mutant of *Magnapothe oryzae* impaired in dihydroxynaphtalene (DHN) melanin biosynthesis is unable to infect healthy rice leaves but is pathogenic on wounded leaves suggesting that DHN melanin is required for fungal penetration. Pathogenicity on healthy leaves was restored when the *alb*$^{-}$ mutant was complemented with scytalone, the first intermediate in the DHN melanin biosynthetic pathway confirming the involvement of melanin in host penetation (Woloshuk *et al.*, 1980; Chumley & Valent, 1990).

Some polyketide-derived SMs are also involved in processes not necessarily involved in the expression of disease symptoms such as sporulation. Mutation of the polyketide synthase (PKS) encoding for the elsinochrome synthase in *Elsinoë fawcettii* resulted in decreased asexual sporulation (Liao & Chung, 2008a). Similarly, zearalenone, a polyketide derived metabolite produced by *Fusarium* spp., is involved in sexual development of the fungus as chemical inhibition of zearalenone production resulted in decreased perithecial production (Wolf & Mirocha, 1973). The polyketide-derived melanin has also been shown to play a crucial role in sporulation and fungal growth by protecting spores and hyphae from damage associated with UV light radiation (Alspaugh *et al.*, 1997).

Siderophores are non-ribosomal peptide synthetase (NRPS)-derived bacterial and fungal SMs specialised in iron uptake and storage via specific Fe^{3+} chelation (Haas *et al.*, 2008). As iron is both an essential nutrient for all living organism and a

potent redox mediator, its uptake and storage modulates the growth and fitness of a given organism. Intracellular siderophores are thought to be involved in cell protection by acting as an antioxidant whereas secreted siderophores are involved in iron uptake (Haas *et al.*, 2008). Extracellular siderophores are involved in virulence of several fungal species such as *Fusarium graminearum* (syn. *Gibberella zeae*), *Alternaria brassicicola* and *Bipolaris maydis* on wheat (*Triticum aestivum*), thale cress (*Arabidopsis thaliana*) and maize (*Zea mays*), respectively (Oide *et al.*, 2006). Extracellular siderophore-mediated virulence was found to be independent of a putative phytotoxic role of these SMs but was instead linked with increased fitness effect as inoculation carried out with mutants impaired in extracellular siderophore production exhibited normal virulence when complemented with iron (Oide *et al.*, 2006). Similarly, intracellular siderophores are also involved in virulence. A ferricrocin deficient mutant of the rice blast fungus *Magnaporthe oryzae* showed reduced virulence compared to the wild-type which was associated with a reduction in host penetration (Hof *et al.*, 2007).

Fungal SMs can also be indirectly involved in disease development by conferring an advantage to the fungus against other micro-organisms potentially competing in the same ecological niche. Anti-competition agents aiming at inhibiting the growth of other organisms typically fall into this category of SMs. The phleichrome isolated from the timothy-grass (*Phleum pratense*) pathogen *Cladosporium phlei* belongs to the perylenequinones family and exert phytotoxic and antibiotic, light-dependent activities (Yoshihara *et al.*, 1975; Araki & Shimanuki, 1983). Phleichrome notably inhibits the growth of bacteria such as *Bacillus subtillis* as well as fungal species such as *Alternaria* species and *Epichloe thyphnia*, a fungal endophyte of timothy-grass plants (Araki & Shimanuki, 1983; Seto *et al.*, 2005). Furthermore, phleichrome biosynthesis was found to be stimulated by the presence of *E. thyphnia* suggesting that this SM plays a major role as anti-competition agent (Seto *et al.*, 2005).

3.1.3. SM-related gene expression in disease development

Many fungal SMs are important virulence determinant and as such, their production and subsequently the expression of the genes that encodes them is expected to vary during disease development depending on their function. The expression of SM-related genes in plant pathogenic fungi varies greatly between species. Patterns of SM-related gene expression depends mostly on the role of the produced SM as well as on the growing conditions of the producing organism with certain SMs being produced under specific pH conditions, in nutrient deprived media or in response to changes in light radiation (Brakhage, 2013).

Some fungal SMs are expressed during the early stages of the infection process. The majority of SMs produced by the hemibiotroph *Colletotrichum higginsianum*, the causal agent of brassica anthracnose, were more highly expressed during the appressoria development phase and to a lower extent during the biotrophic colonisation phase (O'Connell *et al.*, 2012). Similar observations were made in *Colletotrichum orbiculare*, the agent responsible of cucurbit anthracnose, exhibiting down regulation of SM core genes during the necrotrophic phase. These examples suggest that many of the SMs produced by *Colletotrichum* species are likely to be involved in host manipulation during early colonisation phases rather than acting as phytotoxic compounds involved in symptom development (Gan *et al.*, 2013).

The expression profile of SM-related genes in the Rcc sister species *Zymoseptoria tritici* (syn. *Mycosphaerella graminicola*) was found to be different to that of *Colletotrichum* species. Rudd *et al.* (2015) showed that the majority of SM-related genes were expressed during the transition from symptomless phase to necrotrophic lifestyle. This expression pattern of SM-related genes was similar to that observed for putative *Z. tritici* effectors. The preferential expression of SM-related genes at this time of disease development is consistent with that of putative toxins potentially involved in the transition between lifestyles. Contrastingly, in the hemibiotroph *Dothistroma septosporum* the majority of SM-related core genes were shown to be expressed preferentially during the later stages of infection (Bradshaw *et al.*, 2016). Transcript levels of the core gene involved in the production of the known virulence factor dothistromin, *PksA*, were most abundant during the late stages of disease development which is consistent with the observation that dothistromin is mostly found in lesions (Kabir *et al.*, 2015). However, *PksA* was also expressed

during early *D. septosporum* growth in liquid cultures (Schwelm *et al.*, 2008), suggesting this polyketide synthase may be involved in the production of metabolites with diverse biological functions. In *C. fulvum*, the sister species of *D. septosporum*, most of the genes involved in the biosynthesis of the anthraquinone pigment cladofulvin are down-regulated to allow biotrophic fungal growth during disease development further highlighting the importance of SMs in plant-pathogen interactions (Griffiths *et al.*, 2017).

3.1.4. Regulation of secondary metabolism-related genes

3.1.4.1. Regulation of secondary metabolism within cluster

Many fungal SM pathways are regulated by transcription factors (TFs) located within the SM biosynthetic cluster. These regulatory proteins involved in the activation of SM-specific pathways include zinc binuclear proteins, also known as Zn_2-Cys_6 as well as zinc fingers protein or C2H2 also known as Cys2His2, and some proteins containing ankyrin repeat domains (Proctor *et al.*, 1995; Pedley & Walton, 2001; Shwab & Keller, 2008). TFs interact with DNA to activate or repress the expression of genes present in a given cluster or pathway. TOXE, a protein containing ankyrin repeat domains was shown to regulate HC-toxin biosynthesis by binding to a specific motif called the tox-box present in the promoter of all the genes located in the *TOX2* cluster of *Bipolaris zeicola* (Pedley & Walton, 2001). Zn_2-Cys_6 proteins are the most commonly found SM pathway-specific regulator (Brakhage, 2013) and have only been described in fungi (Keller *et al.*, 2005). The well-studied TF *AflR* found in the aflatoxin and sterigmatocystin pathway in *Aspergillus* spp. was shown to bind to the promoter region of eleven genes involved in toxin production, including the core gene *PksA* (Ehrlich *et al.*, 1999). *AflR*-mediated activation was essential for aflatoxin production in *Aspergillus parasiticus* (Cary & Ehrlich, 2000). Similarly, the homolog of *AflR* in *D. septosporum* was required for dothistromin production (Chettri *et al.*, 2013). Putative homologs of pathway-specific TFs such as *AflR* were identified in several clusters in Rcc but their role in SM biosynthesis in this fungus is still unknown (McGrann *et al.*, 2016; Chapter 2 section 2.3.3.2).

However, not all SM biosynthetic pathways contain pathway-specific regulators such as those clusters that regulate production of penicillin or cephalosporin which suggests that control of these pathways depends on a different level of regulation.

3.1.4.2. Master regulators of fungal secondary metabolism

Fungal secondary metabolism can also be controlled by the action of master regulators which unlike pathway-specific TFs are involved in the regulation of several biological pathways including some non-SM pathways such as those involved in asexual reproduction. Master regulators such as *HdaA* and *Kmt6*, involved in histone deacetylation and methylation respectively, act by modifying histones involved in the formation of the nucleosome thus directly modifying the condensation state of chromatin and subsequently the transcription of a section of DNA (Lee *et al.*, 2009; Connolly *et al.*, 2013). The histone methyltransferase *LaeA*, a known master regulator of fungal secondary metabolism (Bok & Keller, 2004), was found to be involved in the demethylation of histone 3 thus initiating the conversion of heterochromatin to euchromatin (Reyes-Dominguez *et al.*, 2010). *LaeA* acts as part of the velvet complex, a light dependent protein complex that regulates gene expression (section 3.1.4.3). *LaeA* positively regulates several SM pathways including sterigmatocystin, penicillin and lovastatin pathways in *Aspergilli* species (Bok & Keller, 2004). As a result, deletion of *LaeA* in *A. fumigatus* resulted in reduced virulence. The function of *LaeA* appears conserved across fungal species as this gene also regulates secondary metabolism in *Penicillium oxalicum* and *Fusarium oxysporum* (López-Berges *et al.*, 2013; Zhang *et al.*, 2016). Contrastingly, in *D. septosporum*, *LaeA* was found to repress the expression of genes involved in dothistromin production (Chettri & Bradshaw, 2016). The adverse effect *LaeA* exhibits on different SMs is partially imputed to its chromatin remodelling nature. Chromatin-mediated regulation largely dependens on the physical location of the cluster on the chromosome; clusters located near the centromere or in subtelomeric regions are more likely to be subject to chromatin-mediated regulation (Osbourn, 2010; Palmer & Keller, 2010).

3.1.4.3. Environmental regulation of fungal secondary metabolism

Production of fungal secondary metabolites can also be regulated by environmental stimuli such as iron availability, redox status or the presence of other microbes (Fox & Howlett, 2008; Haas, 2015). Considering that SMs are often involved in niche exploitation, environmentally regulated expression of the genes encoding these compounds would be required to avoid unnecessary production of a specific SM. The pH of the environment in which a given fungus grows is known to have an impact on fungal secondary metabolism. Barley leaves infected with Rcc, incubated on acidified agar, produced red compounds which were speculated to be SMs of the rubellin group known to be synthesised by this fungus (Miethbauer *et al.*, 2003). Contrastingly, penicillin production was increased in *A. nidulans* in alkaline medium through the action of the TF *PacC* (Espeso *et al.*, 1993) whereas genes involved in the aflatoxin pathway were down-regulated in a genetically-engineered isolate of *A. nidulans* over-expressing *PacC* (Keller *et al.*, 1997). *PacC* was identified as a zinc-finger transcription factor that activates expression of alkaline-dependent genes in *A. nidulans* by binding the consensus sequence 5'-GCCARG-3' in the promoter region of the regulated genes (Tilburn *et al.*, 1995). pH-mediated regulation of SM clusters appeared to be a conserved mechanism as homologs of *PacC* in other fungi have been shown to have a similar role. *PacC* in *Fusarium fujikuroi* (syn. *Gibberella fujikuroi*) represses genes in the bikaverin cluster (Wiemann *et al.*, 2009). Similarly, *PacC* regulates approximately 5% of the *Colletotrichum gloeosporoides* genome which includes genes involved in host colonisation and pathogenesis as *PacC* knockout mutants exhibited reduced virulence (Alkan *et al.*, 2013).

Nutritional conditions such as carbon and nitrogen availability are also known to regulate SMs production. Nitrogen was found to regulate SM-related gene expression via the action of a zinc-finger TF *AreA* involved in chromatin modification (Muro-Pastor *et al.*, 1999). *AreA* negatively regulates the expression of genes involved in

the gibberellin pathway (Schönig *et al.*, 2008) and is required for the biosynthesis of fumonisin B1 in *Fusarium verticillioides* (Kim & Woloshuk, 2008). A zinc-finger TF, *CreA* is involved in carbon signalling (Dowzer & Kelly, 1989). *CreA* was shown to be responsible for down-regulation of SM-related clusters in *Penicillium oxalicum* (Zhang *et al.*, 2016). *Ramularia collo-cygni* cultures when grown in nitrogen-limited conditions, such as minimal medium (MM) without nitrogen exhibit much more intense red coloration of the hyphae than those observed on MM or PDA. Conversely, when grown on MM without carbon the colony exhibits virtually no coloration (McGrann; unpublished data). These observations concur with the appearance of RLS symptoms during leaf senescence, a plant process which is associated with nitrogen remobilisation to the seeds, subsequently depriving Rcc environment from nitrogen (Schützendübel *et al.*, 2008).

Light is also a known factor that regulates fungal SMs production. In the Dothideomycete *Elsinoë fawcettii*, the causative agent of citrus scald, expression of the *PKS1* gene responsible for the production of the perylenequinone toxin elsinochrome was increased when the fungus was grown under constant light conditions (Liao & Chung, 2008a). Similarly, in *Cercospora nicotianae*, another Dothideomycete, cercosporin accumulated in culture exposed to constant light conditions concomitantly with an increase in transcript levels of *CTB1*, the PKS involved in the biosynthesis of cercosporin (Choquer *et al.*, 2005). Furthermore, both cercosporin and elsinochrome are photodynamic toxins that require light activation to induce cell death (Yamazaki *et al.*, 1975; Liao & Chung, 2008b). Light-dependent SM regulation is mediated in fungi by a conserved protein complex known as the velvet complex (Bayram *et al.*, 2008). This complex is formed by two proteins encoded by the genes *VelB* and *VeA*. The VelB protein is involved in asexual reproduction when acting independently, whereas when VelB is bound to VeA, it activates LaeA-mediated SM-related gene expression. In light conditions, translocation of VeA in the nucleus is inhibited which prevents the formation of the velvet complex and results in subsequent decrease of SM-related gene expression (Bayram *et al.*, 2008). The opposite effect was observed in the dark where a decrease of asexual spore production and increase of SM-related gene expression was observed. The velvet complex and its interaction with the protein encoded by *LaeA*

positively regulates SM production such as T-toxin in *B. maydis* (Wu *et al.*, 2012), beauvericin in *F. oxysporum* (López-Berges *et al.*, 2013), fumonisin B1 and fusarin C in *F. fujikuroi* (Wiemann *et al.*, 2010). The velvet complex was found to negatively regulate bikaverin biosynthesis in *F. fujikuroi* further highlighting the fact that master regulators can have contrasting effects on different SMs (Wiemann *et al.*, 2010). In Rcc, the rubellin toxins, the only SM group characterised in this fungus at present, exhibit light-dependent activity as they were shown *in vitro* to induce ROS-mediated fatty acid peroxidation upon light activation, suggesting that light may be involved in rubellin regulation (Heiser *et al.*, 2004). Furthermore, light intensity plays an important role in RLS development as plants grown under high intensity prior to inoculation exhibit increased levels of RLS symptoms potentially linked with the action of light induced SMs production (Makepeace *et al.*, 2008; Brown & Makepeace, 2009; Peraldi *et al.*, 2014).

Due to their action at a large scale via chromatin remodelling, most master regulators play a crucial role in fungal biology as they are not only involved in the regulation of SM-related gene expression but also in the regulation of genes involved in other processes such as asexual reproduction or developmental processes.

3.1.5. Objectives

The aim of this chapter was to investigate the putative role played by Rcc SMs in the infection process by studying the potential link between SM core gene expression and RLS development by:

- Profiling Rcc SM-related genes expression during the infection process in artificially inoculated barley seedlings.
- Investigating known fungal master regulators of secondary metabolism and pathway-specific TFs in Rcc during disease development.
- Investigating the putative role of Rcc SMs in alternative biological processes such as competition with other micro-organisms.

3.2. Materials and Methods

3.2.1. Plant material

The RLS susceptible spring barley cv. Century was sown in 6.5×6.5×6 cm plastic pots (Desch Plantpack Ltd, Maldon, UK) containing Levington M3 compost (ICL, Ipswich, UK). Plants were grown for two weeks until GS 12/13 (Zadoks *et al.*, 1974) in a controlled environment cabinet (Snijders Scientific, Tilburg, Netherlands) at 18°C, with a photoperiod of 16h/8h day/night with 250 µmol m^{-2} s^{-1} light regime and 80% relative humidity.

3.2.2. Barley seedling inoculation with *Ramularia collo-cygni*

Ramularia collo-cygni isolate Rcc001 DK05 ss2 was grown for two weeks in the dark at 15°C on PDA (Sigma, Dorset, UK). Liquid cultures were prepared by adding five 1 cm^2 agar plugs to 250 mL of potato dextrose broth (PDB, Sigma, Dorset, UK) containing 5 µg mL^{-1} of streptomycin. Cultures were incubated for two weeks in the dark at 15°C under constant agitation at 125 rpm. Inoculum was prepared by blending the culture in a food processor (Kenwood Electronics, London, UK) in three runs of 30 seconds each and adding one drop of Tween 20 (Sigma, Dorset, UK) for every 50 mL of inoculum after blending. The inoculum was sprayed on two-week-old barley cv. Century seedlings using an artist's air brush (Clarke Wiz Air®, Clarke International, Essex, UK) at a rate of 0.5 mL per seedling. Seedlings were sprayed evenly from every direction to obtain uniform inoculation. Inoculated plants placed in a plastic tray (50×40×5 cm) and were covered with a clear plastic lid that was sealed to ensure maximum humidity and incubated in the dark for 48h at 18°C. After incubation in the dark the light regime was then restored to a 16h/8h light/dark cycle at 250 µmol m^{-2} s^{-1}. The clear plastic lids covering the inoculated seedlings were removed five days after inoculation and the development of RLS symptoms monitored over a 21-day period.

3.2.3. Assessment of Ramularia leaf spot development on barley seedlings

3.2.3.1. Visual assessment of Ramularia leaf spot

Development of RLS was assessed at 5, 7, 10, 12, 15, 18 and 21 days post inoculation (dpi) to follow the development of the disease during the infection process, from the asymptomatic phase through to the necrotrophic phase. Visual assessment was carried out on the first leaf and disease severity was estimated as the percentage of the leaf area covered by RLS symptoms. The area under disease progress curve (AUDPC; Shaner & Finney, 1977) was calculated to report the development of the disease over time. Green leaf area retention was also visually assessed at each time point as RLS development has been associated with leaf senescence (Schützendübel *et al.*, 2008). Data shows the mean ± standard error calculated on six independent inoculation experiments each of them containing two biological replications of 20 leaves each.

3.2.3.2. Microscopic assessment of *Ramularia collo-cygni* colonisation

Colonisation by Rcc during RLS development was also followed using microscopic observations. Inoculated leaves were harvested after scoring and cleared in 70% ethanol for one week. Leaves were stained with 0.05% trypan blue in lacto-glycerol and briefly de-stained with 100% ethanol prior to observations on a light microscope (Leica DMRBE, Leica Microsystems, Wetlzar, Germany). For each leaf a minimum of 120 stomata were observed over the full length of the leaf. Fungal development stages and the associated host response was scored in three categories (1) stomata were scored for penetration by fungal hyphae, (2) stomata surrounded by necrosis were scored and (3) the presence of fungal conidiophore-like structures emerging from stomata were noted. Data show the mean ± standard error calculated on six independent experiments each of them containing two biological replications of two leaves each.

3.2.3.3.*Ramularia collo-cygni* DNA quantification

Ramularia collo-cygni DNA was quantified during disease development. Two leaves harvested at each time point between 5 and 21 dpi were snap frozen in liquid nitrogen and DNA was extracted using the DNeasy Plant Mini Kit (QIAGEN Ltd, Hilden, Germany) and quantified using a Nanodrop ND1000 spectrophotometer (Labtech international Ltd, Uckfield, UK). Rcc DNA quantification was carried out using qPCR as described by Taylor *et al.* (2010). Data show the average amount of Rcc DNA from five independent inoculation experiments.

3.2.4. Gene expression analysis

3.2.4.1.Expression profiling of secondary metabolite core genes in artificially inoculated seedlings

Transcript levels of selected Rcc genes were assessed during disease development at each time point between 5-21 dpi when RLS symptoms were scored. For each biological replicate two leaves were harvested, pooled together and snap frozen in liquid nitrogen. Total RNA was extracted using the RNeasy Mini Kit (QIAGEN Ltd, Hilden, Germany) following the manufacturer's instructions. RNA extraction was followed by a TURBO DNase I treatment (Ambion®, Thermo Fisher Scientific, Austin, TX, USA) following manufacturer's instructions to remove any traces of genomic DNA from the sample. The presence of residual genomic DNA was assessed by qPCR using 10-fold diluted RNA as template. When no DNA was present, RNA quantity and quality were measured using a Nanodrop ND1000 spectrophotometer. A total amount of 1 µg of RNA was subsequently used for cDNA synthesis using the SuperScript III First-Strand Synthesis System (Invitrogen, Carlsbad, CA, USA) following manufacturer's instructions. The obtained cDNA was diluted 10-fold in sterile distilled water and used in quantitative reverse transcription PCR (qRT-PCR) to quantify transcript levels. qRT-PCR amplification and melting curve analysis were carried out on a Mx3000P thermocycler (Agilent Technologies,

Santa Clara, CA, USA) using the SybrGreen Jump Start^{TM} Taq system (Sigma, Dorset, UK) following the manufacturer's instructions. As described previously (Udvardi *et al.*, 2008), four Rcc reference genes, elongation factor 1 α (EFα); glyceraldehyde-3-phosphate dehydrogenase (GAPDH); α-tubulin and actin, were assessed using GeNorm (Vandesompele *et al.*, 2002) to determine transcript stability under the conditions of this experiment. The two most stable reference genes GAPDH and α-tubulin were used for subsequent cDNA normalisation.

Gene specific primers for Rcc genes of interest were designed using primer3 software (Rozen & Skaletsky, 2000) with the following set of criteria: primer length between 18 bp and 22 bp, GC content 50±10%, Tm=60±1°C, product size between 80 bp and 160 bp. The list of primer sequences is given in Appendix 5. The amplification efficiency of each primer pair was calculated by qRT-PCR using a cDNA dilution series of 1/10, 1/100, 1/1000 and 1/10000 as the template. Primers with amplification efficiency above 80% were used for qRT-PCR gene expression analysis. Transcript quantification was calculated based on the $E^{-\Delta\Delta Ct}$ method (Livak & Schmittgen, 2001). Data are the mean normalised expression values ± standard error of three independent experiments each of them containing two biological replicates with two inoculated leaves pooled in each replicate.

3.2.4.2.Gene expression analysis from naturally inoculated barley leaves

Expression of the SM-related genes identified on Contig 17 by McGrann *et al.* (2016) was carried out by end point RT-PCR. Total RNA was extracted as described previously (section 3.2.4.1) from flag-1 leaves exhibiting RLS symptoms, harvested from field trials at the Bush Estate, Midlothian, Scotland in 2014. cDNA was synthesised and prepared as described above and end-point RT-PCR was carried out using gene specific primers as described in McGrann *et al.* (2016). Amplification was visualised by electrophoresis using a 1.5% agarose gel complemented with GelRed DNA stain (Biotium Inc, Freemont, CA, USA) following manufacturer's instructions; run for one hour at 100V and visualised on an AlphaImager HP (Cell Biosciences, Heidelberg, Germany).

3.2.5. Co-regulation of secondary metabolite-related genes

To investigate potential co-regulation of SM genes by pathway-specific TFs, the *in silico* identification of typical *AflR* binding sites 5'-TCG(N_5)CGR-3' (Ehrlich *et al.*, 1999) and alternative *AflR* binding sites 5'-TCG(N_{10})TCG-3' and 5'-TCG(N_{11})CGR-3' (Fernandes *et al.*, 1998; Zhang *et al.*, 2007) was carried out. The search was restricted to the putative binding site occurring within 1000 bp of the predicted start codon of the putative SM genes.

3.2.6. Fungal competition assay

A competition assay was designed to investigate the putative antifungal effect of SMs produced by Rcc. Rcc isolate DK05 Rcc001 ss2 was tested against fungal species potentially competing with Rcc for its ecological niche in barley seeds and leaves. Commonly occurring barley pathogens *Fusarium poae*, *F. graminearum* and *Pyrenophora teres* were investigated. The assay was carried out in 9 cm-Petri dishes (Sarstedt, Nümbrecht, Germany), on two different media, alkyl ester agar (AEA) and PDA (Sigma, Dorset, UK) containing 5 µg mL^{-1} of streptomycin. The two media were selected based on the differential production of red pigment in these media as the hyphae of Rcc cultures exhibited bright red coloration on PDA compared to a white coloration when grown on AEA. Because of the differential *in vitro* growth rate between Rcc and most of the competing fungi, Rcc was added first on the plate and allowed to grow for two weeks in isolation. An 8 mm plug of Rcc mycelium was extracted from a two-week-old culture plate and placed 2 cm from the border of the Petri dish. Mycelial plugs from competing fungi were taken from two-week-old cultures and placed 3 cm away from the Rcc culture. Competition with *Rhynchosporium commune* was also investigated; however, due to the slow growing nature of both *R. commune* and Rcc on AEA, this assay was only performed on PDA. The mycelial plug of *R. commune* was added at the same time as Rcc and the two plugs were placed 3 cm apart. All fungal cultures were grown in a Sanyo MIR-254 incubator (Sanyo Electric Ltd, Osaka, Japan) in constant darkness at 15°C. Fungal radial growth was measured after 10 days for *P. teres* and *F. poae*, 7 days for

F. graminearum and after 21 days for *R. commune*. The percentage of growth inhibition was calculated by:

$$\text{Growth inhibition (\%)} = 100 - \frac{\text{Radial growth away from the Rcc culture}}{\text{Radial growth towards the Rcc culture}} \times 100$$

The assay was repeated three times for every fungus, each replication consisting of three plates.

3.3. Results

3.3.1. Inoculation assay

3.3.1.1. Visual assessment

Disease development was assessed based on a visual estimation of the percentage of leaf area covered by RLS symptoms. Small RLS "pepper spot" symptoms were first observed at 7 dpi, but typical RLS symptoms appeared only after 10 dpi and steadily increased until 21 dpi. Disease severity increased concomitantly with a decrease in green leaf area (Figure 3.1). This result is supported by previous observations that Rcc becomes more prevalent as the leaf becomes senescent (Schützendübel *et al.*, 2008). Based on this observation, it appeared that Rcc developed asymptomatically until 5 dpi before switching to a symptomatic phase.

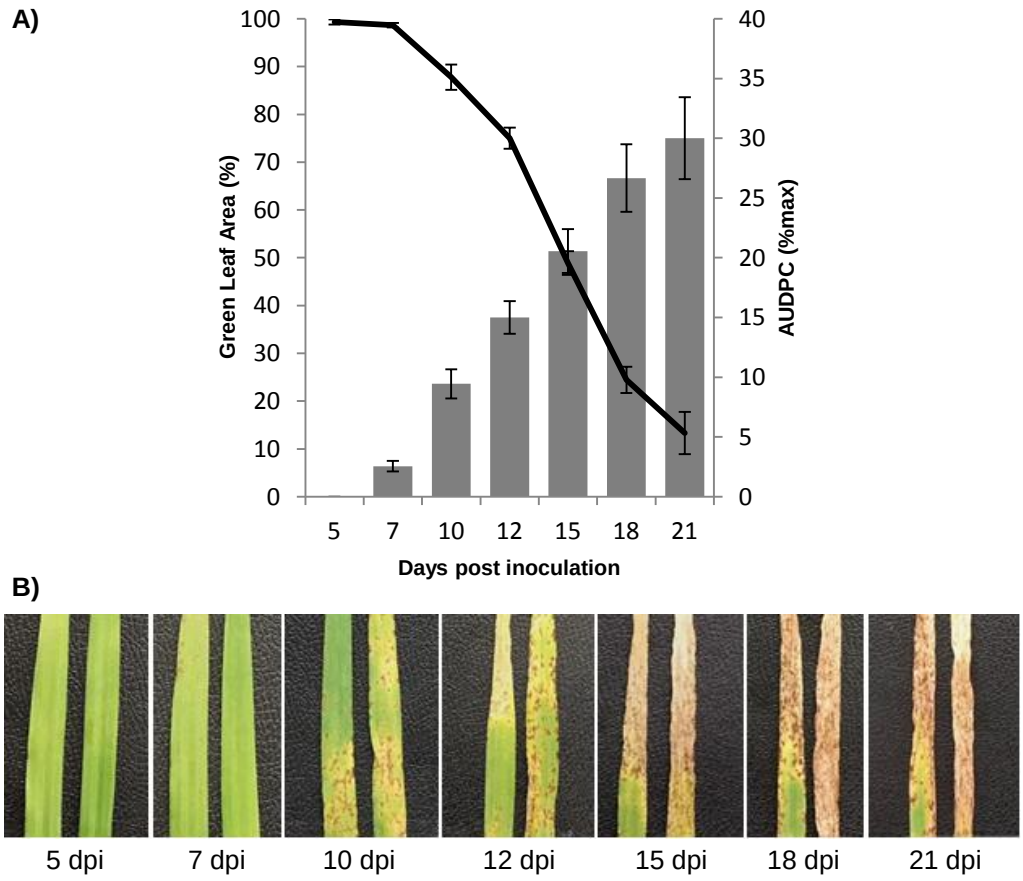

Figure 3.1: Development of Ramularia leaf spot symptoms and green leaf area retention on barley cv. Century.
A) Disease symptom development represented by the area under disease progress curve (AUDPC; grey bars) increases after 5 dpi whilst green leaf area retention (black line) decreases steadily from 7 dpi. Data show the mean ± SE of six independent inoculation experiments. B) Representative images of RLS symptoms on barley cv. Century across the 21 day time course of the bioassay.

3.3.1.2.Fungal development during infection

The formation of the Rcc hyphal network on barley seedlings was studied during disease development. Inoculated leaves were analysed under light microscopy to assess fungal penetration and sporulation as well as fungal-induced necrosis in the host. Fungal penetration of stomata was high after 5 dpi with 85% of stomata penetrated by Rcc hyphae. The number of penetrated stomata steadily increased to reach 92% at 21 dpi (Figure 3.2.A and Figure 3.2.D.i). Further highlighting the typical development of the fungus was the observation of conidiophore-like structures emerging through stomata. Although it was found to occur throughout the

entire time course, the emergence of conidiophore-resembling structures seemed to peak around 15 dpi (Figure 3.2.B and Figure 3.2.D.ii). The observation of necrotic stomata appeared only after 7 dpi suggesting that the fungus behaves as a necrotrophic fungus from 10 dpi onwards, which appears to be correlated with symptom development (Figure 3.2.C and Figure 3.2.D.iii). Taken together, the high level of stomatal penetration by the fungus combined with the lack of necrotic stomata at an early stage of disease development support the hypothesis that Rcc grows asymptomatically until 7 dpi before becoming necrotrophic.

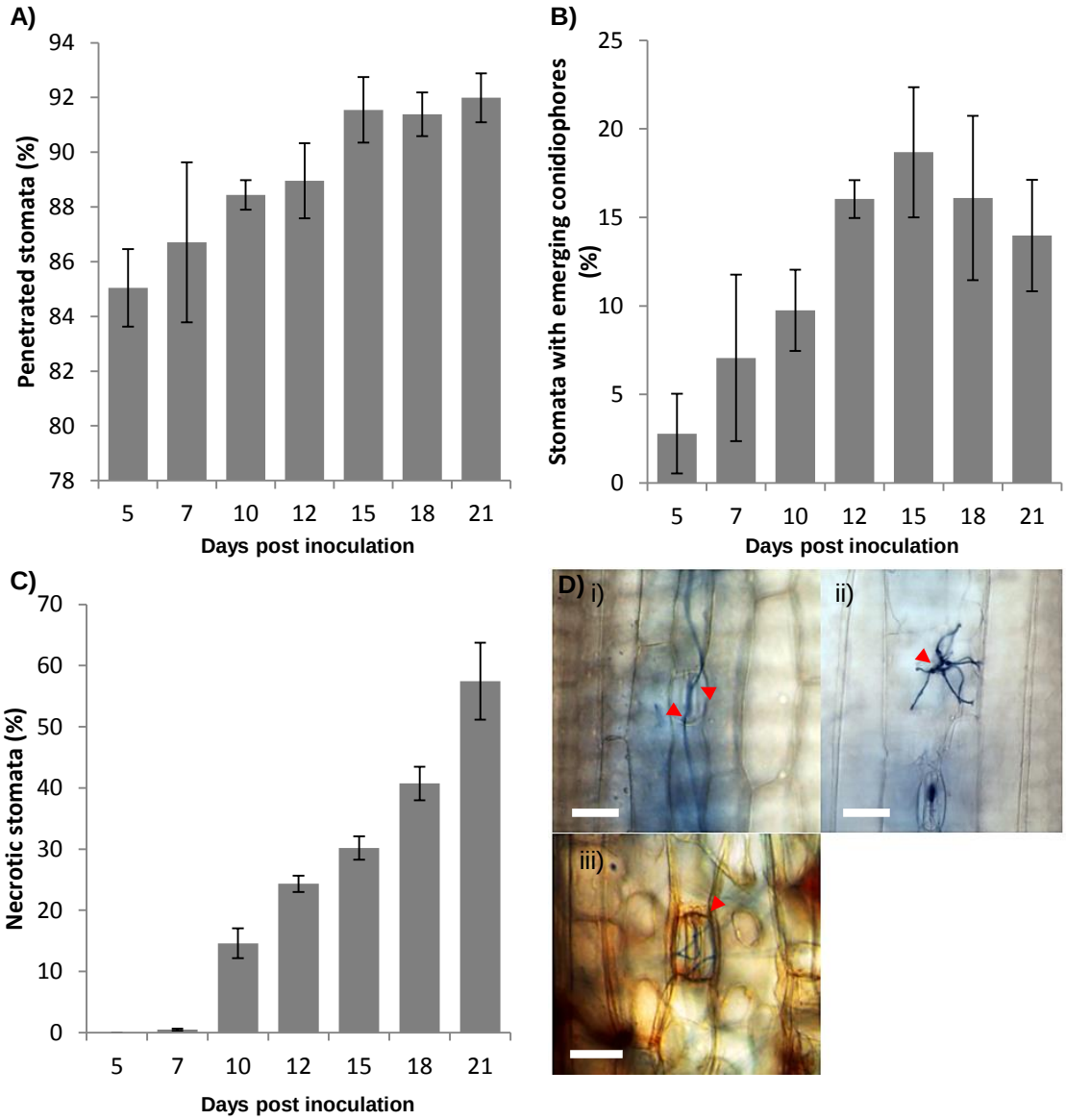

Figure 3.2: Microscopic assessment of Ramularia leaf spot development.
A) Percentage of stomata penetrated by fungal hyphae. B) Percentage of stomata with conidiophore-like structures emerging. C) Percentage of necrotic stomata. D) Light microscopy images of penetrated stomata (i), conidiophore-like structure emerging from stomata (ii) and necrotic stomata (iii). Bar = 50 µm.

The study of disease development on artificially inoculated seedlings suggests that, under these experimental conditions, Rcc early development is asymptomatic, potentially reflecting the endophytic growth phase observed in the field, whereas late development involves appearance of typical RLS lesions.

3.3.2. Expression profiling of *Ramularia collo-cygni* secondary metabolism core genes

A number of core genes identified in Chapter 2 were selected for further *in planta* gene expression profiling. All but one of the putative PKSs identified in SM-related clusters were selected for gene expression. *Pks280-0.23* was not included in the gene expression study because of the two core genes present on the PKS280 cluster, the second core gene, *Nps280-0.11*, was selected as the phylogenetic study suggested that the protein encoded by *Pks280-0.23* is related to *Pks2*, one of the two PKSs involved in T-toxin biosynthesis in *B. maydis*. No other Rcc PKSs showed similarity to *Pks1*, suggesting that Rcc is unlikely to produce T-toxin (Chapter 2, Figure 2.13). In addition, *Pksm46-0.119* was included based both on its domain organisation, which resembles that of known aflatoxin- and dothistromin-pathway PKS core genes, as well as on BLASTp results showing sequence similarity with *A. flavus PksA* (e-value 0.0) and *D. septosporum PksA* (e-value 0.0). Primers suitable for qRT-PCR with amplification efficiencies >80% could not be obtained for *Pks58-0.40, Pks233-0.136* and *Pks60* despite multiple attempts at primer design. Therefore, these three genes were left out of the analysis.

Transcripts of five out of six PKSs examined in this study were most abundant during the asymptomatic and the early symptom formation stage. The expression of *Pks30-1.114, Pks17-1.203, Pksm46-0.119* and *Pksm24-1.219* was highest at 5 dpi and subsequently decreased to much lower level of expression after 10 dpi. *Pks282-0.161* was highly expressed at both 5 and 7 dpi but the expression dropped drastically at 10 dpi and remained low thereafter (Figure 3.3). The NR-PKS *Pks118-3.254* showed consistently low expression levels over the infection time course suggesting that the putative SM produced via *Pks118-3.254* is unlikely to be involved in disease development.

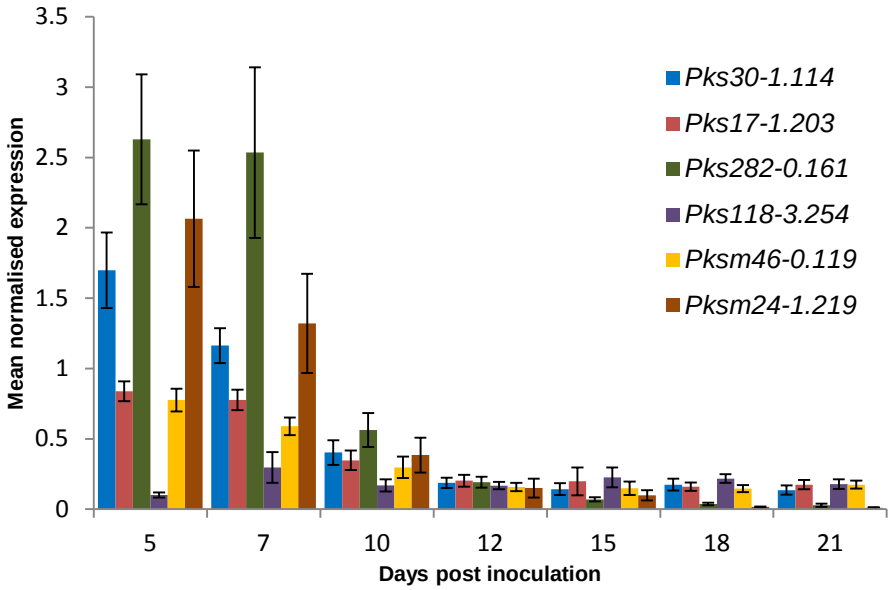

Figure 3.3: Expression profile of selected *Ramularia collo-cygni* polyketide synthases during disease development in artificially inoculated barley seedlings.
Gene expression was obtained by qRT-PCR using gene specific primers carried out on cDNA synthesised from total RNA extracted from inoculated barley seedlings. Data is presented as mean normalised expression based on cDNA normalisation using the two most stable reference genes (GAPDH and α- tubulin).

The expression of all the HPSs identified in the Rcc genome was also studied during disease development. Although the three HPSs were all most highly expressed during the early symptom development phase, the expression profile of *Hps14-0.66* differs from that of the other two HPSs. The expression of *Hps1-2.140* and *Hps38-0.269* peaked at 7 dpi and slowly decreased to reach its minimal level at 21 dpi. *Hps14-0.66* however, was highly expressed at both 5 and 7 dpi before dropping to a low level of expression from 10 dpi onwards (Figure 3.4).

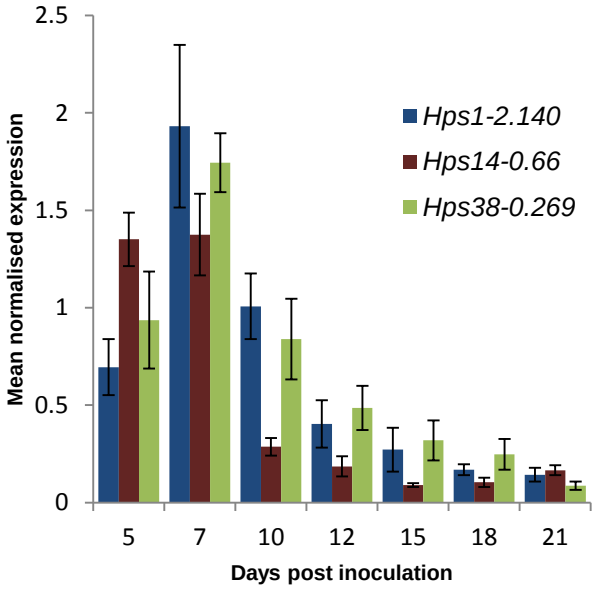

Figure 3.4: Expression profile of selected *Ramularia collo-cygni* PKS/NRPS hybrids during disease development in artificially inoculated barley seedlings.
Gene expression was obtained by qRT-PCR using gene specific primers carried out on cDNA synthesised from total RNA extracted from inoculated barley seedlings. Data is presented as mean normalised expression based on cDNA normalisation using the two most stable reference genes (GAPDH and α- tubulin).

The two NRPSs located on contig 246, *Nps246-0.103* and *Nps246-0.414*, *Nps245-0.245* and *Nps134-0.394* were investigated based on similarity with NRPSs located in secondary metabolism-associated clusters identified in other fungal species. *Nps280-0.11* and *Nps175-0.41* were investigated based on adenylation domain similarity with an unknown NRPS in the Dothideomycete *Parastagonospora nodorum* (syn. *Phaeosphaeria nodorum*) (Chapter 2, Figure 2.15). *Nps55*-3.77 and *Nps100* were investigated based on their location in gene clusters containing a variety of genes with a predicted function associated with SM production such as dehydrogenases and cytochrome P450 monooxygenases. Although all primers set tested for the selected NRPSs showed amplification against *in planta* cDNA, primers exhibiting sufficient amplification efficiency could not be obtained for *Nps246-0.103* which was not investigated further.

Six out of the seven NRPSs investigated showed highest transcript levels during the asymptomatic and early development stages (Figure 3.5). *Nps246-0.414* and

Nps100 exhibited their highest level of expression at both 5 and 7 dpi before being repressed to a low level of expression at 10 dpi until 21 dpi. Similarly, *Nps175-0.41*, *Nps280-0.11*, *Nps55-3.77* and *Nps134-0.394* exhibited their highest level of expression at 5 dpi and decreased to low levels of expression after 10 dpi and remained low until the end of the experiment. Although the expression of *Nps245-0.245* was highest at 5 dpi, the expression profile of this gene was found to be different from that of the other NRPSs as it decreased steadily during the course of the experiment.

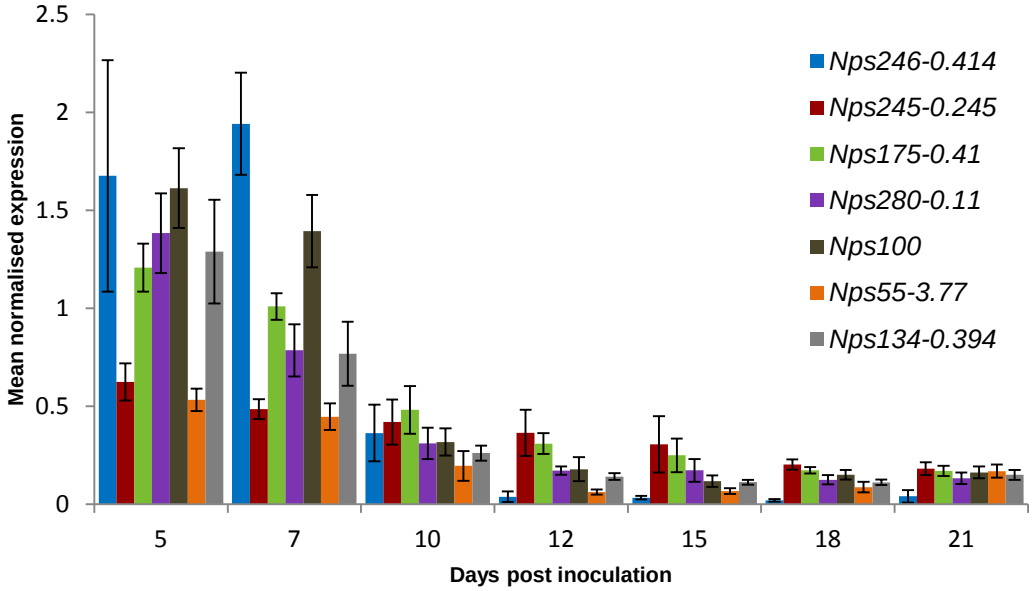

Figure 3.5: Expression profile of selected *Ramularia collo-cygni* non-ribosomal peptide synthetases during disease development in artificially inoculated barley seedlings.
Gene expression was obtained by qRT-PCR using gene specific primers carried out on cDNA synthesised from total RNA extracted from inoculated barley seedlings. Data is presented as mean normalised expression based on cDNA normalisation using the two most stable reference genes (GAPDH and α- tubulin).

To validate that the gene expression data for the SM genes tested can be related to the biology of Rcc in the seedling bioassay, transcript levels of the Rcc catalase gene were also monitored. It has been shown that hydrogen peroxide (H_2O_2) levels increase over time in Rcc infected leaves (McGrann, unpublished data). Therefore,

the expression of catalase, the enzyme involved in the degradation of H_2O_2 is also expected to increase to protect fungal hyphae from ROS-associated damage. A Rcc homolog of *Candida albicans* catalase (BLASTp e-value $1e^{-168}$) was identified in the previously published pathogen-host interaction (PHI) database (McGrann *et al.*, 2016) and expression profiling was carried out as described previously (section 3.2.4). Catalase was found to be mostly expressed after 7 dpi and transcript abundance increased to its highest level from 10 dpi remained constant during the whole necrotic phase until 21 dpi (Figure 3.6). The expression of the present catalase gene increased over time, potentially to protect the fungus from hydrogen peroxide-mediated damage, as the antioxidant system of the plant breaks down during leaf senescence, resulting in increased levels of H_2O_2 in the environement.

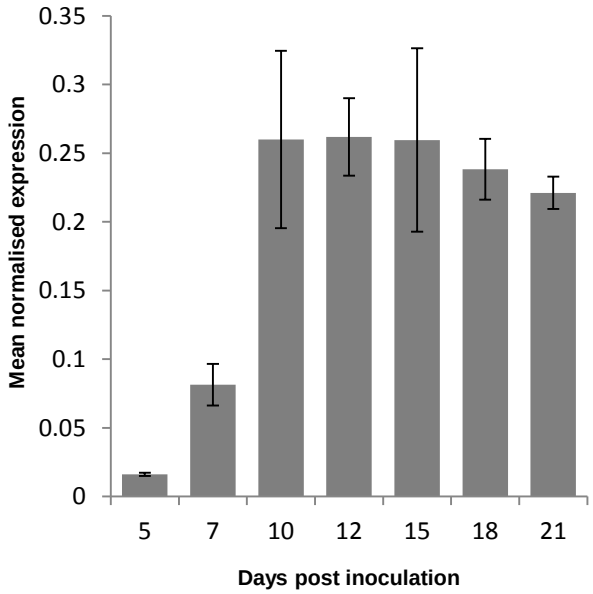

Figure 3.6: Expression profile of a *Ramularia collo-cygni* catalase gene during disease development in artificially inoculated barley seedlings.
Gene expression was obtained by qRT-PCR using gene specific primers carried out on cDNA synthesised from total RNA extracted from inoculated barley seedlings. Data is presented as mean normalised expression based on cDNA normalisation using the two most stable reference genes (GAPDH and α- tubulin).

Furthermore, the amount of fungal DNA was measured over time during the assay and was found to increase as disease symptoms developed which suggests that fungal biomass is increasing over the time course (Figure 3.7). Taken together, these results validate the expression data obtained as the lack of expression at late time points cannot be explained by a reduction in fungal biomass or viability.

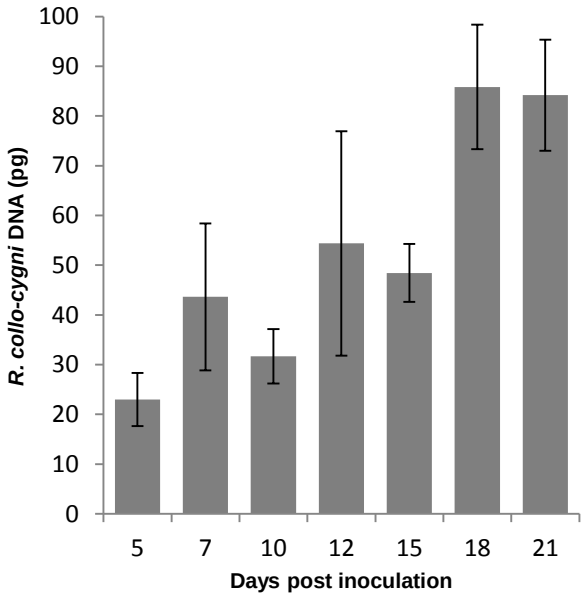

Figure 3.7: *Ramularia collo-cygni* DNA levels during disease development in artificially inoculated barley seedlings.
DNA quantification was carried out by qPCR as described in Taylor *et al.* (2010). DNA levels increased during disease development suggesting that fungal biomass accumulates as Ramularia leaf spot symptoms develop.

The present study showed that the selected SM core genes were most highly expressed *in planta* during earlier stages of Rcc colonisation and RLS symptom formation, suggesting that the role of Rcc SMs in disease development may be through host manipulation such as concealing the fungus from the plants immune system rather than inducing cell death.

3.3.3. Co-regulation of secondary metabolism gene clusters in *Ramularia collo-cygni*

3.3.3.1. Expression profiling of environmental regulators of secondary metabolism

Three master regulators of secondary metabolism associated with the fungal response to environmental stimuli were included in this study. paralogues of the zinc-finger TF *PacC*, *CreA* and *AreA* involved in response to pH, carbon and nitrogen conditions respectively were identified in the Rcc genome using BLASTp (Table 3.1).

Table 3.1: Protein BLAST (BLASTp) hits in *Ramularia collo-cygni* of known regulators of secondary metabolism.

Protein	Organism	Accession number	*R. collo-cygni* corresponding gene model	e-value
PacC	*A. nidulans*	CAA87390.1	maker-contig_178-fgenesh-gene-0.255-mRNA-1	1e-129
CreA	*A. nidulans*	AAR02858.1	maker-contig_44-snap-gene-0.182-mRNA-1	1e-108
AreA	*A. nidulans*	CAA36731.1	genemark-contig_231-processed-gene-0.2-mRNA-1	1e-154
LaeA	*A. fumigatus*	AAR01218	maker-contig_13-fgenesh-gene-0.378-mRNA-1	1e-59
VeA	*A. nidulans*	AAD42946.1	maker-contig_1-fgenesh-gene-1.186-mRNA-1	1e-81

The expression of these regulators was followed during disease development. The expression of *CreA* did not appear to fluctuate during development of RLS. Although *AreA* transcripts were more abundant at 5 and 7 dpi, the level of *AreA* expression dropped at 10 dpi and remained constant at this lower level for the rest of the time course experiment (Figure 3.8). The expression profile of the pH-dependent *PacC* was similar to that observed for the SM core genes as its expression was highest at 5 and 7 dpi before dropping to a lower level at 10 dpi which remained relatively constant from that point onwards. These results suggest that both the pH of the environment in which Rcc grows and nitrogen availability may play a role in SM regulation via the action of *PacC* and *AreA*, respectively. However, these two factors are unlikely to be the only environmental stimuli affecting SM biosynthesis.

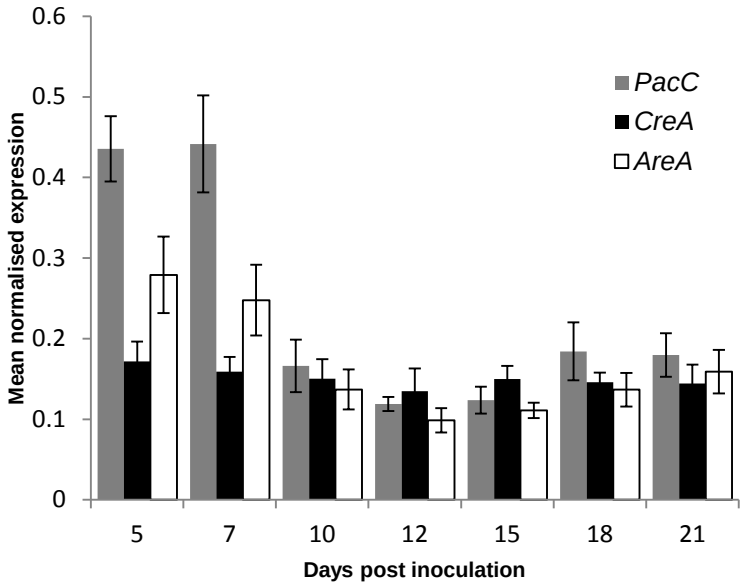

Figure 3.8: Expression profile of *Ramularia collo-cygni* environmental-dependent master regulators of secondary metabolism during disease development in artificially inoculated barley seedlings.
Gene expression was obtained by qRT-PCR using gene specific primers carried out on cDNA synthesised from total RNA extracted from inoculated barley seedlings. Data is presented as mean normalised expression based on cDNA normalisation using the two most stable reference genes (GAPDH and α- tubulin).

It has been reported that high light levels and intensity positively influence RLS severity (Makepeace *et al.*, 2008; Brown & Makepeace, 2009; Peraldi *et al.*, 2014). Therefore, a potential role for the light-regulated fungal velvet complex in SM regulation in Rcc was investigated. Putative paralogues of *VeA* and *LaeA*, two genes involved in the velvet complex in *Aspergilli* spp. were identified in the Rcc genome using BLASTp (Table 3.1). The protein encoded by *VeA* regulates SM gene expression by controlling LaeA protein activity through dimerization with a third protein VelB (Bayram *et al.*, 2008). During seedling infection, *LaeA* expression was highest between 5 and 10 dpi and decreased to be the lowest at 15 dpi, whereas that of *VeA* peaked at 7 dpi (Figure 3.9). The expression profiles of *LaeA* and *VeA* mirrors that of SM core genes which are more abundant during the early stages of the infection.

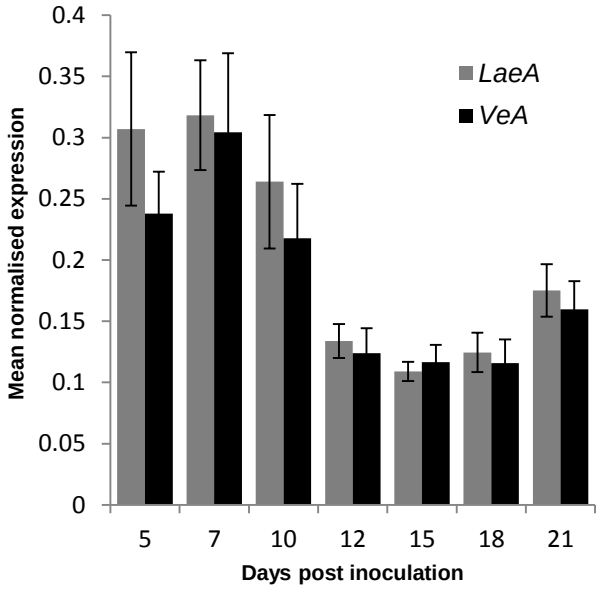

Figure 3.9: Expression profile of genes involved in the velvet complex in *Ramularia collo-cygni* during disease development in artificially inoculated barley seedlings.
Gene expression was obtained by qRT-PCR using gene specific primers carried out on cDNA synthesised from total RNA extracted from inoculated barley seedlings. Data is presented as mean normalised expression based on cDNA normalisation using the two most stable reference genes (GAPDH and α- tubulin).

3.3.3.2.Pathway-specific regulation

Based on the present study, it appeared that secondary metabolism in Rcc may be under the regulation of several master regulator genes such as *LaeA, PacC* and *AreA*. These master regulators have been shown to interact directly with SM cluster-specific TFs. For instance, *LaeA* was found to activate *AflR* in *A. nidulans* (Keller *et al.*, 2005). Therefore, investigating cluster-specific TFs might provide further insights into the regulation of SM-related genes in Rcc. To investigate potential pathway-specific regulation of SM-related genes, the expression of two known transcription factors involved in aflatoxin biosynthesis was investigated. Paralogues of *A. flavus AflR* and *AflJ* (BLASTp e-value of $1e^{-12}$ and $1e^{-50}$, respectively) were identified in Rcc on contig 17 by McGrann *et al.* (2016) in a putative SM cluster that did not contain SM core gene. In order to investigate potential pathway-specific regulation, the expression of the paralogue of the aflatoxin *StcQ* gene (BLASTp e-

value of $1e^{-62}$) found in Rcc in the cluster on contig 17 was followed during disease development. All three genes exhibited similar expression profiles with transcript levels most abundant at 5 dpi that declined at 7 and 10 dpi and remained low from 12 dpi until the end of the experiment (Figure 3.10). This expression profile is reminiscent of that of the two putative *PksA* paralogues *Pksm24-1.219* and *Pksm46-0.119* (BLASTp e-value of 0.0 for both PKSs), *Pks30-1.114*, *Pks17-1.203* (Figure 3.3) as well as the NRPSs *Nps175-041*, *Nps280-0.11*, *Nps55-3.77* and *Nps134-0.394* (Figure 3.5). Taken together, these results suggest that several SM-related genes, including paralogues of aflatoxin biosynthesis genes, are potentially co-regulated by *AflR* and *AflJ*.

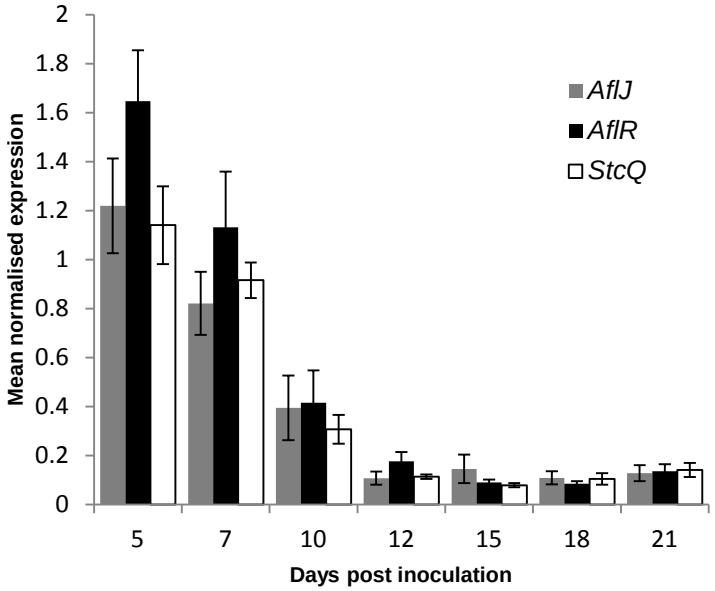

Figure 3.10: Expression profile of aflatoxin-regulatory gene homologs in *Ramularia collo-cygni* during disease development in artificially inoculated barley seedlings.
Gene expression was obtained by qRT-PCR using gene specific primers carried out on cDNA synthesised from total RNA extracted from inoculated barley seedlings. Data is presented as mean normalised expression based on cDNA normalisation using the two most stable reference genes (GAPDH and α- tubulin).

The co-regulation which was found to occur on distant genetic loci as *AflR*, *AflJ*, *StcQ* and the core genes such as *Pksm24-1.219* and *Pksm46-0.119* are located on different clusters, was supported by the identification *in silico* of *AflR* binding sites for nine genes located in the Rcc putative SM cluster identified by McGrann *et al.* (2016) on contig 17 (Table 3.2) and eleven genes located in PKSm24 (Table 3.3) including the *PksA* paralogue *Pksm24-1.219*. In addition, the expression of all the putative SM-related genes identified on contig 17 was investigated in naturally infected barley leaves harvested from field trials at two different growth stages, GS78 which correspond to the onset of leaf senescence and GS83, an advanced leaf senescence stage (McGrann *et al.*, 2016; Appendix 6). Supporting the results of the present study, the RT-PCR-based expression analysis carried out by McGrann *et al.* (2016) showed that all the genes identified in the putative SM cluster on contig 17 were expressed during the earlier time point (GS 78) before the leaves started to senesce while only two were still expressed at an advance senescence stage (GS83).

Table 3.2: Gene expression and number of *AflR* binding site identified in the promoter region of the genes located in the putative secondary metabolism cluster found on contig 17.

Cluster	Predicted function[1]	Typical *AflR* binding site[2]	Alternative *AflR* binding site[3]	Total *AflR* binding sites	RT-PCR expression data[4]					
					In vitro 5d	*In vitro* 10d	*In vitro* 15d	*In vitro* 20d	GS78	GS83
Contig 17	Hyp1	0	1	1	+	+	+	+	+	-
	Hyp2	2	0	2	+	+	+	+	+	-
	AflB	1	1	2	+	+	+	+	+	+
	Hyp3	0	0	0	+	+	+	+	+	-
	OrdB (StcQ)	1	0	1	+	+	+	+	+	-
	AflJ	0	0	0	+	-	+	+	+	-
	AflM	1	0	1	+	-	-	-	+	-
	AflC	0	0	0	-	-	-	-	+	-
	AflR	0	0	0	+	+	+	+	+	-
	Sc Dehydrogenase	0	0	0	+	+	+	+	+	-
	MFS	0	0	0	+	+	+	+	+	+
	P450 superfamilly	1	1	2	-	-	-	-	+	-
	GST	1	1	2	+	+	+	+	+	-
	Scytalone DH	1	0	1	-	-	-	-	+	-
	ABC	0	1	1	+	+	+	+	+	-

[1] Predicted function refers to the naming found in McGrann *et al.* (2016).[2] Typical *AflR* binding site 5'-TCG(N_5)CGR-3' as defined by Ehrlich *et al.* (1999).[3] Alternative binding sites 5'-TCG(N_{10})TCG-3' and 5'-TCG(N_{11})CGR-3' as defined by Fernandes *et al.* (1998) and Zhang *et al.* (2007).[4] Expression data from *in vitro* (PDB) cultures of *Ramularia collo-cygni* and naturally infected field samples (GS 78 and GS 83) reported in McGrann *et al.* (2016). RLS area under disease progress curve (AUDPC) and green leaf area retention for the field samples used for RT-PCR analysis are presented in Appendix 6.

Table 3.3: Number of *AflR* binding site identified in the promoter region of the genes located in the putative secondary metabolism cluster PKSm24.

Cluster	Gene code[1]	Typical AflR binding site[2]	Alternative AflR binding sites[3]	Total AflR binding sites
PKSm24	A	1	2	3
	B	0	1	1
	C	1	1	2
	D	0	1	1
	E	0	2	2
	F	1	2	3
	G	0	0	0
	H	0	0	0
	I	0	0	0
	J	0	0	0
	K	0	1	1
	L	0	0	0
	M	0	0	0
	N	1	0	1
	O	1	1	2
	P	0	1	1
	Pksm24-1.219	0	1	1

[1] Gene code refers to the naming set in Chapter 2, Figure 2.16 of this thesis. [2] Typical AflR binding site 5'-TCG(N_5)CGR-3' as defined by Ehrlich *et al.* (1999). [3] Alternative binding sites 5'-TCG(N_{10})TCG-3' and 5'-TCG(N_{11})CGR-3' as defined by *Fernandes et al.* (1998) and Zhang *et al.* (2007).

Transcripts of genes putatively involved in secondary metabolism in Rcc appear to be most abundantly expressed at an early stage of disease development, typically during the asymptomatic stage or when the earliest disease lesions begin to form. SM core genes seemed to be co-regulated with master regulators as well as pathway-specific TFs such as *AflR*. The preferential expression of SM core genes during the early stages of the infection suggests that if produced by Rcc many of the SMs synthesised by the genes investigated here could play a role in early plant-pathogen interactions such as host manipulation. However, alternative roles for SMs in the biology of Rcc are possible.

3.3.4. Fungal competition assays

To investigate the potential antifungal activity of SMs produced by Rcc, *in vitro* competition assays were carried out between Rcc and common fungal pathogens of barley. Growth of all tested competing fungi was inhibited in the presence of Rcc on both AEA and PDA (Figure 3.11). Growth of *Pyrenophora teres* was inhibited by 66% and 80% on AEA and PDA, respectively. Similarly, the two *Fusarium* species, *F. poae* and *F. graminearum* showed growth inhibition in excess of 50% when in the presence of Rcc on AEA and growth inhibition of more than 65% on PDA. The presence of Rcc also exhibited an antagonistic effect on *Rhynchosporium commune* on PDA. The observation of a red coloration of the medium surrounding Rcc in this assay combined with observation of exudates appearing on Rcc cultures, particularly visible on oatmeal agar suggest that Rcc is producing SMs *in vitro* (Figure 3.12). Taken together, these results suggest that Rcc may release compounds into the growing medium that inhibits the growth of other fungi.

A)

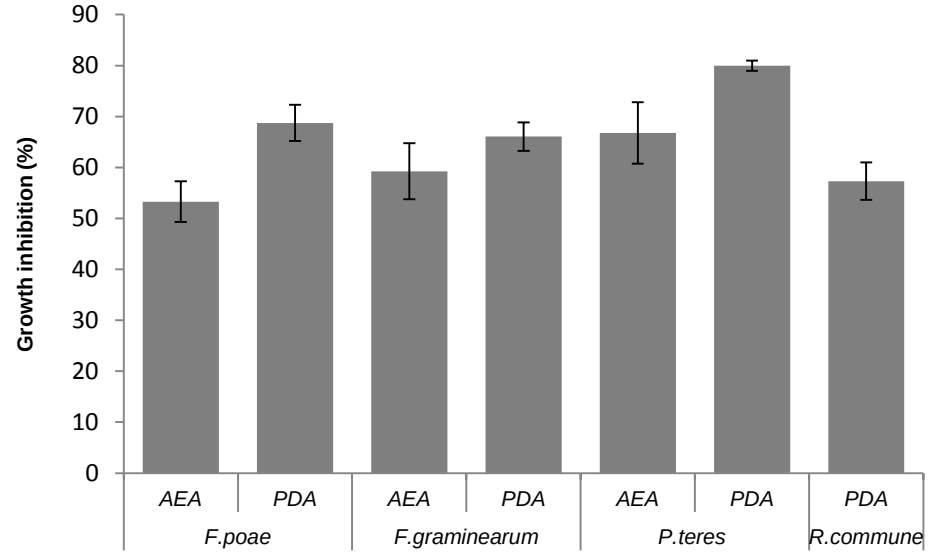

B)

Figure 3.11: Antagonistic effect of *Ramularia collo-cygni* on common fungal barley pathogens.
A) Fungal growth inhibition in to the presence of Rcc. Result shows the average percentage of growth inhibition ± standard error across three independent experiments. B) Representative pictures of the competition assay between Rcc and *F. poae*, *F. graminearum*, *P. teres* and *R. commune* after 10, 7, 10 and 21 days, respectively when grown on AEA (top panel) and PDA (bottom panel).

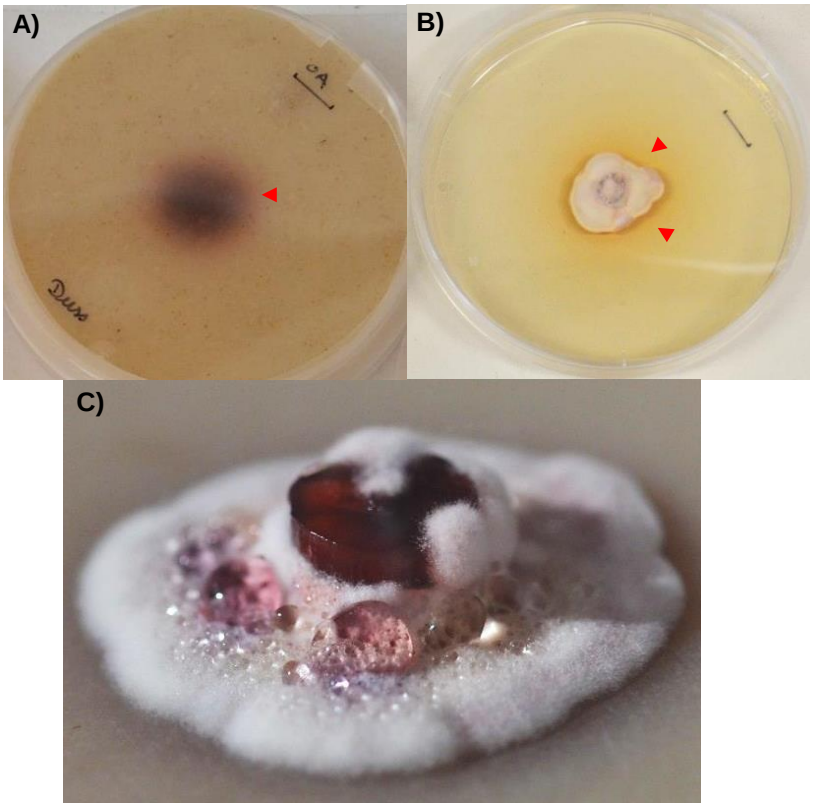

Figure 3.12: Red coloration observed on *Ramularia collo-cygni* cultures.
(A) Red coloration of the medium surrounding the Rcc culture after incubation for 14 days at 15°C in the dark on oatmeal agar. (B) Red coloration of the medium surrounding the Rcc culture after incubation for 14 days at 15°C in the dark on PDA. (C) Exudates of a red compound observed on cultures of Rcc grown for 14 days at 15°C in the dark on oatmeal agar.

3.4. Discussion

Gene expression profiling is commonly used to determine the involvement of fungal genes in virulence or pathogenicity during plant-pathogen interactions. The expression profile of a specific gene or of entire gene families provides valuable insights into the putative role played by these genes during pathogen colonisation and subsequent disease development. Secondary metabolites are frequently involved in plant disease, be it through the action of toxic compounds or by the interaction with the plant host, and are often preferentially expressed *in planta* (Fox & Howlett, 2008). Genes encoding proteins involved in the synthesis of SMs from the Dothideomycetes *Pseudocercospora fijiensis* and *Parastagonospora nodorum* were found to be up-regulated during host infection compared to *in vitro* conditions (Ipcho *et al.*, 2012; Noar & Daub, 2016b). However, not all SM-related genes are highly expressed *in planta*. Collemare *et al.* (2014) showed that the PKSs *PKS1*, *PKS5* and the NRPSs *NPS4*, *NPS8* and *NPS9* in the tomato pathogen *Cladosporium fulvum,* exhibited low levels of expression in the leaves compared to that observed *in vitro*.

Despite the widespread use of gene expression profiling to evaluate changes in fungal transcription during host colonisation there are a limited number of studies that interrogated the expression profile of SM-related genes during the different stages of disease development in the Dothideomycetes. The role of SMs appeared to be unique to each fungal species even within a single taxonomic class. The present study showed that transcript levels of core genes associated with potential secondary metabolism pathways in Rcc are most highly expressed during the asymptomatic and the earliest lesion formation phases of disease development. Two NR-PKSs *Pksm46-0.119* and *Pksm24-1.219* presenting the highest sequence similarity with aflatoxin and dothistromin *PksA* genes were expressed most highly during the asymptomatic phase and early symptoms development stage (Figure 3.3), suggesting that, if their product is a phytotoxin, the SM could be produced early and stored within the hyphae. Previous observations by McGrann *et al.* (2016) which showed that a red compound was found in vesicles within Rcc hyphae support the hypothesis that metabolites such as rubellin could be stored within the fungus until needed. The HR-PKS, *Pks30-1.114*, which was identified in a betaenone-like cluster (Chapter 2,

Figure 2.18) appeared to be expressed at an early time point. Considering the phytotoxic nature of betaenones (Ichihara *et al.*, 1983), if these compounds are produced, it is unlikely that they are released *in planta* when they are synthesised and could also be stored until needed, potentially to induce plant cell death during necrotrophic growth of the fungus to increase nutrient availability.

Transcripts levels of the three HPSs identified in Rcc were also the highest during the early stages of infection. Amongst the HPSs in Rcc, *Hps14-0.66* was previously identified in a putative chaetoglobosin A-like cluster (Chapter 2, Figure 2.22). As such, assuming that the HPS14 cluster is functional and produces a chaetoglobosin-derived SM, the expression profile of *Hps14-0.66* is in accordance with the role of a potential antifungal agent. Chaetoglobosins produced by the endophytic fungus *Chaetomium globosum* were shown to exert potent antifungal activities against *Rhizopus stolonifer* and *Conothirium diplodiella*, two pathogens of plants colonised by *C. globosum* (Ding *et al.*, 2006; Zhang *et al.*, 2013). These observations gave rise to the hypothesis that chaetoglobosins might be involved in competition against other fungi and protection of the endophyte habitat. Therefore, the expression of the core gene of such an SM, if produced in Rcc, is expected to be highest during the asymptomatic and early stages of the disease development to protect the fungus from potential competitors.

All the NRPSs investigated in this study exhibited higher level of expression during the asymptomatic and early symptoms development stages of the infection. Of all the NRPSs examined in this study, only *Nps134-0.394* and *Nps246-0.414* were located in clusters showing similarity to clusters responsible for the biosynthesis of known SMs. The NRPS246-2 cluster exhibited similarity to the gliotoxin cluster in *A. fumigatus* (Chapter 2, Figure 2.25). However, NRPS246-2 exhibited only partial similarity with the *A. fumigatus* gliotoxin biosynthetic cluster as NRPS246-2 contained a significantly higher number of genes than that observed in the *A. fumigatus*. NRPS246-2 was therefore predicted to be unlikely to produce gliotoxin in Rcc. The NRPS134 cluster exhibited similarity to the ferricrocin biosynthetic cluster in *S. pombe* and to a ferricrocin-like cluster in *C. fulvum* (Chapter 2, Figure 2.29). Ferricrocin was found to be involved in virulence in several plant pathogens such as *M. oryzae, B. maydis* and *F. graminearum* (Hof *et al.*, 2007; Oide *et al.*, 2007) and

was highly expressed under iron starvation conditions (Blatzer *et al.*, 2011). These observations could explain the high level of expression of *Nps134-0.394* at an early stage of disease development, as Rcc might have to compete with plant cells for apoplastic iron. Available apoplastic iron is expected to be low due to the fact that 95% of apoplastic iron is bound to cell membranes (Nikolic & Romheld, 2007). Contrastingly, at later stages of disease development available iron might be more abundant due to localised plant cell death. The present results contrast with that of a recent study showing that siderophores-encoding genes in *Colletotrichum graminicola* were down-regulated during biotrophic growth of the fungus *in planta* to avoid plant defence mechanism activation (Albarouki *et al.*, 2014). This difference could be explained by the different lifestyles of the fungi. *C. graminicola* is a hemibiotrophic fungus whereas Rcc which has a long endophytic growth may have evolved other mechanisms to avoid plant defences that do not require down-regulation of fitness-mediating genes such as those involved in siderophore biosynthesis.

Furthermore, based on the previously published RNAseq data (McGrann *et al.*, 2016) one HPS, *Hps14-0.66*, and three NRPSs, *Nps100, Nps280-0.11* and *Nps175-0.41*, were not expressed on PDA after 10-12 days but were demonstrated to be expressed *in planta*. In addition, the PKS *Pks233-0.136*, which was also found not to be expressed *in vitro* was expressed *in planta* despite poor amplification efficiency due to primers design. Similarly, the NRPS *Nps246-0.103*, for which primers yielding sufficient amplification could not be obtained, showed no evidence of expression in the RNAseq data but exhibited *in planta* expression. Based on these results, it appears that at least six SM core genes may be preferentially expressed *in planta*. However, the RNAseq analysis was only carried out at one specific time point *in vitro*, therefore, a more complete *in vitro* study of SM-related gene expression spanning over the growth period of the fungus may provide insights into putative SM core genes expressed preferentially *in planta* and possibly directly involved in the infection process.

Overall, the results of this study showing that Rcc SM core genes are most highly expressed early during the infection process concur with the observation that

SM-related genes in three *Colletotrichum* species, *C. orbiculare, C. higginsianum* and *C. gloeosporioides* were expressed during the early stages of disease development (O'Connell *et al.*, 2012; Gan *et al.*, 2013; Alkan *et al.*, 2015). In *C. higginsianum* most of the SM-related genes were expressed before penetration, during appressoria development. Similarly, the HPS *Ace1* in *Magnaporthe oryzae* is specifically expressed during appressoria differentiation (Fudal *et al.*, 2007). Expression of SM-related genes and *Ace1* was not induced on artificial membranes in *Colletotrichum* and *M. oryzae* respectively, suggesting that the expression of these SM-related genes might be dependent on host cues associated with fungal penetration. In *C. higginsianum*, SM-related gene expression remained high after penetration during the biotrophic phase but was abolished during the necrotrophic phase. A similar finding was observed in the wheat pathogen *Zymoseptoria tritici* where SM gene transcripts were most abundant during the transition phase from biotrophic to necrotrophic growth (Rudd *et al.*, 2015). Secondary metabolites produced during this transition phase are thought to be either involved in defending the fungus from plant defence mechanisms or inducing host cell death therefore facilitating fungal development during the necrotrophic phase. However, secondary metabolism-associated processes were also found to be up-regulated during later stages of disease development, from 21 to 56 dpi, in *Z. tritici* (Palma-Guerrero *et al.*, 2016). Similar results were found in another Dothideomycete closely related to Rcc, *Dothistroma septosporum*, where four core genes including three PKSs and one NRPS were up-regulated during the later stages of infection. However, SM-related gene expression in *D. septosporum* appears to be complex as four genes including one PKS, one NRPS and two HPSs showed a stable level of expression throughout the infection while one NRPS was up-regulated during early fungal development (Bradshaw *et al.*, 2016). A pathway specific study showed that the expression of all the 19 genes involved in the biosynthesis of the dothistromin toxin was found to be maximal at the later stages of infection which concur with previous observations that dothistromin is accumulated in the lesions during disease development (Kabir *et al.*, 2015; Bradshaw *et al.*, 2016). This result contrasts with that of the present study where all the genes present in the cluster located on contig 17 were expressed at GS 78 when leaves were still green at 60% whereas only two of them were expressed at

GS 83 corresponding to an advanced stage of senescence with green leaf area below 30% (Table 3.2, Appendix 6). This could arise from the fact that the putative SM produced by Rcc and dothistromin may have very different roles.

Expression of SM-related genes is the result of a finely tuned balance between secondary metabolism and fungal development (Calvo *et al.*, 2002). As a result, SM-related genes are often co-regulated, allowing for a rapid control of SM production. Rcc SM-related gene expression appeared to be co-regulated with that of several regulators, including the known master regulator *PacC* and the velvet complex. The expression profile of *PacC* suggests that this gene could be involved in regulating SM gene expression in Rcc. Like many SM core genes in the Rcc genome examined here, *PacC* transcripts are most abundant during the asymptomatic and early symptom development phases of the disease, suggesting a possible co-regulatory relationship. Expression of *PacC* was found to be involved in the repression of acidic-induced genes and the activation of alkaline-dependent genes (Tilburn *et al.*, 1995). Rubellins, the only SMs so far characterised in Rcc, were extracted from acidic medium (Miethbauer *et al.*, 2006) which suggests that *PacC* may be involved in the regulation of other SMs in Rcc. Furthermore, considering that the pH in the apoplastic environment is around pH=5 and in the symplast around pH=7 (Nikolic & Romheld, 2007), cell death caused by Rcc may lead to an increase in pH resulting in increased *PacC*-mediated gene expression. However, this study presents contrasting results as all the genes investigated showed decreased expression levels during the necrotrophic phase. A possible hypothesis to explain the co-regulation of *PacC* and the studied SM core genes at an early point in disease development could be that Rcc may induce alkalinisation of its host tissue during the asymptomatic and early symptom development phase. This was reported in the hemi-biotrophic fungus *Colletotrichum coccodes*, a pathogen of fruits, which secretes ammonium ions (NH_4^+) in infected host tissue resulting in localised increase of ambient pH (Alkan *et al.*, 2008). This change in pH is used by the fungus to increase nutrient availability during the necrotrophic phase by activating the expression of nicotinamide adenine dinucleotide phosphate (NADPH) oxidase which results in both hydrogen peroxide-mediated PCD in host tissue (Alkan *et al.*, 2009) as well as up-regulation of salicylic

acid (SA)-dependent genes and down-regulation of jasmonic acid (JA)-dependent genes in the host (Alkan *et al.*, 2012). Both SA and JA pathways are known to be involved in plant defence against biotrophic and necrotrophic pathogen respectively (Spoel *et al.*, 2007). Furthermore, SA was associated with induction of PCD in response to biotrophic pathogens (Brodersen & Malinovsky, 2005). As a result, activation of SA-dependent genes during the necrotrophic growth of *C. coccodes* increased its virulence. It appears that the ability of *C. coccodes* to induce alkalinisation of its environment is crucial to disease development. *PacC* was found to regulate the expression of the genes involved in alkalinisation of host tissue in several unrelated fungal species suggesting this may be a common feature to aid host colonisation by plant pathogenic fungi (Alkan *et al.*, 2013). Therefore, a similar role for *PacC* in Rcc is possible and could explain high transcript levels of SM-related genes during early stages of disease development. Investigating known *PacC* regulated genes involved in alkalinisation or acidification of the medium such as the ammonia exporter *AMET* and ammonia permease *MEPB* could provide insights into the putative role played by *PacC* in Rcc development.

PacC can also exhibit SM-specific effects as seen in *A. nidulans* where *PacC* was found to inhibit sterigmatocystin and aflatoxin production but activated penicillin biosynthesis (Espeso *et al.*, 1993; Keller *et al.*, 1997). In *F. fujikuroi*, *PacC* was found to repress bikaverin biosynthesis genes (Wiemann *et al.*, 2009). Therefore, assuming that *PacC* in Rcc had a similar role to that found in other fungi, *PacC* could differentially regulate specific core genes and SM pathways. However, the expression profile of *PacC* in Rcc closely matches that of most of the SM core genes investigated suggesting that many Rcc SMs could be expressed under alkaline conditions. Based on the previously published RNAseq data (McGrann *et al.*, 2016), *PacC* appears to be expressed *in vitro* on PDA after 10-12 days of incubation. Therefore, an *in vitro* assay following *PacC* expression in Rcc cultures grown over a range of different pH may provide evidence for the role of *PacC* as a pH-dependent regulator in this fungus. Furthermore, a detailed study of the promoter region of the putative SM core genes could reveal the presence of *PacC* specific 5'-GCCARG-3' binding sites (Tilburn *et al.*, 1995) which would support the hypothesis that *PacC* may be involved in SM regulation. Because *PacC* was also found to be involved in

virulence in *F. oxysporum* (Caracuel *et al.*, 2003), *Colletotrichum gloeosporioides* (Alkan *et al.*, 2013) and *Aspergillus fumigatus* (Bertuzzi *et al.*, 2014), obtaining Rcc *PacC* knockout (KO) mutants and assessing the fitness and the ability of the fungus to infect barley could provide insights into the role of pH-response during the infection process.

The velvet complex also appeared to be involved in SM core gene expression in Rcc as observed in *A. nidulans* (Park *et al.*, 2012), *F. fujikuroi* (Wiemann *et al.*, 2010), *F. oxysporum* (López-Berges *et al.*, 2013) and *B. maydis* (Wu *et al.*, 2012). The action of the velvet complex varies between SMs and in the same fungus the velvet complex can activate one SM pathway and repress another. This study suggests that in Rcc, the *VeA* and *LaeA* genes involved in the velvet complex may be involved in regulating SM core gene expression. Most of the core genes studied in Rcc showed higher transcript levels at the earliest stages of fungal colonisation concomitant with high level of *VeA* and *LaeA* expression. This result contrasts with the findings by Chettri & Bradshaw (2016) showing that *LaeA* negatively regulated expression of dothistromin biosynthesis genes in the pine pathogen *D. septosporum*. As dothistromin is structurally related to rubellin and *D. septosporum* is closely related to Rcc (McGrann *et al.*, 2016), the hypothesis that the paralogue of *DsPksA* in Rcc may be involved in rubellin production was proposed. The results of this study suggest that the two paralogues of *DsPksA* in Rcc, *Pksm24-1.219* and *Pksm46-0.119*, are co-regulated with *LaeA*. However, Rcc genome analysis revealed that Rcc does not possess the full dothistromin biosynthetic pathway suggesting that Rcc is unlikely to produce dothistromin (McGrann *et al.*, 2016). Therefore, the role of *LaeA* in rubellin production may be different from that found for dothistromin. Furthermore, *LaeA* deletion in *D. septosporum* yielded mutants that produced a new uncharacterised SM (Chettri & Bradshaw, 2016). This suggests a cross-regulation between dothistromin and this new SM resulting in the expression of the dothistromin pathway whilst maintaining this unknown SM pathway cryptic. A similar regulation is possible in Rcc and may explain why at present only one SM family has been characterised in Rcc despite exhibiting the genetic ability to produce a wide range of SMs.

The velvet complex also negatively regulated developmental processes, such as asexual sporulation, by repressing the action of free VelB protein (Bayram *et al.*, 2008; Wiemann *et al.*, 2010; Park *et al.*, 2012). Deletion of *VeA* in *A. nidulans* resulted in increased sporulation associated with a decrease in SM production (Kato *et al.*, 2003). Peak emergence of Rcc conidiophore-like structures from stomata was observed at 15 dpi, which coincided with the lowest level of expression of *VeA* and *LaeA*, suggesting the velvet complex could be involved in regulating sporulation in Rcc. The results of this study suggest that the velvet complex may be involved in SM gene expression regulation in Rcc; however, some discrepancies appeared particularly at 10 dpi when *VeA* and *LaeA* level remained high while SM core genes level started to drop. This suggests that other regulators of secondary metabolism may be at play. Further work including putative KO mutants is required to elaborate a clear relationship between the velvet complex and SM-related gene expression in Rcc. Although Rcc rarely sporulates *in vitro* (Frei, 2002), obtaining KO mutants impaired in the velvet complex may also provide information on the role of this complex in asexual sporulation in Rcc as recent studies reported the presence of microconidia and chlamydospores in Rcc grown on straw bran agar (Frei & Gindro, 2015). Previous studies reported a causative link between light intensity and RLS development as plants grown in conditions of high light intensity before inoculation exhibited more symptoms than plants grown in low light conditions (Makepeace *et al.*, 2008; Brown & Makepeace, 2009; Peraldi *et al.*, 2014). Moreover, the development of RLS is thought to be linked with the production and release *in planta* of the photodynamic toxins rubellins (Heiser & Liebermann, 2006; Makepeace *et al.*, 2008). Taken together these studies suggest that light plays an important role in RLS development which could potentially be explained by light-regulated production and subsequent release of SMs *in planta*. Therefore, *in vitro* experiments carried out in different light conditions may provide insights into the potential involvement of the velvet complex in light-dependent regulation of secondary metabolism in Rcc.

Master regulators such as *LaeA* acting on chromatin compaction state were shown to be involved in the regulation of SM clusters located primarily in subtelomeric regions (Shwab *et al.*, 2007; Osbourn, 2010; Palmer & Keller, 2010). Determining the chromosomal location of the gene clusters involved in certain SM

pathways may provide valuable information regarding the role of master regulators in specific pathways. Regulation of gene expression by *LaeA* in *A. nidulans* largely depends on the physical location of the target genes. Insertion of a non-SM-related gene in the sterigmatocystin biosynthetic cluster, which is under *LaeA* regulation mediated by *AflR*, resulted in silencing of this gene in an *A. nidulans laeA* deficient mutant strain (Bok *et al.*, 2006). Furthermore, the observation that complementation of this mutant with a functional *AflR* gene inserted outside of the sterigmatocystin cluster restored sterigmatocystin production further highlights the importance of physical location in *LaeA*-mediated regulation (Bok *et al.*, 2006). Therefore, karyotyping Rcc could prove informative in regards to SM gene cluster location and putative subsequent regulation by master regulators such as *LaeA*.

The results of this study suggest that regulation of secondary metabolism in Rcc may also occur at an SM cluster level. Rcc paralogues of the pathway-specific TFs *AflR* and *AflJ*, both involved in aflatoxin and dothistromin regulation in *A. flavus* and *D. septosporum* respectively, showed a similar transcription profile to that observed for the putative Rcc paralogues of the *StcQ* and *PksA* genes, also involved in aflatoxin and dothistromin biosynthesis. This result correlates with that observed in *Leptosphaeria maculans* where genes involved in the biosynthesis of sirodesmin PL were co-regulated with the zinc finger TF *SirZ* also located in the sirodesmin biosynthetic cluster (Gardiner *et al.*, 2004). Furthermore, because the two putative *PksA* paralogues in Rcc were identified in different clusters from that containing the *AflR*, *AflJ* and *StcQ* genes, this suggests that *AflR*-mediated regulation may occur at separate loci. Similar results were found in *D. septosporum* where dothistromin biosynthetic genes located in different clusters were co-regulated (Schwelm *et al.*, 2008). Further supporting the role of *AflR*-mediated regulation in dothistromin biosynthesis was the observation that co-regulated genes possessed in their promoter region specific *AflR* binding sites whereas genes lacking these sites exhibited different transcription profiles (Chettri *et al.*, 2013). Genes located in the clusters on contig 17 and PKSm24, including the *StcQ* and *PksA* paralogues, were found to possess *AflR* binding sites in their promoter regions suggesting that they may be under regulation of an *AflR*-like TF in Rcc.

The competition assay presented in this study proposed another possible role for Rcc SMs. When in the vicinity of Rcc cultures *in vitro*, other fungal pathogen of barley such as *R. commune*, *P. teres*, *F. graminearum* and *F. poae* all exhibited reduced growth. These observations are reminiscent of that made when *F. graminearum*, known to produce the mycotoxin zearalenone, inhibited the growth of other *Fusarium* species such as *F. moniliforme* and *F. proliferatum* that produce the mycotoxin fumonisin B1 (Velluti *et al.*, 2000). Similarly, the characterisation of massariphenone and ergosterol peroxide, two SMs isolated from an unidentified *Verticillium* species endophytic of *Rehmannia glutinosa*, an *Orobanchaceae*, exhibiting antifungal activity against *Fusarium* and *Rhizoctonia* species (You *et al.*, 2009), highlighted further the involvement of SMs in conferring an ecological advantage to the producing organism. However, the observation that the non-aflatoxigenic isolate of *Aspergillus flavus* AF36 inhibited the colonisation of maize kernel by the aflatoxigenic isolate AF70, suggested that not all SMs are involved in inhibiting the growth of competitors. The antimicrobial activity of rubellin toxins produced by Rcc reported by Miethbauer *et al.* (2008) being light-dependent and this assay having been carried out in constant darkness, the results of this study are unlikely to be linked with rubellins activity. However, the discovery of a gene cluster resembling that involved in the biosynthesis of the known antifungal agent chaetoglobosin A (Chapter 2, Figure 2.22), suggest that Rcc possesses the genetic ability to produce SMs potentially involved in antagonistic effects towards other fungi.

The results presented in this chapter showed that most of the Rcc PKSs, all HPSs and approximately half of the NRPS genes tested are expressed during the earliest stages of Rcc colonisation. Secondary metabolites expressed at early stages of disease development if involved in disease expression may be interacting with the host, for instance through manipulating host defence mechanism or concealing the pathogen from host recognition. Taken together with the results of the second chapter of this thesis, it appears that Rcc has the genetic ability to produce a wide range of SM and that most of the core genes identified are expressed during the infection.

However, the expression of the core gene does not always result in SM production in fungal pathogens. Therefore, despite the fact that Rcc appears to have the genetic equipment to produce a diverse range of SMs, it is possible that this fungus may only produce few SM products. The next chapter will focus on understanding the role of the only SM family characterised in Rcc by interrogating the mode of action of rubellin D, one member of this family.

Chapter 4:

Determining the *in planta* mode of action of rubellin D, a phytotoxin produced by *Ramularia collo-cygni*.

4.1. Introduction

It is commonly understood that secondary metabolism products play a crucial role in interactions between pathogens and their hosts. Fungal secondary metabolites (SMs) can protect the pathogen from recognition by the host defence system, suppress host defence responses or can induce host cell death to increase nutrient availability for the pathogen. In this chapter the role and mode of action of a known phytotoxin, rubellin D, produced by *Ramularia collo-cygni* (Rcc) was investigated.

4.1.1. Rubellins: toxins produced by *Ramularia collo-cygni*

As stated in the Chapter 1, section 1.4.5, to date only one family of SM, the rubellins, has been confirmed to be produced by Rcc. Rubellins were first identified in culture of *Mycosphaerella rubella* grown on malt-peptone-glucose agar and shown to induce cell death in a number of plant species, including tobacco (*Nicotiana tabacum*), wild angelica (*Angelica sylvestris*), barley (*Hordeum vulgare*), as well as animal cells (Arnone *et al.*, 1986; Heiser *et al.*, 2004; Miethbauer *et al.*, 2008). Therefore, rubellins were classified as non-host specific toxins. Based on their chemical structure, which is that of a dimer of anthracene-9,10-dione, particularly visible on rubellin A and B, rubellins were classified among the anthraquinone-derived toxins (Arnone *et al.*, 1986). Furthermore, because these SMs exhibit light-dependent activity such as cytotoxicity, rubellins were classified as photosensitisers (Miethbauer *et al.*, 2006).

4.1.2. Role of known anthraquinone toxins in plant pathogenic fungi

The anthraquinones are a family of cyclic compounds characterised by an anthracene-9,10-dione backbone with the formula $C_{14}H_8O_2$ and are a major class of SMs produced by plant pathogenic fungi (Muria-Gonzalez *et al.*, 2015). Phytotoxic activities are often found for anthraquinone-derived SMs, such as catenarin and dothistromin produced by respectively *Pyrenophora tritici-repentis* and *Dothistroma septosporum* (syn. *Dothistroma pini*), respectively, the agents responsible for tan spot

of wheat and needle blight of pine trees (Bassett *et al.*, 1970; Bouras & Strelkov, 2008). Catenarin and dothistromin can induce cell death in plant tissues, however, the activity of catenarin does not appear to depend on light, whereas dothistromin-induced cell death requires light activation (Shain & Franich, 1981; Bouras & Strelkov, 2008). Similarly, lentisone, a recently characterised anthraquinone produced by *Ascochyta lentis*, the causative agent of ascochyta blight of lentils, was shown to exert light-dependent phytotoxic activity in a wide range of *Fabaceae* crops, including chickpea, lentils and pea (Andolfi *et al.*, 2013). Interestingly, not all anthraquinones were found to be phytotoxic, suggesting that these toxins can play alternative roles depending on the infection strategy and biology of the fungus. The most widely studied anthraquinone derived metabolites are arguably aflatoxins because of their potent carcinogenic effects on humans and animals (Wild & Turner, 2002). Although the chemical structure of aflatoxins differs significantly from that of most anthraquinones as the cyclic anthracene backbone is not present in the final product, these SMs are classified as belonging to the anthraquinone family as their precursors averantin, averufanin or versicolorin B contain the anthracene backbone (Yu *et al.*, 2004). Emodin is an anthraquinone SM produced by both plants and plant pathogenic fungi such as *Pyrenochaeta terrestris*, a pathogen of *Alliaceae* plants, and *P. tritici-repentis* (Izhaki, 2002; Brase *et al.*, 2009). Although the role of emodin in fungal pathogenesis is still unclear, this anthraquinone has been extensively studied due to its numerous potential medicinal uses, as emodin was shown to affect the human immune system and vasomotor system as well as exhibit antimicrobial, antioxidant and anti-inflammatory activities (Izhaki, 2002). Many anthraquinone-derived SMs produced by plant pathogenic fungi are involved in disease development through phytotoxic or cytotoxic effects in the host. The phytotoxic activity of anthraquinones is thought to be associated with the inhibition of the electron transport chain in the photosystem II, therefore negatively impacting photosynthesis (Oettmeier *et al.*, 1988). This mode of action is likely to explain the phytotoxic activity of rubellins produced by Rcc although these SMs also induce fatty acid peroxidation *in vitro* via light-dependent production of reactive oxygen species (ROS), primarily singlet oxygen (Heiser *et al.*, 2004) which is reminiscent of the mode of action of photosensitisers. Although the biosynthetic pathways involved

in the production of some anthraquinone-derived metabolites, such as cladofulvin produced by *Cladosporium fulvum* (syn. *Passalora fulva*), is well understood (Griffiths *et al.*, 2016), the role and mode of action of many anthraquinone-derived metabolites in hosts remains largely unclear.

4.1.3. Role of photosensitisers in plant pathogenic fungi

Photosensitisers are molecules that, when activated by visible light wavelengths, induce cell death in a given tissue through the production of ROS (Spikes, 1989). The mechanism behind photosensitisation is that of energy transfer. Photosensitisers are able to transform light energy into the chemical energy of ROS such as hydrogen peroxide (H_2O_2), singlet oxygen ($^1O_2$), hydroxyl radicals ($OH^{\bullet}$) or superoxide ($O_2^{\bullet-}$) (Spikes, 1989). Many plant pathogenic fungi utilise photosensitising toxins to modify cellular processes in their hosts. The non-host specificity of many photosensitising toxins may largely be imputed to the fact that ROS are potent toxic compounds for a large range of cells. Cercosporin, a perylenequinone toxin produced by *Cercospora* species that are related to Rcc (Churchill, 2011; McGrann *et al.*, 2016), was shown to induce cell death in tobacco (*Nicotiana tabacum*), chard (*Beta vulgaris*), mustard (*Brassica juncea*), rapeseed (*Brassica napus*) and wild radish (*Raphanus raphanistrum*) (Guchu & Cole, 1994; Gunasinghe *et al.*, 2016). Cercosporin has been studied as the model photosensitising toxin and its mode of action is well understood. Upon light activation, cercosporin is converted to a highly energetic state that reacts with oxygen molecules to yield superoxide and singlet oxygen (Daub & Chung, 2007). Singlet oxygen was found to play a major role in cercosporin-induced cell death, as the singlet oxygen quenchers 1,4-diazabicyclo[2,2,2]octane (DABCO) and bixin increased cell survival in presence of cercosporin (Daub, 1982). This highly reactive ROS subsequently induces membrane lipid peroxidation, thus damaging cell integrity and ultimately leading to cell death (Daub & Briggs, 1983). ROS-mediated cell death has been identified in several other photosensitisers from the perylenequinone family such as the elsinochrome, isolated from *Elsinoë fawcettii*, the agent responsible of the citrus scab, which produces both singlet oxygen and superoxide (Liao & Chung, 2008b). Similarly, altertoxin produced by *Alternaria*

species was shown to induce superoxide formation upon light activation (Hartman *et al.*, 1989). Anthraquinone photosensitisers also appear to operate with a mode of action related to ROS-mediated cell death. Rubellins were shown *in vitro* to induce fatty acid peroxidation through the production of ROS, especially singlet oxygen (Heiser *et al.*, 2004). However, the mode of action of rubellins may differ slightly from that of cercosporin as the presence of ferrous ions (Fe^{2+}) increased rubellin-induced fatty acid peroxidation, whereas Fe^{2+} treatment reduced cercosporin-mediated fatty acid peroxidation (Heiser *et al.*, 2004). Furthermore, singlet oxygen is closely associated with genetically determined response to oxidative stress *in planta*. Upon pathogen challenge plants accumulate high levels of ROS, including singlet oxygen as part of the defence response (Wojtaszek, 1997). The oxidative burst has several consequences as it plays a role in triggering the hypersensitive response (HR), a form of programmed cell death (PCD) that blocks biotrophic pathogen growth at the site of infection (Levine *et al.*, 1994). One mechanism behind singlet oxygen-mediated HR was identified in *flu* mutants of *Arabidopsis thaliana* that accumulate high levels of singlet oxygen and initiate PCD after shifting from dark to light conditions (op den Camp *et al.*, 2013). Singlet oxygen-mediated PCD is orchestrated by the *EXECUTER1* and *EXECUTER2* genes encoding protein localised in the chloroplasts that perceive singlet oxygen (Wagner *et al.*, 2004; Danon *et al.*, 2005; Kim *et al.*, 2012). In addition, the oxidative burst is followed by salicylic acid (SA) accumulation (Hammond-Kosack *et al.*, 1996). SA is a known regulator of plant defence mechanisms, for instance it induces stomatal closure following bacterial infection (Melotto *et al.*, 2006). SA is also involved in the induction of systemic acquired resistance (SAR) against a broad spectrum of pathogens away from the infection site (Durrant & Dong, 2004).

4.1.4. Salicylic acid in plant defence mechanism

Salicylic acid (SA) is a phenolic acid naturally synthesised by a wide range of organisms including both prokaryotes and eukaryotes. In plants, SA acts as a phytohormone that regulates plant defences and control cell's fate following pathogen infection through its action as a cell death agonist in tissues around the

infection point (Fu *et al.*, 2012). Although SA has many roles in plants, including in developmental processes such as growth, germination or flowering (Rivas-San Vicente & Plasencia, 2011), the present study will mostly focus on the role of SA in plant immunity.

4.1.4.1.Salicylic acid biosynthesis in higher plants

Biosynthesis of SA plays an important role in plant defence. Following pathogen challenge, the level of SA in the plant cell increases significantly which ultimately decides the fate of the cell and therefore, decides the success or failure of the infection. SA biosynthesis and its induction upon pathogen infection in plants are achieved by two pathways occurring in different cell compartments. In the cytoplasm, SA can be synthesised from the amino acid phenylalanine via phenylalanine ammonia lyase (PAL) and benzoic acid-2-hydroxylase (BA2H) (Lee *et al.*, 1995). The second pathway, localised in the chloroplasts, is responsible for the majority of SA biosynthesis and uses chorismate as a precursor, which is converted through the action of isochorismate synthase (ICS) to isochorismate and subsequently transformed into SA (Wildermuth *et al.*, 2001). *Arabidopsis thaliana* possesses two genes encoding for ICS called *ICS1* and *ICS2*. The *salicylic acid induction deficient 2* (*sid2*) mutant is impaired in *ICS1* and compared to wild-type exhibits lower SA accumulation and reduced *Pathogenesis-related-1* (*PR-1*) gene expression following pathogen infection (Nawrath & Métraux, 1999; Wildermuth *et al.*, 2001). Although the ICS pathway is responsible for more than 95% of SA biosynthesis, the role of the PAL pathway is crucial in pathogen-induced SA biosynthesis required for SAR (Chen *et al.*, 2009).

4.1.4.2. Salicylic acid in plant immunity

Upon pathogen recognition, plants undergo both localised and systemic changes. The HR takes place locally surrounding the site of pathogen infection and involves physiological processes such as modification of cell wall composition and PCD which blocks the development of biotrophic pathogens (Levine *et al.*, 1994). SA is a

major component of HR by acting as a cell death agonist. Transgenic plants carrying the *nahG* gene encoding for a bacterial SA hydroxylase that completely degrades SA into catechol fail to trigger HR and allow avirulent pathogen growth (Delaney *et al.*, 1994; Rairdan & Delaney, 2002). Away from the site of infection, distant tissues also see an increase in defence-related gene expression such as those encoding for phytoalexins and pathogenesis-related (PR) genes. This distal response is termed systemic acquired resistance (SAR), which confers resistance to a broad spectrum of pathogens (Ryals *et al.*, 1996). SA plays a crucial role in SAR induction. Upon pathogen recognition, accumulation of SA in systemic tissue induces *PR* gene expression, resulting in increased resistance in these tissues (Yalpani *et al.*, 1991). SA-induction deficient *A. thaliana sid* mutants lacking SA accumulation after pathogen challenge, exhibit lower level of PR-1 proteins and impaired SAR (Nawrath & Métraux, 1999). Furthermore, transgenic plants expressing bacterial *nahG* lack SA and are impaired in SAR induction (Gaffney *et al.*, 1993). SA induces expression of defence-related genes through the action of the transcription cofactor Nonexpresser of PR genes 1 (NPR1). Plants carrying the *npr1* mutation lack SA-mediated *PR* induction and exhibit higher susceptibility to pathogens (Cao *et al.*, 1994). NPR1 activates *PR* gene expression by binding to the TGACG *cis*-element-binding protein (TGA) family of a basic leucine zipper (bZIP) transcription factor (Zhang *et al.*, 1999; Zhou *et al.*, 2000; Alves *et al.*, 2014). Induction of *PR* gene expression by NPR1 is modulated by perception of SA by NPR3 and NPR4, two paralogues of NPR1 (Fu *et al.*, 2012). Both NPR3 and NPR4 were shown to bind SA, however, NPR4 exhibited the highest affinity (Fu *et al.*, 2012). NPR3 and NPR4 differentially interact with NPR1 in a SA-dependent manner. The NPR1-NPR3 interaction was promoted upon SA binding by NPR3, whereas SA binding by NPR4 disrupted the interaction with NPR1 (Fu *et al.*, 2012). Interactions between NPR1 and NPR3 or NPR4 play a crucial role in modulating defence responses. NPR3 and NPR4 act as substrate adaptors for a Cullin3-based (CUL3) ubiquitin E3 ligase that ubiquitinates NPR1 and targets it for proteasome-mediated degradation (Spoel *et al.*, 2009). Degradation of NPR1 plays diverse roles in regulating immunity. The degradation of NPR1 by the 26S proteasome, a multi-subunit ATP-dependent protease complex, allows a new NPR1 to bind to the TGA transcription factor which

prolongs and amplifies the immune response (Spoel *et al.*, 2009). Therefore, SA indirectly modulates the plant immune response through its ambivalent role in regulating NPR1 degradation in a NPR3/NPR4-dependent manner.

In cells unchallenged by pathogens, NPR1 is mostly present in the cytosol in an oligomeric form bound via disulphide bounds and only a small amount of monomeric NPR1 translocates to the nucleus (Mou *et al.*, 2003). In the nucleus, most NPR1 is bound by NPR4 which initiates CUL3-mediated ubiquitination and targets NPR1 for proteasome-mediated degradation to prevent unnecessary *PR* gene expression (Spoel *et al.*, 2009). Furthermore, in unchallenged cells, low SA concentration promotes the phosphorylation of free NPR1 at the Serine 55 and Serine 59 residues which results in NPR1 binding to the transcription repressor WRKY70 (Saleh *et al.*, 2015). A simplified model of the role of SA and NPR1 in unchallenged cells is presented in Figure 4.1.A.

Upon pathogen challenge, changes in cellular redox state result in thioredoxin (TRX)-mediated reduction of oligomeric NPR1 in the cytosol and subsequent release of monomeric NPR1 that translocates to the nucleus (Tada *et al.*, 2008). Concomitantly, accumulation of SA promotes NPR1 sumoylation (addition of small ubiquitin-like modifiers; SUMO) resulting in NPR1 switching its interaction with WRKY70 repressors for TGA transcription activators (Saleh *et al.*, 2015). In addition, SA induces phosphorylation of NPR1 at the Serine 11 and Serine 15 residues, which facilitates recruitment of the CUL3-based ubiquitin ligase, resulting in NPR1 ubiquitination and degradation by the proteasome (Spoel *et al.*, 2009). SA-induced NPR1 turnover is thought to be necessary for continuous delivery of "fresh" transcriptionally active NPR1 to SA-responsive gene promoters (Spoel *et al.*, 2009; Furniss & Spoel, 2015). A simplified model of the role of SA and NPR1 in unchallenged cells is presented in Figure 4.1.B.

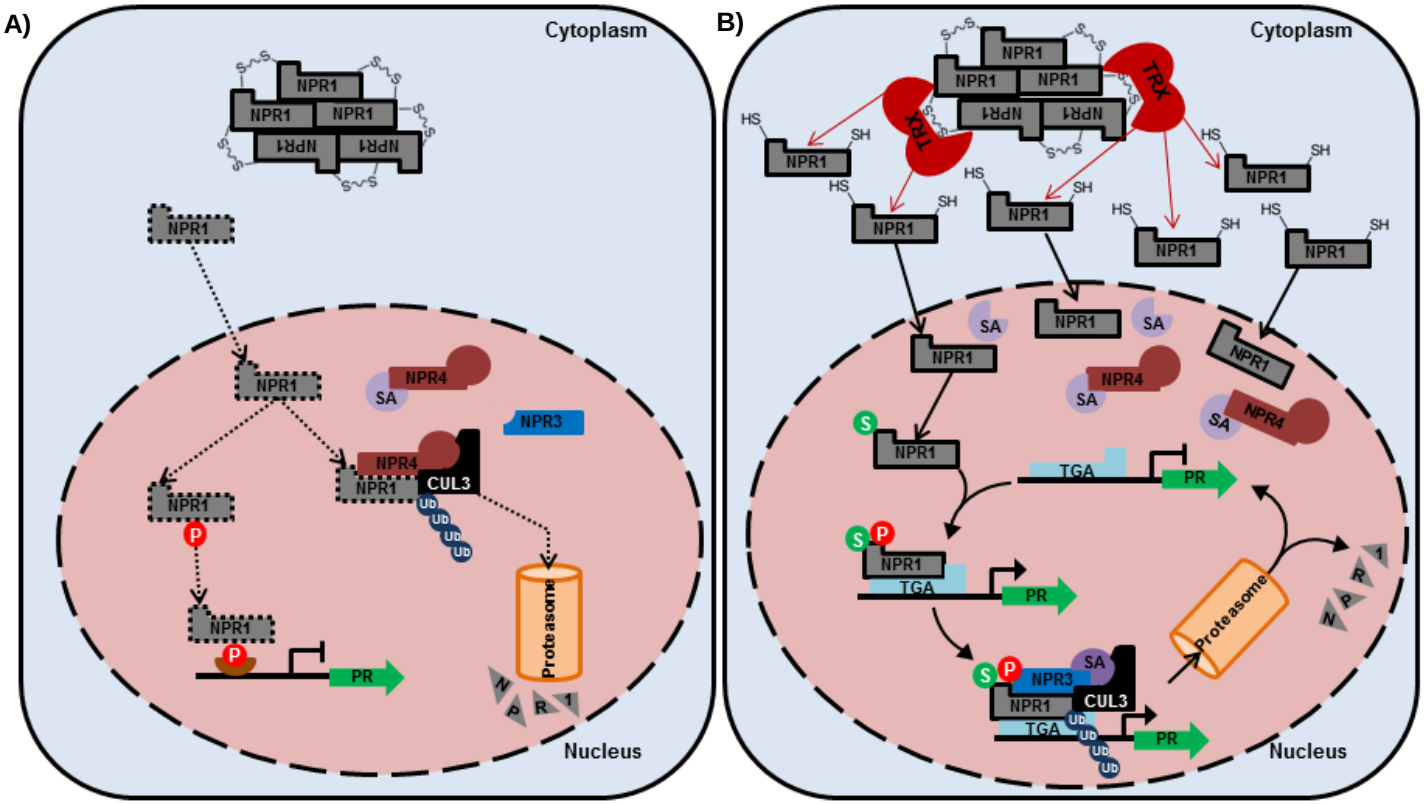

Figure 4.1: Role of salicylic acid in immunity in unchallenged and challenged cells.
A) In unchallenged cells NPR1 is mostly present in the cytoplasm as oligomers. Only a small amount of monomeric NPR1 translocates in the nucleus where under low SA levels it interacts with NPR4. The NPR1-NPR4 complex is recognised by a cullin3-based ubiquitin E3 ligase (CUL3) which promotes NPR1 ubiquitination (Ub) and it subsequent degradation by the proteasome. In addition, free NPR1 is phosphorylated (P) at the Serine 55/59 residues which promotes its interaction with WRKY70 transcription repressor to prevent unnecessary SAR gene expression. B) Upon pathogen challenge, changes in cell redox state results in thioredoxin (TRX)-mediated reduction of disulphide bonds between NPR1 and subsequent release of monomeric NPR1 which translocates in large amount the nucleus. The elevated levels of SA promote SUMOylation (S) of NPR1 resulting in its activation via phosphorylation at the Serine11/15 residues. Activated NPR1 binds TGA transcription factors and activates SAR gene expression. Activated NPR1 interacts, in a SA-dependent manner, with NPR3 which serves as an adaptor to recruit CUL3 and promotes subsequent ubiquitination of NPR1 that is targeted for proteasomal degradation. Free TGA can be bound to a newly activated NPR1 and amplify SAR. Adapted from Spoel et al. 2009; Spoel & Loake 2011; Fu et al. 2012; Saleh et al. 2015.

4.1.4.3.Salicylic acid regulates cell death during the immune response

Salicylic acid plays a crucial role in deciding cell fate upon pathogen infection. The identification of *accelerated cell death 2* (*acd2*), *lesion simulating disease resistance response* (*lsd*) and *hypersensitive response-like lesion 1* (*hrl1*) mutants (Dietrich *et al.*, 1994; Greenberg *et al.*, 1994; Devadas *et al.*, 2002), exhibiting spontaneous HR-induced cell death lesions uncovered the link between pathogen-induced PCD and SA. In these three mutants SA was found to play a major role in PCD induction. The *acd2* and *hrl1* mutant exhibit higher level of SA than wild-type plants (Greenberg *et al.*, 1994; Devadas *et al.*, 2002), while in the *lsd1* mutant, treatment with SA or the SA analogues 2,6-dichloroisonictinic acid (INA) or benzothiadiazole-S-methylester (BTH) was sufficient to induce HR-like PCD (Dietrich *et al.*, 1994; Rusterucci *et al.*, 2001). The observation that mutation of the *Pad4* gene, which encodes a lipase-like protein required for SA accumulation upon pathogen infection (Jirage *et al.*, 1999), in a *lsd1* genetic background abolished PCD upon BTH treatment or pathogen inoculation, strengthened the link between SA and HR-like PCD induction (Rusterucci *et al.*, 2001). Conversely, *lsd* mutations in a *nahG* genetic background that completely lacks SA does not lead to spontaneous formation of lesions, confirming the role of SA in HR-like PCD induction (Weymann *et al.*, 1995). Similarly, *hrl1* mutation in a *nahG* background delayed HR-like lesions formation further highlighting the importance of SA in PCD induction (Devadas *et al.*, 2002). Furthermore, the interaction between SA and NPR1 also mediates PCD. The accumulation of NPR1 monomer in SA-induced cells is also thought to act as a signal that promotes cell survival by negatively regulating pathogen-induced PCD. In *npr3 npr4* double mutant plants that accumulate excessive amounts of NPR1 protein, pathogen effector-triggered PCD by nucleotide-binding leucine rich repeat domain-containing (NB-LRR) receptors was abolished, whereas NB-LRR-mediated PCD was restored in an *npr1 npr3 npr4* triple mutant supporting an antagonistic role for *NPR1* towards PCD (Rate & Greenberg, 2001; Fu *et al.*, 2012). Furthermore, the observation that NPR1 is not necessary for NB-LRR-induced PCD supports the hypothesis that levels of NPR1 acts as a cell survival

signal rather than an inducer of PCD (Rairdan & Delaney, 2002). Indeed, genetic analysis of *npr1* mutants has previously revealed a role for NPR1 in suppression of NB-LRR-induced PCD (Rate & Greenberg, 2001). The differential affinity to bind SA of NPR3 and NPR4 combined with the contrasting effect on NPR1 degradation controlled by NPR1-NPR3 and NPR1-NPR4 interactions appears to be crucial to modulate plant cell's fate upon pathogen infection (Fu *et al.*, 2012) therefore directly mediating the interactions between the plant and pathogens.

To date, no studies have investigated the role and mode of action of the phytotoxins produced by Rcc *in planta*. As rubellins are non-host specific, this study investigated the mode of action of rubellin D using the model plant *A. thaliana* (thale cress). Using *A. thaliana* as a model offers several advantages, including the availability of numerous mutants and transgenic plants altered in pathways involved in plant-pathogen interaction. Although rubellin B is predominant in barley infected leaves, rubellin D is the most stable and soluble rubellin *in planta* (Miethbauer *et al.*, 2003). Therefore, rubellin D was used to investigate the mode of action of rubellins *in planta* to determine how this toxin interacts with plants.

4.1.5. Objectives

This chapter aims at understanding the putative role and *in planta* mode of action of the most stable and plant soluble rubellin, produced by Rcc, rubellin D, by:

- Determining the relationship between leaf sensitivity to rubellin D-induced cell death in barley plants and disease susceptibility.
- Characterising the mode of action of *in planta* rubellin D-induced cell death and the role of the SA pathway in this interaction using the model plant *Arabidopsis thaliana*.

4.2. Material and methods

4.2.1. Infiltration solutions used in this study

Rubellin D (Enzo Life Sciences, Farmingdale, NY, USA) was dissolved into dimethyl sulfoxide (DMSO; Sigma, Dorset, UK) to obtain a stock solution (10 mM) and stored at -20°C. Working solutions were made fresh on the day of use by diluting the stock solution in 10 mM magnesium chloride ($MgCl_2$; Sigma, Dorset, UK). A pilot assay in which leaves of *A. thaliana* were infiltrated with different concentrations of rubellin D was used to determine the final working concentration of rubellin D. Lesions were observed after 24 hours under the conditions described in section 4.2.3.1 (Appendix 7). The working solution concentration was set at 50 µM as this concentration of rubellin D yielded lesions that were easily visible without exhibiting an activity too destructive on plant tissues. Control leaves were treated with 10 mM $MgCl_2$ supplemented with DMSO equivalent to that of the rubellin D treatment.

The proteasome inhibitor MG132 (Cambridge Biosciences, Cambridge, UK) was dissolved in DMSO to obtain a stock solution (20 mM) and stored at -20°C. Working solutions were made fresh on the day of use by diluting the stock solution in 10 mM $MgCl_2$ to obtain a concentration of 100 µM as previously described (Spoel *et al.*, 2009).

Salicylic acid (Sigma, Dorset, UK) and the SA analogue benzothiadiazole-S-methylester (BTH; Sigma, Dorset, UK) were dissolved in DMSO to obtain stock solutions (10mM). Working solutions were made fresh on the day of use by diluting the stock solutions in 10 mM $MgCl_2$ to obtain solutions at a concentration of 500 µM. Concentrations of SA and BTH were set based on previous studies (Cao *et al.*, 1994; Fu *et al.*, 2012; Saleh *et al.*, 2015).

4.2.2. Plant materials used in this study

4.2.2.1.Barley plant materials used in this study

Several barley lines were used in this study including landraces, elite cultivars and mutants. Landraces were selected based on disease assessment in field conditions in 2012 at the SRUC trial site in Lanark, Scotland. Two RLS resistant landraces PFLUGS INTENSIV and Midas showing less than 5% RLS leaf coverage, two landraces with an intermediate RLS response Wiebe F13 and Hordeum9, exhibiting between 5 and 10% RLS leaf coverage and the susceptible Hor.3322 exhibiting more than 10% RLS leaf coverage were used.

Elite spring barley cultivars that have been described on the UK AHDB recommended list for commercial use since their release were also used, including two RLS resistant cultivars, Sanette and Power, and two RLS susceptible cultivars, Shaloo and Braemar.

The *sln1d*, *bri1* and two *mlo5* barley mutants that have been previously reported to exhibit different behaviour towards RLS were also investigated. The *Slender 1* (*Sln1*) gene encodes a DELLA protein known to be a repressor of gibberllic acid (GA)-induced growth response. The mutant *sln1d* is a *Sln1* gain of function mutant resulting in a dwarfing phenotype and was shown to exhibit higher susceptibility to RLS than its wild-type Himalaya (Saville *et al.*, 2012). The *bri1* mutant lacks *Brassinosteroid-insensitive 1*, the main receptor for brassinosteroids (Friedrichsen *et al.*, 2000) which are a family of phytohormones known to regulate several physiological processes including growth and plant defence responses. The mutated *bri1* allele results in a semi-dwarf phenotype but does not appear to have an impact on RLS susceptibility (Goddard *et al.*, 2014). The *MLO* (*mildew locus O*) gene encodes a seven transmembrane-domain protein responsible for susceptibility to *Blumeria graminis f.sp hordei*, the biotrophic fungus causative of powdery mildew, by negatively regulating plant defence (Kim *et al.*, 2002). Barley lines carrying *mlo* mutations are fully resistant to powdery mildew (Piffanelli *et al.*, 2002) but highly susceptible to RLS (McGrann *et al.*, 2014). In this study, two *mlo5* mutants and their

respective wild-type Ingrid and Pallas were used. Barley lines used in this study are presented in Table 4.1.

Table 4.1: Ramularia leaf spot resistance status of the barley plant materials used in this study.

Name	Line type	RLS resistance status	Source
PFLUGS INTENSIV	Landraces	Resistant	Field trials
Midas	Landraces	Resistant	Field trials
Wiebe F13	Landraces	Intermediate	Field trials
Hordeum9	Landraces	Intermediate	Field trials
Hor.3322	Landraces	Susceptible	Field trials
Sanette	Cultivars	Resistant	AHDB Recommended list
Shaloo	Cultivars	Susceptible	AHDB Recommended list
Power	Cultivars	Resistant	AHDB Recommended list
Braemar	Cultivars	Susceptible	AHDB Recommended list
sln1d (Himalaya)	Mutant	Increased susceptibility	Saville *et al.* (2012)
Himalaya	Wild-type	-	
bri1 (Bowman)	Mutant	No effect	Goddard *et al.* (2014)
Bowman	Wild-type	-	
mlo5 (Ingrid)	Mutant	Increased susceptibility	McGrann *et al.* (2014)
Ingrid	Wild-type	-	
mlo5 (Pallas)	Mutant	Increased susceptibility	McGrann *et al.* (2014)
Pallas	Wild-type	-	

4.2.2.2.*Arabidopsis thaliana* plant materials used in this study

The ecotype Columbia-0 (Col-0) of *A. thaliana* was used in this study to investigate the role of rubellin D. Two *A. thaliana* mutants carrying *mlo* mutations were also used: *Atmlo2* and *Atmlo2/6/12*. *A. thaliana* possesses three *MLO* genes which are homologs to the barley *MLO*, *AtMLO2*, *AtMLO6* and *AtMLO12*. However, *AtMLO2* was the most important *MLO* gene in conferring resistance to powdery mildew as the *Atmlo2* single mutant exhibited partial resistance to *Golovinomyces orontii* the causative agent of powdery mildew whereas the *Atmlo6* and *Atmlo12* single mutants exhibited disease level similar to that observed in the wild-type Col-0. The double mutants *Atmlo2/6* and *Atmlo2/12* also showed reduced infection and sporulation compared to that of the wild-type which was not observed for the double mutant *Atmlo6/12*. The triple mutant *Atmlo2/6/12* showed complete resistance to *G. orontii* (Consonni *et al.*, 2006).

Several mutants impaired in the SA pathway were also investigated in this study. The *npr1-2* mutant accumulates SA upon pathogen challenge but fails to achieve SAR and *PR* gene expression which results in compromised immune response (Cao *et al.*, 1997). *A. thaliana nahG* plants express a transgene encoding for a bacterial SA hydroxylase which is involved in SA degradation into catechol, resulting in SAR abolition and higher disease susceptibility (Delaney *et al.*, 1994). The *pad4* mutant (*phytoalexin deficient 4*) is impaired in the expression of the gene encoding a lipase-like protein involved in SA-induced expression of defence response-related genes such as *PR* genes or the phytoalexin camalexin biosynthesis genes (Jirage *et al.*, 1999). *PAD4* acts upstream of SA and is thought to be involved in SA accumulation after pathogen challenge (Feys *et al.*, 2001; Brodersen *et al.*, 2006). Upon pathogen challenge, plants carrying *pad4* mutation exhibited lower level of SA accumulation than that observed in wild-type plants despite exhibiting a normal behaviour when exogenous SA was applied (Zhou *et al.*, 1998). Similarly, the *sid2* (*salicylic acid induction deficient 2*) mutant is impaired in SA biosynthesis through disruption of the *ICS1* gene encoding for the isochorismate synthase (Wildermuth *et al.*, 2001). Accumulation of SA following pathogen inoculation and expression of *PR-1* are reduced in *sid2* mutants. However, in contrast to *pad4* mutants levels of camalexin and the *PR* genes *PR-2* and *PR-5* are not altered in *sid2* mutants (Nawrath & Métraux, 1999).

4.2.3. Chemical infiltration of barley and *Arabidopsis thaliana* leaves to determine the *in planta* effect of rubellin D

4.2.3.1. Infiltration of barley leaves with rubellin D

First leaves of two week old barley plants at GS 11-12 (Zadoks *et al.*, 1974) were infiltrated with 100 µL of rubellin D using a 1 mL syringe. Infiltration was performed on the abaxial side of the leaf on either side of the central vein at the approximate middle section of the leaf. Lesions were photographed after 72 hours at 18°C, 80% relative humidity, 250 mol m^{-2} s^{-1} and a 16h/8h light/dark photoperiod. The area of rubellin D induced lesions were measured using the ImageJ software

(Abràmoff *et al.*, 2004). Data were analysed in GenStat 16th edition (VSN International, Rothamsted, UK). Three independent experiments consisting of ten leaves each were carried out for the rubellin D infiltration of barley landraces and mutants whereas two independent experiments of 15 leaves each were carried out for the infiltration of barley cultivars. Raw data were analysed by general linear model (GLM), using the model Line*Experiment.

4.2.3.2. Infiltrations of *Arabidopsis thaliana* leaves with rubellin D

Infiltrations of *A. thaliana* were performed on the abaxial side of the third or fourth leaf of 4-week-old *A. thaliana* plants grown at 18°C, 16h light photoperiod, 80% relative humidity and 250 mol m^{-2} s^{-1} light intensity. In contrast to the barley infiltrations, the full leaf area was infiltrated. Lesions were photographed and measured after 24 hours using ImageJ (Abràmoff *et al.*, 2004). Results are expressed as the percentage of the total leaf area covered by necrosis.

Infiltration of 50 µM rubellin D was performed on *A. thaliana mlo* mutants as well as on the ecotype Columbia-0 (Col-0) to assess rubellin D sensitivity. Raw data from three independent experiments of ten leaves each were analysed in GenStat 16th edition by GLM, using the model Experiment*Line.

This assay was also used to investigate the role of the plant proteasome in rubellin D-induced cell death following rubellin D infiltration and co-infiltration with the proteasome inhibitor MG132 in *A. thaliana* Col-0 plants. Control consisted in $MgCl_2$ or MG132 supplemented with DMSO equivalent to that of the treatment. Raw data from three independent experiments of ten leaves each were LOG transformed and analysed using GLM with the model Experiment*Treatment.

Infiltration of rubellin D was used to assess the sensitivity of mutants impaired in the SA pathway towards the toxin. Mutants and wild-type *A. thaliana* leaves were infiltrated with rubellin D, rubellin D + SA or rubellin D + BTH. Control consisted in $MgCl_2$, SA and BTH, respectively, supplemented with DMSO equivalent to that of the treatment. Raw data from three independent experiment of ten leaves each were analysed using GLM with the model Experiment+Line*Treatment.

4.2.4. Electrolyte leakage assay

Measurement of electrolyte leakage can be used as a reflection of membrane permeability. Electrolyte leakage assays are widely used to directly quantify cell death (del Pozo & Lam, 1998). Cell degradation results in increased ion leakage and thus higher levels of ionic conductivity in the extracellular environment are measured. Electrolyte leakage was used to assess cell death following co-infiltration of rubellin D with the proteasome inhibitor MG132 in *A. thaliana* ecotype Col-0. The third or fourth leaf of four weeks old *A. thaliana* plants were infiltrated with a solution of rubellin D, rubellin D + MG132 or $MgCl_2$ as a control. Leaves were allowed to stand for 15 minutes in the dark to absorb the infiltrated compound before a 5 mm diameter disc was excised from the middle of the leaf and washed extensively with distilled water for 30 minutes. Leaf discs were transferred in a 50 mL Falcon tube containing 1 mL of distilled water per leaf disc and the tubes were placed in an incubator at 18°C with constant lights (250 µmol m^{-2} s^{-1}). Electrical conductivity of the water of each tube was measured with a Treaceable© conductimeter (Fisher Scientific International, NH, USA) every hour for 24 hours. At the end of the experiment, total electrolyte leakage was measured after an intense heat treatment consisting of 1 min at 100°C. Results are expressed as a percentage of total electrolyte leakage over time based on three independent experiments each containing three biological replicates of ten leaf discs each.

Electrolyte leakage was also used to assess sensitivity of the *A. thaliana npr1-2* mutant to rubellin D compared to that of the wild-type Col-0. The assay was carried out as described above. Results are expressed as a percentage of total electrolyte leakage over time based on three independent experiments each containing four biological replicates of ten leaf discs each.

All electrolyte leakage raw data were analysed in GenStat 16^{th} edition using restricted maximum likelihood (REML) for repeated measurments using the Uniform correlation/Split-plot in time covariance matrix. The model used to analyse the data obtained in the proteasome inhibitor assay was Experiment+Treatment*Time. Raw data from the *npr1-2* mutant assay were analysed using the model Experiment+Line*Treatment*Time.

4.3. Results

4.3.1. Relationship between rubellin D-induced necrosis and Ramularia leaf spot development in barley

To investigate to role of rubellins in disease symptom development, rubellin D was infiltrated into the leaves of five barley landraces that have adapted to local environmental and agricultural conditions (PFLUGS INTENSIV, Midas, Hor.3322, Wiebe F13 and Hordeum9), four elite cultivars (Sanette, Shaloo, Power and Braemar) and two barley mutants (*sln1d* and *bri1*) and their respective wild-type cultivars (Himalaya and Bowman). These different barley lines all exhibited differential RLS susceptibility (section 4.2.2.1, Table 4.1). Rubellin D infiltrations in barley leaves did not produce typical RLS symptoms. However, necrotic lesions were formed, composed of dehydrated tissue that was surrounded by a brown discolouration (Figure 4.2). The two resistant landraces, PFLUGS INTENSIV and Midas, exhibited similar sensitivity to rubellin D based on the size of the lesion formed 72 hours post infiltration to that observed for the susceptible line, Hor.3322, whereas the two landraces showing intermediate resistance to RLS, Wiebe F13 and Hordeum9, showed significantly lower sensitivity to the toxin ($P<0.05$) than the resistant ones (Figure 4.3.A). Similarly, the RLS resistant cultivar Power exhibited an equivalent sensitivity to rubellin D to that observed for the susceptible cultivar Shaloo (Figure 4.3.B). However, the RLS resistant cultivar Sanette exhibited the smallest rubellin-induced lesions, whereas the RLS susceptible cultivar Braemar had the highest sensitivity to the toxin. Rubellin infiltration of the barley *sln1* and *bri1* mutants and their respective wild-type cultivars showed that the *sln1d* mutant exhibited significantly ($P<0.001$) smaller rubellin D-induced lesions than its wild-type Himalaya, whereas the *bri1* mutant did not exhibit a different behaviour than its wild-type Bowman ($P=0.105$) (Figure 4.3.C). Taken together, these results suggest that the link between rubellin D-induced *in planta* necrosis and RLS is more complex than previously thought. Increased rubellin sensitivity alone does not correlate with higher susceptibility to RLS. In addition, the observed phenotype of rubellin-induced cell death differs from typical RLS symptoms. Therefore, a causal link between

rubellin and RLS development appears to be unlikely; however, rubellin may still be involved in disease development as a virulence factor. Understanding the mode of action *in planta* of the toxin produced by Rcc may provide insights into its potential role in modulating disease severity.

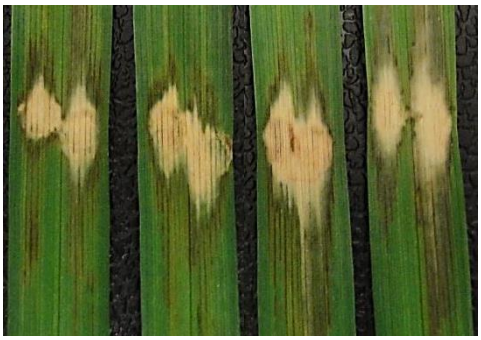

Figure 4.2: Rubellin D-induced lesions in barley cultivar Concerto.
Lesions observed on four barley leaves cv. Concerto photographed 72 hours post infiltration at 18°C, 80% relative humidity, 250 mol m^{-2} s^{-1} and 16h/8h light/dark photoperiod.

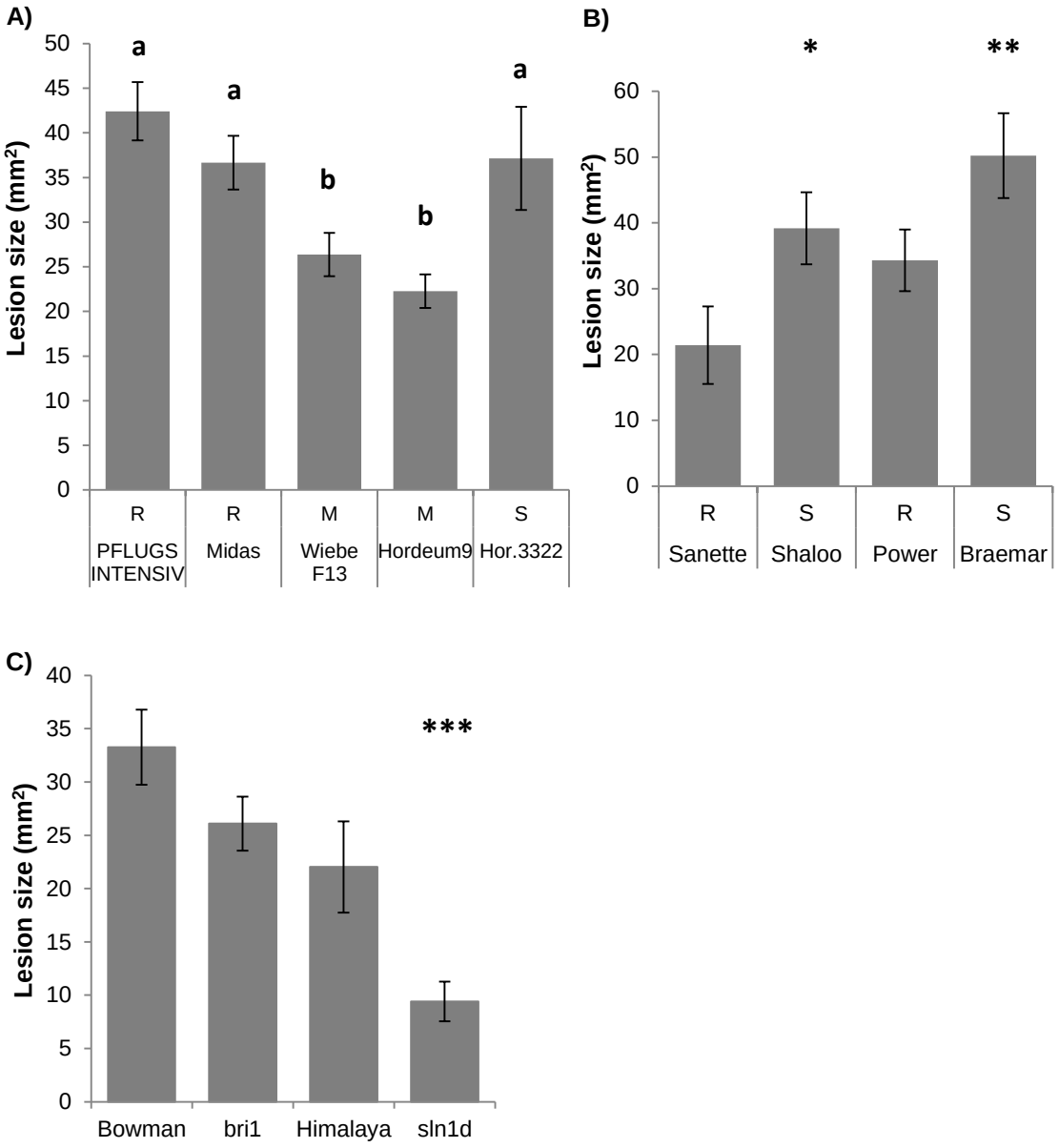

Figure 4.3: Lesion size observed in barley leaves following a rubellin D infiltration treatment.

A) Infiltration of rubellin D in barley landraces. Resistance (R), susceptibility (S) or intermediate resistance (M) to RLS is indicated above the line's name. Bars sharing the same letters were not significantly different at $P<0.05$. Data represent predicted mean ± SE. B) Infiltration of rubellin D of selected resistant (R), and susceptible (S) barley cultivars. Data represent predicted mean ± SE. C) Infiltration of rubellin D on the barley *sln1d* and *bri1* mutants. Data represent predicted mean ± SE. *** P <0.001; ** P <0.01, * P <0.05.

4.3.2. Analysis of the *in planta* mode of action of rubellin D

4.3.2.1. Assessing the suitability of *A. thaliana* as a model for studying the *in planta* mode of action of rubellin D

As Rcc rubellins have been previously reported to be non-host specific toxins (Heiser *et al.*, 2004), the *in planta* mode of action of rubellin D was investigated in the model organism *A. thaliana*. To assess the suitability of *A. thaliana* as a model for the effect of rubellin D *in planta*, infiltrations were carried out on barley *mlo* mutants that are highly susceptible to RLS (McGrann *et al.*, 2014) and compared with *A. thaliana* carrying mutations in the homologous genes. The role of the *MLO* gene in conferring susceptibility to powdery mildew to both barley and *A. thaliana* is described in sections 4.2.2.1 and 4.2.2.2, respectively.

The phenotype of rubellin D-induced lesions in the two barley *mlo5* mutants and their respective wild-type (Figure 4.4.A) exhibited a similar phenotype to that described previously of collapsed dehydrated tissue surrounded by a brown discoloration (section 4.3.1, Figure 4.2). In *A. thaliana* the phenotype observed following rubellin D infiltrations showed well contained lesions with typical dehydrated collapsed tissue that was particularly visible on *A. thaliana* wild-type Col-0 (Figure 4.4.A). This phenotype is reminiscent to that of programmed cell death (PCD) occurring during the hypersensitive response (HR) (Greenberg, 1996). Similar phenotypes have been observed in the *acd2*, *lsd* and *hrl1* mutants that exhibit spontaneous HR-like PCD (Dietrich *et al.*, 1994; Greenberg *et al.*, 1994; Devadas *et al.*, 2002). Despite exhibiting slightly different rubellin D-induced phenotypes, both barley and *A. thaliana* behaved similarly following rubellin D infiltrations as smaller lesions were observed in the *mlo* mutants compared to their respective wild-type lines (Figure 4.4.B). Taken together these results suggest that *A. thaliana* appears to be a good model to study the interaction between rubellin D and plant cells. Therefore, the mode of action of this toxin was further studied in *A. thaliana* grown in controlled conditions.

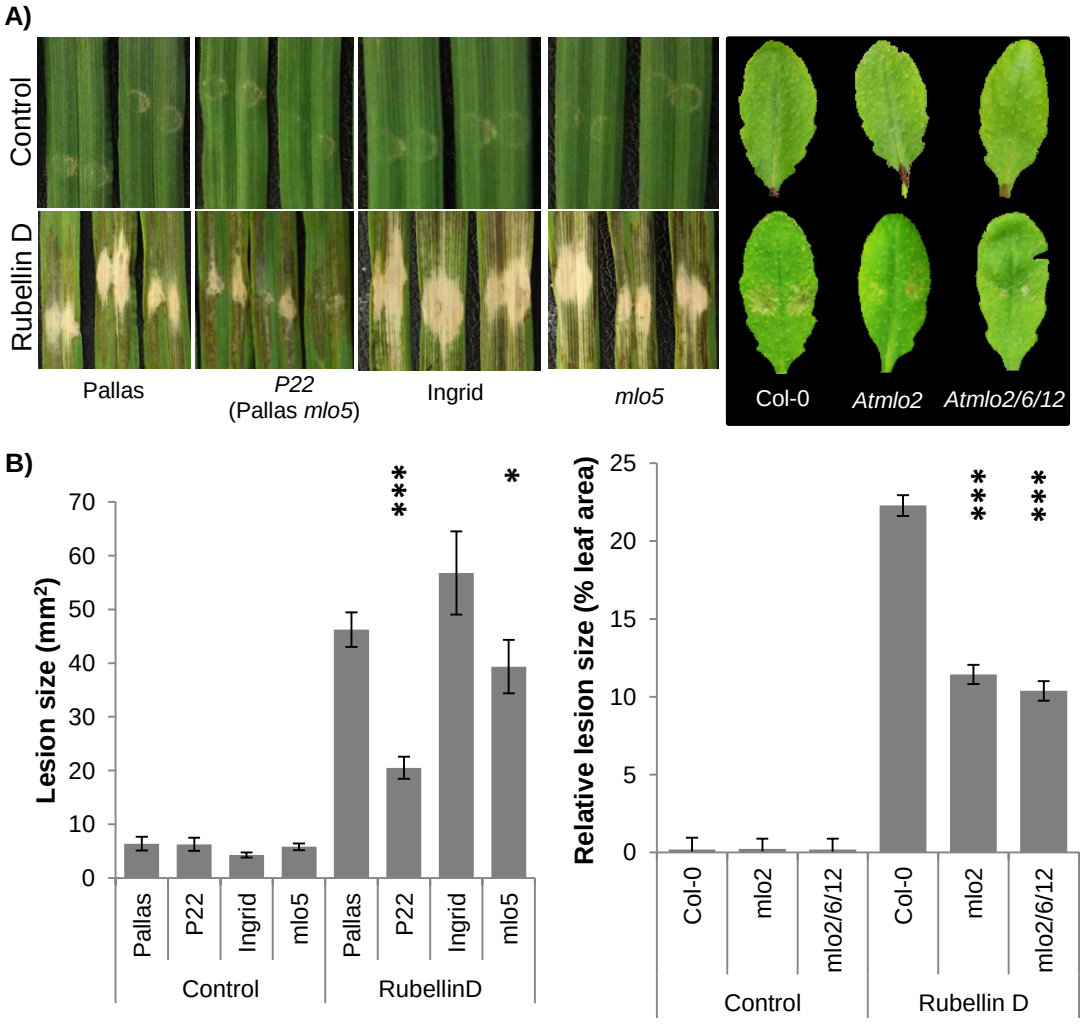

Figure 4.4: Rubellin D infiltration in *mlo* mutants of barley and *A. thaliana*.
A) Infiltration of rubellin D in barley and *A. thaliana* leaves showed a similar type of response with the *mlo* mutants exhibiting smaller lesions that their respective wild-types. B) Lesion size was measured 72 hours and 24 hours post infiltrations in barley and *A. thaliana* respectively. Data show predicted mean of three independent experiments of 10 leaves each ± SE. *** P <0.001; * P <0.05.

4.3.2.2.Role of the salicylic acid pathway in rubellin D-induced cell death

Rubellin D-induced lesions in *A. thaliana* (described in section 4.3.2.1) phenotypically resemble HR-like PCD lesions observed in the *acd2*, *lsd* and *hrl1* mutants. As SA has been shown to play a major role in regulating lesion formation in these mutants (Weymann *et al.*, 1995; Rusterucci *et al.*, 2001; Devadas *et al.*, 2002), the role of the SA pathway was investigated in rubellin D-induced cell death.

Four lines of *A. thaliana* impaired in the SA pathway were studied. The wild-type Col-0 was included as a control and compared with SA-deficient *nahG*, *sid2* and *pad4* plants, as well as with *npr1-2* mutants impaired SA signalling. Lesion formation on the selected mutants was studied following infiltration with rubellin D. All the mutants exhibited significantly larger lesions ($P<0.01$ for *pad4* and $P<0.001$ for *nahG*, *npr1-2* and *sid2*) than wild-type Col-0 when infiltrated with rubellin D (Figure 4.5). *A. thaliana nahG* plants in which SA is completely degraded was the most sensitive to rubellin D as illustrated by the largest lesion size on these plants. Mutants with basal levels of SA such as *pad4* and *sid2* exhibited larger lesions than Col-0 but smaller than *nahG*, suggesting that after infiltration, Rubellin D may be able to induce a moderate SA accumulation which could explain the difference observed between the wild-type Col-0 and the *nahG*, *sid2* and *pad4* plants that are unable to do so. Moderate induction of SA accumulation may result in partial NPR1 stabilisation, via the action of SA on NPR3- and NPR4-mediated degradation of NPR1, thus promoting cell survival (Fu *et al.*, 2012). In this hypothesis, mutation of NPR1 naturally leads to increased rubellin D-induced cell death, which was observed in the *npr1-2* mutant (Figure 4.5). The observation that lesion size increased the most in *nahG* plants, which completely lacks SA therefore cannot stabilise NPR1, further support this hypothesis. Therefore, both a basal level of SA which is lacking in *nahG* plants and SA accumulation that is lacking in *sid2* and *pad4* mutants (Zhou *et al.*, 1998; Wildermuth *et al.*, 2001) may be able to dampen the effect of rubellin D-induced PCD on foliar necrosis.

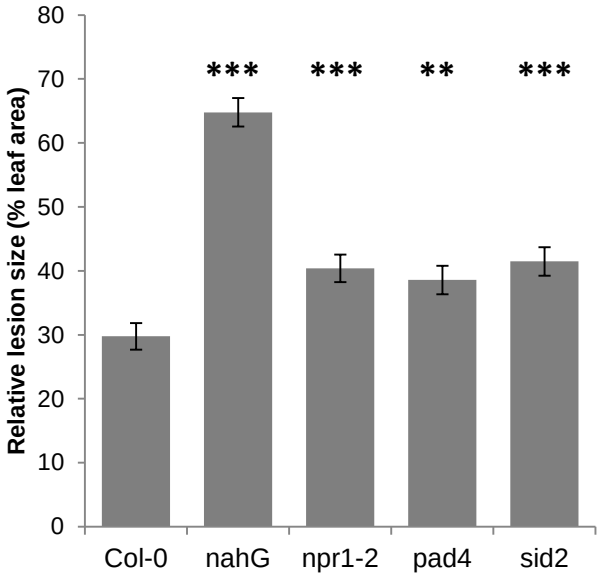

Figure 4.5: Lesions induced by rubellin D infiltrations in *A. thaliana* mutants impaired in the salicylic acid pathway.
Relative lesions sizes in leaves infiltrated with rubellin D (50 µM) measured after 24 hours. Data represent predicted average relative lesion size ± SE of three independent experiments of 10 leaves each. *** *P* <0.001; ** *P* <0.01.

Taken together these results indicate that a functional SA/NPR1 signalling pathway is required to reduce sensitivity to rubellin D. To confirm this hypothesis, leaves of *nahG*, *sid2*, *pad4* and *npr1-2* plants were also co-infiltrated with rubellin D and either exogenous SA or BTH, a potent structural analogue of SA. Assuming that this hypothesis is correct, treatment with exogenous SA or an SA analogue is expected to partially reduce lesion size of the plants impaired in the SA pathway.

In wild-type Col-0 plants, co-infiltration with rubellin D and BTH significantly decreased (P<0.001) lesion size compared to infiltration with rubellin D alone. Although a decrease in lesion size was observed in Col-0 following co-infiltration of SA with rubellin D, this reduction was not significant. In the *nahG* plants, co-infiltration of rubellin D with SA showed no reduction in lesion size compared to infiltration with rubellin D alone, whereas co-infiltration with the structural SA analogue BTH significantly (P<0.001) reduced lesion size (Figure 4.6.B). No effect on lesion size was observed in the *sid2* mutant after co-infiltrations of rubellin D

with either SA or BTH when compared to infiltrations with rubellin D alone. Smaller lesions were observed in the *pad4* mutants co-infiltrated with rubellin D and BTH ($P<0.001$) compared to that infiltrated with rubellin D alone but no significant effects on lesion size were observed in *pad4* co-infiltrated with rubellin D and SA. In the *npr1-2* mutant, both an addition of exogenous SA or BTH co-infiltrated with rubellin D significantly ($P<0.001$) reduced lesions size compared to treatment with rubellin D alone (Figure 4.6.B). This suggests that rubellin D-induced cell death may also involve a NPR1-independent pathway. Reduction in lesion size in the transgenic *nahG* plants treated with BTH supports the hypothesis that rubellin D-induced cell death is dependent of the SA pathway. Furthermore, the phenotype of the lesions observed in the *nahG* transgenic plant differs from that of the mutant and wild-type plants. Rubellin D-induced lesions in *nahG* appeared water soaked and spread over the whole leaf compared to the well contained dehydrated collapsed tissue observed in the other plants. This phenotype was partially rescued in *nahG* upon treatment with the SA analogue BTH (Figure 4.6.A). Taken together, these results suggest that basal levels of SA as well as RubD-induced accumulation of endogenous SA play critical roles in regulating HR-like PCD induction after rubellin D infiltrations.

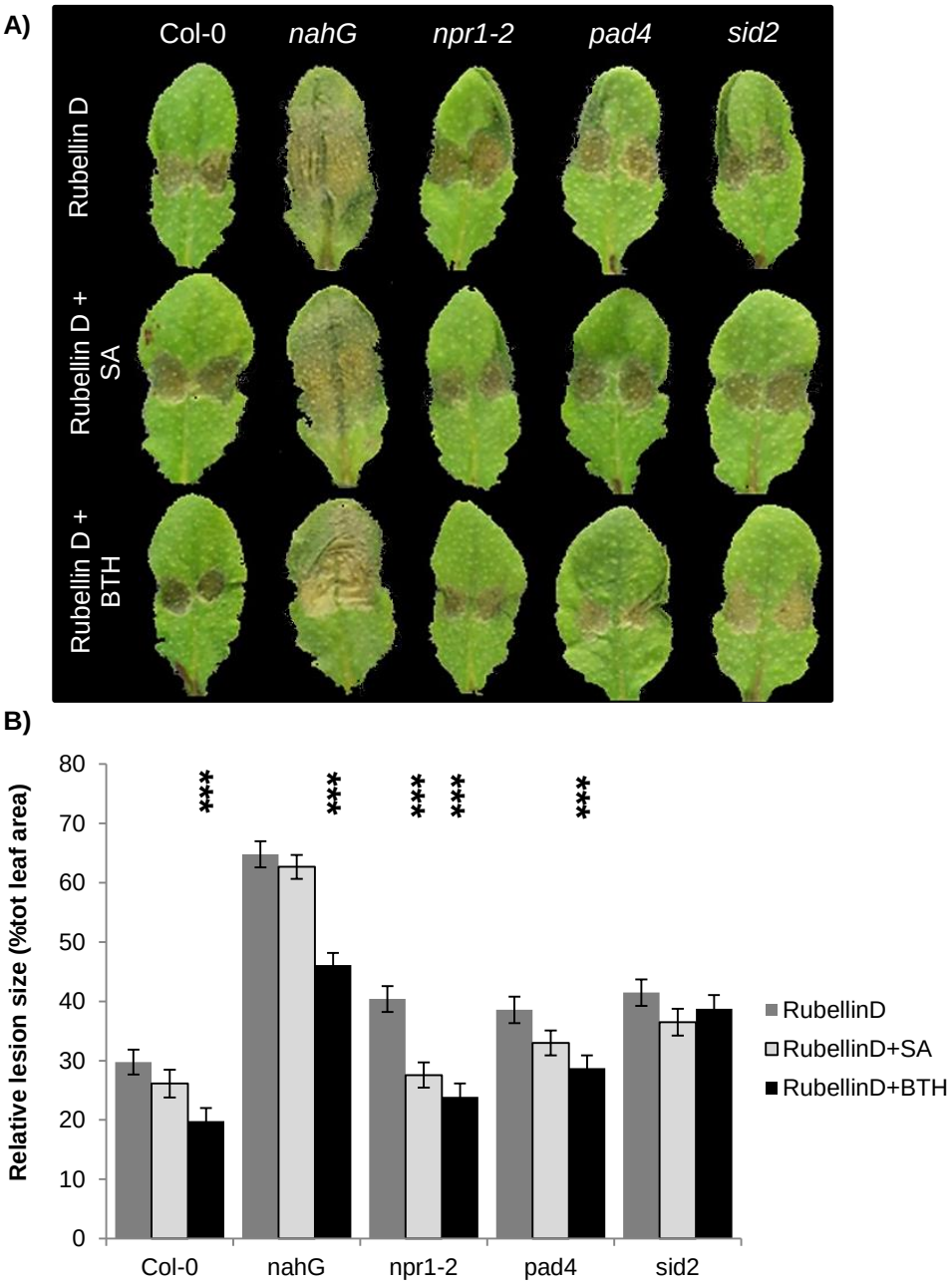

Figure 4.6: Effect of co-infiltration of salicylic acid (SA) or benzothiadiazole-S-methylester (BTH) in rubellin D-induced lesion formation in *A. thaliana* plants impaired in the SA pathway.

A) Representative images of the lesions observed 24 hours post infiltration. B) Relative lesions sizes in leaves infiltrated with rubellin D (50 µM), rubellin D + SA (500 µM) or rubellin D + BTH (500 µM) measured after 24 hours. Data represent predicted average relative lesion size ± SE of three independent experiments of 10 leaves each. *** *P* <0.001.

Within the SA pathway, NPR1 is a master regulator of SA-induced plant defence mechanism including SAR (Dong, 2004) and was found to regulate PCD (Lorrain *et al.*, 2003; Fu *et al.*, 2012; Furniss & Spoel, 2015). Therefore the effect of rubellin D was investigated further in the *npr1-2* mutant to assess whether increased lesion size was a reflection of cell death. Rubellin D-induced lesions were measured 24 hours post infiltrations and cell death was assessed by electrolyte leakage assay. Again larger rubellin D-induced lesions were observed in the *npr1-2* mutant compared to wild-type leaves (Figure 4.7.A and Figure 4.7.B). Moreover, leaves of the *npr1-2* mutant infiltrated with rubellin D exhibited significantly ($P<0.001$) higher electrolyte leakage throughout the time course experiment than leaves of wild-type Col-0, indicating that more cell death occurred in *npr1-2* (Figure 4.7.C). Taken together these results demonstrate that disruption of the *NPR1* gene, which acts in the SA pathway as a regulator of HR-like PCD, leads to an increased sensitivity to rubellin D.

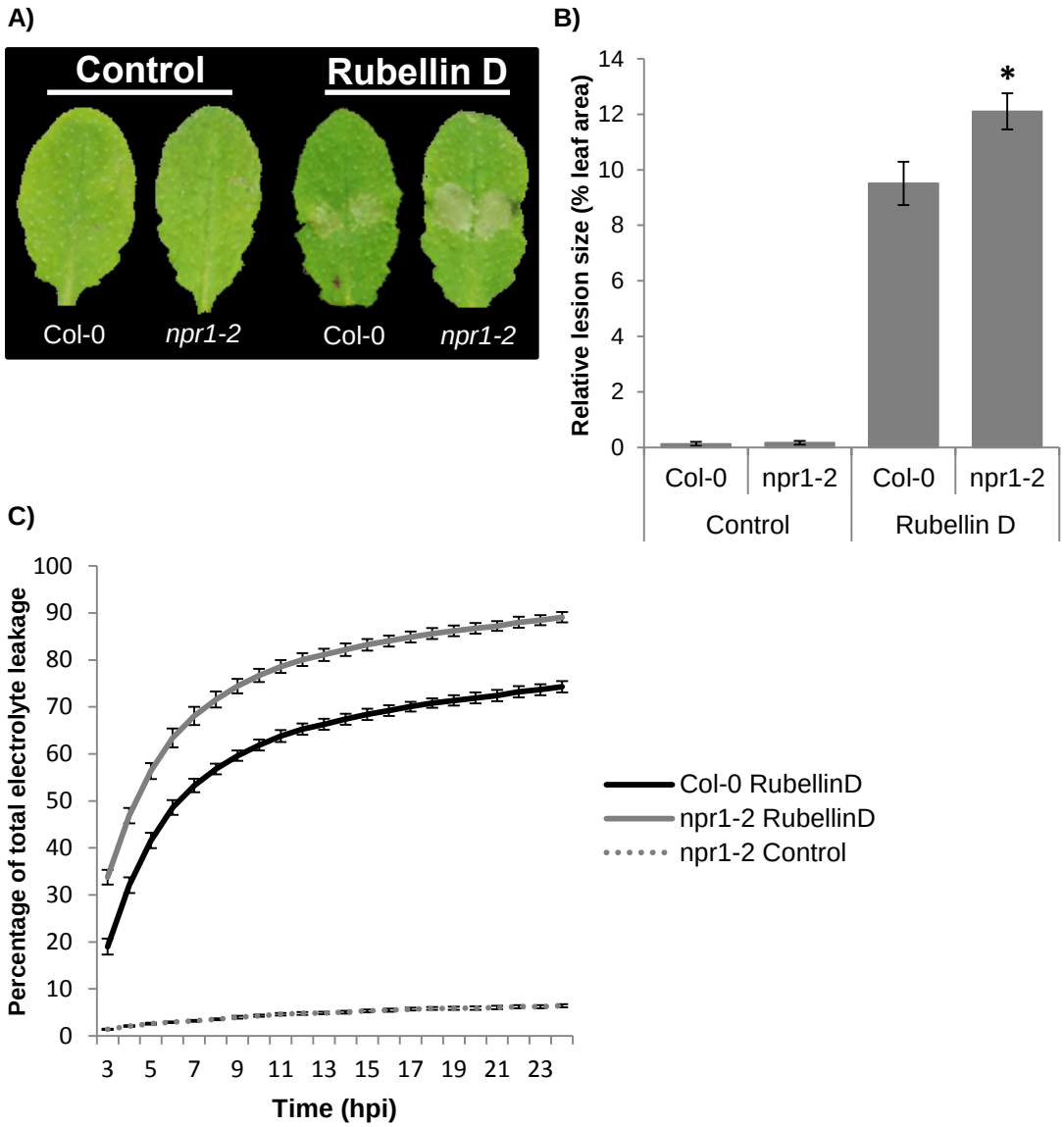

Figure 4.7: Rubellin D-induced lesions and cell death after infiltrations in the *npr1-2* mutant.

A) Representative images of the lesions observed 24 hours post infiltration. B) Relative lesions sizes in leaves infiltrated with rubellin D (50 µM) in the *npr1-2* mutant and in the wild-type Col-0 measured after 24 hours. Data represent predicted average relative lesion size ± SE of three independent experiments of 10 leaves each. * P <0.05. C) Electrolyte leakage following rubellin D infiltration. Data represent predicted mean percentage of total electrolyte leakage ± SE based on three independent experiments. Each experiment contained four biological replications consisting of 10 leaf discs per treatment.

4.3.2.3.Role of the proteasome in rubellin D induced cell death

Given the prominent function the proteasome plays in SA- and NPR1-mediated immune gene expression and pathogen-induced PCD (Spoel *et al.*, 2009; Fu *et al.*, 2012; Furniss & Spoel, 2015), the role of the proteasome in rubellin-induced PCD was investigated further. The proteasome itself is known to function as a master regulator of PCD (Drexler *et al.*, 2000; Kim *et al.*, 2003). The proteasome is a key player in inducing HR-related PCD in *A. thaliana*. Upon infection by avirulent bacterial pathogens, such as *Pseudomonas syringae* pv. *tomato*, inhibition of the proteasome resulted in impaired PCD response which allowed pathogen growth (Hatsugai *et al.*, 2009). Mutation of the proteasome being embryo lethal in *A. thaliana*, chemical inhibition of the proteasome was carried out using the inhibitor MG132. Co-infiltration of *A. thaliana* leaves (Col-0) with rubellin D and the proteasome inhibitor MG132 showed that inhibiting the proteasome significantly ($P<0.001$) increased rubellin D-induced lesion size (Figure 4.8.A and Figure 4.8.B). Furthermore, leaves co-infiltrated with rubellin D and the proteasome inhibitor MG132 exhibited significantly ($P<0.001$) higher electrolyte leakage than leaves infiltrated with rubellin D alone throughout the time course experiment (Figure 4.8.C). As electrolyte leakage is a direct measure of the cell death occurring in a given tissue, these observations demonstrate that rubellin D-induced cell death is increased in proteasome inhibited leaves, indicating a role for the proteasome in reducing rubellin D-induced cell death.

Taken together, the data presented in this study demonstrate that both the SA/NPR1 signalling pathway and the 26S proteasome may be involved in rubellin-induced PCD.

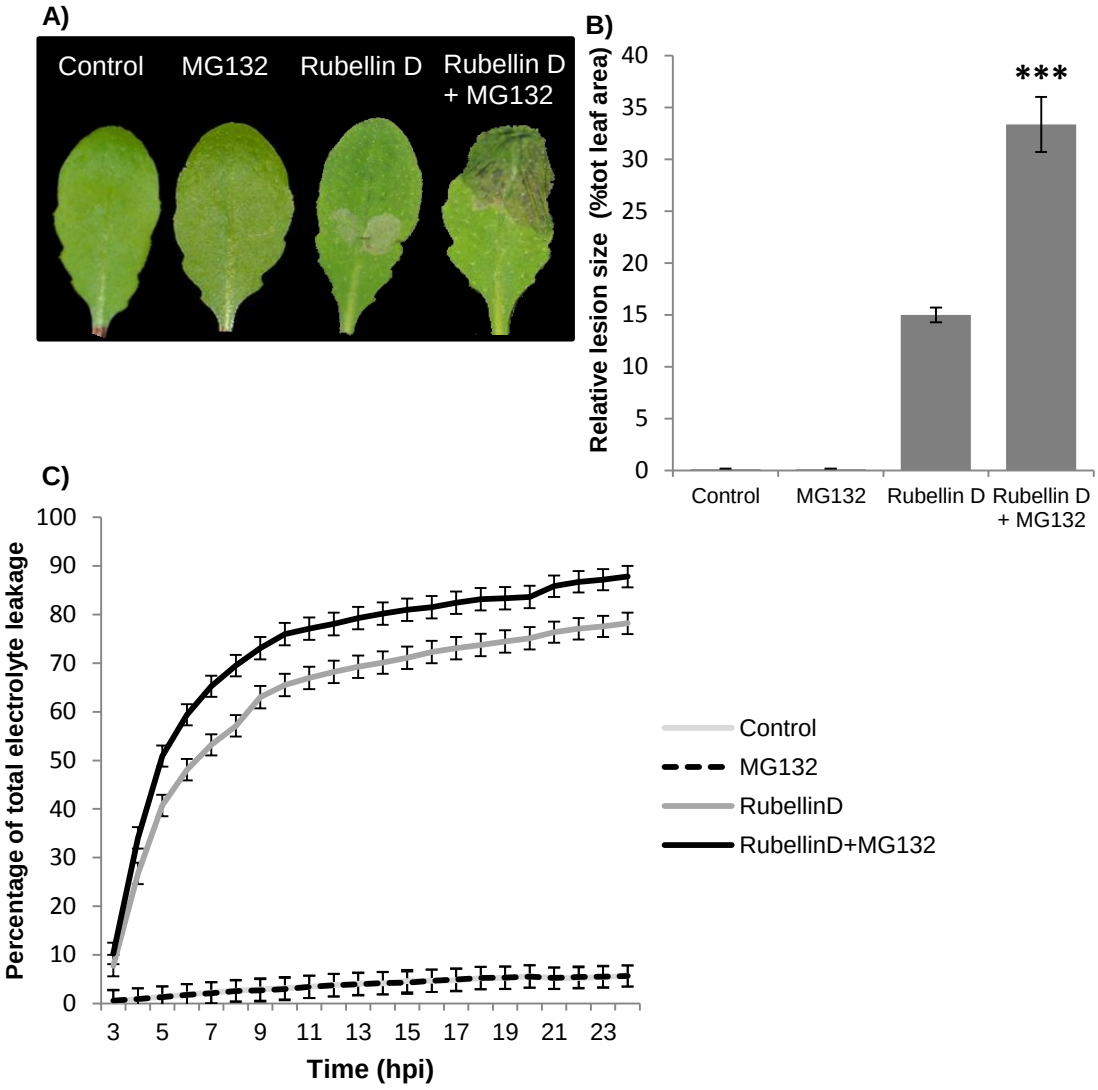

Figure 4.8: Proteasome inhibition increases lesion size and cell death induced by rubellin D in *A. thaliana* Col-0.

A) Representative images of the lesions observed 24 hours post infiltration. B) Relative lesions sizes in leaves infiltrated with rubellin D (50 µM) alone and co-infiltrated with rubellin D and the proteasome inhibitor MG132 (100 µM) measured after 24 hours. Data represent predicted average relative lesion size ± SE of three independent experiments of 10 leaves each. *** *P* <0.001. C) Electrolyte leakage following rubellin D infiltration and co-infiltration with the proteasome inhibitor MG132. Data represent predicted mean percentage of total electrolyte leakage ± SE based on three independent experiments. Each experiment contained three biological replications consisting of 10 leaf discs per treatment.

4.4. Discussion

The present study aimed at understanding the *in planta* mode of action of the known Rcc phytotoxic product rubellin D in the model plant *A. thaliana*. Based on this study, *A. thaliana* appears to be a suitable model to further study at the molecular level the interactions between rubellins and plant cells. This study presents the first insights into the *in vivo* biology of rubellin D-induced cell death by showing that a functional salicylic acid pathway and a functional proteasome may contribute to reducing rubellin D-induced cell death.

The rubellin phytotoxins produced by Rcc were shown to exert light-dependent, non-host specific phytotoxic properties (Heiser *et al.*, 2003; Miethbauer *et al.*, 2003). The phytotoxic effect of rubellins C, B and D was attributed to ROS-mediated disruption of cell membranes as rubellins exhibited *in vitro* singlet oxygen-dependent fatty acid peroxidation (Heiser *et al.*, 2004). These findings were in accordance with previous results describing the mode of action of other photosensitisers such as that of the cercosporin toxin produced by *Cercospora* species. Cercosporin, a red perylenequinone light-activated toxin, induces lipid peroxidation through the production of singlet oxygen (Cavallini *et al.*, 1979; Daub & Ehrenshaft, 2000). Although the identified mode of action of these two toxins seems similar, their role in disease development may vary greatly. In the study presented here, the absence of a clear association between rubellin D sensitivity and RLS susceptibility in barley cultivars, landraces and mutants supports the hypothesis that rubellin is not the sole factor in disease symptoms development. The rubellin D response in barley is different to those in related pathogens such as *Cercospora oryzae* in rice where a direct correlation between cercosporin sensitivity and susceptibility to the disease was observed (Batchvarova *et al.*, 1992). High sensitivity to cercosporin was associated with increased susceptibility to Cercospora leaf spot in sugar beet (Balis & Payne, 1971), whilst susceptibility to white leaf spot in *B. juncea*, *B. napus* and *R. raphanistrum* was impacted by the degree of resistance to cercosporin (Gunasinghe *et al.*, 2016). However, in the present study, the rubellin D response was only investigated in a small population consisting of five landraces and four elite cultivars. The release date of the four cultivars may also have played a role in differential

rubellin sensitivity, as Sanette and Shaloo, which are more recent cultivars than Power and Breamar, exhibited lower rubellin D sensitivity (Figure 4.3.B). Furthermore, the assay used in this study is relatively artificial as the amount of rubellin D infiltrated is approximately 50 times higher than that observed in naturally infected barley leaves (Miethbauer *et al.*, 2003). High concentrations of rubellin D were used in order to observe a phenotype; therefore the observation made in this study may exagerate some aspects of rubellin D biology compared to what is the case in the field. Furthermore, this study provides evidence that rubellin D sensitivity can be modulated by single interactions mediated by one gene. The *MLO* and *SLN1* genes were found to mediate rubellin D sensitivity, as two barley mutants carrying *mlo5* and the DELLA mutant *sln1d* exhibited lower rubellin D sensitivity than their respective wild-types (Figure 4.3.C and Figure 4.4) but higher RLS susceptibility (Saville *et al.*, 2012; McGrann *et al.*, 2014). Therefore, the genetic background of the tested barley lines may have influenced this assay as it is unlikely that these two genes are the only ones influencing rubellin D sensitivity. For instance, genes involved in ROS detoxification in host cells, such as catalases and peroxidases that transform hydrogen peroxide (H_2O_2) into water and oxygen, or superoxide dismutases that detoxify superoxide ($O_2^{\bullet-}$), may play an important role in controlling rubellin-induced cell death (Ananieva *et al.*, 2004). Similarly, carotenoids being strong singlet oxygen ($^1O_2$) quenchers in plant cells (Tripathy & Oelmüller, 2012), variations of carotenoids content between different barley lines may result in differential rubellin sensitivity. To support the observation that rubellin D sensitivity may not relate with RLS susceptibility a more extensive study is required. Assessing rubellin D sensitivity in a larger collection of barley elite cultivars released at different times, with the same *mlo* status and different RLS resistance ratings may help identify or confirm the absence of a putative link between disease susceptibility and rubellin D sensitivity.

Previous studies demonstrated that rubellin B- or rubellin D-induced lesions observed in barley leaves following rubellin uptake through cut leaf edges exhibited a different phenotype than that of typical RLS symptoms (Heiser *et al.*, 2003; Miethbauer *et al.*, 2003). In this study, the phenotype observed following rubellin D

infiltrations into barley also did not resemble that of typical RLS symptoms (Figure 4.2) as infiltrations of barley leaves with rubellin D exhibited dehydrated necrotic tissue at the site of infiltration, similar to the necrotic lesions observed previously after rubellin D uptake in barley (Heiser et al. 2003) or infiltrations in tobacco leaves (Heiser *et al.*, 2004). However, in this study, the necrotic tissue was surrounded by a brown area which was also weakly seen when rubellin was absorbed by barley leaves but was not present on tobacco infiltrated leaves (Heiser *et al.*, 2003, 2004). These results contrast with that of previous studies showing that several toxins involved in disease either as virulence or pathogenicity factors were able to reproduce disease symptoms. The anthraquinone derived toxin dothistromin produced by *D. septosporum* is a virulence factor that was shown to reproduce typical Dothistroma needle blight symptoms when infiltrated into pine needles (Shain & Franich, 1981; Kabir *et al.*, 2015). Although infiltrations with the non-host specific toxin dothistromin, produced by *D. septosporum*, induced lesions similar to the symptoms observed during Dothistroma needle blight (Shain & Franich, 1981), this toxin was not found to be required for pathogenicity. Mutants of *D. septosporum* impaired in dothistromin production where able to infect pine trees and induce needle blight symptoms, despite the fact that lesion formation was not as severe in mutants compared to wild-type isolates (Kabir *et al.*, 2015). Similarly, infiltrations of soybean leaves with the non-host specific toxin cercosporin isolated from *Cercospora kikuchii*, induced lesions similar to the symptoms observed during Cercospora leaf blight development (Upchurch *et al.*, 1991). Mutants of *C. kikuchii* impaired in cercosporin production failed to infect soybean plants, further highlighting the relationship between the pathogenicity factor cercosporin and disease development (Upchurch *et al.*, 1991). Despite the fact that Cercosporin was found to be a pathogenicity factor in *C. kikuchii*, this toxin is thought to act as a virulence factor in *Pseudecercosporella capsella* as hyphal solutions of *P. capsella* that contained no detectable cercosporin were still able to cause disease on *Brassica juncea* and *B. napus* similar to that observed with a solution containing cercosporin (Gunasinghe *et al.*, 2016). However, it is possible that *P. capsella* could synthesise cercosporin *in planta* rapidly after inoculation. Until mutants of *P. capsella* impaired in cercosporin production are generated, the role of cercosporin as pathogenicity or virulence factor

in white leaf spot remains unclear. Similarly, cerato-ulmin, a toxin produced by the fungus responsible of the Dutch elm disease *Ophiostoma ulmi* (syn. *Graphium ulmi*), induces similar lesions to that observed on diseased plants but is not required for pathogenicity and acts as a virulence factor determining the severity of the symptoms (Takai, 1974; Bowden *et al.*, 1996; Temple *et al.*, 1997). Taken together these results highlight the close relationship between both pathogenicity and virulence factors, which in many pathosystems are sufficient to induce typical disease lesion formation, and disease development as these toxins mediate successful infection or disease severity respectively. Therefore, considering that rubellin D failed to reproduce typical RLS lesions, the role of this SM in disease development appears to be more complex than originally thought.

In this thesis, the mode of action of rubellin D was studied in the model plant *A. thaliana* and rubellin D-induced cell death phenotype was found to be similar to that observed in PCD. At the site of infiltration in wild-type plants, rubellin D-induced lesions appeared well contained and exhibited typical dehydrated tissue collapse similar to that seen in *acd2, lsd* and *hrl1* mutants exhibiting spontaneous HR lesions, a form of PCD (Dietrich *et al.*, 1994; Greenberg *et al.*, 1994; Weymann *et al.*, 1995; Devadas *et al.*, 2002). The role of the SA pathway, which is known to regulate HR (Alvarez, 2000; Raffaele *et al.*, 2006), was also investigated after rubellin D infiltrations. Rubellin D-induced lesion size and PCD were increased when the *A. thaliana* SA pathway was impaired (Figure 4.5 and figure 4.7). Furthermore, in the *nahG* transgenic plant that degrades SA into catechol, the phenotype of the lesions appeared to be different from that observed in mutants with a basal level of SA (Figure 4.6.A). Instead of a localised dehydrated tissue, *nahG* exhibited water soaked lesions, which was partially rescued by application of the SA analogue BTH (Figure 4.6.A). The *sid2* mutants were the only plants that did not respond to either exogenous SA or BTH treatment which could be explained by the existence of a positive feedback loop from SA on the expression of *ICS1* (Shah, 2003). Similarly, the lack of response to SA in *pad4* compared to the significant response to BTH (Figure 4.6.B) could potentially be attributed to the fact that BTH is a more potent and stable inducer of plant defence responses than SA (Friedrich *et al.*, 1996). Within

the SA pathway the function of the transcription co-factor NPR1, which is a cell survival promoting factor (Fu *et al.*, 2012; Furniss & Spoel, 2015), appeared to be required to reduce rubellin D-induced PCD as *npr1-2* mutants exhibited larger lesions and higher cell death than the wild-type after rubellin D infiltration (Figure 4.7). However, the observation that lesion size was reduced in *npr1*-2 upon SA or BTH treatment suggests that rubellin-induced lesion size may be regulated via both SA-induced NPR1-dependent and -independent pathways (Figure 4.9). NPR1 independent pathways have been previously reported in *A. thaliana* (Shah *et al.*, 1999; Kachroo *et al.*, 2000; Rairdan *et al.*, 2001; Rate & Greenberg, 2001). Taken together, the results of this study imply that the *A. thaliana* SA pathway mediates the plant defence mechanisms against rubellin D-induced cellular necrosis and PCD.

In addition to the SA pathway, the proteasome also appeared to mediate rubellin D-induced cell death. In the present study, chemical inhibition of the 26S proteasome resulted in increased lesion size and cell death upon rubellin D infiltration (Figure 4.8). Although the proteasome is known to regulate PCD in the SA pathway through its degradation activity of the cell survival factor NPR1 (Spoel *et al.*, 2009; Fu *et al.*, 2012), the observation that both inhibition of the proteasome and mutation of the *NPR1* gene resulted in increased rubellin D-induced cell death suggests that the proteasome acts independently of the SA pathway (Figure 4.9). Regulation of PCD by the plant proteasome independently from that occurring in the immune response has previously been reported after observing that virus-induced gene silencing of the α6 and RPN9 subunits of the *Nicotiana bethamiana* proteasome triggered PCD but did not activate defence-related gene expression (Kim *et al.*, 2003). The proteasome-mediated regulation of PCD has been further understood with the observation that the PBA1 subunit of the proteasome promoted membrane fusion of a large central vacuole with the cell plasma membrane which resulted in PCD induction (Hatsugai *et al.*, 2009). Upon fusion, the vacuole which contains mainly anti-microbial compounds and vacuolar processing enzymes (VPE), which exhibit PCD-inducing caspase-like activity (Hatsugai *et al.*, 2004; Kuroyanagi *et al.*, 2005), releases its content into the apoplast, thus acting as a signal to activate PCD (Hatsugai *et al.*, 2009; Pajerowska-Mukhtar & Dong, 2009). Co-infiltrating rubellin D with inhibitors

of VPEs such as Ac-YVAD-CMK which inhibits caspase-1-like activity or Ac-DEVD-CMK, a potent caspase-3 inhibitor, may provide insights into the role played by the proteasome in rubellin D-induced PCD. Similarly, assessing the expression of the plant metacaspases, known to be involved in activating PCD, following rubellin D infiltration and co-infiltration with chemical inhibitors of VPEs may confirm the involvement of this activation of PCD by the proteasome independently from that occurring during the immune response.

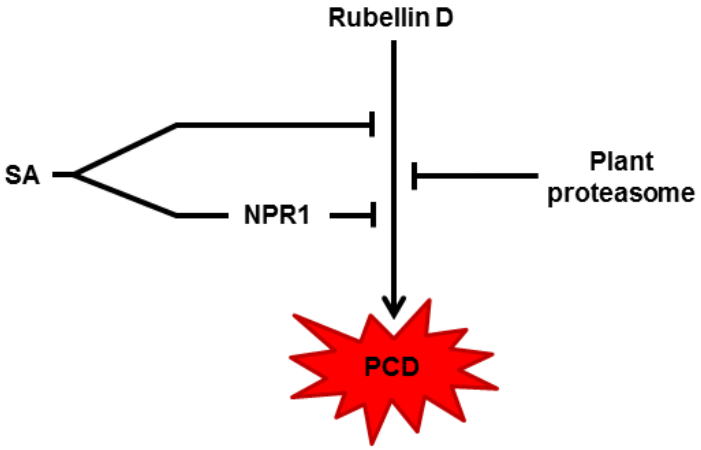

Figure 4.9: Proposed model of how SA, NPR1 and the proteasome affect rubellin D-induced programmed cell death in A. *thaliana*.
Salicylic acid reduces rubellin D-induced PCD (blocked arrows) in a NPR1-dependent and NPR1-independent manner. The 26S proteasome also reduces rubellin D-induced PCD.

The involvement of plant defence mechanisms in toxin-induced cell death was also shown to occur in lesion formation caused by dothistromin infiltration into pine needles. Franich et al. (1986) reported an accumulation of benzoic acid which was speculated to act as a phytoalexin. More recently, benzoic acid was also found to accumulate in tobacco cells infected with the *Tobacco mosaic virus* or elicited with an extract from the oomycete *Phytophtora megasperma* (Chong *et al.*, 2001). Benzoic acid is known to act as a precursor of SA in the phenylalanine amonia lyase (PAL) pathway where it is converted into SA by the action of the benzoic-acid-2-hydroxylase (BA2H) (Métraux, 2002; Shah, 2003). Therefore, the accumulation of benzoic acid after dothistromin infiltration suggests that dothistromin-induced lesion formation also involves the SA pathway. Notwithstanding the fact that rubellin- and

dothistromin-induced cell deaths appear to be modulated by plant defence mechanisms, some discrepancies arise between the two toxins. Rubellin-induced cell death was reduced by a functional SA pathway whereas for dothistromin, plant defences are thought to amplify the effect of this toxin (Franich *et al.*, 1986). Interfering with host defence signalling has also previously been reported for bacterial pathogens such as *Ralstonia solanacearum* or *Pseudomonas syringae*. However, in the case of *R. solanacearum*, a pathogen of *Solanaceae* plants, the bacteria directly interacts with the SA pathway by degrading SA through a set of reactions catalysed by enzymes encoded in the *Nag* operon (Lowe-Power *et al.*, 2016). The case of *P. syringae,* although significantly different from that of Rcc, appears to be more relevant for the present study as the interaction with the SA pathway is mediated by the polyketide-derived toxin coronatine (Bender *et al.*, 1996; Brooks *et al.*, 2005; Uppalapati *et al.*, 2007). Coronatine, which mimics the action of the plant hormone jasmonic acid (JA) uses the antagonistic cross-talk between JA and SA to activate transcription repressors regulating genes involved in SA biosynthesis such as *ICS1* (Laurie-Berry *et al.*, 2006; Zheng *et al.*, 2012). Therefore, interfering with host defence signalling appears to be a strategy found in other organisms and has been linked with at least one toxin.

Rubellin D-induced PCD was affected by the status of the *A. thaliana* SA pathway. Within the SA pathway, the *NPR1* gene is a master transcriptional regulator that controls many SA-dependent plant responses (Dong, 2004). Infiltration of rubellin D into the *npr1-2* mutant resulted in increased cell death. Binding of NPR1 to TGA transcription factor activates the expression of SAR genes, which includes *PR* and phytoalexin encoding genes, upon pathogen-induced SA accumulation (Cao *et al.*, 1994). The subsequent SA-dependent degradation of NPR1 by the 26S proteasome, which also appears to mediate rubellin D-induced cell death, was shown to regulate the intensity of the immune response (Spoel *et al.*, 2009). In addition to SAR genes, NPR1 was also shown to have primary target genes encoding proteins involved in secretion such as transmembrane proteins as well as genes involved in protein folding, including the chaperone-encoding gene *BIP2* (*luminal binding protein 2*) (Wang *et al.*, 2005). BIP2 is located in the endoplasmic reticulum (ER)

and is involved in recognition of unfolded or misfolded proteins (Hetz, 2012). To prevent ER stress due to enhanced secretion of defence proteins during pathogen infection and establishment of SAR, NPR1 induces the expression of *BIP2* and other secretory pathway genes (Wang *et al.*, 2005). Upon elicitation with the SA analogue INA, *bip2* mutants were unable to mount SAR and exhibited unfolded protein response (UPR)-mediated PCD (Wang *et al.*, 2005). In mammalian cells, under normal conditions, BIP proteins were shown to bind the ER transmembrane protein inositol-requiring enzyme 1 (IRE1) (Bertolotti *et al.*, 2000). A similar pathway is believed to exist in plants where mutation of *IRE1* analogues in *A.thaliana* resulted in impaired SAR induction (Moreno *et al.*, 2012), further indicating that NPR1-mediated SAR induction requires a functional UPR pathway. Under ER stress conditions such as accumulation of unfolded or misfolded proteins, BIP proteins bind to unfolded proteins allowing IRE1 to dimerise (Walter & Ron, 2012). Upon dimerization, a transduction cascade, involving splicing of the mRNA of the transcription activator X-box binding protein 1 (XBP1), results in the activation of the UPR (Yoshida *et al.*, 2006). UPR includes diverse processes such as lipid and chaperones biosynthesis, involved in ER biogenesis which aims at dampening ER stress, as well as ER-associated degradation (ERAD) of unfolded proteins which is partially mediated by the 26S proteasome (Yoshida *et al.*, 2003). ERAD was shown to occur after severe ER stress and involves both lysosome- and proteasome-mediated degradation of misfolded proteins (Ron & Walter, 2007; Chiang *et al.*, 2012). Treatment with proteasome inhibitors resulted in increased cell death following accumulation of unfolded proteins (Lee *et al.*, 2003). Taken together these data highlight the interaction between SA-induced immunity and the UPR. Based on the present study, it appears that both the SA pathway and the proteasome mediate rubellin D-induced PCD. Therefore, investigating the phenotypes of both *bip2* and *ire1* mutants following rubellin D infiltration may prove informative regarding the potential action of rubellin D in the UPR. Furthermore, ER-mediated protein quality control, which involves the UPR, is involved in the plant immunity by promoting the production of pathogen-associated molecular pattern (PAMPs) receptors (Li *et al.*, 2009), resulting in early recognition of attempted pathogen infection (Jones & Dangl, 2006; Zipfel, 2009). Therefore, by targeting the ER rubellin may also be involved in

suppressing basal defences to facilitate endophytic growth. Another hypothesis could be that by targeting the ER, which is a widely conserved organelle across organism, rubellins may ensure successful cell death induction via UPR-mediated PCD in every organisms surrounding Rcc.

This study was the first to date to investigate the action of a Rcc rubellin *in planta*. Although further studies are required to elucidate the exact plant pathway(s) targeted by rubellin D, this study suggests that a functional SA pathway is required to reduce PCD induced by this non-host specific toxin.

Chapter 5:
General discussion

This study investigated aspects of secondary metabolism in *Ramularia collo-cygni* (Rcc), the causative agent of Ramularia leaf spot (RLS), which is an increasingly important disease of barley (*Hordeum vulgare*) occurring in temperate regions worldwide. The aim of this project was to increase the understanding of the interactions occurring between Rcc and barley during RLS development by studying fungal secondary metabolism, a key component that often mediates these interactions. Using a combined *in silico* and molecular approach, the genome of Rcc was studied to identify genes predicted to be involved in the biosynthesis of secondary metabolite (SM) products derived from the polyketide and non-ribosomal peptide pathways. Expression of these SM-associated core genes was investigated during RLS development to assess changes in transcript levels in relation with symptom development. Furthermore, by determining the *in planta* mode of action of the only currently characterised Rcc SM, the phytotoxin rubellin D, this study aimed to provide insights into the interaction between the pathogen and its host at a molecular level to assess how these interactions modulate RLS severity.

The onset of disease development in plants involves, among other processes, a complex cross-talk at the molecular level between a pathogen and its host (Jones & Dangl, 2006). Secondary metabolites are mediators of this chemical dialogue between plants and fungi (Pusztahelyi *et al.*, 2015). For instance, in the presence of 13S-hydroperoxy linolenic acid, a plant SM of the oxylipin family, which includes the phytohormone jasmonic acid (JA) involved in plant defence against necrotrophic pathogens (Glazebrook, 2005), the biosynthesis of fungal SMs aflatoxin and sterigmatocystin was repressed in *Aspergillus flavus*, *A. nidulans* and *A. parasiticus* (Burow & Nesbitt, 1997). However, this dialogue between a phytopathogen and its host rapidly turn into a battle with SMs produced by both the pathogen and the plant that will determine the final outcome of the interaction.

Plant SMs are involved in activating defence mechanisms and inhibiting the growth of the pathogen. As part of the response to pathogen infection, the phytohormone salicylic acid (SA), a product of plant secondary metabolism, accumulates in plant tissue and acts as a transduction signal triggering global defence responses including systemic acquired resistance (SAR) (Durrant & Dong, 2004). In

addition, upon pathogen infection plants also synthesise antimicrobial SMs known as phytoalexins (Ahuja *et al.*, 2012). The terpene-derived phytoalexins zealexins are produced by maize (*Zea mays*) following infection by pathogenic fungi such as *Fusarium graminearum* (syn. *Gibberella zeae*), *Colletotrichum sublineolum*, *Bipolaris maydis* (syn. *Cochliobolus heterostrophus*) as well as the opportunistic fungal pathogen *A. flavus* and were shown to inhibit the growth of several fungal species including *F. graminearum* and *A. flavus* (Huffaker *et al.*, 2011).

Pathogens produce a large array of SMs involved in the infection process and disease development. Some SMs, such as that encoded by the *ACE1* gene cluster identified in the rice blast fungus *Magnaporthe oryzae*, are associated with physiological processes occurring during host penetration including differentiation and maturation of infection-specific structures known as appressoria (Collemare *et al.*, 2008). Other fungal SMs act as phytotoxins and induce cell death in the host tissue which increases nutrient availability for the fungus. The fungal class of the Dothideomycetes, which includes Rcc, is one of the most important groups of toxin-producing fungi (Stergiopoulos *et al.*, 2013). Victorin, a non-ribosomal peptide-derived SM produced by *Bipolaris victoriae* (syn. *Cochliobolus victoriae*), the necrotrophic fungus responsible of Victoria blight of oats, induces cell death in its host by triggering programmed cell death (PCD) in susceptible lines carrying the *Pc-2* gene that confers resistance against crown rust disease caused by the biotrophic fungus *Puccinia coronata* (Navarre & Wolpert, 1999). Such trade-off between biotroph and necrotroph resistance is reminiscent to that seen in barley lines carrying *mlo* mutation that confers resistance against powdery mildew caused by the biotrophic fungus *Blumeria graminis f. sp. hordei* but increases susceptibility to RLS (McGrann *et al.*, 2014). Another group of SMs is thought to be involved in host manipulation, for instance to prevent pathogen recognition by the host. Previous transcriptomic studies in the hemibiotrophic fungi *Colletotrichum higginsianum* and *C. orbiculare* reported that many SM-related gene clusters were expressed during the biotrophic phase of disease development in these species which led the authors to hypothesise that these SMs may be involved in host manipulation to prevent the pathogen from being detected during early fungal colonisation (O'Connell *et al.*, 2012; Gan *et al.*, 2013).

The present study demonstrated that the genome of Rcc, like that of many phytopathogenic fungi belonging to the Dothideomycetes, encodes a large number of genes with a predicted function associated with secondary metabolism (Chapter 2). Within these SM-related genes, this study identified 23 core genes belonging to the polyketide synthases (PKSs), non-ribosomal peptide synthetases (NRPSs) and hybrid PKS/NRPS (HPS) families that presented a domain organisation resembling that of functional core genes. In addition, four genes encoding for terpene cyclases (TCs) were found in the genome of Rcc in previous study but no dimethylallyl tryptophan synthases (DMATSs) were identified (McGrann *et al.*, 2016). Taken together these results suggest that the genome of Rcc contains at least 27 SM-related core genes whereas that of Rcc sister species *Zymoseptoria tritici* (syn. *Mycosphaerella graminicola*) contains 26 SM core genes (Ohm *et al.*, 2012). Although the methods used between the present study and that of Ohm *et al.* (2012) differs, the number of core genes identified in Rcc is similar to the number of core genes found in the genomes of many phytopathogenic Dothideomycetes of the order of the Capnodiales (Ohm *et al.*, 2012). *Sphaerulina musiva* (syn. *M. populorum*) and its sister species *Septoria populicola* (syn. *M. populicola*) possess 26 and 28 SM core genes, respectively and their related species *Pseudocercospora fijiensis* (syn. *M. fijiensis*) has 25 SM-related core genes. Similarly, *Cladosporium fulvum* (syn. *Passalora fulva*) and its sister species *Dothistroma septosporum* (syn. *M. pini*) which are both closely related to Rcc and *Z. tritici* possess 27 and 20 SM core genes respectively. Taken together these results led Ohm *et al.* (2012) to hypothesise that the genome of the last common ancestor of the Capnodiales contained 24 SM core genes. This number differs significantly from that estimated to be present in the genome of the last common ancestor of other orders within the Dothideomycetes such as the Pleosporales and the Hysteriales which have 40 and 46 SM core genes respectively, suggesting that genome evolution in the Dothideomycetes is accompanied by gain or loss of SM-related genes (Ohm *et al.*, 2012). Furthermore, the observation that of all the NRPSs and PKSs identified in the genome of 18 Dothideomycetes, only one NRPS was conserved in every species supports the hypothesis that gene deletion or gain drives genome evolution. Loss or gain of genes, specifically SM-related genes,

can be a reflection of the evolution of fungi towards different lifestyles as genes conferring an advantage to thrive in a specific ecological niche are likely to be retained whereas genes that may have become irrelevant are unlikely to be retained.

Analysis of Rcc genome revealed that this fungus possesses the genetic ability to potentially produce a wide range of SMs as gene clusters exhibiting similarity with known fungal SM clusters involved in the biosynthesis of previously characterised SMs were identified. Furthermore, clusters exhibiting similarity to uncharacterised SM biosynthetic clusters where the function of the SM has not yet been determined in other species were also discovered (Chapter 2). Rcc clusters were frequently found to be similar to clusters identified in other Dothideomycetes including members of the Capnodiales such as the Rcc sister species *Z. tritici*, as well as members of the Pleosporales such as *Bipolaris sorokiniana* (syn. *Cochliobolus sativus*). This further supports the phylogenetic relationship between Rcc and the Dothideomycetes. In addition, 40% (6 out of 15) of the clusters identified in Rcc exhibited similarity to species belonging to the Eurotiomycetes and Sordariomycetes. The presence in Rcc of gene sets from both closely and distantly related species raises the question of the origin of these genes. Two different explanations are possible and both are likely to have played a role in Rcc genome evolution. Secondary metabolite clusters exhibiting similarity with SM gene clusters identified in closely related species may indicate that they originate from a set of genes inherited from a common ancestor that has been retained over time. The identification in Rcc of putative paralogues of the 18 genes involved in dothistromin biosynthesis in the related species *D. septosporum* supports this hypothesis. However, only nine of the putative dothistromin biosynthesis genes found in Rcc are predicted to be true paralogues (McGrann *et al.*, 2016). Similar observations were made for other Dothideomycetes where fungal genomes in this class contained mostly paralogues of the dothistromin biosynthetic genes (Ohm *et al.*, 2012). A complete set of orthologous genes to that found in dothistromin biosynthesis was identified in *C. fulvum*, the sister species of *D. septosporum*. Furthermore, the genomic locus near every PKS, NRPS and HPS in *D. septosporum* was conserved in *C. fulvum* supporting the hypothesis that some gene sets may have been inherited from a common ancestor (de Wit *et al.*, 2012;

Ohm *et al.*, 2012). Horizontal gene transfer (HGT) is another mechanism that could explain the presence in Rcc of sets of genes found in distantly related species and absent in closely related ones. HGT is defined as the exchange of genetic information between different species (Doolittle, 1999). Although HGT was originally thought to occur mostly in prokaryotes, recent evidence showed that HGT events are frequent in the fungal kingdom and play an important role in genome evolution (Marcet-Houben & Gabaldón, 2010). Furthermore, HGT can also affect genes involved in secondary metabolism. The Sordariomycete *Podospora anserina* gained the ability to produce sterigmatocystin, a toxic intermediate of aflatoxin, through a HGT event resulting in the transfer of the complete functional sterigmatocystin biosynthetic cluster from the Eurotiomycete *A. nidulans* (Slot & Rokas, 2011). Therefore, similar mechanisms may explain the presence of SM gene clusters in Rcc exhibiting similarity with unrelated or distantly related fungi. For instance, the cluster identified at the HPS14 locus in Rcc (Chapter 2, Figure 2.22) exhibited similarity with the chaetoglobosin A cluster originally described in the Sordariomycete *Chaetomium globosum* (Ishiuchi *et al.*, 2013) and the PKS30 cluster (Chapter 2, Figure 2.18) exhibited similarity to the betaenone biosynthetic cluster identified in *Phoma betae* (syn. *Pleospora betae*), a member of the Pleosporales order (Ichihara *et al.*, 1983; Oikawa *et al.*, 1988). If these gene clusters have been horizontaly transferred to Rcc, they may have been retained in the genome because the SMs produced by these clusters might confer an advantage to Rcc. The ability to produce an anti-fungal compound, such as chaetoglobosin A, by Rcc, a slow growing fungus that lives as an endophyte for a long period of time during the growing season, may facilitate host colonisation by inhibiting faster growing competing fungi such as *Fusarium* spp.. Similarly, the phytotoxin betaenone may increase Rcc fitness during necrotrophic growth by inducing plant cell death, thus increasing nutrient availability for the fungus.

It appears that HGT may play a major role in the evolution of the biology of a given pathogen. The transfer via HGT of SM-related genes and *a fortiori* of complete SM clusters could result in the emergence of new properties such as the ability to produce SMs conferring an advantage in the colonisation of a specific ecological niche. HGT could also result in the ability to synthesise new phytotoxins thus broadening the host range of a pathogen or increasing its virulence on an already

known host. Several HGT events relating to the *ToxA* locus support this hypothesis. ToxA is a host specific phytototoxic proteinaceous effector and a major determinant of virulence of *Pyrenophora tritici-repentis* (syn. *Dreschlera tritici-repentis*), the causative agent of tan spot of wheat (Friesen *et al.*, 2003). It was found that *P. tritici-repentis* most probably gained the *ToxA* locus from another wheat pathogen *Parastagonospora nodorum* (Syn. *Phaeosphaeria nodorum*) through a HGT event that most likely occurred in the early 1940's which resulted in increased virulence and possible emergence of tan spot as a new disease of wheat (Friesen *et al.*, 2006; Stukenbrock & McDonald, 2007). More recently, a 12 kb *ToxA* locus almost identical to that found in *P. tritici-repentis* and *P. nodorum* was identified in twelve isolates of *B. sorokiniana*, the causative agent of spot blotch of wheat, that exhibited increased virulence compared to isolates lacking ToxA (McDonald *et al.*, 2017). Taken together, these results suggest that the transfer of virulence determinant via HGT can lead to an increased profile of a given pathogen. Combining this with the results of this study, this raises the question of whether a recent HGT event involving the transfer of a virulence factor such as an effector or a SM cluster could have occurred in Rcc and resulted in the emergence of RLS as an important disease of barley. This could explain the relatively recent importance of RLS as a barley disease although other factors which may have influenced RLS emergence cannot be excluded. The increased control of other barley diseases such as leaf scald or head blight caused by *Rhynchosporium commune* and *Fusarium* spp. respectively, which was achieved in recent history via the use of fungicides, may also explain the appearance of RLS. Control of these phytopathogens that normally compete with Rcc for the same ecological niche may have facilitated the development of Rcc by removing this competition. Furthermore, controlling foliar diseases, late season application of nitrogen fertilizers and the use of fungicides that increase green leaf area retention may have resulted in delayed senescence which is one of the stimuli that has been linked with the onset of RLS development (McGrann *et al.*, 2015a). Finally, the wide usage of the *mlo*-mediated resistance to powdery mildew in spring barley which increases susceptibility to RLS (McGrann *et al.*, 2014) may also have contributed to the recent emergence of RLS. Therefore, it is possible that a recent HGT affecting Rcc conferring increased virulence may be part of a combination of

factors that have resulted in rapid and successful colonisation of barley fields worldwide by Rcc.

Secondary metabolites are key players in the interactions between a pathogen and its host and understanding the biosynthetic pathway of potential virulence determinants in a particular pathogen may help to control its development. RLS development is thought to be been linked with the *in planta* action of a set of SMs known as rubellins (Heiser *et al.*, 2004). The biosynthetic pathway involved in rubellin biosynthesis remains undetermined. This study may contribute to a better understanding of rubellin production as some genes potentially involved in this pathway might have been identified. The chemical structure of rubellins resembles that of several fungal SMs belonging to the anthraquinone family (Chapter 1, Figure 1.5). Many anthraquinone SMs were shown to be synthesised through the polyketide pathway and involved the action of a non-reducing PKS (NR-PKS). Endocrocin, emodin and cladofulvin, a dimer of nataloe-emodin, are SMs exhibiting the anthracene-9,10-dione (also known as dioxoanthracene) backbone characteristic of anthraquinones and were found to be synthesised by the NR-PKSs *EncA*, *MdpG* and *ClaG*, in *A. fumigatus*, *A. nidulans* and *C. fulvum*, respectively (Chiang *et al.*, 2010; Lim *et al.*, 2012; Griffiths *et al.*, 2016). Although, the anthraquionone-derived aflatoxins and dothistromin do not exhibit the dioxoanthracene backbone, some of their intermediates such as versicolorin or averantin do (Yu *et al.*, 2004; Bradshaw & Zhang, 2006). Early steps in the biosynthesis of both aflatoxins and dothistromin involve the action of NR-PKSs called *PksA* in *A. flavus* and *D. septosporum* (Chang *et al.*, 1995; Bradshaw *et al.*, 2006). In this study three NR-PKSs have been identified, *Pks118-3.254*, *Pksm24-1.219* and *Pksm46-0.119* (Chapter 2, Figure 2.6). However, *Pks118-3.254* is unlikely to be involved in the biosynthesis of rubellin. The domain organisation of the protein encoded by this gene, which includes a methyltransferase (MT) domain and lacks a product template (PT) domain, differs significantly from that of the NR-PKSs involved in the biosynthesis of the above-mentioned anthraquinone toxins (Figure 5.1). This suggests that NR-PKS *Pks118-3.254* may be involved in the biosynthesis of a different SM, which was also supported by the phylogenetic analysis that showed that the protein encoded by

Pks118-3.254 did not appear to be related to the PKSs involved in anthraquinone-derived SMs (Chapter 2, Figure 2.13). Both *Pksm24-1.219* and *Pksm46-0.119* present the domain structure of typical NR-PKSs. The protein encoded by *Pksm46-0.119* shows a domain organisation similar to that found in *AfPksA* and *DsPksA* with SAT-KS-AT-PT-$(ACP)_n$-TE, with n=1 in *AfPksA*, n=2 in *Pksm46-0.119* and n=3 in *DsPksA*, suggesting that *Pksm46-0.119* may be involved in the biosynthesis of anthraquinone-derived SMs. However, the NR-PKSs encoded by *CTB1*, *Pks1* and *Cppks1* involved in the biosynthesis of the perylenequinone toxins cercosporin, elsinochrome and phleichrome, isolated from *Cercospora nicotianae*, *Elsinoë fawcettii* and *Cladosporium phlei*, respectively (Choquer *et al.*, 2005; Liao & Chung, 2008a; So *et al.*, 2015), exhibit the same domain organisation as that of *Pksm46-0.119* (Figure 5.1). Furthermore, the phylogenetic analysis of PKS proteins presented in this thesis suggests that the protein encoded by *Pksm46-0.119* is more closely related to the elsinochrome synthase Pks1 in *E. fawcettii* and the phleichrome synthase Cppks1 in *C. phlei* which are located on a different clade than AfPksA and DsPksA (Chapter2, Figure 2.13). Taken together these results suggest that *Pksm46-0.119* may be involved the production of an anthraquinone-derived SM such as rubellin but could also be involved in the biosynthesis of a different type of SMs, potentially belonging to the perylenequinone family. The third NR-PKS identified in Rcc, *Pksm24-1.219*, encodes a protein exhibiting the same domain organisation as the proteins encoded by *MdpG*, *EncA* and *ClaG*, the core genes involved in the biosynthesis of the anthraquinone SMs monodictyphenone, endocrocin and cladofulvin, respectively (Chiang *et al.*, 2010; Lim *et al.*, 2012; Griffiths *et al.*, 2016) (Figure 5.1). In addition, the protein encoded by *Pksm24-1.219* appeared to be closely related to that encoded by the core genes *MdpG, EncA, ClaG* as well as *Acas*, which is responsible for the biosynthesis of atrochrysone carboxylic acid, a precursor of endocrocin, emodin and cladofulvin (Awakawa *et al.*, 2009; Griffiths *et al.*, 2016)(Chapter 2, Figure 2.13). Furthermore, *Pksm24-1*.219 is located in a cluster alongside genes exhibiting similarity to genes identified in the monodictyphenone biosynthetic cluster which is also involved in emodin biosynthesis (Chiang *et al.*, 2010)(Chapter 2 Figure 2.16). Considering that rubellins, especially rubellin A and B, and uredinorubellins reported from Rcc (Miethbauer *et al.*, 2008) exhibit a

chemical structure resembling that of a dimer of emodin derivatives (Chapter 1, Figure 1.5), *Pksm24-1.219* appears to be a strong candidate to play a role in the rubellin biosynthetic pathway. Core genes are often involved in the early steps of SM biosynthesis because they are generally responsible for the synthesis of the SM chemical backbone. Therefore, if *Pksm24-1.219* is involved in rubellin biosynthesis, it is likely that the enzyme encoded by this gene will be recruited early in this pathway. However, the possibility that the two NR-PKSs, *Pksm24-1.219* and *Pksm46-0.119*, may also be involved in rubellin biosynthesis cannot be excluded. These two enzymes could act synergistically, each being involved in the synthesis of one part of the future toxin. Similar results have been found in *F. graminearum* where two PKSs, the NR-PKS *Pks13* and the highly reducing (HR)-PKS *Pks4*, act together to produce the mycotoxin zearalenone (Kim *et al.*, 2005). Until knockout (KO) mutants of Rcc impaired in the expression of the two NR-PKSs *Pksm24-1.219* and *Pksm46-0.119* are generated, the SM(s) synthesised by the biosynthetic pathway involving these two NR-PKSs will remain uncertain.

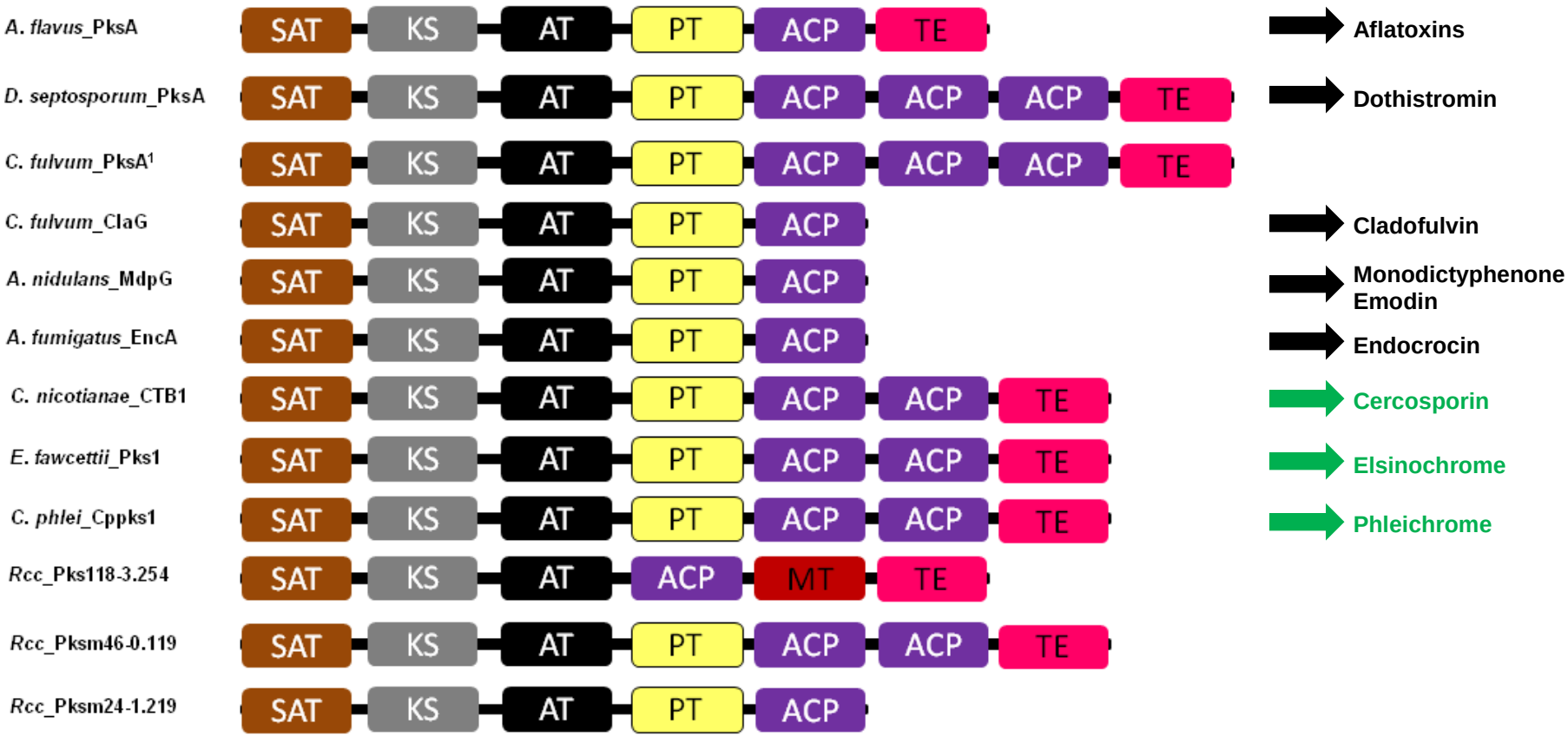

Figure 5.1: Comparison of the domain organisation of fungal non-reducing polyketide synthases (NR-PKSs) involved in the biosynthesis of anthraquinone- and perylenequinone-derived secondary metabolites and putative NR-PKSs identified in *Ramularia collo-cygni*.
From the N-terminus to the C-terminus the NR-PKS domains are labelled: Starter unit: Acyl-carrier protein transacylase (SAT), keto-synthase (KS), acyl transferase (AT), product template (PT), acyl carrier protein (ACP), methyltransferase (MT) and thiolesterase (TE). [1] *D. septosporum PksA* as well as all the genes involved in dothistromin biosynthesis are conserved in *C. fulvum* but dothistromin production has not been reported for *C. fulvum* (de Wit *et al.*, 2012). The SM products synthesised by the pathway involving the NR-PKS may belong to the anthraquinone (black arrows) or the perylenequinone (green arrows) family.

In addition to the unknown biosynthetic pathway leading to the production of rubellin, our understanding of the *in planta* mode of action and role of these SMs produced by Rcc is rather limited. Sutton & Waller (1988) hypothesised that a phytotoxin may be released by the fungus *in planta* to account for the observation of cell death occurring in tissue located away from fungal hyphae. Combined with the discovery of rubellins in infected leaves (Miethbauer *et al.*, 2003) and the non-host specific phytotoxicity of rubellins (Heiser *et al.*, 2003) the link between RLS development and rubellin was quickly made. However, this study suggests that the relationship between rubellin and RLS symptom expression may be more complex than previously thought. Rubellin sensitivity does not appear to correlate with RLS susceptibility as the extent of rubellin D-induced necrosis did not reflect the level of disease susceptibility of the tested barley lines (Chapter 4, Figure 4.3). Furthermore, infiltration of barley leaves with rubellin D failed to reproduce lesions that are characteristic of RLS symptoms (Chapter 4, Figure 4.2) suggesting that, if involved in RLS expression, rubellins may not be the only element responsible for symptom development. These results contrast with previous findings relating to relationship of known fungal virulence factors such as dothistromin and disease symptom expression. The observation that *D. septosporum* mutants impaired in dothistromin biosynthesis were able to infect pine trees and develop typical Dothistroma needle blight symptoms suggested that dothistromin is not required for the disease to occur (Schwelm *et al.*, 2009). However, infiltration of the toxin into pine needles was sufficient to induce typical red band needle blight symptoms (Shain & Franich, 1981). A potential role for dothistromin started to emerge with the observation that dothistromin-lacking mutants induced smaller lesions, associated with lower mesophyll colonisation than that observed with the wild-type pathogen, and these mutants were also affected in sporulation (Kabir *et al.*, 2015). As the genes involved in dothistromin biosynthesis are preferentially expressed during the later stages of disease development, including mesophyll colonisation and sporulation (Bradshaw *et al.*, 2016), these results suggest a link between dothistromin and fungal development processes such as sporulation. Similar results were found in *D. septosporum* sister species, *C. fulvum* where cladofulvin, although not required for disease development, has contrasting effects on disease severity and sporulation. Overexpression of the

cladofulvin core gene *ClaG* in *C. fulvum* resulted in increased lesion formation on tomato leaves but reduced sporulation (Griffiths *et al.*, 2017). In this thesis, transcript levels of several putative SM core genes involved in secondary metabolism of Rcc were investigated including the two potential candidates involved in rubellin biosynthesis, *Pksm24-1.219* and *Pksm46-0.119*, which both showed a similar expression profile with a highest level of expression occurring as early as 5 and 7 days post inoculation (dpi)(Chapter 3, Figure 3.3). This observation appears to be incompatible with a potential role during sporulation as the formation of conidiophore-like structures peaked during the later stages of disease development, typically from 15 dpi onwards (Chapter 3, Figure 3.2.B). However, vesicles carrying a red compound, potentially rubellin, within Rcc hyphae have been observed (McGrann *et al.*, 2016) indicating that some SMs synthesised by Rcc at an early stage of host colonisation may be stored for later use. Therefore, SMs such as rubellin may possibly be involved in processes occurring concomitantly with sporulation despite SM core gene transcription being highest during the early stages of fungal colonisation. In addition, this study showed that rubellin D-induced phytotoxicity was phenotypically similar to programmed cell death (PCD). The link between rubellin-induced lesions and PCD was supported by the observation that mutants impaired in the salicylic acid (SA) pathway, a key regulator of PCD, exhibited larger lesions than wild-type plants (Chapter 4, Figure 4.5 and Figure 4.6). Inhibition of the plant 26S proteasome, another key player in the induction of PCD, resulted in larger lesions compared to plants with a functional proteasome (Chapter 4, Figure 4.8). Based on these results, a role for rubellin in the fungal life cycle can be proposed. Rubellins may be released in the host tissue to increase nutrient availability for the fungus through induction of plant PCD, during the early stages of the necrotrophic colonisation of Rcc, thus providing the fungus with sufficient energy to sporulate. Similar findings were reported in the sister species of Rcc, *Z. tritici* where the necrotrophic growth of the fungus was associated with PCD induction which correlated with an increased concentration of carbohydrates and amino acids in the apoplast (Keon *et al.*, 2007). Shortly after the first signs of PCD, such as DNA laddering or cytochrome c release, were detected in wheat plants, *Z. tritici* biomass increased significantly as increased nutrient availability in the

apoplast was recorded. Furthermore, several SMs have been linked with sporulation in fungi. The presence of butyrolactone I produced by *Aspergillus terreus* induces sporulation of the producing fungus (Schimmel *et al.*, 1998). Similarly, the mycotoxin zearalenone regulates sporulation in a dose-dependent manner as low levels of toxin induced sporulation in *F. graminearum* but the opposite was observed at high levels (Wolf & Mirocha, 1973). Furthermore, observations that sporulation in the model organism *Saccharomyces cerevisae* is directly dependent on the metabolic and energetic status of the yeast support this hypothesis (Aon *et al.*, 1996). Another possibility linked with sporulation, could be that rubellins may act as pigments to protect conidia from abiotic stresses as well as from host defences. Cladofulvin, an anthraquinone SM produced by the Dothideomycete *C. fulvum* protects conidia from UV radiation and freezing temperature (Griffiths *et al.*, 2017). Similarly, melanin a polyketide-derived pigment acting as a virulence factor in many fungi is involved in conidial cell wall development in *A. fumigatus* and *Alternaria alternata* and protection from UV lights in *A. alternata* (Kawamura *et al.*, 1999; Pihet *et al.*, 2009). Rubellin may also be involved in other biological processes such as inhibiting the growth of competing micro-organisms or manipulating the host to conceal Rcc from the plant defence mechanisms.

Most of Rcc SM core genes identified in this study are expressed in the early stages of disease development, typically during the asymptomatic and early lesion formation stages. Most of the PKSs and NRPSs studied showed highest expression at 5 and 7 dpi (Chapter 3, Figures 3.3 and 3.5) and all HPSs transcript levels were highest at 5, 7 and 10 dpi (Chapter 3, Figure 3.4). Similar observations were made in numerous species of hemibiotrophic fungi such as *Colletotrichum* species and in the Rcc sister species *Z. tritici* (O'Connell *et al.*, 2012; Gan *et al.*, 2013; Alkan *et al.*, 2015; Rudd *et al.*, 2015). In these fungi, SMs were speculated to function in processes relating to colonisation such as concealing the pathogen from the host defence system, promoting host penetration or inducing localised cell death to facilitate fungal development prior to the start of necrotrophic growth. Based on this study, defining a general role for the SMs produced by Rcc would be unrealistic and it seems unlikely that all of the SMs produced by this fungus will have similar roles

and actions. Furthermore, it is important to be aware that although most of the SM core genes are expressed during the early stages of infection, their action may occur at a different time during the fungal life cycle. Considering that Rcc has been described as an endophytic fungus with a recently acquired necrotrophic phase (Salamati & Reitan, 2006), the role of some of Rcc SMs may resemble that of SMs found in endophytes. The interactions between plants and endophytes, which involve SMs from both sides, have been subject to numerous hypotheses and the balanced antagonism hypothesis (Schulz & Boyle, 2005) is of particular interest for the case of Rcc. In this hypothesis, both endophytes and pathogens produce virulence-confering SMs that act antagonistically to the defence-related SMs from the plant, yet, in the endophytic interaction, fungal and plant SMs counteract each other (Figure 5.2.A) whereas in pathogenic interaction fungal SMs overpower the plant defence responses (Figure 5.2.D). A similar role for some of Rcc secondary metabolism products can be proposed. In addition, the hypothesis that many endophytes could be latent pathogen only undergoing pathogenic growth in response to environmental stimuli (Arnold 2008) is reminiscent of the biology of Rcc which showed increased virulence on light-stressed plants (Makepeace *et al.,* 2008; Peraldi *et al.*, 2014). The transition from endophytic to pathogenic colonisation (Figure 5.2.C) may be mediated by an increased production of SM or by the synthesis or release of new metabolites absent in the endophytic lifestyle. It was shown in the perennial rye grass endophyte *Epichloë festucae* that a loss of function mutation of the *sakA* gene encoding for a stress- and mitogen-activated protein kinase, results in a transition from endophytic to pathogenic growth which is accompanied by major modifications in SM-related genes expression (Eaton *et al.*, 2010). However, in *E. festucae sakA* mutants, most of the SM-related genes investigated were constitutively down-regulated rather than up-regulated. Another important component of the interaction between endophytes and their hosts is in defensive mutualism (Clay, 1988). In this interaction, SMs from both the plant and the endophyte act synergistically (Figure 5.2.B) to prevent pathogen infection (Kusari *et al.*, 2012)(Figure 5.2.E). Many SMs from fungal endophytes have been shown to be involved in antagonistic effects against herbivorous, insects and fungal, bacterial and viral pathogens (Schardl *et al.*, 2004). Alkaloid SMs produced by *Epichloë coenophiala*, an endophyte of *Lolium* species, were shown to

protect the host plants from several aphid species (Siegl *et al.*, 1990). Similarly, phenone-derived SMs produced by the tree endophytes *Pestalotiospis foedan* and *P. adusta*, exhibited antifungal activity against the pathogenic fungi *F. graminearum*, *F. culmorum* and *Verticillium albo-atrum* (Ding *et al.*, 2008; Li *et al.*, 2008). This study suggests that some SMs produced by Rcc may also be involved in host protection during the endophytic and early necrotrophic stage. This synergistic action between Rcc SMs and barley could therefore also occur during the necrotrophic growth of the fungus (Figure 5.2.F). The presence of Rcc inhibited the growth of other barley leaf pathogens such as *Rhynchosporium commune*, the hemibiotrophic fungus responsible of leaf scald, or *Pyrenophora teres*, the causative agent of net blotch. Rcc also inhibited the growth of the pathogenic fungi *Fusarium graminearum* and *F. poae*, causative agents of Fusarium head blight (Chapter 3, Figure 3.11). Considering that a seed borne stage is known to be predominant in Rcc dispersal (Havis *et al.*, 2006; Matusinsky *et al.*, 2011), the ability to inhibit major seed pathogens may confer an advantage to Rcc to compete for this ecological space. Whether or not the SMs involved in this inhibition are synthesised or released in the seed remains to be determined. This poses several human and animal health-related questions regarding risks associated with Rcc infected grain. Many fungal SMs, such as mycotoxins or antibiotics are stable potent toxic compounds that could subsequently be found in the marketed foodstuffs. The discovery of a metabolic cluster resembling that of the known antifungal agent chaetoglobosin A (Chapter 2, Figure 2.22) combined with observations that Rcc is a slow growing fungus (Salamati *et al.*, 2002), could explain the production of antifungal agents by Rcc potentially resulting in host protection and inhibiting the growth of fungal competitors thus allowing Rcc to colonise effectively the host mesophyll.

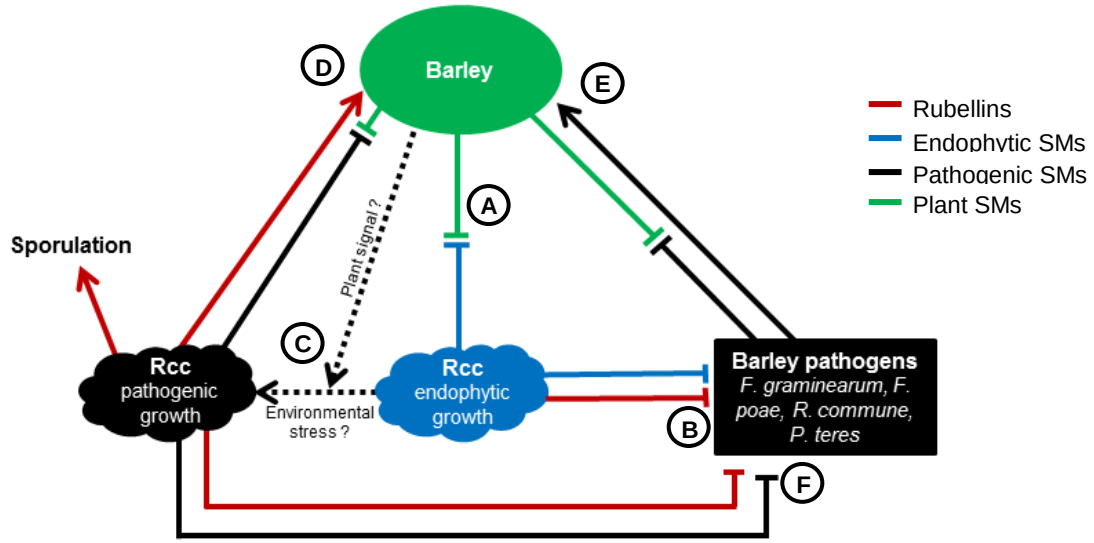

Figure 5.2: Proposed model presenting the putative roles of secondary metabolites in the interactions between *Ramularia collo-cygni* and its environment.
During the endophytic phase SMs produced by Rcc (blue blocked arrow) may be involved in blocking plant defence mechanism (green arrow) in a balanced antagonism between the host and pathogen (A). At this stage, some SMs including rubellin (red arrows) may be involved in inhibiting the growth of fungal pathogen (B) synergistically with plant defence SMs in a mutualistic defence interaction potentially preventing disease (E). In response to unknown stimuli, possibly derived from the host plant (dotted black arrows), Rcc undergoes a transition from endophytic to pathogenic lifestyle (C) most likely accompanied by the production of new SMs or the release of stored SMs associated with pathogenic lifestyle (black arrow), which unbalances the balanced antagonism and results in disease development (D). Rubellin may also be involved in the transition from endophytic to necrotrophic growth by unbalancing the antagonism between plants and fungal SMs. During pathogenic growth, Rcc may produce SMs, potentially rubellin, which inhibit the growth of other fungal pathogens of barley to provide an advantage to Rcc to successfully colonise its host (F). In addition, rubellin may also be involved in sporulation by increasing nutrient availability through host cell death induction. Adapted from Clay, 1988; Schulz & Boyle, 2005; Arnold, 2008; Kusari *et al.*, 2012.

In order to better understand the role of secondary metabolism in the biology and infection strategy of Rcc, further work is required. Based on the results of this study, it appears that Rcc possesses the genetic equipment to synthesise a wide range of SMs. Characterising the arsenal of SMs produced by Rcc may provide deeper insight into the infection biology of Rcc and may help determine the role of the secondary metabolism in this fungus. SMs being key players in the interactions between a pathogen and its host, characterising new SMs may help understand better these interactions and could help identify targets conferring resistance to RLS, or identify putative fungicide targets. Growing Rcc *in vitro* in a wide range of different conditions including pH, iron and nitrogen sources and concentrations or light

conditions may result in production of new SMs. Extracting and analysing exudates produced by Rcc using liquid- or gas-chromatography-mass spectrometry (GC-MS; LC-MS) may help identify new SMs which in turn, could improve understanding of the interactions between Rcc and its environment. Similarly, creating KO mutants of Rcc deficient in the expression of master regulators of secondary metabolism such as *PacC, AreA, CreA* known to regulate SM production in response to pH, nitrogen and carbon sources respectively (Espeso & Peñalva, 1992; Tilburn *et al.*, 1995; Kim & Woloshuk, 2008), or components of the velvet complex *VeA, VelB* and *LaeA*, involved in light-mediated regulation of secondary metabolism (Bayram *et al.*, 2008), may results in the expression of pathways maintained cryptic under normal conditions. However, a similar approach carried out in *C. fulvum* did not appear to induce cryptic SM biosynthesis (Griffiths *et al.*, 2015). Using a chemical epigenetics approach, which consists of using inhibitors of epigenetic factors such as histone deacetylase or methyltransferases may be another way of discovering cryptic pathways in Rcc as many transcriptional master regulators act on chromatin condensation state (Palmer & Keller, 2010). Inhibition of fungal DNA methyltransferases, which includes the master regulator *LaeA*, resulted in the production of new SMs in several fungal species including the Dothideomycete *Cladosporium cladosporioides* (Williams *et al.*, 2008). Similarly, inhibition of histone deacetylases, which includes the master regulator of secondary metabolism *HdaA*, resulted in a drastic remodelling of the secondary metabolome of *A. niger* exemplified by the biosynthesis of a new SM identified as nygerone A (Henrikson *et al.*, 2009). In addition to providing further insights into the infection biology of Rcc, characterising the complete arsenal of SMs produced by this fungus may identify metabolites of interest for medical research such as antifungal agent or antibiotics.

Investigating the secondary metabolome of Rcc in different isolates, both *in silico* and *in vivo*, may also provide insights into the importance of the secondary metabolism in Rcc biology. Genomic variations in SM-related genes between different Rcc isolates may result in different sets of SMs being produced which could affect the interactions between these isolates and their hosts. Therefore, assessing the arsenal of SMs produced or the amount of a given SM produced by different Rcc

isolates may help understand variation in virulence between isolates. Isolate-specific variations of the secondary metabolome were found in *Penicillium crustosum*, *P. paneum* and *P. roqueforti* where different strains produced different sets of SMs (Sonjak *et al.*, 2005; O'Brien *et al.*, 2006). These variations were observed even between isolates originating from the same ecological niche. In addition, characterising the secondary metabolome of Rcc isolated from different hosts, such as wheat or wild grasses may help identify SMs preferentially expressed in alternative hosts. However, a study carried out in *P. expansum* showed that the set of SM produced by this fungus was independent of the substrate from which the fungus was isolated as most isolates of *P. expansum* consistently produced a set of SMs that includes chaetoglobosins, citrinins, communesins, patulin and roquefortin C (Andersen *et al.*, 2004). Therefore, it appears that, even within the same genus, the set of SMs produced by a species may or may not drastically differ between isolates. Adding another level of complexity to the role of secondary metabolism in fungal biology is the fact that the effect of a given SM may vary between isolates. The action of the virulence factor botrydial, a polyketide-derived SM produced by *Botrytis cinerea*, appears to be isolate-specific as a loss of function mutation of *bcbot1*, a gene encoding for a cytochrome P450 monooxygenase involved in botrydial biosynthesis, resulted in reduced virulence in only one out of four isolates of *B. cinerea* (Siewers *et al.*, 2005). A large scale RNAseq experiment following the expression of the SM-related genes identified in the clusters presented in Chapter 2 carried out in different Rcc isolates from different hosts may help address several questions relating to how transcriptional regulation of SM in Rcc is linked to RLS expression and host specificity. First, such an experiment could confirm results from this study suggesting that many SM-related genes are co-regulated during RLS development (Chapter 3). Second, this experiment could help identify genes or gene clusters exhibiting different expression patterns across isolates potentially reflecting variations of the secondary metabolome which could be related to variation in Rcc biology including virulence, fungal growth or reproduction.

The *in planta* function of rubellin D is still unclear. However, the study of the *in planta* mode of action of this phytotoxin has provided insights into the link between

rubellin D-induced necrosis and plant cell death. To further determine how rubellin D induces cell death in plants, *A. thaliana* mutants can be used to assess whether this toxin involves endoplasmic reticulum (ER)-related stress response such as the unfolded protein response (UPR) to activate the plant PCD response. Infiltration of rubellin D into mutants with a disrupted UPR pathway such as the *bip2* or *ire1* mutants impaired in sensing ER stress and triggering the UPR respectively, should be of particular interest to determine if the ER is a potential target for rubellin D. Understanding the interaction between Rcc and its host which appeared to be mediated at least partially by rubellins could provide putative targets for barley breeders to select lines for increased resistance against Rcc.

This study opens up a new chapter in the research on Rcc and, although more work is needed to understand fully the interactions between Rcc and barley as well as the processes involved in disease development, it is the first study to investigate the secondary metabolism of Rcc both at a genetic and molecular level. This study has revealed that Rcc, like many fungal plant pathogens, appears to have the genetic equipment to produce several chemically diverse SMs. Furthermore, the results of this study provided insight into the molecular biology of the known secondary metabolite rubellin D produced by Rcc which constitute the first step in understanding the *in planta* mode of action of this toxin and its complex role in the biology of Rcc.

References

Abid-Essefi S, Ouanes Z, Hassen W, Baudrimont I, Creppy E, Bacha H. **2004**. Cytotoxicity, inhibition of DNA and protein syntheses and oxidative damage in cultured cells exposed to zearalenone. *Toxicology in Vitro* **18**: 467–474.

Abràmoff MD, Magalhães PJ, Ram SJ. **2004**. Image processing with imageJ. *Biophotonics International* **11**: 36–41.

Ahn J-H, Walton JD. **1997**. A fatty acid synthase gene in *Cochliobolus carbonum* required for production of HC-Toxin, cyclo(D-prolyl-L-alanyl-D-alanyl-L-2-amino-9,10-epoxi-8-oxodecanoyl). *Molecular Plant-Microbe Interactions: MPMI* **10**: 207–214.

Ahuja I, Kissen R, Bones AM. **2012**. Phytoalexins in defense against pathogens. *Trends in Plant Science* **17**: 73–90.

Akar T, Muzaffer A, Fazil D. **1999**. *Barley: Post-harvest Operations* (D Mejia, Ed.). Ankara, Turkey.

Albarouki E, Schafferer L, Ye F, von Wirén N, Haas H, Deising HB. **2014**. Biotrophy-specific downregulation of siderophore biosynthesis in *Colletotrichum graminicola* is required for modulation of immune responses of maize. *Molecular Microbiology* **92**: 338–355.

Alkan N, Davydov O, Sagi M, Fluhr R, Prusky D. **2009**. Ammonium secretion by *Colletotrichum coccodes* activates host NADPH oxidase activity enhancing host cell death and fungal virulence in tomato fruits. *Molecular Plant-Microbe Interactions : MPMI* **22**: 1484–1491.

Alkan N, Fluhr R, Prusky D. **2012**. Infection modulates salicylic and jasmonic acid pathways of ripe and unripe tomato fruit. *Molecular Plant-Microbe Interactions: MPMI* **25**: 85–96.

Alkan N, Fluhr R, Sherman A, Prusky D. **2008**. Role of ammonia secretion and pH modulation on pathogenicity of *Colletotrichum coccodes* on tomato fruit. *Molecular Plant-Microbe Interaction: MPMI* **21**: 1058–1066.

Alkan N, Friedlander G, Ment D, Prusky D, Fluhr R. **2015**. Simultaneous transcriptome analysis of *Colletotrichum gloeosporioides* and tomato fruit pathosystem reveals novel fungal pathogenicity and fruit defense strategies. *New Phytologist* **205**: 801–815.

Alkan N, Meng X, Friedlander G, Reuveni E, Sukno S, Sherman A, Thon M, Fluhr R, Prusky D. **2013**. Global aspects of *PacC* regulation of pathogenicity genes in *Colletotrichum gloeosporioides* as revealed by transcriptome analysis. *Molecular Plant-Microbe Interactions: MPMI* **26**: 1345–1358.

Alspaugh JA, Perfect JR, Heitman J. **1997**. *Cryptococcus neoformans* mating and virulence are regulated by the G-protein alpha subunit GPA1 and cAMP. *Genes and Development* **11**: 3206–3217.

Altschul S, Gish W, Miller W, Meyers E, DJ L. **1990**. Basic local alignment research tool. *Journal of Molecular Biology* **215**: 403–410.

Alvarez ME. **2000**. Salicylic acid in the machinery of hypersensitive cell death and disease resistance. *Plant Molecular Biology* **44**: 429–442.

Alves M, Dadalto S, Gonçalves A, de Souza G, Barros V, Fietto L. **2014**. Transcription factor functional protein-protein interactions in plant defense responses. *Proteomes* **2**: 85–106.

Amri A, Ouammou L, Nassif F. **1994**. Barley-based food in southern Morocco. In: Grando S, Gomez Macpherson H, eds. Food barley: Importance, uses and local knowledge.22–28.

Ananieva EA, Christov KN, Popova LP. **2004**. Exogenous treatment with salicylic acid leads to increased antioxidant capacity in leaves of barley plants exposed to paraquat. *Journal of plant physiology* **161**: 319–328.

Andersen B, Smedsgaard J, Frisvad JC. **2004**. *Penicillium expansum*: consistent production of patulin,chaetoglobosins, and other secondary metabolites in culture and their natural occurrence in fruit products. *Journal of Agricultural and Food Chemistry* **52**: 2421–2428.

Andolfi A, Cimmino A, Villegas-Fernández AM, Tuzi A, Santini A, Melck D, Rubiales D, Evidente A. **2013**. Lentisone, a new phytotoxic anthraquinone produced by *Ascochyta lentis*, the causal agent of ascochyta blight in *Lens culinaris*. *Journal of Agricultural and Food Chemistry* **61**: 7301–7308.

Andriole VT. **2005**. The quinolones : past, present, and future. *Clinical Infectious Diseases* **41**: 113–119.

Aon JC, Rapisarda VA, Cortassa S. **1996**. Metabolic fluxes regulate the success of sporulation in *Saccharomyces cerevisiae*. *Experimental cell research* **222**: 157–162.

Araki T, Shimanuki T. **1983**. Phleichrome, a non-host specific toxin produced by the causal organism of timothy purple spot, *Cladosporium phlei*, and its toxic influence on timothy leaf blades and leat surface microorganisms. *Journal of Japanese Society of Grassland Science* **28**: 427–431.

Arnold A. **2008**. Endophytic fungi: hidden components of tropical community ecology. In: Carson W, Schnitzer S, eds. Tropical Forest Community Ecology. West Sussex, UK, 254–271.

Arnone A, Camarda L, Nasini G. **1986**. Structure elucidation of rubellins A and B, two novel anthraquinone metabolites from *Mycosphaerella rubella*. *Journal of Chemical Society* **1**: 255–260.

Atkinson NJ, Urwin PE. **2012**. The interaction of plant biotic and abiotic stresses: from genes to the field. *Journal of experimental botany* **63**: 3523–3544.

Avrova A, Knogge W. **2012**. *Rhynchosporium commune*: a persistent threat to barley cultivation. *Molecular Plant Pathology* **13**: 986–997.

Awakawa T, Yokota K, Funa N, Doi F, Mori N, Watanabe H, Horinouchi S. **2009**. Physically discrete beta-lactamase-type thioesterase catalyzes product release in atrochrysone synthesis by iterative type I polyketide synthase. *Chemistry and Biology* **16**: 613–623.

Axford LC, Simpson TJ, Willis CL. **2004**. Synthesis and incorporation of the first polyketide synthase free intermediate in monocerin biosynthesis. *Angewandte Chemie - International Edition* **43**: 727–730.

Badr A, Muller K, Schafer-Pregl R, Rabey HE, Effgen S, Ibrahim HH, Pozzi C, Rohde W, Salamini F. **2000**. On the origin and domestication history of barley (*Hordeum vulgare*). *Molecular Biology and Evolution* **17**: 499–510.

Bailey AM, Cox RJ, Harley K, Lazarus CM, Simpson TJ, Skellam E. **2007**. Characterisation of 3-methylorcinaldehyde synthase (MOS) in *Acremonium strictum*: first observation of a reductive release mechanism during polyketide biosynthesis. *Chemical communications*: 4053–4055.

Baker SE, Kroken S, Inderbitzin P, Asvarak T, Li B, Shi L, Yoder OC, Turgeon BG. **2006**. Two polyketide synthase-encoding genes are required for biosynthesis of the polyketide virulence factor, T-toxin, by *Cochliobolus heterostrophus*. *Molecular Plant-Microbe Interactions: MPMI* **19**: 139–149.

Balis C, Payne MG. **1971**. Triglycerides and cercosporin from *Cercospora beticola*: fungal growth and cercosporin production. *Phytopathology* **61**: 1477–1484.

Balz T, Prigge G, Krieg U, Sattler U, Von Tiedemann A. **2006**. Strategies of chemical control of *Ramularia collo-cygni*. In: Koopmann B, Oxley S, Schützendübel A, von Tiedemann A, eds. Proceedings of the first European Ramularia workshop - *Ramularia collo-cygni*: a new disease and challenge in barley production. Gottingen, Germany, 120–121.

Bassett C, Buchanan M, Gallagher R, Hodges R. **1970**. A toxic difuroanthraquinone from *Dothistroma pini*. *Chemistry and Industry* **52**: 1652–1660.

Batchvarova RB, Reddy VS, Bennett J. **1992**. Cellular-resistance in rice to cercosporin, a toxin of *Cercospora*. *Phytopathology* **82**: 642–646.

Bayram Ö, Krappmann S, Ni M, Bok JW, Helmstaedt K, Yu J, Braus GH. **2008**. VelB/VeA/LaeA complex coordinates light signal with fungal development and secondary metabolism. *Science* **320**: 1504–1506.

Bender C, Palmer D, Peñaloza-Vázquez A, Rangaswamy V, Ullrich M. **1996**. Biosynthesis of coronatine, a thermoregulated phytotoxin produced by the phytopathogen *Pseudomonas syringae*. *Archives of Microbiology* **166**: 71–75.

Bentley R. **2001**. Bartolomeo Gosio, 1863-1944: an appreciation. *Advanced Applied Microbiology* **48**: 229–250.

Bérdy J. **2005**. Bioactive microbial metabolites. *The Journal of antibiotics* **58**: 1–26.

Berestetskiy AO. **2008**. A review of fungal phytotoxins: from basic studies to practical use. *Applied Biochemistry and Microbiology* **44**: 453–465.

Bertolotti A, Zhang Y, Hendershot LM, Harding HP, Ron D. **2000**. Dynamic interaction of BiP and ER stress transducers in the unfolded-protein response. *Nature cell biology* **2**: 326–332.

Bertuzzi M, Schrettl M, Alcazar-Fuoli L, Cairns TC, Muñoz A, Walker LA, Herbst S, Safari M, Cheverton AM, Chen D, *et al.* 2014. The pH-responsive *PacC* transcription factor of *Aspergillus fumigatus* governs epithelial entry and tissue invasion during pulmonary Aspergillosis. *PLoS Pathogens* **10**: e1004413.

Bhetariya PJ, Prajapati M, Bhaduri A, Mandal RS, Varma A, Madan T, Singh Y, Sarma PU. **2016**. Phylogenetic and structural analysis of polyketide synthases in *Aspergilli*. *Evolutionary Bioinformatics* **12**: 109–119.

Binder EM, Tan LM, Chin LJ, Handl J, Richard J. **2007**. Worldwide occurrence of mycotoxins in commodities, feeds and feed ingredients. *Animal Feed Science and Technology* **137**: 265–282.

Bistrich H, Breun J, Emmert G, Fleck A, Jaiser H, Kempe H, Lemmens M. **2006**. Screening for leaf spot resistance-results and impact on practical breeding. In: Koopmann B, Oxley S, Schützendübel A, von Tiedemann A, eds. Proceedings of the first European Ramularia workshop - *Ramularia collo-cygni*: a new disease and challenge in barley production. Gottingen, Germany, 83–84.

Blatzer M, Schrettl M, Sarg B, Lindner HH, Pfaller K, Haas H. **2011**. SidL, an *Aspergillus fumigatus* transacetylase involved in biosynthesis of the siderophores ferricrocin and hydroxyferricrocin. *Applied and Environmental Microbiology* **77**: 4959–4966.

Blin K, Medema MH, Kazempour D, Fischbach MA, Breitling R, Takano E, Weber T. **2013**. antiSMASH 2.0-a versatile platform for genome mining of secondary metabolite producers. *Nucleic acids research* **41**: 204–212.

Bok JW, Keller NP. **2004**. LaeA, a regulator of secondary metabolism in *Aspergillus* spp. *Eukaryotic cell* **3**: 527–535.

Bok JW, Noordermeer D, Kale SP, Keller NP. **2006**. Secondary metabolic gene cluster silencing in *Aspergillus nidulans*. *Molecular Microbiology* **61**: 1636–1645.

Borel JF, Feurer C, Gubler HU, Stähelin H. **1976**. Biological effects of cyclosporin A: a new antilymphocytic agent. *Agents and Actions* **6**: 468–475.

Bottalico A, Perrone G. **2002**. Toxigenic *Fusarium* species and mycotoxins associated with head blight in small-grain cereals in Europe. *European Journal of Plant Pathology* **108**: 611–624.

Bouras N, Strelkov SE. **2008**. The anthraquinone catenarin is phytotoxic and produced in leaves and kernels of wheat infected by *Pyrenophora tritici-repentis*. *Physiological and Molecular Plant Pathology* **72**: 87–95.

Bove FJ. **1970**. *The story of Ergot*. Basel (Switzerland): Karger.

Bowden CG, Smalley E, Guries RP, Hubbes M, Temple B, Horgen PA. **1996**. Lack of association between cerato-ulmin production and virulence in *Ophiostoma novo-ulmi*. *Molecular Plant-Microbe Interactions: MPMI* **9**: 556–564.

Bradshaw RE, Guo Y, Sim AD, Kabir MS, Chettri P, Ozturk IK, Hunziker L, Ganley RJ, Cox MP. **2016**. Genome-wide gene expression dynamics of the fungal pathogen *Dothistroma septosporum* throughout its infection cycle of the gymnosperm host *Pinus radiata*. *Molecular Plant Pathology* **17**: 210–224.

Bradshaw RE, Jin H, Morgan BS, Schwelm A, Teddy OR, Young CA, Zhang S. **2006**. A polyketide synthase gene required for biosynthesis of the aflatoxin-like toxin, dothistromin. *Mycopathologia* **161**: 283–294.

Bradshaw RE, Zhang S. **2006**. Biosynthesis of dothistromin. *Mycopathologia* **162**: 201–213.

Brakhage AA. **2013**. Regulation of fungal secondary metabolism. *Nature Reviews Microbiology* **11**: 21–32.

Brase S, Encinas A, Keck J, Nising CF. **2009**. Chemistry and biology of mycotoxins and related fungal metabolites. *Chemical Reviews* **109**: 3903–3990.

Brodersen P, Malinovsky F. **2005**. The role of salicylic acid in the induction of cell death in Arabidopsis *acd11*. *Plant physiology* **138**: 1037–1045.

Brodersen P, Petersen M, Nielsen HB, Zhu S, Newman MA, Shokat KM, Rietz S, Parker J, Mundy J. **2006**. Arabidopsis MAP kinase 4 regulates salicylic acid- and jasmonic acid/ethylene-dependent responses via EDS1 and PAD4. *Plant Journal* **47**: 532–546.

Brooks DM, Bender CL, Kunkel BN. **2005**. The *Pseudomonas syringae* phytotoxin coronatine promotes virulence by overcoming salicylic acid-dependent defences in *Arabidopsis thaliana*. *Molecular Plant Pathology* **6**: 629–639.

Brown J, Makepeace J. **2009**. The effet of genetic variation in barley on responses to *Ramularia collo-cygni*. *Aspects of Applied Biology* **92**: 43–47.

Brunner PC, Schürch S, McDonald BA. **2007**. The origin and colonization history of the barley scald pathogen *Rhynchosporium secalis*. *Journal of evolutionary biology* **20**: 1311–1321.

Bullerman LB, Bianchini A. **2007**. Stability of mycotoxins during food processing. *International Journal of Food Microbiology* **119**: 140–146.

Burow GB, Nesbitt TC. **1997**. Seed lipoxygenase products modulate *Aspergillus* mycotoxin biosynthesis. *Molecular Plant-Microbe Interactions: MPMI* **10**: 380–387.

Bushley KE, Turgeon BG. **2010**. Phylogenomics reveals subfamilies of fungal nonribosomal peptide synthetases and their evolutionary relationships. *BMC evolutionary biology* **10**: 26.

Caboche S, Pupin M, Leclère V, Fontaine A, Jacques P, Kucherov G. **2008**. NORINE: A database of nonribosomal peptides. *Nucleic Acids Research* **36**: 326–331.

Calvo AM, Wilson RA, Bok JW, Keller NP. **2002**. Relationship between secondary metabolism and fungal development. *Microbiology and molecular biology reviews : MMBR* **66**: 447–459.

Cao H, Bowling SA, Gordon AS. **1994**. Characterization of an Arabidopsis mutant that is nonresponsive to inducers of systemic acquired resistance. *The Plant cell* **6**: 1583–1592.

Cao H, Glazebrook J, Clarke JD, Volko S, Dong X. **1997**. The Arabidopsis *NPR1* gene that controls systemic acquired resistance encodes a novel protein containing ankyrin repeats. *Cell* **88**: 57–63.

Caracuel Z, Roncero MIG, Espeso EA, González-Verdejo CI, García-Maceira FI, Di Pietro A. **2003**. The pH signalling transcription factor *PacC* controls virulence in the plant pathogen *Fusarium oxysporum*. *Molecular Microbiology* **48**: 765–779.

Caron D, Maumene C, Maufras J-Y, Beauvallet G. **2009**. La Ramulariose des orges en France : Importance et management de *Ramularia collo-cygni*. AFPP-9eme conférence internationale sur les maladies des plantes. Tours, 254–262.

Cary J, Ehrlich K. **2000**. Generation of *aflR* disruption mutants of *Aspergillus parasiticus*. *Applied microbiology and biotechnology* **53**: 680–684.

Cavallini L, Bindoli A, Macri F, Vianello A. **1979**. Lipid peroxidation induced by cercosporin as a possible determinant of its toxicity. *Chemico-Biological Interaction* **28**: 139–146.

Cavara F. **1893**. Über einige parasitische Pilze auf dem Getreide. *Zeitschrift für Pflanzenkrankheit* **3**: 16–26.

Chang PK, Cary JW, Yu J, Bhatnagar D, Cleveland TE. **1995**. The *Aspergillus parasiticus* polyketide synthase gene *pksA*, a homolog of *Aspergillus nidulans wA*, is required for aflatoxin B1 biosynthesis. *Molecular & General Genetics* **248**: 270–277.

Chang P-K, Matsushima K, Takahashi T, Yu J, Abe K, Bhatnagar D, Yuan G-F, Koyama Y, Cleveland TE. **2007**. Understanding nonaflatoxigenicity of *Aspergillus sojae*: a windfall of aflatoxin biosynthesis research. *Applied microbiology and biotechnology* **76**: 977–984.

Chang T-C, Salvucci A, Crous PW, Stergiopoulos I, Arias P, Dankers C, Liu P, Pilkauskas P, Heslop-Harrison J, Schwarzacher T, *et al.* 2016. Comparative genomics of the Sigatoka disease complex on banana suggests a link between parallel evolutionary changes in *Pseudocercospora fijiensis* and *Pseudocercospora eumusae* and increased virulence on the banana host. *PLOS Genetics* **12**: e1005904.

Chen FQ, Prehn D, Hayes PM, Mulrooney D, Corey A, Vivar H. **1994**. Mapping genes for resistance to barley stripe rust (*Puccinia striiformis f.sp. hordei*). *Theoretical and Applied Genetics* **Vol 88**: 215–219.

Chen Z, Zheng Z, Huang J, Lai Z, Fan B. **2009**. Biosynthesis of salicylic acid in plants. *Plant signaling & behavior* **4**: 493–496.

Cheng Y, Ahn J, Walton JD. **1999**. A putative branched-chain-amino-acid transaminase gene required for HC-toxin biosynthesis and pathogenicity in *Cochliobolus carbonum*. *Microbiology* **145**: 3539–3546.

Chettri P, Bradshaw RE. **2016**. LaeA negatively regulates dothistromin production in the pine needle pathogen *Dothistroma septosporum*. *Fungal Genetics and Biology* **97**: 24–32.

Chettri P, Ehrlich KC, Cary JW, Collemare J, Cox MP, Griffiths SA, Olson MA, de Wit PJGM, Bradshaw RE. **2013**. Dothistromin genes at multiple separate loci are regulated by *AflR*. *Fungal genetics and biology : FG & B* **51**: 12–20.

Chiang W-C, Messah C, Lin JH. **2012**. IRE1 directs proteasomal and lysosomal degradation of misfolded rhodopsin. *Molecular biology of the cell* **23**: 758–770.

Chiang YM, Szewczyk E, Davidson AD, Entwistle R, Keller NP, Wang CCC, Oakley BR. **2010**. Characterization of the aspergillus nidulans monodictyphenone gene cluster. *Applied and Environmental Microbiology* **76**: 2067–2074.

Chong J, Pierrel M-A, Atanassova R, Werck-Reichhart D, Fritig B, Saindrenan P. **2001**. Free and conjugated benzoic acid in tobacco plants and cell cultures. Induced accumulation upon elicitation of defense responses and role as salicylic acid precursors. *Plant Physiology* **125**: 318–328.

Choquer M, Dekkers KL, Chen H, Cao L, Ueng PP, Daub ME, Chung K. **2005**. The *CTB1* gene encoding a fungal polyketide synthase is required for cercosporin biosynthesis and fungal virulence of *Cercospora nicotianae*. *Molecular Plant-Microbe Inetractions: MPMI* **18**: 468–476.

Chumley FG, Valent B. **1990**. Genetic analysis of melanin-deficient, nonpathogenic mutants of *Magnaporthe grisea*. *Molecular Plant-Microbe Interactions: MPMI* **3**: 135–143.

Churchill ACL. **2011**. Pathogen profile *Mycosphaerella fijiensis*, the black leaf streak pathogen of banana: progress towards understanding pathogen biology and detection, disease development, and the challenges of control. *Molecular plant pathology* **12**: 307–328.

Clay K. **1988**. Fungal endophytes of grasses: a defensive mutualism between plants and fungi. *Ecology* **69**: 10–16.

Clemente G, Quintana S, Aguirre N, Rosso A, Cordi N, Havis ND. **2014**. State of art of *Ramularia collo-cygni* (leaf spot of barley) in Argentina and detection and quantification of *R. collo-cygni* by Real Time PCR in barley plantlets and seeds treated with fungicide. Proceeding of the 11th Conference of the European Foundation for Plant Pathology. Krakow, Poland, 116–118.

Coleman JJ, Ghosh S, Okoli I, Mylonakis E. **2011**. Antifungal activity of microbial secondary metabolites. *PLoS ONE* **6**: e25321.

Collemare J, Griffiths S, Iida Y, Karimi Jashni M, Battaglia E, Cox RJ, de Wit PJGM. **2014**. Secondary metabolism and biotrophic lifestyle in the tomato pathogen *Cladosporium fulvum*. *PLoS ONE* **9**: e85877.

Collemare J, Pianfetti M, Vial M, Houlle A, Morin D, Camborde L, Gagey M, Lebrun MH, Bohnert H. **2008**. *Magnaporthe grisea* avirulence gene *ACE1* belongs to an infection specific gene cluster involved in secondary metabolism. *New Phytologist* **179**: 196–208.

Connolly LR, Smith KM, Freitag M. **2013**. The *Fusarium graminearum* histone H3 K27 methyltransferase KMT6 regulates development and expression of secondary metabolite gene clusters. *PLoS Genetics* **9**.

Consonni C, Humphry ME, Hartmann HA, Livaja M, Durner J, Westphal L, Vogel J, Lipka V, Kemmerling B, Schulze-Lefert P, *et al.* 2006. Conserved requirement for a plant host cell protein in powdery mildew pathogenesis. *Nature genetics* **38**: 716–720.

Correia T, Grammel N, Ortel I, Keller U, Tudzynski P. **2003**. Molecular cloning and analysis of the ergopeptine assembly system in the ergot fungus *Claviceps purpurea*. *Chemistry & biology* **10**: 1281–1292.

Cox RJ. **2007**. Polyketides, proteins and genes in fungi: programmed nano-machines begin to reveal their secrets. *Organic & biomolecular chemistry* **5**: 2010–2026.

Crawford JM, Dancy BCR, Hill EA, Udwary DW, Townsend CA. **2006**. Identification of a starter unit acyl-carrier protein transacylase domain in an iterative type I polyketide synthase. *Proceedings of the National Academy of Sciences of the United States of America* **103**: 16728–16733.

Crawford JM, Korman TP, Labonte JW, Vagstad AL, Hill EA, Kamari-Bidkorpeh O, Tsai S-C, Townsend CA. **2009**. Structural basis for biosynthetic programming of fungal aromatic polyketide cyclization. *Nature* **461**: 1139–1143.

Crawford J, Thomas P, Scheerer J, Vagstad A, Kelleher N, Townsend C. **2008**. Deconstruction of iterative multidomain polyketide synthase function. *Science* **320**: 243–246.

Crawford J, Townsend C. **2010**. New insights into the formation of fungal aromatic polyketides. *Nature Reviews Microbiologie* **8**: 879–889.

Cromey MG, Harvey IC, Sheridan JE, Grbavac N. **2002**. Occurrence, importance, and control of *Ramularia collo-cygni* in New-Zealand. In: Yahyaoui A, Brader L, Tekauz A, Wallwork H, Steffenson B, eds. Proceedings of the 2nd International Workshop on Barley Leaf Blights. Aleppo, Syria, 337–342.

Crous P, Aptroot A, Kang J-C, Braun U, MJ W. **2000**. The genus *Mycosphaerella* and its anamorphs. *Studies in Mycology* **45**: 107–121.

Cruz-Cruz CA, García-Sosa K, Escalante-Erosa F, Peña-Rodríguez LM. **2011**. Physiological effects of the hydrophilic phytotoxins produced by *Mycosphaerella fijiensis*, the causal agent of black sigatoka in banana plants. *Journal of General Plant Pathology* **77**: 93–100.

Cuq F, Herrmann-Gorline S, Klaebe A, Rossignol M, Petitprez M. **1993**. Monocerin in *Exserohilum turcicum* isolates from maize and a study of its phytotoxicity. *Phytochemistry* **34**: 1265–1270.

Dalmais B, Schumacher J, Moraga J, Le Pecheur P, Tudzynski B, Collado IG, Viaud M. **2011**. The *Botrytis cinerea* phytotoxin botcinic acid requires two polyketide synthases for production and has a redundant role in virulence with botrydial. *Molecular Plant Pathology* **12**: 564–579.

Danon A, Delorme V, Mailhac N, Gallois P. **2000**. Plant programmed cell death : A common way to die. *Plant Physiology and Biochemistry* **38**: 647–655.

Danon A, Miersch O, Felix G, op den Camp RGL, Apel K. **2005**. Concurrent activation of cell death-regulating signaling pathways by singlet oxygen in *Arabidopsis thaliana*. *The Plant Journal* **41**: 68–80.

Daub ME. **1982**. Cercosporin, a photosensitizing toxin from *Cercospora* species. *Phytopathology* **71**: 370–374.

Daub ME, Briggs SP. **1983**. Changes in tobacco cell membrane composition and structure caused by cercosporin. *Plant physiology* **71**: 763–766.

Daub M, Chung K-R. **2007**. Cercosporin: a photoactivated toxin in plant disease. *APSnet feature* **Online**.

Daub ME, Ehrenshaft M. **2000**. The photoactivated *Cercospora* toxin cercosporin: contributions to plant disease and fundamental biology. *Annual review of phytopathology* **38**: 461–490.

Daub ME, Herrero S, Chung KR. **2005**. Photoactivated perylenequinone toxins in fungal pathogenesis of plants. *FEMS Microbiology Letters* **252**: 197–206.

Delaney TP, Uknes S, Vernooij B, Friedrich L, Negrotto D, Gaffney T, Gut-rella M, Kessmann H, Delaney TP, Uknes S, *et al.* 1994. A central role of salicylic acid in plant disease resistance. *Science* **266**: 1247–1250.

Demain A. **2014**. Valuable secondary metabolites from fungi. In: Marin J-F, Garcia-Estrada C, Zeilinger S, eds. Biosynthesis and Molecular Genetics of Fungal Secondary Metabolites. Springer, 351.

Desjardins AE, Proctor RH. **2007**. Molecular biology of *Fusarium* mycotoxins. *International Journal of Food Microbiology* **119**: 47–50.

Devadas SK, Enyedi A, Raina R. **2002**. The Arabadopsis *hrl1* mutation reveals novel overlapping roles for salicyclic acid, jasmonic acid, and ethylene signaling in cell death and defence against pathogens. *The Plant Journal* **30**: 467–480.

Dietrich R, Delaney T, Uknes S, Ward E, Ryals J, Dangl J. **1994**. Arabidopsis mutants simulating disease resistance response. *Cell* **77**: 565–577.

Ding G, Liu S, Guo L, Zhou Y, Che Y. **2008**. Antifungal metabolites from the plant endophytic fungus *Pestalotiopsis foedan*. *Journal of Natural Products* **71**: 615–618.

Ding G, Song YC, Chen JR, Xu C, Ge HM, Wang XT, Tan RX. **2006**. Chaetoglobosin U, a cytochalasan alkaloid from endophytic *Chaetomium globosum* IFB-E019. *Journal of Natural Products* **69**: 302–304.

Djurle A, Rasmussen M. **2006**. Ramularia leaf spot in barley. A new disease in Sweden? In: Koopmann B, Oxley S, Schützendübel A, von Tiedemann A, eds.

Proceedings of the first European Ramularia workshop - *Ramularia collo-cygni*: a new disease and challenge in barley production. Gottingen, Germany, 45–46.

Dolan SK, O'Keeffe G, Jones GW, Doyle S. **2015**. Resistance is not futile: Gliotoxin biosynthesis, functionality and utility. *Trends in Microbiology* **23**: 419–428.

Dong X. **2004**. NPR1, all things considered. *Current Opinion in Plant Biology* **7**: 547–552.

Doolittle FW. **1999**. Lateral genomics. *Trends in Biochemical Sciences* **24**: 5–8.

Dowzer CEA, Kelly JM. **1989**. Cloning of the *creA* gene from *Aspergillus nidulans*: a gene involved in carbon catabolite repression. *Current Genetics* **15**: 457–459.

Dreiseitl A. **2012**. Frequency of powdery mildew resistances in spring barley cultivars in Czech variety trials. *Plant Protection Science* **48**: 17–20.

Drexler HC, Risau W, Konerding MA. **2000**. Inhibition of proteasome function induces programmed cell death in proliferating endothelial cells. *FASEB journal : Federation of American Societies for Experimental Biology* **14**: 65–77.

Du L, Lou L. **2010**. PKS and NRPS release mechanisms. *Natural product reports* **27**: 255–78.

Dunn BJ, Cane DE, Khosla C. **2013**. Mechanism and specificity of an acyltransferase domain from a modular polyketide synthase. *Biochemistry* **52**: 1839–1841.

Durrant WE, Dong X. **2004**. Systemic Acquired Resistance. *Annual Review of Phytopathology* **42**: 185–209.

Eaton CJ, Cox MP, Ambrose B, Becker M, Hesse U, Schardl CL, Scott B. **2010**. Disruption of signaling in a fungal-grass symbiosis leads to pathogenesis. *Plant physiology* **153**: 1780–1794.

Eguchi N, Kondo KI, Yamagishi N. **2009**. Bait twig method for soil detection of *Rosellinia necatrix*, causal agent of white root rot of Japanese pear and apple, at an early stage of tree infection. *Journal of General Plant Pathology* **75**: 325–330.

Ehrlich KC, Montalbano BG, Cary JW. **1999**. Binding of the C6-zinc cluster protein, AFLR, to the promoters of aflatoxin pathway biosynthesis genes in *Aspergillus parasiticus*. *Gene* **230**: 249–257.

Endo A, Kuroda M, Tanzawa K. **1977**. Competitive inhibition of 3-hydroxy-3-methylglutaryl coenzyme A reductase by ML-236A and ML-236B fungal metabolites, having hypocholesterolemic activity. *FEBS letters* **72**: 323–326.

Espeso EA, Peñalva MA. **1992**. Carbon catabolite repression can account for the temporal pattern of expression of a penicillin biosynthetic gene in *Aspergillus nidulans*. *Molecular microbiology* **6**: 1457–1465.

Espeso EA, Tilburn J, Arst HN, Peñalva MA. **1993**. pH regulation is a major determinant in expression of a fungal penicillin biosynthetic gene. *The EMBO journal* **12**: 3947–3956.

European Commission. **2006**. *Commission Regulation (EC) No 1881/2006*.

Faino L, Seidl MF, Datema E, Van Den Berg GCM, Janssen A, Wittenberg AHJ, Thomma BPHJ. **2015**. Single-Molecule Real-Time sequencing combined with optical mapping yields completely finished fungal genome. *mBio* **6**: e00936–15.

FAOSTAT. **2014**. Production: crops. *Food and Agriculture Organisation of the United Nations*.

Fernandes M, Keller NP, Adams TH. **1998**. Sequence-specific binding by *Aspergillus nidulans* AflR, a C6 zinc cluster protein regulating mycotoxin biosynthesis. *Molecular Microbiology* **28**: 1355–1365.

Feys BJ, Moisan LJ, Newman MA, Parker JE. **2001**. Direct interaction between the Arabidopsis disease resistance signaling proteins, EDS1 and PAD4. *EMBO Journal* **20**: 5400–5411.

Finking R, Marahiel MA. **2004**. Biosynthesis of nonribosomal peptides. *Annual Review of Microbiology* **58**: 453–488.

Fisch KM. **2013**. Biosynthesis of natural products by microbial iterative hybrid PKS–NRPS. *RSC Advances* **3**: 18228–18247.

Fitzpatrick DA. **2012**. Horizontal gene transfer in fungi. *FEMS Microbiology Letters* **329**: 1–8.

Fountaine JM, Fraaije BA. **2009**. Development of QoI resistant alleles in populations of *Ramularia collo-cygni*. *Aspects of Applied Biology* **92**: 123–126.

Fox EM, Howlett BJ. **2008**. Secondary metabolism: regulation and role in fungal biology. *Current Opinion in Microbiology* **11**: 481–487.

FRAG. **2013**. *Fungicide Resistance Management in Cereals - Ramularia collo-cygni*.

Franich RA, Carson MJ, Carson SD. **1986**. Synthesis and accumulation of benzoic acid in *Pinus radiata* needles in response to tissue injury by dothistromin, and correlation with resistance of *P. radiata* families to *Dothistroma pini*. *Physiological and Molecular Plant Pathology* **28**: 267–286.

Frei P. **2002**. *Ramularia collo-cygni*: cultivation, storage, and artificial infection of barley and weed grasses under controlled conditions. In: Yahyaoui A, Brader L, Tekauz A, Wallwork H, Steffenson B, eds. Proceedings of the 2nd International Workshop on Barley Leaf Blights. Aleppo, Syria, 351–354.

Frei P, Gindrat D. **2000**. Le champignon *Ramularia collo-cygni* provoque une forme de grillures sur les feuilles d'orge d'automne et de gramineés adventices. *Revue Suisse d'Agriculture* **32**: 229–233.

Frei P, Gindro K. **2015**. *Ramularia collo-cygni* - un nouveau champignon pathogene de l'orge. *Recherche Agronomique Suisse* **6**: 210–217.

Frei P, Gindro K, Richter H, Schurch S. **2007**. Direct-PCR detection and epidemiology of *Ramularia collo-cygni* associated with barley necrotic leaf spots. *Journal of Phytopathology* **155**: 281–288.

Friedrich L, Lawton K, Ruess W, Masner P, Specker N, Rella MG, Meier B, Dincher S, Staub T, Uknes S, *et al.* 1996. A benzothiadiazole derivative induces systemic acquired resistance in tobacco. *The Plant Journal* **10**: 61–70.

Friedrichsen DM, Joazeiro CA, Li J, Hunter T, Chory J. **2000**. Brassinosteroid-insensitive-1 is a ubiquitously expressed leucine-rich repeat receptor serine/threonine kinase. *Plant physiology* **123**: 1247–1256.

Friesen TL, Ali S, Kianian S, Francl LJ, Rasmussen JB. **2003**. Role of host sensitivity to Ptr ToxA in development of tan spot of wheat. *Phytopathology* **93**: 397–401.

Friesen T, Stukenbrock E, Liu Z, Meinhardt S, Ling H, Faris J, Rasmussen J, Solomon P, McDonald B, Oliver R. **2006**. Emergence of a new disease as a result of interspecific virulence gene transfer. *Nature Genetics* **38**: 953–956.

Fu ZQ, Yan S, Saleh A, Wang W, Ruble J, Oka N, Mohan R, Spoel SH, Tada Y, Zheng N, *et al.* 2012. NPR3 and NPR4 are receptors for the immune signal salicylic acid in plants. *Nature* **486**: 228–232.

Fudal I, Collemare J, Böhnert HU, Melayah D, Lebrun MH. **2007**. Expression of *Magnaporthe grisea* avirulence gene *ACE1* is connected to the initiation of appressorium-mediated penetration. *Eukaryotic Cell* **6**: 546–554.

Furniss JJ, Spoel SH. **2015**. Cullin-RING ubiquitin ligases in salicylic acid-mediated plant immune signaling. *Frontiers in Plant Science* **6**: Article 154.

Gaffney T, Friedrich L, Vernooij B, Negrotto D, Nye G, Uknes S, Ward E, Kessmann H, Ryals J. **1993**. Requirement of salicylic acid for the induction of systemic acquired resistance. *Science* **261**: 754–756.

Gan P, Ikeda K, Irieda H, Narusaka M, O'Connell RJ, Narusaka Y, Takano Y, Kubo Y, Shirasu K. **2013**. Comparative genomic and transcriptomic analyses reveal the hemibiotrophic stage shift of *Colletotrichum* fungi. *New Phytologist* **197**: 1236–1249.

Gardiner DM, Cozijnsen AJ, Wilson LM, Pedras MSC, Howlett BJ. **2004**. The sirodesmin biosynthetic gene cluster of the plant pathogenic fungus *Leptosphaeria maculans*. *Molecular Microbiology* **53**: 1307–1318.

Gardiner DM, Jarvis RS, Howlett BJ. **2005a**. The ABC transporter gene in the sirodesmin biosynthetic gene cluster of *Leptosphaeria maculans* is not essential for sirodesmin production but facilitates self-protection. *Fungal Genetics and Biology* **42**: 257–263.

Gardiner DM, Waring P, Howlett BJ. **2005b**. The epipolythiodioxopiperazine (ETP) class of fungal toxins: distribution, mode of action, functions and biosynthesis. *Microbiology* **151**: 1021–1032.

Gill M. **2001**. The biosynthesis of pigments in basidiomycetes. *Australian Journal of Chemistry* **54**: 721–734.

Glazebrook J. **2005**. Contrasting mechanisms of defense against biotrophic and necrotrophic pathogens. *Annual Review of Phytopathology* **43**: 205–227.

Goddard R, Peraldi A, Ridout C, Nicholson P. **2014**. Enhanced disease resistance caused by *BRI1* mutation is conserved between *Brachypodium distachyon* and barley (*Hordeum vulgare*). *Molecular Plant-Microbe Interactions: MPMI* **27**: 1095–1106.

Gostincar C, Ohm RA, Kogej T, Sonjak S, Turk M, Zajc J, Zalar P, Grube M, Sun H, Han J, *et al.* 2014. Genome sequencing of four *Aureobasidium pullulans* varieties: biotechnological potential, stress tolerance, and description of new species. *BMC Genomics* **15**: 549.

Granum E, Pérez-Bueno ML, Calderón CE, Ramos C, de Vicente A, Cazorla FM, Barón M. **2015**. Metabolic responses of avocado plants to stress induced by *Rosellinia necatrix* analysed by fluorescence and thermal imaging. *European Journal of Plant Pathology* **142**: 625–632.

Greenberg JT. **1996**. Programmed cell death : A way of life for plants. *Proceedings of the National Academy of Sciences* **93**: 12094–12097.

Greenberg JT, Guo A, Klessig DF, Ausubet FM. **1994**. Programmed cell death in plants: a pathogen-triggered response activated coordinately with multiple defense functions. *Cell* **77**: 551–563.

Greenwood C, Thomson A-W. **1959**. A comparison of the starches from barley and malted barley. *Journal of the Institue of Brewing* **65**: 346–353.

Greif P. **2002**. Importance of leaf spot *Ramularia collo-cygni* for barley growers and breeders. In: Yahyaoui A, Brader L, Tekauz A, Wallwork H, Steffenson B, eds. Proceedings of the 2nd International Workshop on Barley Leaf Blights. Aleppo, Syria, 331–336.

Griffiths S, Mesarich CH, Overdijk EJR, Saccomanno B, de Wit PJGM, Collemare J. **2017**. Down-regulation of cladofulvin biosynthesis is required for biotrophic growth of *Cladosporium fulvum* on tomato. *Molecular plant pathology*: in press.

Griffiths S, Mesarich CH, Saccomanno B, Vaisberg A, de Wit PJGM, Cox R, Collemare J. **2016**. Elucidation of cladofulvin biosynthesis reveals a cytochrome P450 monooxygenase required for anthraquinone dimerization. *Proceedings of the National Academy of Sciences* **113**: 6851–6856.

Griffiths S, Saccomanno B, de Wit PJGM, Collemare J. **2015**. Regulation of secondary metabolite production in the fungal tomato pathogen *Cladosporium fulvum*. *Fungal Genetics and Biology* **84**: 52–61.

Guchu HS, Cole DL. **1994**. The toxicity of phytotoxins from *Cercospora arachidicola* and cercosporin from *Cercospora* species to tobacco, Swiss chard and groundnut plants. *Mycological Research* **98**: 1245–1252.

Gunasinghe N, You MP, Cawthray GR, Barbetti MJ. **2016**. Cercosporin from *Pseudocercosporella capsellae* and its critical role in white leaf spot development. *Plant Disease* **100**: 1521–1531.

Haas H. **2015**. How to trigger a fungal weapon. *eLife* **4**: e10504.

Haas H, Eisendle M, Turgeon BG. **2008**. Siderophores in fungal physiology and virulence. *Annual review of phytopathology* **46**: 149–187.

Hamad B. **2010**. The antibiotics market. *Nature Reviews Drug Discovery* **9**: 675–676.

Hammond-Kosack KE, Silverman P, Raskin I, Jones J. **1996**. Race-specific elicitors of *Cladosporium fulvum* induce changes in cell morphology and the synthesis of ethylene and salicylic acid in tomato plants carrying the corresponding *Cf* disease resistance gene. *Plant physiology* **110**: 1381–1394.

Hansen FT, Sorensen JL, Giese H, Sondergaard TE, Frandsen RJN. **2012**. Quick guide to polyketide synthase and nonribosomal synthetase genes in *Fusarium*. *International Journal of Food Microbiology* **155**: 128–136.

Hartman PE, Suzuki CK, Stack ME. **1989**. Photodynamic production of superoxide in vitro by altertoxins in the presence of reducing agents. *Applied and Environmental Microbiology* **55**: 7–14.

Harvey IC. **2002**. Epidemiology and control of leaf and awn spot of barley caused by *Ramularia collo-cygni*. *New Zealand Plant Protection Society* **55**: 331–335.

Hatsugai N, Iwasaki S, Tamura K, Kondo M, Fuji K. **2009**. A novel membrane fusion-mediated plant immunity against bacterial pathogens. *Genes & Development*: 2496–2506.

Hatsugai N, Kuroyanagi M, Yamada K, Meshi T, Tsuda S, Kondo M, Nishimura M, Hara-Nishimura I. **2004**. A plant vacuolar protease, VPE, mediates virus-induced hypersensitive cell death. *Science (New York, N.Y.)* **305**: 855–8.

Havis ND, Brown JKM, Clemente G, Frei P, Jedryczka M, Kaczmarek J, Kaczmarek M, Matusinsky P, McGrann GRD, Piotrowska M, *et al.* 2015. *Ramularia collo-cygni* - an emerging pathogen of barley crops. *Phytopathology* **105**: 895–904.

Havis ND, Nyman M, Oxley SJP. **2010**. Potential of seed treatment to control *Ramularia collo-cygni* in barley. Crop protection in Northern Britain, Dundee, United Kingdom.97–102.

Havis ND, Nyman M, Oxley SJP. **2014**. Evidence for seed transmission and symptomless growth of *Ramularia collo-cygni* in barley (*Hordeum vulgare*). *Plant Pathology* **63**: 929–936.

Havis ND, Oxley SJP, Piper SR, Langrell SRH. **2006**. Rapid nested PCR-based detection of *Ramularia collo-cygni* direct from barley. *FEMS microbiology letters* **256**: 217–223.

Havis ND, Piper SR, Oxley SJP, Langrell SRH. **2002**. Development of a PCR based identification and detection assay for *Ramularia collo-cygni* direct from barley leaf tissue. In: Yahyaoui A, Brader L, Tekauz A, Wallwork H, Steffenson B, eds. Proceedings of the 2nd International Workshop on Barley Leaf Blights. Aleppo, Syria, 343–350.

Hayes PM, Castro A, Marquez-cedillo L, Corey A, Henson C, Jones BL, Kling J, Diane M, Matus I, Rossi C, *et al.* 2003. Genetic diversity for quantitatively inherited agronomic and malting quality traits. In: Von Bothmer R, Van Hintum T, Sato K, eds. Diversity in Barley (Hordeum vulgare). Amsterdam, Netherlands, 201–226.

Heiser I, Heß M, Schmidtke K-U, Vogler U, Miethbauer S, Liebermann B. **2004**. Fatty acid peroxidation by rubellin B, C and D, phytotoxins produced by *Ramularia collo-cygni* (Sutton et Waller). *Physiological and Molecular Plant Pathology* **64**: 135–143.

Heiser I, Liebermann B. **2006**. Phytotoxins from *Ramularia collo-cygni*: mode of action and contribution to pathogenicity. In: Koopmann B, Oxley S, Schützendübel A, von Tiedemann A, eds. Proceedings of the first European Ramularia workshop -

Ramularia collo-cygni: a new disease and challenge in barley production. Gottingen, Germany, 57–62.

Heiser I, Sachs E, Liebermann B. **2003**. Photodynamic oxygen activation by rubellin D, a phytotoxin produced by *Ramularia collo-cygni* (Sutton et Waller). *Physiological and Molecular Plant Pathology* **62**: 29–36.

Henikoff S, Henikoff JG. **1992**. Amino acid substitution matrices from protein blocks. *Proceedings of the National Academy of Sciences of the United States of America* **89**: 10915–10919.

Henrikson JC, Hoover AR, Joyner PM, Cichewicz RH. **2009**. A chemical epigenetics approach for engineering the in situ biosynthesis of a cryptic natural product from *Aspergillus niger*. *Organic and biomolecular chemistry* **7**: 435–438.

Henry R. 1943. The mode of action of sulfonamides. *Bacteriology Reviews* **7**: 175–262.

Hertweck C. **2009**. The biosynthetic logic of polyketide diversity. *Angewandte Chemie International Edition* **48**: 4688–4716.

Hetz C. **2012**. The unfolded protein response: controlling cell fate decisions under ER stress and beyond. *Nature reviews. Molecular cell biology* **13**: 89–102.

HGCA. **2013**. *Ramularia leaf spot in barley*.

Hof C, Eisfeld K, Welzel K, Antelo L, Foster AJ, Anke H. **2007**. Ferricrocin synthesis in *Magnaporthe grisea* and its role in pathogenicity in rice. *Molecular Plant Pathology* **8**: 163–172.

Hopwood DA. **1997**. Genetic contributions to understanding polyketide synthases. *Chemical reviews* **97**: 2465–2498.

Horbach R, Navarro-Quesada AR, Knogge W, Deising HB. **2011**. When and how to kill a plant cell: infection strategies of plant pathogenic fungi. *Journal of Plant Physiology* **168**: 51–62.

Huffaker A, Kaplan F, Vaughan MM, Dafoe NJ, Ni X, Rocca JR, Alborn HT, Teal PEA, Schmelz EA. **2011**. Novel acidic sesquiterpenoids constitute a dominant class of pathogen-induced phytoalexins in maize. *Plant Physiology* **156**: 2082–2097.

Huss H. **2002**. The biology of *Ramularia collo-cygni*. In: Yahyaoui A, Brader L, Tekauz A, Wallwork H, Steffenson B, eds. Proceedings of the 2nd International Workshop on Barley Leaf Blights. Aleppo, Syria, 321–328.

Huss H, Mayerhofer H, Wetschnig W. **1987**. *Ophiocladum hordei* CAV. (Fungi imperfecti), ein für Österreich neuer parasitischer Pilz der Gerste. *Der Pflanzenarzt* **40**: 167–169.

Ichihara A, Oikawa H, Hayashi K, Sakamura S. **1983**. Structures of betaenones A and B, novel phytotoxins from *Phoma betae* Fr. *Journal of the American Chemical Society* **105**: 2907–2908.

Ipcho SVS, Hane JK, Antoni EA, Ahren D, Henrissat B, Friesen TL, Solomon PS, Oliver RP. **2012**. Transcriptome analysis of *Stagonospora nodorum*: gene models, effectors, metabolism and pantothenate dispensability. *Molecular Plant Pathology* **13**: 531–545.

Ishiuchi K, Nakazawa T, Yagishita F, Mino T, Noguchi H, Hotta K, Watanabe K. **2013**. Combinatorial generation of complexity by redox enzymes in the chaetoglobosin A biosynthesis. *Journal of the American Chemical Society* **135**: 7371–7377.

Izhaki I. **2002**. Emodin–a secondary metabolite with multiple ecological functions in higher plants. *New Phytologist* **155**: 205–217.

Jarosch B, Kogel K, Schaffrath U. **1999**. The ambivalence of the barley Mlo locus : mutations conferring resistance against powdery mildew (*Blumeria graminis f. sp. hordei*) enhance susceptibility to the rice blast fungus *Magnaporthe grisea*. *Molecular Plant-Microbe Interactions: MPMI* **12**: 508–514.

Jez JM, Ferrer JL, Bowman ME, Dixon RA, Noel JP. **2000**. Dissection of malonyl-coenzyme A decarboxylation from polyketide formation in the reaction mechanism of a plant polyketide synthase. *Biochemistry* **39**: 890–902.

Jirage D, Tootle TL, Reuber TL, Frost LN, Feys BJ, Parker JE, Ausubel FM, Glazebrook J. **1999**. *Arabidopsis thaliana* PAD4 encodes a lipase-like gene that is important for salicylic acid signaling. *Proceedings of the National Academy of Sciences* **96**: 13583–13588.

Jones J, Dangl J. **2006**. The plant immune system. *Nature* **444**: 323–329.

Jørgensen JH. **1992**. Discovery, characterization and exploitation of Mlo powdery mildew resistance in barley. *Euphytica* **63**: 141–152.

Jorgensen L, Christiansen A, Lemmens M. **2006**. Control of Ramularia in winter barley and spring barley using different fungicides-experiences from Denmark. In: Koopmann B, Oxley S, Schützendübel A, von Tiedemann A, eds. Proceedings of the first European Ramularia workshop - *Ramularia collo-cygni*: a new disease and challenge in barley production. Gottingen, Germany, 113–119.

Kabir MS, Ganley RJ, Bradshaw RE. **2015**. Dothistromin toxin is a virulence factor in dothistroma needle blight of pines. *Plant Pathology* **64**: 225–234.

Kachroo P, Yoshioka K, Shah J, Dooner HK, Klessig DF. **2000**. Resistance to turnip crinkle virus in Arabidopsis is regulated by two host genes and is salicylic acid

dependent but NPR1, ethylene, and jasmonate independent. *The Plant cell* **12**: 677–690.

Kaczmarek M, Piotrowska MJ, Fountaine JM, Gorniak K, McGrann GRD, Armstrong A, Wright KM, Newton AC, Havis ND. **2017**. Infection strategy of *Ramularia collo-cygni* and development of Ramularia leaf spot on barley and alternative graminaceous hosts. *Plant Pathology* **46**: 45–55.

Kaeberlein T, Lewis K, Epstein SS. **2002**. Isolating 'uncultivable' microorganisms in pure culture in a simulated natural environment. *Science* **296**: 1127–1129.

Kallberg Y, Oppermann U, Jörnvall H, Persson B. **2002**. Short-chain dehydrogenases/reductases (SDRs). Coenzyme-based functional assignments in completed genomes. *European Journal of Biochemistry* **269**: 4409–4417.

Kato N, Brooks W, Calvo AM. **2003**. The expression of sterigmatocystin and penicillin genes in *Aspergillus nidulans* is controlled by *veA*, a gene required for sexual development. *Eukaryotic Cell* **2**: 1178–1186.

Kawamura C, Tsujimoto T, Tsuge T. **1999**. Targeted disruption of a melanin biosynthesis gene affects conidial development and UV tolerance in the Japanese pear pathotype of *Alternaria alternata*. *Molecular Plant-Microbe Interactions: MPMI* **12**: 59–63.

Kaysser L, Bernhardt P, Nam SJ, Loesgen S, Ruby JG, Skewes-Cox P, Jensen PR, Fenical W, Moore BS. **2012**. Merochlorins A-D, cyclic meroterpenoid antibiotics biosynthesized in divergent pathways with vanadium-dependent chloroperoxidases. *Journal of the American Chemical Society* **134**: 11988–11991.

Keller NP, Hohn TM. **1997**. Metabolic pathway gene cluster in filamentous fungi. *Fungal Genetics and Biology* **21**: 17–29.

Keller NP, Nesbitt C, Sarr B, Phillips TD, Burow GB. **1997**. pH regulation of sterigmatocystin and aflatoxin biosynthesis in *Aspergillus* spp. *Postharvest Pathology and Mycotoxins* **87**: 643–648.

Keller NP, Turner G, Bennett JW. **2005**. Fungal secondary metabolism — from biochemistry to genomics. *Nature Reviews Microbiology* **3**: 937–947.

Keon J, Antoniw J, Carzaniga R, Deller S, Ward JL, Baker JM, Beale MH, Hammond-Kosack K, Rudd JJ. **2007**. Transcriptional adaptation of *Mycosphaerella graminicola* to programmed cell death (PCD) of its susceptible wheat host. *Molecular Plant-Microbe Interactions: MPMI* **20**: 178–193.

Khan MR, Fischer S, Egan D, Doohan FM. **2006**. Biological control of *Fusarium* seedling blight disease of wheat and barley. *Phytopathology* **96**: 386–394.

Khosla C. **2009**. Structures and mechanisms of polyketide synthases. *Journal of Organic Chemistry* **74**: 6416–6420.

Kim M, Ahn JW, Jin UH, Choi D, Paek KH, Pai HS. **2003**. Activation of the programmed cell death pathway by inhibition of proteasome function in plants. *Journal of Biological Chemistry* **278**: 19406–19415.

Kim YT, Lee YR, Jin J, Han KH, Kim H, Kim JC, Lee T, Yun SH, Lee YW. **2005**. Two different polyketide synthase genes are required for synthesis of zearalenone in *Gibberella zeae*. *Molecular Microbiology* **58**: 1102–1113.

Kim C, Meskauskiene R, Zhang S, Lee KP, Lakshmanan Ashok M, Blajecka K, Herrfurth C, Feussner I, Apel K. **2012**. Chloroplasts of Arabidopsis are the source and a primary target of a plant-specific programmed cell death signaling pathway. *The Plant Cell* **24**: 3026–3039.

Kim M, Panstruga R, Elliott C, Muller J, Devoto A, Yoon H, Park H, Cho M, Schulze-Lefert P. **2002**. Calmodulin interacts with MLO protein to regulate defence against mildew in barley. *Nature* **416**: 447–450.

Kim H, Woloshuk CP. **2008**. Role of AREA, a regulator of nitrogen metabolism, during colonization of maize kernels and fumonisin biosynthesis in *Fusarium verticillioides*. *Fungal Genetics and Biology* **45**: 947–953.

Kroken S, Glass NL, Taylor JW, Yoder OC, Turgeon BG. **2003**. Phylogenomic analysis of type I polyketide synthase genes in pathogenic and saprobic ascomycetes. *Proceedings of the National Academy of Sciences of the United States of America* **100**: 15670–15675.

Kroll M, Arenzana-Seisdedos F, Bachelerie F, Thomas D, Friguet B, Conconi M. **1999**. The secondary fungal metabolite gliotoxin targets proteolytic activities of the proteasome. *Chemistry and Biology* **6**: 689–698.

Kumaran RS, Choi Y, Lee S, Jeon HJ, Kim HJ. **2012**. Isolation of taxol, an anticancer drug produced by the endophytic fungus, *Phoma betae*. *African Journal of Biotechnology* **11**: 950–960.

Kuroyanagi M, Yamada K, Hatsugai N, Kondo M, Nishimura M, Hara-Nishimura I. **2005**. Vacuolar processing enzyme is essential for mycotoxin-induced cell death in *Arabidopsis thaliana*. *The Journal of biological chemistry* **280**: 32914–20.

Kusari S, Hertweck C, Spiteller M. **2012**. Chemical ecology of endophytic fungi: Origins of secondary metabolites. *Chemistry and Biology* **19**: 792–798.

Laurie-Berry N, Joardar V, Street IH, Kunkel BN. **2006**. The *Arabidopsis thaliana JASMONATE INSENSITIVE 1* gene is required for suppression of salicylic

acid-dependent defenses during infection by *Pseudomonas syringae*. *Molecular Plant-Microbe Interactions: MPMI* **19**: 789–800.

Lee A-H, Iwakoshi NN, Anderson KC, Glimcher LH. **2003**. Proteasome inhibitors disrupt the unfolded protein response in myeloma cells. *Proceedings of the National Academy of Sciences of the United States of America* **100**: 9946–9951.

Lee H, Leon J, Raskin I. **1995**. Biosynthesis and metabolism of salicylic acid. *Plant signaling behavior* **92**: 493–496.

Lee I, Oh JH, Keats Shwab E, Dagenais TRT, Andes D, Keller NP. **2009**. HdaA, a class 2 histone deacetylase of *Aspergillus fumigatus*, affects germination and secondary metabolite production. *Fungal Genetics and Biology* **46**: 782–790.

Leistrumaite A, Liatukas Ž. **2006**. Resistance of spring barley cultivars to the new disease Ramularia leaf spot , caused by *Ramularia collo-cygni*. *Agronomy Research* **4**: 251–255.

Levine A, Tenhaken R, Dixon R, Lamb C. **1994**. H2O2 from the oxidative burst orchestrates the plant hypersensitive disease resistance response. *Cell* **79**: 583–593.

Li Y, Chooi YH, Sheng Y, Valentine JS, Tang Y. **2011**. Comparative characterization of fungal anthracenone and naphthacenedione biosynthetic pathways reveals an a-hydroxylation-dependent claisen-like cyclization catalyzed by a dimanganese thioesterase. *Journal of the American Chemical Society* **133**: 15773–15785.

Li E, Jiang L, Guo L, Zhang H, Che Y. **2008**. Pestalachlorides A-C, antifungal metabolites from the plant endophytic fungus *Pestalotiopsis adusta*. *Bioorganic and Medicinal Chemistry* **16**: 7894–7899.

Li CS, Ren G, Yang BJ, Miklossy G, Turkson J, Fei P, Ding Y, Walker LA, Cao S. **2016**. Meroterpenoids with antiproliferative activity from a Hawaiian-plant associated fungus *Peyronellaea coffeae-arabicae* FT238. *Organic Letters* **18**: 2335–2338.

Li J, Zhao-Hui C, Batoux M, Nekrasov V, Roux M, Chinchilla D, Zipfel C, Jones JDG. **2009**. Specific ER quality control components required for biogenesis of the plant innate immune receptor EFR. *Proceedings of the National Academy of Sciences of the United States of America* **106**: 15973–15978.

Liao HL, Chung KR. **2008a**. Genetic dissection defines the roles of elsinochrome Phytotoxin for fungal pathogenesis and conidiation of the citrus pathogen *Elsinoë fawcettii*. *Molecular Plant-Microbe Interactions: MPMI* **21**: 469–479.

Liao HL, Chung KR. **2008b**. Cellular toxicity of elsinochrome phytotoxins produced by the pathogenic fungus, *Elsinoë fawcettii* causing citrus scab. *New Phytologist* **177**: 239–250.

Lim FY, Hou Y, Chen Y, Oh JH, Lee I, Bugni TS, Keller NP. **2012**. Genome-based cluster deletion reveals an endocrocin biosynthetic pathway in *Aspergillus fumigatus*. *Applied and Environmental Microbiology* **78**: 4117–4125.

Linne U, Doekel S, Marahiel MA. **2001**. Portability of epimerization domain and role of peptidyl carrier protein on epimerization activity in nonribosomal peptide synthetases. *Biochemistry* **40**: 15824–15834.

Linne U, Stein DB, Mootz HD, Marahiel MA. **2003**. Systematic and quantitative analysis of protein-protein recognition between nonribosomal peptide synthetases investigated in the tyrocidine biosynthetic template. *Biochemistry* **42**: 5114–5124.

Livak KJ, Schmittgen TD. **2001**. Analysis of relative gene expression data using real-time quantitative PCR and the $2^{-\Delta\Delta Ct}$ method. *Methods* **25**: 402–408.

López-Berges MS, Hera C, Sulyok M, Schäfer K, Capilla J, Guarro J, Di Pietro A. **2013**. The velvet complex governs mycotoxin production and virulence of *Fusarium oxysporum* on plant and mammalian hosts. *Molecular Microbiology* **87**: 49–65.

Lorang JM, Carkaci-Salli N, Wolpert TJ. **2004**. Identification and characterization of victorin sensitivity in *Arabidopsis thaliana*. *Molecular Plant-Microbe Interactions: MPMI* **17**: 577–582.

Lorrain S, Vailleau F, Balagué C, Roby D. **2003**. Lesion mimic mutants: keys for deciphering cell death and defense pathways in plants? *Trends in Plant Science* **8**: 263–271.

Lowe-Power TM, Jacobs JM, Ailloud F, Fochs B, Prior P, Allen C. **2016**. Degradation of the plant defense signal salicylic acid protects *Ralstonia solanacearum* from toxicity and enhances virulence on tobacco. *mBio* **7**: e00656–16.

Ma L-J, Geiser DM, Proctor RH, Rooney AP, O'Donnell K, Trail F, Gardiner DM, Manners JM, Kazan K. **2013**. *Fusarium* pathogenomics. *Annual Review of Microbiology* **67**: 399–416.

Ma J, Li Y, Ye Q, Li J, Hua Y, Ju D, Zhang D, Cooper R, Chang M. **2000**. Constituents of red yeast rice, a traditional Chinese food and medicine. *Journal of Agricultural and Food Chemistry* **48**: 5220–5225.

Ma SM, Zhan J, Xie X, Watanabe K, Tang Y, Zhang W. **2008**. Redirecting the cyclization steps of fungal polyketide synthase. *Journal of the American Chemical Society* **130**: 38–39.

Makepeace JC, Havis ND, Burke JI, Oxley SJP, Brown JKM. **2008**. A method of inoculating barley seedlings with *Ramularia collo-cygni*. *Plant Pathology* **57**: 991–999.

Manninger K, Mátrai T, Murányi I. **2009**. Occurrence and spread of a new disease, Ramularia leaf spot on winter and spring barley in Hungary. *Aspects of Applied Biology* **92**: 111–116.

Manzoni M, Rollini M. **2002**. Biosynthesis and biotechnological production of statins by filamentous fungi and application of these cholesterol-lowering drugs. *Applied Microbiology and Biotechnology* **58**: 555–564.

Marahiel MA, Stachelhaus T, Mootz HD. **1997**. Modular peptide synthetases involved in nonribosomal peptide synthesis. *Chemical Reviews* **97**: 2651–2674.

Marcet-Houben M, Gabaldón T. **2010**. Acquisition of prokaryotic genes by fungal genomes. *Trends in Genetics* **26**: 5–8.

Matusinsky P, Gubis J, Hudcovicova M, Klcova L, Gubisova M, Marik P, Tvaruzek L, Minarikova V. **2011**. Impact of the seed-borne stage of *Ramularia collo-cygni* in barley. *Journal of Plant Pathology* **93**: 679–689.

Matusinsky P, Leisova-Svobodova L, Marik P, Tvaruzek L, Stemberkova L, Hanusova M, Minarikova V, Vysohlidova M, Spitzer T. **2010**. Frequency of a mutant allele of cytochrome b conferring resistance to QoI fungicides in the Czech population of *Ramularia collo-cygni*. *Journal of Plant Diseases and Protection* **117**: 248–252.

McDonald MC, Ahren DAG, Simpfendorfer S, Milgate A, Solomon PS. **2017**. The discovery of the virulence gene *ToxA* in the wheat and barley pathogen *Bipolaris sorokiniana*. *Molecular Plant Pathology*: 2–26.

McGrann GRD, Andongabo A, Sjökvist E, Trivedi U, Dussart F, Kaczmarek M, Mackenzie A, Fountaine JM, Taylor JMG, Paterson LJ, *et al.* 2016. The genome of the emerging barley pathogen *Ramularia collo-cygni*. *BMC Genomics* **17**: 584.

McGrann GRD, Stavrinides A, Russell J, Corbitt MM, Booth A, Chartrain L, Thomas WTB, Brown JKM. **2014**. A trade off between mlo resistance to powdery mildew and increased susceptibility of barley to a newly important disease, Ramularia leaf spot. *Journal of experimental botany* **65**: 1025–1037.

McGrann GRD, Steed A, Burt C, Goddard R, Lachaux C, Bansal A, Corbitt M, Gorniak K, Nicholson P, Brown JKM. **2015a**. Contribution of the drought tolerance-related stress-responsive NAC1 transcription factor to resistance of barley to Ramularia leaf spot. *Molecular Plant Pathology* **16**: 201–209.

McGrann GRD, Steed A, Burt C, Nicholson P, Brown JKM. **2015b**. Differential effects of lesion mimic mutants in barley on disease development by facultative pathogens. *Journal of experimental botany* **66**: 3417–3428.

McIntosh R, Wellings C, Park R. **1995**. *Wheat Rusts: an Atlas of Resistance Genes* (K Jeans and A Cloud-Guest, Eds.). Melbourne: CSIRO publishing.

Melotto M, Underwood W, Koczan J, Nomura K, He SY. **2006**. Plant stomata function in innate immunity against bacterial invasion. *Cell* **126**: 969–980.

Métraux JP. **2002**. Recent breakthroughs in the study of salicylic acid biosynthesis. *Trends in Plant Science* **7**: 332–334.

Miethbauer S, Günther W, Schmidtke K-U, Heiser I, Gräfe S, Gitter B, Liebermann B. **2008**. Uredinorubellins and caeruleoramularin, photodynamically active anthraquinone derivatives produced by two species of the genus *Ramularia*. *Journal of natural products* **71**: 1371–1375.

Miethbauer S, Haase S, Schmidtke K-U, Günther W, Heiser I, Liebermann B. **2006**. Biosynthesis of photodynamically active rubellins and structure elucidation of new anthraquinone derivatives produced by *Ramularia collo-cygni*. *Phytochemistry* **67**: 1206–1213.

Miethbauer S, Heiser I, Liebermann B. **2003**. The phytopathogenic fungus *Ramularia collo-cygni* produces biologically active rubellins on infected barley leaves. *Journal of Phytopathology* **151**: 665–668.

Milaire H. **1982**. Resistance des organismes vivants aux substances chimiques. *Cahier de Liaison O.P.I.E* **44**: 3–6.

Minarikova V, Marik P, Stemberkova L. **2002**. Occurrence of a new fungal pathogen on barley, *Ramularia collo-cygni*, in the Czech Republic. In: Yahyaoui A, Brader L, Tekauz A, Wallwork H, Steffenson B, eds. Proceedings of the 2nd International Workshop on Barley Leaf Blights. Aleppo, Syria, 360–364.

Mingeot-Leclercq MP, Glupczynski Y, Tulkens PM. **1999**. Aminoglycosides: activity and resistance. *Antimicrobial Agents and Chemotherapy* **43**: 727–737.

Minowa Y, Araki M, Kanehisa M. **2007**. Comprehensive analysis of distinctive polyketide and nonribosomal peptide structural motifs encoded in microbial genomes. *Journal of Molecular Biology* **368**: 1500–1517.

Mootz HD, Schwarzer D, Marahiel MA. **2002**. Ways of assembling complex natural products on modular nonribosomal peptide synthetases. *ChemBioChem* **3**: 490–504.

Moreno AA, Mukhtar MS, Blanco F, Boatwright JL, Moreno I, Jordan MR, Chen Y, Brandizzi F, Dong X, Orellana A, *et al.* 2012. IRE1/bZIP60-mediated unfolded protein response plays distinct roles in plant immunity and abiotic stress responses. *PLoS ONE* **7**: e31944.

Mou Z, Fan W, Dong X. **2003**. Inducers of plant systemic acquired resistance regulate NPR1 function through redox changes. *Cell* **113**: 935–944.

Mullbacher A, Waring P, Tiwari-Palni U, Eichner RD. **1986**. Structural relationship of epipolythiodioxopiperazines and their immunomodulating activity. *Molecular Immunology* **23**: 231–236.

Munns R, Tester M. **2008**. Mechanisms of salinity tolerance. *Annual review of plant biology* **59**: 651–681.

Muria-Gonzalez MJ, Chooi YH, Breen S, Solomon PS. **2015**. The past, present and future of secondary metabolite research in the Dothideomycetes. *Molecular Plant Pathology* **16**: 92–107.

Muro-Pastor MI, Gonzalez R, Strauss J, Narendja F, Scazzocchio C. **1999**. The GATA factor AreA is essential for chromatin remodelling in a eukaryotic bidirectional promoter. *The EMBO journal* **18**: 1584–1597.

Navarre DA, Wolpert TJ. **1999**. Victorin induction of an apoptotic/senescence-like response in oats. *The Plant cell* **11**: 237–249.

Nawrath C, Métraux JP. **1999**. Salicylic acid induction-deficient mutants of Arabidopsis express *PR-2* and *PR-5* and accumulate high levels of camalexin after pathogen inoculation. *The Plant Cell* **11**: 1393–1404.

Nevo E, Fu Y-B, Pavlicek T, Khalifa S, Tavasi M, Beiles A. **2012**. Evolution of wild cereals during 28 years of global warming in Israel. *Proceedings of the National Academy of Sciences of the United States of America* **109**: 3412–3415.

Newman R, Newman C, Graham H. **1989**. The hypocholesterolemic function of barley beta glucan. *Cereal Foods World* **34**: 883–886.

Newton AC, Flavell AJ, George TS, Leat P, Mullholland B, Ramsay L, Revoredo-Giha C, Russell J, Steffenson BJ, Swanston JS, *et al.* 2011. Crops that feed the world 4. Barley: a resilient crop? Strengths and weaknesses in the context of food security. *Food Security* **3**: 141–178.

Nikolic M, Romheld V. **2007**. The dynamics of iron in the leaf apoplast. In: Sattelmacher B, Horst WJ, eds. The Apoplast of Higher Plants: Compartment of Storage, Transport and Reactions.353–371.

Noar RD, Daub ME. **2016a**. Bioinformatics prediction of polyketide synthase gene clusters from *Mycosphaerella fijiensis*. *PLoS ONE* **11**: e0158471.

Noar RD, Daub ME. **2016b**. Transcriptome sequencing of *Mycosphaerella fijiensis* during association with *Musa acuminata* reveals candidate pathogenicity genes. *BMC genomics* **17**: 690.

Norred WP, Wang E, Yoo H, Riley RT, Merrill AH. **1992**. In vitro toxicology of fumonisins and the mechanistic implications. *Mycopathologia* **117**: 73–78.

O'Brien M, Nielsen KF, O'Kiely P, Forristal PD, Fuller HT, Frisvad JC. **2006**. Mycotoxins and other secondary metabolites produced in vitro by *Penicillium paneum* Frisvad and *Penicillium roqueforti* Thom isolated from baled grass silage in Ireland. *Journal of agricultural and food chemistry* **54**: 9268–9276.

O'Connell RJ, Thon MR, Hacquard S, Amyotte SG, Kleemann J, Torres MF, Damm U, Buiate EA, Epstein L, Alkan N, *et al.* 2012. Lifestyle transitions in plant pathogenic *Colletotrichum* fungi deciphered by genome and transcriptome analyses. *Nature genetics* **44**: 1060–1065.

O'Sullivan E. **2002**. *Ramularia collo-cygni* - a new pathogen associated with spotting of barley in Ireland. In: Yahyaoui A, Brader L, Tekauz A, Wallwork H, Steffenson B, eds. Proceedings of the 2nd International Workshop on Barley Leaf Blights. Aleppo, Syria, 385–390.

Oettmeier W, Masson K, Donner A. **1988**. Anthraquinone inhibitors of photosystem II electron transport. *FEBS letters* **23**: 259–262.

Ohm RA, Feau N, Henrissat B, Schoch CL, Horwitz BA, Barry KW, Condon BJ, Copeland AC, Dhillon B, Glaser F, *et al.* 2012. Diverse lifestyles and strategies of plant pathogenesis encoded in the genomes of eighteen Dothideomycetes fungi. *PLoS pathogens* **8**: e1003037.

Ohtsubo K, Saito M, Sekita S, Yoshihira K, Natori S. **1978**. Acute toxic effects of chaetoglobosin A, a new cytochalasan compound produced by *Chaetomium globosum*, on mice and rats. *Japanese journal of experimental medicine* **48**: 105–110.

Oide S, Krasnoff SB, Gibson DM, Turgeon BG. **2007**. Intracellular siderophores are essential for ascomycete sexual development in heterothallic *Cochliobolus heterostrophus* and homothallic *Gibberella zeae*. *Eukaryotic Cell* **6**: 1339–1353.

Oide S, Moeder W, Krasnoff S, Gibson D, Haas H, Yoshioka K, Turgeon BG. **2006**. *NPS6*, encoding a nonribosomal peptide synthetase involved in siderophore-mediated iron metabolism, is a conserved virulence determinant of plant pathogenic Ascomycetes. *the Plant Cell Online* **18**: 2836–2853.

Oikawa H, Ichihara A, Sakamura S. **1988**. Biosynthetic study of betaenone B: origin of the oxygen atoms and accumulation of a deoxygenated intermediate using P450 inhibitor. *Journal of Chemical Society*: 600–602.

op den Camp R, Przybyla D, Ochsenbein C, Laloi C, Kim C, Danon A, Wagner D, Hideg É, Göbel C, Nater M, *et al.* 2013. Rapid induction of distinct stress responses after the release of singlet oxygen in Arabidopsis. *The Plant Cell* **15**: 2320–2332.

Osbourn A. **2010**. Secondary metabolic gene clusters: evolutionary toolkits for chemical innovation. *Trends in Genetics* **26**: 449–457.

Oxley SJP, Havis ND. **2010**. Managing *Ramularia collo-cygni* through varietal resistance, seed health and forecasting. *HGCA Report No463*: 55.

Oxley SJP, Havis ND, Brown JMK, Makepeace JC, Fountaine JM. **2008**. *Impact and interactions of Ramularia collo-cygni and oxidative stress in barley*.

Oxley SJP, Havis ND, Hackett R. **2006**. Impact of fungicides and varietal resistance on *Ramularia collo-cygni* in spring barley. Proceedings of the first European Ramularia workshop - *Ramularia collo-cygni*: a new disease and challenge in barley production. Gottingen, Germany, 103–112.

Pahl BHL, Kraub B, Schulze-osthoff K, Decker T, Traenckner EB, Myersfl C, Parksfl T, Warring P, Miihlbacher IIA, Czernilofiky A, *et al.* 1996. The immunosuppressive fungal metabolite gliotoxin specifically inhibits transcription factor NF-kB. *Journal of Experimental Medicine* **183**: 1829–1840.

Pajerowska-Mukhtar K, Dong X. **2009**. A kiss of death-proteasome-mediated membrane fusion and programmed cell death in plant defense against bacterial infection. *Genes & development* **23**: 2449–2454.

Palma-Guerrero J, Torriani SFF, Zala M, Carter D, Courbot M, Rudd JJ, Mcdonald BA, Croll D. **2016**. Comparative transcriptomic analyses of *Zymoseptoria tritici* strains show complex lifestyle transitions and intraspecific variability in transcription profiles. *Molecular Plant Pathology* **17**: 845–859.

Palmer JM, Keller NP. **2010**. Secondary metabolism in fungi: does chromosomal location matter? *Current Opinion in Microbiology* **13**: 431–436.

Pardo J, Urban C, Galvez EM, Ekert PG, Müller U, Kwon-Chung J, Lobigs M, Müllbacher A, Wallich R, Borner C, *et al.* 2006. The mitochondrial protein Bak is pivotal for gliotoxin-induced apoptosis and a critical host factor of *Aspergillus fumigatus* virulence in mice. *Journal of Cell Biology* **174**: 509–519.

Park HS, Ni M, Jeong KC, Kim YH, Yu JH. **2012**. The role, interaction and regulation of the velvet regulator VelB in *Aspergillus nidulans*. *PLoS ONE* **7**: e45935.

Pedley KF, Walton JD. **2001**. Regulation of cyclic peptide biosynthesis in a plant pathogenic fungus by a novel transcription factor. *Proceedings of the National Academy of Sciences of the United States of America* **98**: 14174–14179.

Peraldi A, Griffe LL, Burt C, McGrann GRD, Nicholson P. **2014**. *Brachypodium distachyon* exhibits compatible interactions with *Oculimacula* spp. and *Ramularia collo-cygni*, providing the first pathosystem model to study eyespot and ramularia leaf spot diseases. *Plant Pathology* **63**: 554–562.

Periyannan S, Moore J, Ayliffe M, Bansal U, Wang X, Huang L, Deal K, Luo M, Bariana H, Mago R, *et al.* 2013. The gene *Sr33*, an ortholog of barley *Mla* genes, encodes resistance to wheat stem rust race Ug99. *Science* **341**: 786–788.

Pestka JJ, Smolinski AT. **2005**. Deoxynivalenol: toxicology and potential effects on humans. *Journal of toxicology and environmental health. Part B, Critical reviews* **8**: 39–69.

Pfohl-Leszkowicz A. **1999**. Mycotoxines dans l'aliment: effets sur la sante humaine. Mycologie Medicale.161–212.

Piffanelli P, Zhou F, Casais C, Orme J, Jarosch B, Schaffrath U, Collins NC, Panstruga R, Schulze-Lefert P. **2002**. The barley MLO modulator of defense and cell death is responsive to biotic and abiotic stress stimuli. *Plant physiology* **129**: 1076–1085.

Pihet M, Vandeputte P, Tronchin G, Renier G, Saulnier P, Georgeault S, Mallet R, Chabasse D, Symoens F, Bouchara J-P. **2009**. Melanin is an essential component for the integrity of the cell wall of *Aspergillus fumigatus* conidia. *BMC microbiology* **9**: 177.

Pinnschmidt HO, Sindberg SA, Willas J. **2006**. Resistant barley varieties may facilitate control of Ramularia leaf spot. *Danish Research Centre for Organic Farming*.

Piotrowska MJ, Fountaine JM, Ennos RA, Kaczmarek M, Burnett FJ. **2016a**. Characterisation of *Ramularia collo-cygni* laboratory mutants resistant to succinate dehydrogenase inhibitors. *Pest Management Science*.

Piotrowska MJ, Havis ND, McKenzie A, Burnett FJ. **2016b**. Fungicide sensitivity monitoring in cereals, forest and minor crop pathogens in the UK. In: Deising H, Fraaje B, Mehl A, Oerke E, Sierotzki H, Stammler G, eds. Modern Fungicides and Antifungal Compounds, Vol. III.6.

Del Pozo O, Lam E. **1998**. Caspases and programmed cell death in the hypersensitive response of plants to pathogens. *Current Biology Biol* **8**: 1129–1132.

Proctor RH, Hohn TM, McCormick SP, Desjardins AE. **1995**. *Tri6* encodes an unusual zinc finger protein involved in regulation of trichothecene biosynthesis in *Fusarium sporotrichioides*. *Applied and Environmental Microbiology* **61**: 1923–1930.

Pusztahelyi T, Holb IJ, Pocsi I. **2015**. Secondary metabolites in fungus-plant interactions. *Frontiers in Plant Science* **6**: 1–23.

Qi X, Niks RE, Stam P, Lindhout P. **1998**. Identification of QTLs for partial resistance to leaf rust (*Puccinia hordei*) in barley. *Theoretical and Applied Genetics* **96**: 1205–1215.

Raffaele S, Rivas S, Roby D. **2006**. An essential role for salicylic acid in *AtMYB30*-mediated control of the hypersensitive cell death program in Arabidopsis. *FEBS Letters* **580**: 3498–3504.

Rairdan GJ, Delaney TP. **2002**. Role of salicylic acid and NIM1/NPR1 in race-specific resistance in Arabidopsis. *Genetics* **161**: 803–811.

Rairdan GJ, Donofrio NM, Delaney TP. **2001**. Salicylic acid and NIM1 / NPR1-independent gene induction by incompatible *Peronospora parasitica* in Arabidopsis. *Molecular Plant-Microbe Interactions: MPMI* **14**: 1235–1246.

Rate DN, Greenberg JT. **2001**. The Arabidopsis aberrant growth and death2 mutant shows resistance to *Pseudomonas syringae* and reveals a role for NPR1 in suppressing hypersensitive cell death. *Plant Journal* **27**: 203–211.

Rawlings BJ. **1998**. Biosynthesis of fatty acids and related metabolites. *Natural Product Reports* **15**: 275–308.

Reyes-Dominguez Y, Bok JW, Berger H, Shwab EK, Basheer A, Gallmetzer A, Scazzocchio C, Keller N, Strauss J. **2010**. Heterochromatic marks are associated with the repression of secondary metabolism clusters in *Aspergillus nidulans*. *Molecular Microbiology* **76**: 1376–1386.

Richard JL. **2007**. Some major mycotoxins and their mycotoxicoses-An overview. *International Journal of Food Microbiology* **119**: 3–10.

Rivas-San Vicente M, Plasencia J. **2011**. Salicylic acid beyond defence: Its role in plant growth and development. *Journal of Experimental Botany* **62**: 3321–3338.

Rohlfs M, Albert M, Keller NP, Kempken F. **2007**. Secondary chemicals protect mould from fungivory. *Biology Letters* **3**: 523–525.

Ron D, Walter P. **2007**. Signal integration in the endoplasmic reticulum unfolded protein response. *Nature reviews* **8**: 519–529.

Röttig M, Medema MH, Blin K, Weber T, Rausch C, Kohlbacher O. **2011**. NRPSpredictor2 - A web server for predicting NRPS adenylation domain specificity. *Nucleic Acids Research* **39**: 1–6.

Rouse M, Jin Y. **2009**. Aggressiveness of races TTKSK and QFCSC of *Puccinia graminis f. sp. tritici* at various temperatures. In: Akkaya MS, ed. Proceedings of the 12th International Cereal Rusts and Powdery Mildew Conference.

Rouxel T, Chupeau Y, Fritz R, Kollman A, Bousquet J-F. **1988**. Biological effects of sirodesmin PL, a phytotoxin produced by *Leptosphaeria maculans*. *Plant Science* **57**: 45–53.

Rozen S, Skaletsky HJ. **2000**. Primer3 on the WWW for general users and for biologist programmers. In: Krawetz SMS, ed. Bioinformatics Methods and Protocols: Methods in Molecular Biology. Totowa, NJ, U.S.A., 365–386.

Rudd JJ, Kanyuka K, Hassani-Pak K, Derbyshire M, Andongabo A, Devonshire J, Lysenko A, Saqi M, Desai NM, Powers SJ, *et al.* 2015. Transcriptome and metabolite profiling of the infection cycle of *Zymoseptoria tritici* on wheat reveals a biphasic interaction with plant immunity involving differential pathogen chromosomal contributions and a variation on the hemibiotrophic lifestyle definition. *Plant physiology* **167**: 1158–1185.

Rusterucci C, Aviv DH, Holt BF, Dangl JL, Parker JE. **2001**. The disease resistance signaling components EDS1 and PAD4 are essential regulators of the cell death pathway controlled by LSD1 in Arabidopsis. *the Plant Cell* **13**: 2211–2224.

Ryals JA, Neuenschwander UH, Willits MG, Molina A, Steiner HY, Hunt MD. **1996**. Systemic acquired resistance. *The Plant cell* **8**: 1809–1819.

Sachs E. **2002**. A 'new' leaf spot disease of barley caused by *Ramularia collo-cygni*: description, diagnosis and comparison with other leaf spots. In: Yahyaoui A, Brader L, Tekauz A, Wallwork H, Steffenson B, eds. Proceedings of the 2nd International Workshop on Barley Leaf Blights. Aleppo, Syria, 365–369.

Sachs E, Greif P, Amelung D, Huss H. **1998**. *Ramularia collo-cygni*-a re-discovered barley pathogen in Europe. *Mitt BBA* **357**: 96–97.

Salamati S, Reitan L. **2006**. *Ramularia collo-cygni* on spring barley, an overview of its biology and epidemiology. In: Koopmann B, Oxley S, Schützendübel A, von Tiedemann A, eds. Proceedings of the first European Ramularia workshop - *Ramularia collo-cygni*: a new disease and challenge in barley production. Gottingen, Germany, 19–35.

Salamati S, Reitan L, Flataker KE. **2002**. Occurrence of *Ramularia collo-cygni* on spring barley in Norway. In: Yahyaoui A, Brader L, Tekauz A, Wallwork H, Steffenson B, eds. Proceedings of the 2nd International Workshop on Barley Leaf Blights. Aleppo, Syria, 355–359.

Saleh A, Withers J, Mohan R, Marqués J, Gu Y, Yan S, Zavaliev R, Nomoto M, Tada Y, Dong X. **2015**. Posttranslational modifications of the master transcriptional regulator NPR1 enable dynamic but tight control of plant immune responses. *Cell Host and Microbe* **18**: 169–182.

Salvi M, Bozac A, Toninello A. **2004**. Gliotoxin induces Mg^{2+} efflux from intact brain mitochondria. *Neurochemistry International* **45**: 759–764.

Saville RJ, Gosman N, Burt CJ, Makepeace J, Steed A, Corbitt M, Chandler E, Brown JKM, Boulton MI, Nicholson P. **2012**. The 'Green Revolution' dwarfing

genes play a role in disease resistance in *Triticum aestivum* and *Hordeum vulgare*. *Journal of experimental botany* **63**: 1271–1283.

Schardl CL, Leuchtmann A, Spiering MJ. **2004**. Symbioses of grasses with seedborne fungal endophytes. *Annual Review of Plant Biology* **55**: 315–340.

Scherlach K, Boettger D, Remme N, Hertweck C. **2010**. The chemistry and biology of cytochalasans. *Natural product reports* **27**: 869–886.

Schimmel TG, Coffman AD, Parsons SJ. **1998**. Effect of butyrolactone I on the producing fungus, *Aspergillus terreus*. *Applied and Environmental Microbiology* **64**: 3707–3712.

Schönig B, Brown DW, Oeser B, Tudzynski B. **2008**. Cross-species hybridization with *Fusarium verticillioides* microarrays reveals new insights into *Fusarium fujikuroi* nitrogen regulation and the role of *AreA* and *NMR*. *Eukaryotic Cell* **7**: 1831–1846.

Schulz B, Boyle C. **2005**. The endophytic continuum. *Mycological research* **109**: 661–686.

Schumann J, Hertweck C. **2007**. Molecular basis of cytochalasan biosynthesis in fungi: gene cluster analysis & evidence for involvement of a PKS-NRPS hybrid synthase by RNA silencing. *Journal of the American Chemical Society* **129**: 9564–9565.

Schützendübel A, Stadler M, Wallner D, von Tiedemann A. **2008**. A hypothesis on physiological alterations during plant ontogenesis governing susceptibility of winter barley to ramularia leaf spot. *Plant Pathology* **57**: 518–526.

Schwecke T, Göttling K, Durek P, Dueñas I, Käufer NF, Zock-Emmenthal S, Staub E, Neuhof T, Dieckmann R, Von Döhren H. **2006**. Nonribosomal peptide synthesis in *Schizosoccharomyces pombe* and the architectures of ferrichrome-type siderophore synthetases in fungi. *ChemBioChem* **7**: 612–622.

Schwelm A, Barron NJ, Baker J, Dick M, Long PG, Zhang S, Bradshaw RE. **2009**. Dothistromin toxin is not required for dothistroma needle blight in *Pinus radiata*. *Plant Pathology* **58**: 293–304.

Schwelm A, Barron NJ, Zhang S, Bradshaw RE. **2008**. Early expression of aflatoxin-like dothistromin genes in the forest pathogen *Dothistroma septosporum*. *Mycological research* **112**: 138–146.

Seto Y, Kogami Y, Shimanuki T, Takahashi K, Matsuura H, Yoshihara T. **2005**. Production of phleichrome by *Cladosporium phlei* as stimulated by diketopiperadines of *Epichloe typhina*. *Bioscience, biotechnology, and biochemistry* **69**: 1515–1519.

Shah J. **2003**. The salicylic acid loop in plant defense. *Current Opinion in Plant Biology* **6**: 365–371.

Shah J, Kachroo P, Klessig DF. **1999**. The Arabidopsis *ssi1* mutation restores pathogenesis-related gene expression in *npr1* plants and renders defensin gene expression salicylic acid dependent. *The Plant cell* **11**: 191–206.

Shain L, Franich RA. **1981**. Induction of Dothistroma blight symptoms with dothistromin. *Physiological Plant Pathology* **19**: 49–55.

Shaner G, Finney RE. **1977**. The effect of nitrogen fertilization on the expression of slow-mildewing resistance in knox wheat. *Phytopathology* **77**: 1051–1056.

Shimizu T, Kinoshita H, Ishihara S, Sakai K, Nagai S. **2005**. Polyketide synthase gene responsible for citrinin biosynthesis in *Monascus purpureus*. *Applied and Environmental Microbiology* **71**: 3453–3457.

Shwab EK, Jin WB, Tribus M, Galehr J, Graessle S, Keller NP. **2007**. Histone deacetylase activity regulates chemical diversity in *Aspergillus*. *Eukaryotic Cell* **6**: 1656–1664.

Shwab EK, Keller NP. **2008**. Regulation of secondary metabolite production in filamentous ascomycetes. *Mycological Research* **112**: 225–230.

Siegl M, Latch G, Bush L, Fannin F, Rowan D, Tapper B, Bacon C, Johnson M. **1990**. Fungal endophyte-infected grasses: alkaloid accumulation and aphid response. *Journal of Chemical Ecology* **16**: 3301–3315.

Siewers V, Viaud M, Jimenez-Teja D, Collado IG, Gronover CS, Pradier J-M, Tudzynski B, Tudzynski P. **2005**. Functional analysis of the cytochrome P450 monooxygenase gene *bcbot1* of *Botrytis cinerea* indicates that botrydial is a strain-specific virulence factor. *Molecular Plant-Microbe Interactions: MPMI* **602**: 602–612.

Simpson TJ. **2012**. Genetic and biosynthetic studies of the fungal prenylated xanthone shamixanthone and related metabolites in *Aspergillus* spp. revisited. *ChemBioChem* **13**: 1680–1688.

Slot JC, Rokas A. **2011**. Horizontal transfer of a large and highly toxic secondary metabolic gene cluster between fungi. *Current Biology* **21**: 134–139.

So K, Chung Y, Kim J, Kim B, Park S, Kim D. **2015**. Identification of a polyketide synthase gene in the synthesis of phleichrome of the phytopathogenic fungus *Cladosporium phlei*. *Molecules and Cells* **38**: 1105–1110.

Sock J, Hoppe H-H. **1999**. Pathogenicity of sirodesmin-deficient mutants of Phoma lingam. *Journal of Phytopathology* **147**: 169–173.

Sonjak S, Frisvad JC, Gunde-Cimerman N. **2005**. Comparison of secondary metabolite production by *Penicillium crustosum* strains, isolated from Arctic and other various ecological niches. *FEMS Microbiology Ecology* **53**: 51–60.

Spikes J. **1989**. Photosensitization. In: Smith K, ed. The Science of Photobiology. New-York, 79–110.

Spoel SH, Johnson JS, Dong X. **2007**. Regulation of tradeoffs between plant defenses against pathogens with different lifestyles. *Proceedings of the National Academy of Sciences of the United States of America* **104**: 18842–18847.

Spoel SH, Loake GJ. **2011**. Redox-based protein modifications: the missing link in plant immune signalling. *Current Opinion in Plant Biology* **14**: 358–364.

Spoel SH, Mou Z, Tada Y, Spivey NW, Genschik P, Dong X. **2009**. Proteasome-mediated turnover of the transcription coactivator NPR1 plays dual roles in regulating plant immunity. *Cell* **137**: 860–72.

Sprague R. **1946**. Additions to the fungi imperfecti on grasses in the United States. *Mycological Society of America* **38**: 52–64.

Stabentheiner E, Minihofer T, Huss H. **2009**. Infection of barley by *Ramularia collo-cygni*: scanning electron microscopic investigations. *Mycopathologia* **168**: 135–143.

Stachelhaus T, Mootz HD, Marahiel MA. **1999**. The specificity-conferring code of adenylation domains in nonribosomal peptide synthetases. *Chemistry and Biology* **6**: 493–505.

Stamatakis A, Ludwig T, Meier H. **2005**. RAxML-III: A fast program for maximum likelihood-based inference of large phylogenetic trees. *Bioinformatics* **21**: 456–463.

Stergiopoulos I, Collemare J, Mehrabi R, De Wit PJGM. **2013**. Phytotoxic secondary metabolites and peptides produced by plant pathogenic Dothideomycete fungi. *FEMS Microbiology Reviews* **37**: 67–93.

Stierle A, Strobel G, Stierle D. **1993**. Taxol and taxane production by *Taxomyces andreanae*, an endophytic fungus of Pacific yew. *Science* **260**: 214–216.

Stukenbrock EH, McDonald BA. **2007**. Geographical variation and positive diversifying selection in the host-specific toxin *SnToxA*. *Molecular Plant Pathology* **8**: 321–332.

Suarez C, Gudiol F. **2009**. Beta-lactam antibiotics. *Enfermedades Infecciosas y Microbiología Clínica* **27**: 116–129.

Sutton BC, Waller JM. **1988**. Taxonomy of *Ophiocladium hordei*, causing leaf lesions on Triticale and other *Gramineae*. *Transactions of the British Mycological Society* **90**: 55–61.

Sweat TA, Wolpert TJ. **2007**. Thioredoxin h5 is required for victorin sensitivity mediated by a CC-NBS-LRR gene in Arabidopsis. *The Plant cell* **19**: 673–87.

Tada Y, Kusaka K, Betsuyaku S, Shinogi T, Sakamoto M, Ohura Y, Hata S, Mori T, Tosa Y, Mayama S. **2005**. Victorin triggers programmed cell death and the defense response via interaction with a cell surface mediator. *Plant & cell physiology* **46**: 1787–98.

Tada Y, Spoel SH, Pajerowska-mukhtar K, Mou Z, Song J, Wang C, Zuo J, Dong X. **2008**. Plant immunity requires conformational charges of NPR1 via S-nitrosylation and thioredoxins. *Science* **321**: 952–956.

Takai S. **1974**. Pathogenicity and cerato-ulmin production in *Ceratocystis ulmi*. *Nature* **252**: 124–126.

Takano Y, Kubo Y, Kawamura C, Tsuge T, Furusawa I. **1997**. The *Alternaria alternata* melanin biosynthesis gene restores appressorial melanization and penetration of cellulose membranes in the melanin-deficient albino mutant of *Colletotrichum lagenarium*. *Fungal genetics and biology : FG & B* **21**: 131–140.

Tanaka A, Tapper BA, Popay A, Parker EJ, Scott B. **2005**. A symbiosis expressed non-ribosomal peptide synthetase from a mutualistic fungal endophyte of perennial ryegrass confers protection to the symbiotum from insect herbivory. *Molecular Microbiology* **57**: 1036–1050.

Taylor JMG, Paterson LJ, Havis ND. **2010**. A quantitative real-time PCR assay for the detection of *Ramularia collo-cygni* from barley (*Hordeum vulgare*). *Letters in applied microbiology* **50**: 493–499.

Temple B, Horgen PA, Bernier L, Hintz WE. **1997**. Cerato-ulmin, a hydrophobin secreted by the causal agents of Dutch elm disease, is a parasitic fitness factor. *Fungal genetics and biology : FG & B* **22**: 39–53.

Thirugnanasambandam, A, Wright, KM, Havis, N, Whisson, SC, Newton, AC. **2011**. Agrobacterium-mediated transformation of the barley pathogen *Ramularia collo-cygni* with fluorescent marker tags and live tissue imaging of infection development. *Plant Pathology*. **60**: 929–937

Throckmorton K, Lim FY, Kontoyiannis DP, Zheng W, Keller NP. **2016**. Redundant synthesis of a conidial polyketide by two distinct secondary metabolite clusters in *Aspergillus fumigatus*. *Environmental Microbiology* **18**: 246–259.

Tilburn J, Sarkar S, Widdick DA, Espeso EA, Orejas M, Mungroo J, Peñalva MA, Arst HN. **1995**. The *Aspergillus PacC* zinc finger transcription factor mediates

regulation of both acid- and alkaline-expressed genes by ambient pH. *The EMBO journal* **14**: 779–790.

Tripathy BC, Oelmüller R. **2012**. Reactive oxygen species generation and signaling in plants. *Plant Signaling & Behavior* **7**: 1621–1633.

Udvardi MK, Czechowski T, Scheible W-R. **2008**. Eleven golden rules of quantitative RT-PCR. *The Plant cell* **20**: 1736–1737.

Ugai T, Minami A, Fujii R, Tanaka M, Oguri H, Gomi K, Oikawa H. **2015**. Heterologous expression of highly reducing polyketide synthase involved in betaenone biosynthesis. *Chemical communications* **51**: 1878–1881.

Upchurch RG, Walker DC, Rollins JA, Ehrenshaft M, Daub ME. **1991**. Mutants of *Cercospora kikuchii* altered in cercosporin synthesis and pathogenicity. *Applied and environmental microbiology* **57**: 2940–2945.

Uppalapati SR, Ishiga Y, Wangdi T, Kunkel BN, Anand A, Mysore KS, Bender CL. **2007**. The phytotoxin coronatine contributes to pathogen fitness and is required for suppression of salicylic acid accumulation in tomato inoculated with *Pseudomonas syringae* pv. *tomato* DC3000. *Molecular Plant-Microbe Interactions: MPMI* **20**: 955–965.

Valenzeno DP, Pooler JP. **1987**. Photodynamic Action. *BioScience* **37**: 270–276.

Vandesompele J, De Preter K, Pattyn F, Poppe B, Van Roy N, De Paepe A, Speleman F. **2002**. Accurate normalization of real-time quantitative RT-PCR data by geometric averaging of multiple internal control genes. *Genome biology* **3**: 0034.1–0034.11.

Vanhaute E, Paping R, O'Grada C. **2006**. The European subsistence crisis of 1845 – 1850 : a comparative perspective. In: Paping R, Vanhaute E, O'Grada C, eds. When the Potato Failed. Causes and Effects of the Last European Subsistence Crisis, 1845-1850.15–40.

Velluti A, Marín S, Bettucci L, Ramos AJ, Sanchis V. **2000**. The effect of fungal competition on colonization of maize grain by *Fusarium moniliforme*, *F. proliferatum* and *F. graminearum* and on fumonisin B1 and zearalenone formation. *International Journal of Food Microbiology* **59**: 59–66.

Wagner D, Przybyla D, op den Camp R, Kim C, Landgraf F, Lee KP, Wu M. **2004**. The genetic basis of singlet oxygen-induced stress responses of *Arabidopsis thaliana*. *Science* **306**: 1183–1186.

Walsh CT, Chen H, Keating TA, Hubbard BK. **2001**. Tailoring enzymes that modify nonribosomal peptides during and after chain elongation on NRPS assembly lines. *Current Opinion in Chemical Biology* **5**: 525–534.

Walter P, Ron D. **2012**. The unfolded protein response: from stress pathway to homeostatic regulation. *Science* **334**: 1081 – 1086.

Walters DR, Havis ND, Oxley SJP. **2008**. *Ramularia collo-cygni*: the biology of an emerging pathogen of barley. *FEMS microbiology letters* **279**: 1–7.

Walton JD. **2006**. HC-toxin. *Phytochemistry* **67**: 1406–1413.

Wang L, Newman R, Newman C, Hofer P. **1992**. Barley beta glucans alter intestinal viscosity and reduce plasma cholesterol concentrations in chicks. *Journal of Nutrition* **122**: 2292–2297.

Wang D, Weaver ND, Kesarwani M, Dong X. **2005**. Induction of protein secretory pathway is required for systemic acquired resistance. *Science* **308**: 1036–1040.

Wasil Z, Pahirulzaman KAK, Butts CP, Simpson TJ, Lazarus CM, Cox RJ. **2013**. One pathway, many compounds: heterologous expression of a fungal biosynthetic pathway reveals its intrinsic potential for diversity. *Chemical Science* **4**: 3845–3856.

Watanabe CM, Wilson D, Linz JE, Townsend CA. **1996**. Demonstration of the catalytic roles and evidence for the physical association of type I fatty acid synthases and a polyketide synthase in the biosynthesis of aflatoxin B1. *Chemistry & biology* **3**: 463–469.

Weissman KJ. **2015**. The structural biology of biosynthetic megaenzymes. *Nature Chemical Biology* **11**: 660–670.

Weymann K, Hunt M, Uknes S, Neuenschwander U, Lawton K, Steiner HY, Ryals J. **1995**. Suppression and restoration of lesion formation in Arabidopsis *lsd* mutants. *Plant Cell* **7**: 2013–2022.

Wiemann P, Brown DW, Kleigrewe K, Bok JW, Keller NP, Humpf HU, Tudzynski B. **2010**. *FfVel1* and *FfLae1*, components of a velvet-like complex in *Fusarium fujikuroi*, affect differentiation, secondary metabolism and virulence. *Molecular Microbiology* **77**: 972–994.

Wiemann P, Willmann A, Straeten M, Kleigrewe K, Beyer M, Humpf HU, Tudzynski B. **2009**. Biosynthesis of the red pigment bikaverin in *Fusarium fujikuroi*: genes, their function and regulation. *Molecular Microbiology* **72**: 931–946.

Wight WD, Kim K, Lawrence CB, Walton JD. **2009**. Biosynthesis and role in virulence of the histone deacetylase inhibitor depudecin from *Alternaria brassicicola*. *Molecular Plant-Microbe Interactions: MPMI* **22**: 1258–1267.

Wild CP, Turner PC. **2002**. The toxicology of aflatoxins as a basis for public health decisions. *Mutagenesis* **17**: 471–481.

Wildermuth MC, Dewdney J, Wu G, Ausubel FM. **2001**. Isochorismate synthase is required to synthesize salicylic acid for plant defence. *Nature* **414**: 562–565.

Williams RB, Henrikson JC, Hoover AR, Lee AE, Cichewicz RH. **2008**. Epigenetic remodeling of the fungal secondary metabolome. *Organic & biomolecular chemistry* **6**: 1895–1897.

De Wit PJGM, van der Burgt A, Ökmen B, Stergiopoulos I, Abd-Elsalam KA, Aerts AL, Bahkali AH, Beenen HG, Chettri P, Cox MP, *et al.* 2012. The genomes of the fungal plant pathogens *Cladosporium fulvum* and *Dothistroma septosporum* reveal adaptation to different hosts and lifestyles but also signatures of common ancestry. *PLoS genetics* **8**: e1003088.

Wojtaszek P. **1997**. Oxidative burst: an early plant response to pathogen infection. *The Biochemical journal* **322**: 681–692.

Wolf JC, Mirocha CJ. **1973**. Regulation of sexual reproduction in *Gibberella zeae* (*Fusarium roseum 'Graminearum'*) by F-2 (zearalenone). *Canadian Journal of Microbiology* **19**: 725–734.

Woloshuk CP, Foutz KR, Brewer JF, Bhatnagar D, Cleveland TE, Payne GA. **1994**. Molecular characterization of *aflR*, a regulatory locus for aflatoxin biosynthesis. *Applied and environmental microbiology* **60**: 2408–2414.

Woloshuk CP, Sisler HD, Tokousbalides MC, Dutky SR. **1980**. Melanin biosynthesis in *Pyricularia oryzae*: site of tricyclazole inhibition and pathogenicity of melanin-deficient mutants. *Pesticide Biochemistry and Physiology* **14**: 256–264.

Wu D, Oide S, Zhang N, Choi MY, Turgeon BG. **2012**. *ChLae1* and *ChVel1* regulate T-toxin production, virulence, oxidative stress response, and development of the maize pathogen *Cochliobolus heterostrophus*. *PLoS Pathogens* **8**.

Wu Y-X, von Tiedemann A. **2004**. Light-dependent oxidative stress determines physiological leaf spot formation in barley. *Phytopathology* **94**: 584–592.

Xu W, Cai X, Jung ME, Tang Y. **2010**. Analysis of intact and dissected fungal polyketide synthase-nonribosomal peptide synthetase in vitro and in *Saccharomyces cerevisiae*. *Journal of the American Chemical Society* **132**: 13604–13607.

Yalpani N, Silverman P, Wilson MA, Kleier DA, Raskin I. **1991**. Salicylic acid is a systemic signal and an inducer of pathogenesis-related proteins in virus-infected tobacco. *The Plant Cell* **3**: 809–818.

Yamazaki S, Okubo A, Akiyama Y, Fuwa K. **1975**. Cercosporin: a novel photodynamic pigment isolated from *Cercospora kikuchii*. *Agricultural and Biological Chemistry* **39**: 287–288.

Yoshida H, Matsui T, Hosokawa N, Kaufman RJ, Nagata K, Mori K. **2003**. A time-dependent phase shift in the mammalian unfolded protein response. *Developmental Cell* **4**: 265–271.

Yoshida H, Oku M, Suzuki M, Mori K. **2006**. pXBP1(U) encoded in *XBP1* pre-mRNA negatively regulates unfolded protein response activator pXBP1(S) in mammalian ER stress response. *Journal of Cell Biology* **172**: 565–575.

Yoshihara T, Shimanuki T, Araki T, Sakamura S. **1975**. Phleichrome; a new phytotoxic compound produced by *Cladosporium phlei*. *Agricultural and Biological Chemistry* **39**: 1683–1684.

You F, Han T, Wu JZ, Huang BK, Qin LP. **2009**. Antifungal secondary metabolites from endophytic *Verticillium* sp. *Biochemical Systematics and Ecology* **37**: 162–165.

Yu J, Chang P, Ehrlich KC, Cary JW, Bhatnagar D, Cleveland TE, Payne GA, Linz JE, Woloshuk CP, Bennett JW. **2004**. Clustered pathway genes in aflatoxin biosynthesis. *Applied and environmental microbiology* **70**: 1253–1262.

Zadoks J, Chang T, Konzak C. **1974**. A decimal code for the growth stages of cereals. *Weed research* **14**: 415–421.

Zhan J, Fitt BDL, Pinnschmidt HO, Oxley SJP, Newton AC. **2007**. Resistance, epidemiology and sustainable management of *Rhynchosporium secalis* populations on barley. *Plant Pathology* **57**: 1–14.

Zhang Y, Fan W, Kinkema M, Li X, Dong X. **1999**. Interaction of NPR1 with basic leucine zipper protein transcription factors that bind sequences required for salicylic acid induction of the *PR-1* gene. *Proceedings of the National Academy of Sciences of the United States of America* **96**: 6523–6528.

Zhang S, Schwelm A, Jin H, Collins LJ, Bradshaw RE. **2007**. A fragmented aflatoxin-like gene cluster in the forest pathogen *Dothistroma septosporum*. *Fungal genetics and biology : FG & B* **44**: 1342–1354.

Zhang G, Zhang Y, Qin J. **2013**. Antifungal metabolites produced by *Chaetomium globosum* No.04, an endophytic fungus isolated from *Ginkgo biloba*. *Indian Journal of Microbiology* **53**: 175–180.

Zhang X, Zhu Y, Bao L, Gao L, Yao G, Li Y, Yang Z, Li Z, Zhong Y, Li F, *et al.* 2016. Putative methyltransferase LaeA and transcription factor CreA are necessary for proper asexual development and controlling secondary metabolic gene cluster expression. *Fungal Genetics and Biology* **94**: 32–46.

Zheng XY, Spivey NW, Zeng W, Liu PP, Fu ZQ, Klessig DF, He SY, Dong X. **2012**. Coronatine promotes *Pseudomonas syringae* virulence in plants by activating a

signaling cascade that inhibits salicylic acid accumulation. *Cell Host and Microbe* **11**: 587–596.

Zhou N, Tootle TL, Tsui F, Klessig DF, Glazebrook J. **1998**. PAD4 functions upstream from salicylic acid to control defense responses in Arabidopsis. *The Plant cell* **10**: 1021–1030.

Zhou JM, Trifa Y, Silva H, Pontier D, Lam E, Shah J, Klessig DF. **2000**. NPR1 differentially interacts with members of the TGA/OBF family of transcription factors that bind an element of the PR-1 gene required for induction by salicylic acid. *Molecular Plant-Microbe Interactions: MPMI* **13**: 191–202.

Zipfel C. **2009**. Early molecular events in PAMP-triggered immunity. *Current Opinion in Plant Biology* **12**: 414–420.

Zohary D, Hopf M. **2000**. *Domestication of Plants in the Old World. The origin and spread of cultivated plants in West Asia, Europe and the Nile Valley*. New York, USA: Oxford University Pres Inc.

Thesis outputs

- Publications:

McGrann GRD, Andongabo A, Sjökvist E, Trivedi U, **Dussart F**, Kaczmarek M, Mackenzie A, Fountaine JM, Taylor JMG, Paterson LJ, Gorniak K, Burnett F, Kanyuka K, Hammond-Kosack KE, Rudd JJ, Blaxer M, Havis, ND. 2016. The genome of the emerging barley pathogen *Ramularia collo-cygni*. *BMC Genomics* 17: 584

- Planned publications:

Authors: **Dussart F**, Douglas R, Sjökvist E, Hoebe P, Spoel SH, McGrann GRD.
Proposed title: Identification and characterisation of secondary metabolism-associated core genes in *Ramularia collo-cygni*, the causative agent of Ramularia leaf spot disease of barley.

Authors: **Dussart F**, Williams L, Hoebe P, McGrann GRD, Spoel SH.
Proposed title: The phytotoxin rubellin D produced by the barley pathogen *Ramularia collo-cygni* induces plant cell death mediated by the salicylic acid pathway.

- Conference posters:

Authors: **Dussart F**, Hoebe P, Spoel SH, McGrann GRD
Title: Poisonned plants: unravelling the mystery of rubellins.
Conference: Institute of Molecular Plant Sciences symposium, September 2015, Edinburgh, UK

Authors: **Dussart F**, Spoel SH, Hoebe, P, McGrann GRD
Title: Identification and characterisation of polyketide synthases in the barley pathogen *Ramularia collo-cygni*.
Conference: 29th Fungal Genetics Conference, March 2017, Asilomar, Pacific Grove, CA, USA

Appendix

Appendix 1: Proteins used in the phylogenetic study and their respective organisms

A) Polyketide synthases

Name	Species	Accession number
ZymtrPks56913	*Zymoseptoria tritici*	XP_003856913.1
PhobeBet1	*Phoma betae*	BAQ25466.1
FusgrFsl1	*Fusarium graminearum*	XP_011319443.1
BotciPks6	*Botrytis cinerea*	CAP58786.1
FusoxFum1	*Fusarium oxysporum*	ACB12550.1
AltbrDep5	*Alternaria brassicicola*	ACZ57548.1
BotciPks9	*Botrytis cinerea*	CBX87032.1
MacphPks16355	*Macrophomina phaseolina*	EKG16355.1
BipmaPks1	*Bipolaris maydis*	AAB08104.3
BipmaPks2	*Bipolaris maydis*	ABB76806.1
AspniAN1036	*Aspergillus nidulans*	EAA65604.1
PenciMlcB	*Penicillium citrinum*	BAC20566.1
AspteLDKS	*Aspergillus terreus*	AAD34559.1
MonpiMkB	*Monascus pilosus*	ABA02240.1
SceapLovF	*Scedosporium apiospermum*	XP_016645297.1
ZymbrPks98396	*Zymoseptoria brevis*	KJX98396.1
AltsoPksN	*Alternaria solani*	BAD83684.1
Aspno08214	*Aspergillus nominus*	XP_015408214.1
FusgrPks4	*Fusarium graminearum*	ABB90283.1
HypsuHpm8	*Hypomyces subiculosus*	ACD39767.1
Podan04114	*Podspora anserina*	XP_001904114.1
Settu28124	*Setosphaeria turcica*	XP_008028124.1
AspocAomsas	*Aspergillus ochraceus*	AAS98200.1
Bisni6Msas	*Byssochlamys nivea*	AAK48943.1
PengrMsas	*Penicillium griseofulvum*	P22367.1
MonpuPksCT	*monasus purpureus*	BAD44749.1
AspniAN1034	*Aspergillus nidulans*	EAA65602.1
PenbrMpaC	*Penicillium brevicompactum*	ADY00130.1
ZymtrPks55816	*Zymoseptoria tritici*	XP_003855816.1
FusgrPks13	*Fusarium graminearum*	ABB90282.1
HypsuHpm3	*Hypomyces subiculosus*	ACD39762.1
ClafuClaG	*Cladosporium fulvum*	184395*
AspfuEncA	*Aspergillus fumigatus*	XP_746435.1
AspteAcas	*Aspergillus terreus*	XP_001217072.1
AspniMdpG	*Aspergillus nidulans*	XP_657754.1
BipviPks555313	*Bipolaris victoriae*	XP_014555313.1
ClaphPks1	*Cladosporium phlei*	AFP89389.1
ElsfaPks1	*Elsino* ë *fawcettii*	ABU63483.1
PsefiPksA	*Pseudocercospora fijiensis*	XP_007931490.1
ZymtrPksA	*Zymoseptoria tritici*	XP_003848644.1
GlaloPks1	*Glarea lozoyensis*	AAN59953.1
NodspPks1	*Nodulisporium sp. ATCC74245*	AAD38786.1
CollaPks1	*Colletotrichum lagenaria*	BAA18956.1

Appendix 1 (Continued): Proteins used in the phylogenetic study and their respective organisms

MagorAlb1	*Magnaporthe oryzae*	XP_003715434.1
SormaPks1	*Sordaria macrospora*	CAM35471.1
PodanPks1	*Podospora anserina*	XP_001910795.1
CerniCtb1	*Cercospora nictianae*	AAT69682.1
AspflPksA	*Aspergillus flavus*	AAS90093.1
AspniStcA	*Aspergillus nidulans*	AAC49191.1
DotsePksA	*Dothistroma septosporum*	EME39092.1
ClafuPksA	*Cladosporium fulvum*	194256*
NechaPKSN	*Nectria haematococca*	AAS48892.1
FusgrPks12	*Fusarium graminearum*	AAU10633.1
FusfuBik1	*Fusarium fujikuroi*	CAB92399.1
AspfuAlb1	*Aspergillus fumigatus*	AAC39471.1
AspniYwa1	*Aspergillus nidulans*	CAA46695.2
AspnigAlbA	*Aspergillus niger*	EHA28527.1

*: protein ID in the jgi database

B) Hybrids Polyketide synthase/Non-ribosomal peptide synthetases

Name	Species	Accession number
Chagl15110	*Chaetomium globosum*	XP_001220460.1
MagorAce1	*Magnaporthe oryzae*	CAG28797.1
Pano251	*Parastagonospora nodorum*	XP_001790998.1
MagorSyn2	*Magnaporthe oryzae*	CAG28798.1
AspclCssA	*Aspergillus clavatus*	XP_001270543.1
Cocim06629	*Coccidioides imitis*	XP_001242733.1
Uncre03815	*Uncinocarpus reesii*	EEP78969.1
PodanHps05191	*Podospora anserina*	XP_001905191.1
Aspcl023380	*Aspergillus clavatus*	XP_001269050.1
FusheEqiS	*Fusarium heterosporum*	AGO86662.1
Fusox9586	*Fusarium oxysporum*	EGU88865.1
FusvePks1	*Fusarium verticillioides*	AAR92208.1
AspfuPsoA	*Aspergillus fumigatus*	ABS87601.1
Aspte00325	*Aspergillus terreus*	EAU38971.1
SphmuHps08749	*Sphaerulina musiva*	EMF08749.1
MetanNgs1	*Metarhizium anisopliae*	ACS68554.1
FusveFusS	*Fusarium verticillioides*	AAT28740.1
FusfuFusC	*Fusarium fujikuroi*	KLP11216.1
AsporCpaA	*Aspergillus oryzae*	BAK26562.1
AspflCpaA	*Aspergillus flavus*	BAI43678.1
AspniApdA	*Aspergillus nidulans*	XP_681681.1
SphmuHyb1	*Sphaerulina musiva*	XP_016760307.1
BeabaTenS	*Beauveria bassiana*	CAL69597.1
BeabaDmbS	*Beauveria bassiana*	ADN43685.1
PenexCheA	*Penicillium expansum*	CAO91861.1
AspleNps14	*Aspergillus lentulus*	GAQ05296.1

Appendix 1 (Continued): Proteins used in the phylogenetic study and their respective organisms

C) Non-ribosomal peptide synthetases

Name	Species	Accession number
BipmaNps1	*Bipolaris maydis*	AAX09983.1
BipmaNps3	*Bipolaris maydis*	AAX09985.1
BipzeHts1	*Bipolaris zeicola*	AAA33023.2
FuseqEsyn1	*Fusarium equiseti*	Q00869.2
AspfuPes1	*Aspergillus fumigatus*	XP_752404.1
ClapuLpsA1	*Claviceps purpurea*	AET79183.1
AspkaNps	*Aspergillus kawachii*	GAA82422.1
ZymbrNpsT139	*Zymoseptoria brevis*	KJX92939.1
BipmaNps5	*Bipolaris maydis*	AAX09987.1
BipmaNps4	*Bipolaris maydis*	AAX09986.1
AltalAmt	*Alternaria alternata*	AAF01762.1
AspudNps8	*Aspergillus udagawae*	GAO84820.1
RosneNps	*Rosellinia necatrix*	GAP90069.1
FusgrNps6	*Fusarium graminearum*	EYB32861.1
AspfuSidD	*Aspergillus fumigatus*	XP_748662.1
MagorSsm2	*Magnaporthe oryzae*	XP_003714007.1
ParnoSNOG09488	*Parastagonospora nodorum*	XP_001799780.1
EpifePerA	*Epichloe festucae*	BAE06845.2
BipmaNps8	*Bipolaris maydis*	AAX09990.1
AspfuGliP	*Aspergillus fumigatus*	XP_750855.1
CorcoNps	*Cordyceps confragosa*	OAA76647.1
EndpuNps	*Endocarpon pusillum*	XP_007802349.1
UstmaSid2	*Ustillago maydis*	AAB93493.1
MagorSsm1	*Magnaporthe oryzae*	XP_003719607.1
BipmaNps2	*Bipolaris maydis*	AAX09984.1
DotseNps	*Dothistroma septosporum*	EME41700.1
AspfuSidC	*Aspergillus fumigatus*	XP_753088.1
UstmaFer3	*Ustillago maydis*	DAA04939.1
SchpoSib1	*Schizosaccharomyces pombe*	CAB72227.1
OmpolFso1	*Omphalotus olearius*	AAX49356.1

Appendix 2: BLASTp hits in *Ramularia collo-cygni* for every search carried out to identify putative core genes.
Protein sequence query used: A) *A. flavus* PksA, B) *D. septosporum* PksA, C) *C. nicotianae* CTB1, D) *A. terreus* LovF, E) *B. maydis* Pks1, F) *F. graminearum* Pks4, G) *A. flavus* GliP, H) *A. fumigatus* GliP, I) *A. fumigatus* SidC, J) *B. zeicola* HTS1. The name presented corresponds to the Rcc gene model. The grade is calculated by Geneious using the e-value, query cover and identity and is a representation of the longest and highest identity.

A)

E Value	Name	Query coverage	Pairwise Identity	Grade
0	augustus_masked-scaffold_m24-processed-gene-1.219-mRNA-1	73.68%	35.70%	61.80%
0	maker-scaffold_m46-fgenesh-gene-0.119-mRNA-1	86.91%	37.80%	68.50%
6.11E-106	maker-contig_118-augustus-gene-3.254-mRNA-1	41.73%	30.00%	45.90%
6.11E-101	snap_masked-contig_187-processed-gene-0.130-mRNA-1	41.20%	30.90%	45.60%
3.06E-99	augustus_masked-contig_233-processed-gene-0.136-mRNA-1	41.30%	30.20%	45.60%
4.21E-99	maker-contig_282-snap-gene-0.161-mRNA-1	43.24%	30.10%	46.60%
3.45E-95	augustus_masked-contig_14-processed-gene-0.66-mRNA-1	41.44%	30.80%	45.70%
1.45E-89	maker-contig_301-snap-gene-0.98-mRNA-1	38.55%	29.00%	44.30%
2.97E-85	augustus_masked-contig_280-processed-gene-0.23-mRNA-1	41.44%	27.10%	45.70%
8.09E-83	maker-contig_38-fgenesh-gene-0.269-mRNA-1	43.53%	29.20%	46.80%
9.85E-83	maker-contig_17-augustus-gene-1.203-mRNA-1	41.68%	27.50%	45.80%
1.05E-80	fgenesh_masked-contig_30-processed-gene-1.114-mRNA-1	41.68%	28.90%	45.80%
1.61E-61	snap_masked-contig_60-processed-gene-2.105-mRNA-1	19.77%	33.00%	34.90%
4.87E-61	snap_masked-contig_118-processed-gene-3.158-mRNA-1	29.16%	27.90%	39.60%
8.31E-59	genemark-contig_58-processed-gene-0.40-mRNA-1	24.13%	29.10%	37.10%
9.48E-39	maker-contig_1-fgenesh-gene-2.140-mRNA-1	21.86%	29.60%	35.90%
3.09E-38	maker-contig_146-augustus-gene-0.150-mRNA-1	18.87%	26.00%	34.40%
9.07E-24	augustus_masked-contig_5-processed-gene-0.137-mRNA-1	17.40%	26.20%	33.70%
2.11E-23	maker-contig_220-fgenesh-gene-0.9-mRNA-1	10.29%	30.30%	30.10%
6.63E-21	maker-contig_60-snap-gene-2.193-mRNA-1	14.04%	26.30%	15.40%
2.53E-11	genemark-contig_17-processed-gene-1.45-mRNA-1	9.96%	25.70%	5.00%
1.45E-08	augustus_masked-contig_1-processed-gene-3.280-mRNA-1	8.16%	31.10%	4.10%
6.11E-05	maker-scaffold_m40-fgenesh-gene-0.149-mRNA-1	4.88%	27.90%	2.40%

B)

E Value	Name	Query coverage	Pairwise Identity	Grade
0	augustus_masked-scaffold_m24-processed-gene-1.219-mRNA-1	66.40%	35.50%	58.20%
0	maker-scaffold_m46-fgenesh-gene-0.119-mRNA-1	81.45%	36.50%	65.70%
1.00E-110	maker-contig_118-augustus-gene-3.254-mRNA-1	36.81%	32.10%	43.40%
9.72E-99	maker-contig_301-snap-gene-0.98-mRNA-1	36.39%	30.00%	43.20%
1.45E-97	snap_masked-contig_187-processed-gene-0.130-mRNA-1	36.89%	32.10%	43.40%
2.82E-95	augustus_masked-contig_14-processed-gene-0.66-mRNA-1	36.85%	30.60%	43.40%
1.43E-94	maker-contig_282-snap-gene-0.161-mRNA-1	38.10%	30.20%	44.00%
2.35E-93	augustus_masked-contig_233-processed-gene-0.136-mRNA-1	37.35%	29.60%	43.70%
5.09E-90	maker-contig_38-fgenesh-gene-0.269-mRNA-1	36.52%	30.40%	43.30%
1.11E-84	maker-contig_17-augustus-gene-1.203-mRNA-1	36.93%	28.10%	43.50%
3.40E-84	augustus_masked-contig_280-processed-gene-0.23-mRNA-1	37.56%	27.60%	43.80%
1.16E-78	fgenesh_masked-contig_30-processed-gene-1.114-mRNA-1	36.52%	29.50%	43.30%
2.34E-66	snap_masked-contig_60-processed-gene-2.105-mRNA-1	17.22%	35.30%	33.60%
7.30E-58	snap_masked-contig_118-processed-gene-3.158-mRNA-1	25.76%	28.70%	37.90%
3.57E-56	genemark-contig_58-processed-gene-0.40-mRNA-1	20.38%	30.00%	35.20%
1.09E-45	maker-contig_146-augustus-gene-0.150-mRNA-1	15.80%	28.10%	32.90%
1.04E-37	maker-contig_1-fgenesh-gene-2.140-mRNA-1	22.72%	28.20%	36.40%
1.38E-23	maker-contig_220-fgenesh-gene-0.9-mRNA-1	8.42%	31.20%	29.20%
7.76E-23	augustus_masked-contig_5-processed-gene-0.137-mRNA-1	14.51%	26.50%	32.10%
6.57E-21	maker-contig_60-snap-gene-2.193-mRNA-1	14.67%	27.50%	15.90%
3.00E-11	augustus_masked-contig_1-processed-gene-3.280-mRNA-1	10.75%	27.20%	5.40%
6.53E-09	genemark-contig_17-processed-gene-1.45-mRNA-1	8.63%	24.80%	4.30%
7.62E-03	maker-scaffold_m40-fgenesh-gene-0.149-mRNA-1	3.83%	26.10%	1.90%

C)

E Value	Name	Query coverage	Pairwise Identity	Grade
0	augustus_masked-scaffold_m24-processed-gene-1.219-mRNA-1	72.09%	36.00%	61.00%
0	maker-scaffold_m46-fgenesh-gene-0.119-mRNA-1	99.41%	36.70%	74.70%
1.05E-100	maker-contig_118-augustus-gene-3.254-mRNA-1	40.57%	30.50%	45.30%
1.18E-90	augustus_masked-contig_233-processed-gene-0.136-mRNA-1	45.22%	27.80%	47.60%
1.54E-87	maker-contig_38-fgenesh-gene-0.269-mRNA-1	50.36%	27.70%	50.20%
2.37E-86	maker-contig_301-snap-gene-0.98-mRNA-1	41.53%	28.00%	45.80%
3.95E-85	maker-contig_17-augustus-gene-1.203-mRNA-1	40.94%	28.80%	45.50%
9.34E-85	augustus_masked-contig_14-processed-gene-0.66-mRNA-1	44.31%	28.40%	47.20%
1.16E-83	maker-contig_282-snap-gene-0.161-mRNA-1	41.07%	28.20%	45.50%
8.30E-81	snap_masked-contig_187-processed-gene-0.130-mRNA-1	39.85%	28.90%	44.90%
2.07E-74	fgenesh_masked-contig_30-processed-gene-1.114-mRNA-1	45.81%	25.80%	47.90%
2.97E-66	augustus_masked-contig_280-processed-gene-0.23-mRNA-1	40.35%	25.60%	45.20%
1.03E-60	snap_masked-contig_60-processed-gene-2.105-mRNA-1	18.31%	33.40%	34.20%
1.42E-60	genemark-contig_58-processed-gene-0.40-mRNA-1	21.13%	30.80%	35.60%
4.28E-50	snap_masked-contig_118-processed-gene-3.158-mRNA-1	19.63%	31.50%	34.80%
3.63E-34	maker-contig_146-augustus-gene-0.150-mRNA-1	18.76%	27.20%	34.40%
3.05E-31	maker-contig_1-fgenesh-gene-2.140-mRNA-1	25.14%	26.20%	37.60%
1.23E-20	maker-contig_220-fgenesh-gene-0.9-mRNA-1	9.70%	28.30%	4.80%
4.81E-18	augustus_masked-contig_5-processed-gene-0.137-mRNA-1	13.30%	24.60%	6.60%
8.60E-18	maker-contig_60-snap-gene-2.193-mRNA-1	12.07%	28.60%	6.00%
2.91E-07	maker-scaffold_m40-fgenesh-gene-0.149-mRNA-1	4.92%	32.40%	2.50%
2.64E-06	augustus_masked-contig_1-processed-gene-3.280-mRNA-1	13.30%	22.40%	6.60%
5.45E-06	genemark-contig_17-processed-gene-1.45-mRNA-1	13.39%	24.60%	6.70%
7.94E-02	maker-contig_247-fgenesh-gene-0.52-mRNA-1	3.87%	29.90%	1.90%

D)

E Value	Name	Query coverage	% Pairwise Identity	Grade
0	augustus_masked-contig_14-processed-gene-0.66-mRNA-1	68.84%	31.80%	59.40%
0	augustus_masked-contig_280-processed-gene-0.23-mRNA-1	99.33%	31.50%	74.70%
0	fgenesh_masked-contig_30-processed-gene-1.114-mRNA-1	68.60%	31.40%	59.30%
0	genemark-contig_58-processed-gene-0.40-mRNA-1	76.46%	39.30%	63.20%
0	maker-contig_17-augustus-gene-1.203-mRNA-1	46.64%	36.40%	48.30%
0	maker-contig_38-fgenesh-gene-0.269-mRNA-1	68.68%	32.40%	59.30%
0	maker-contig_60-snap-gene-2.193-mRNA-1	78.52%	29.30%	64.30%
0	maker-contig_282-snap-gene-0.161-mRNA-1	50.28%	34.80%	50.10%
0	maker-contig_301-snap-gene-0.98-mRNA-1	92.06%	31.60%	71.00%
0	snap_masked-contig_187-processed-gene-0.130-mRNA-1	38.47%	38.10%	44.20%
7.49E-169	augustus_masked-contig_233-processed-gene-0.136-mRNA-1	45.50%	34.00%	47.70%
1.68E-110	snap_masked-contig_60-processed-gene-2.105-mRNA-1	16.07%	44.70%	33.00%
1.53E-108	maker-contig_187-snap-gene-0.262-mRNA-1	43.84%	29.40%	46.90%
3.02E-100	augustus_masked-scaffold_m24-processed-gene-1.219-mRNA-1	36.10%	29.70%	43.00%
1.35E-97	maker-contig_220-fgenesh-gene-0.8-mRNA-1	23.93%	33.10%	37.00%
1.88E-95	maker-scaffold_m46-fgenesh-gene-0.119-mRNA-1	36.02%	29.70%	43.00%
1.59E-89	snap_masked-contig_118-processed-gene-3.158-mRNA-1	27.76%	30.70%	38.90%
1.94E-79	maker-contig_1-fgenesh-gene-2.140-mRNA-1	22.95%	34.60%	36.50%
9.02E-77	maker-contig_118-augustus-gene-3.254-mRNA-1	31.87%	29.30%	40.90%
4.33E-44	maker-contig_220-fgenesh-gene-0.9-mRNA-1	8.45%	40.70%	29.20%
4.97E-23	augustus_masked-contig_5-processed-gene-0.137-mRNA-1	12.48%	27.40%	31.10%
2.63E-20	maker-contig_51-augustus-gene-4.195-mRNA-1	11.69%	25.60%	5.80%
1.79E-18	fgenesh_masked-contig_112-processed-gene-1.91-mRNA-1	11.41%	26.20%	5.70%
1.74E-17	fgenesh_masked-contig_27-processed-gene-0.105-mRNA-1	10.70%	29.10%	5.40%
3.71E-13	maker-contig_61-snap-gene-2.323-mRNA-1	11.77%	25.70%	5.90%
1.13E-11	maker-contig_147-fgenesh-gene-0.136-mRNA-1	11.97%	25.10%	6.00%

D) (Continued)

8.56E-08	maker-contig_38-fgenesh-gene-0.280-mRNA-1	12.01%	26.20%	6.00%
2.28E-07	maker-contig_301-snap-gene-0.99-mRNA-1	3.16%	31.30%	1.60%
3.03E-07	maker-contig_137-fgenesh-gene-2.388-mRNA-1	9.44%	23.90%	4.70%
4.92E-07	maker-contig_169-fgenesh-gene-0.301-mRNA-1	8.85%	24.40%	4.40%
1.93E-06	maker-contig_330-augustus-gene-0.55-mRNA-1	4.58%	26.70%	2.30%
4.12E-06	augustus_masked-contig_1-processed-gene-3.280-mRNA-1	9.83%	25.20%	4.90%
8.59E-06	maker-contig_238-fgenesh-gene-0.34-mRNA-1	4.62%	30.40%	2.30%
1.54E-05	maker-contig_37-fgenesh-gene-5.166-mRNA-1	3.28%	36.20%	1.60%
2.20E-05	fgenesh_masked-contig_37-processed-gene-1.97-mRNA-1	4.90%	31.00%	2.40%
4.20E-05	fgenesh_masked-contig_37-processed-gene-6.81-mRNA-1	5.96%	30.50%	3.00%
5.79E-05	maker-contig_192-fgenesh-gene-0.151-mRNA-1	12.56%	20.90%	6.30%
7.70E-05	maker-scaffold_m24-fgenesh-gene-0.152-mRNA-1	11.18%	24.50%	5.60%
3.28E-04	snap_masked-contig_134-processed-gene-0.169-mRNA-1	9.40%	24.00%	4.70%
6.47E-04	augustus_masked-scaffold_m46-processed-gene-1.151-mRNA-1	7.54%	22.40%	3.80%
8.05E-04	fgenesh_masked-contig_29-processed-gene-0.97-mRNA-1	11.77%	24.60%	5.90%
1.59E-03	augustus_masked-contig_5-processed-gene-2.153-mRNA-1	2.84%	32.00%	1.40%
1.85E-03	genemark-scaffold_m42-processed-gene-2.33-mRNA-1	6.28%	25.40%	3.10%
1.85E-03	maker-scaffold_m29-augustus-gene-0.308-mRNA-1	5.77%	27.20%	2.90%
5.01E-03	maker-contig_118-fgenesh-gene-2.177-mRNA-1	4.54%	25.80%	2.30%
5.58E-03	augustus_masked-scaffold_m42-processed-gene-3.173-mRNA-1	6.56%	28.80%	3.30%
1.02E-02	maker-contig_247-fgenesh-gene-0.52-mRNA-1	4.34%	31.70%	2.20%
1.91E-02	maker-contig_152-fgenesh-gene-1.285-mRNA-1	3.55%	29.30%	1.80%
2.77E-02	augustus_masked-contig_193-processed-gene-0.126-mRNA-1	3.63%	27.40%	1.80%
2.77E-02	maker-contig_58-augustus-gene-0.193-mRNA-1	1.50%	31.60%	0.80%
3.08E-02	maker-contig_123-fgenesh-gene-1.175-mRNA-1	2.57%	34.80%	1.30%
6.18E-02	maker-scaffold_m42-augustus-gene-2.162-mRNA-1	5.09%	29.20%	2.50%
6.56E-02	fgenesh_masked-contig_3-processed-gene-0.66-mRNA-1	3.20%	29.80%	1.60%
7.89E-02	maker-contig_127-augustus-gene-0.442-mRNA-1	5.69%	25.70%	2.80%
8.29E-02	maker-contig_14-fgenesh-gene-0.72-mRNA-1	3.52%	25.50%	1.80%

E)

E Value	Name	Query coverage	Pairwise Identity	Grade
0	augustus_masked-contig_14-processed-gene-0.66-mRNA-1	61.12%	32.40%	55.60%
0	augustus_masked-contig_280-processed-gene-0.23-mRNA-1	99.09%	29.70%	74.50%
0	fgenesh_masked-contig_30-processed-gene-1.114-mRNA-1	41.85%	37.30%	45.90%
0	genemark-contig_58-processed-gene-0.40-mRNA-1	75.24%	31.10%	62.60%
0	maker-contig_17-augustus-gene-1.203-mRNA-1	51.11%	38.20%	50.60%
0	maker-contig_38-fgenesh-gene-0.269-mRNA-1	70.85%	29.80%	60.40%
0	maker-contig_60-snap-gene-2.193-mRNA-1	77.10%	27.90%	63.50%
0	maker-contig_282-snap-gene-0.161-mRNA-1	52.18%	35.80%	51.10%
0	maker-contig_301-snap-gene-0.98-mRNA-1	92.01%	30.50%	71.00%
0	snap_masked-contig_187-processed-gene-0.130-mRNA-1	39.12%	38.30%	44.60%
5.04E-180	augustus_masked-contig_233-processed-gene-0.136-mRNA-1	47.67%	35.40%	48.80%
2.37E-115	snap_masked-contig_60-processed-gene-2.105-mRNA-1	15.63%	45.30%	32.80%
1.67E-103	maker-contig_220-fgenesh-gene-0.8-mRNA-1	24.41%	35.40%	37.20%
9.58E-92	maker-scaffold_m46-fgenesh-gene-0.119-mRNA-1	36.51%	28.50%	43.30%
5.32E-91	augustus_masked-scaffold_m24-processed-gene-1.219-mRNA-1	36.51%	28.60%	43.30%
2.37E-85	maker-contig_187-snap-gene-0.262-mRNA-1	43.43%	27.80%	46.70%
9.06E-82	snap_masked-contig_118-processed-gene-3.158-mRNA-1	25.44%	30.70%	37.70%
1.87E-80	maker-contig_1-fgenesh-gene-2.140-mRNA-1	22.82%	37.10%	36.40%
1.90E-77	maker-contig_118-augustus-gene-3.254-mRNA-1	36.71%	27.40%	43.40%
9.88E-35	maker-contig_220-fgenesh-gene-0.9-mRNA-1	7.99%	35.60%	29.00%
2.11E-22	augustus_masked-contig_5-processed-gene-0.137-mRNA-1	10.44%	29.70%	29.70%
1.31E-18	maker-contig_51-augustus-gene-4.195-mRNA-1	12.34%	25.50%	6.20%
3.18E-17	fgenesh_masked-contig_112-processed-gene-1.91-mRNA-1	10.44%	26.30%	5.20%
4.22E-13	maker-contig_137-fgenesh-gene-2.388-mRNA-1	9.06%	25.90%	4.50%
2.20E-12	fgenesh_masked-contig_27-processed-gene-0.105-mRNA-1	10.32%	26.00%	5.20%
1.09E-11	augustus_masked-contig_1-processed-gene-3.280-mRNA-1	9.69%	24.90%	4.80%
5.99E-10	maker-contig_61-snap-gene-2.323-mRNA-1	8.62%	26.00%	4.30%
8.57E-09	maker-scaffold_m17-fgenesh-gene-0.247-mRNA-1	10.25%	22.60%	5.10%
2.33E-08	fgenesh_masked-contig_29-processed-gene-0.97-mRNA-1	11.31%	23.00%	5.70%
6.01E-08	maker-contig_330-augustus-gene-0.55-mRNA-1	4.91%	27.40%	2.50%

E) (Continued)

9.05E-08	maker-contig_37-fgenesh-gene-5.166-mRNA-1	5.50%	28.10%	2.70%
1.49E-07	maker-contig_301-snap-gene-0.99-mRNA-1	2.06%	34.60%	1.00%
2.76E-07	snap_masked-contig_240-processed-gene-0.40-mRNA-1	6.69%	26.40%	3.30%
2.81E-07	maker-contig_147-fgenesh-gene-0.136-mRNA-1	7.83%	23.10%	3.90%
4.10E-07	genemark-contig_17-processed-gene-1.45-mRNA-1	8.98%	25.50%	4.50%
3.37E-06	maker-contig_227-fgenesh-gene-0.178-mRNA-1	8.23%	26.10%	4.10%
5.95E-06	maker-contig_238-fgenesh-gene-0.34-mRNA-1	7.75%	24.00%	3.90%
2.56E-05	genemark-scaffold_m42-processed-gene-2.33-mRNA-1	6.76%	27.80%	3.40%
4.61E-05	maker-scaffold_m24-fgenesh-gene-0.152-mRNA-1	7.95%	25.20%	4.00%
6.08E-05	snap_masked-contig_134-processed-gene-0.169-mRNA-1	9.22%	22.90%	4.60%
1.45E-04	augustus_masked-contig_37-processed-gene-0.142-mRNA-1	8.62%	23.60%	4.30%
4.89E-04	maker-contig_1-augustus-gene-2.157-mRNA-1	10.21%	22.90%	5.10%
5.92E-04	augustus_masked-scaffold_m24-processed-gene-1.213-mRNA-1	6.45%	22.60%	3.20%
9.67E-04	maker-contig_10-augustus-gene-1.205-mRNA-1	8.23%	20.70%	4.10%
1.97E-03	maker-contig_127-augustus-gene-0.442-mRNA-1	5.42%	26.20%	2.70%
1.97E-03	maker-contig_169-fgenesh-gene-0.301-mRNA-1	6.84%	26.10%	3.40%
2.34E-03	maker-scaffold_m29-augustus-gene-0.308-mRNA-1	4.31%	27.20%	2.20%
3.05E-03	maker-contig_112-snap-gene-1.295-mRNA-1	6.05%	23.30%	3.00%
5.03E-03	maker-contig_38-fgenesh-gene-0.280-mRNA-1	6.25%	28.30%	3.10%
5.38E-03	fgenesh_masked-contig_37-processed-gene-1.97-mRNA-1	5.93%	24.30%	3.00%
9.33E-03	maker-contig_71-fgenesh-gene-1.178-mRNA-1	4.55%	26.10%	2.30%
9.73E-03	augustus_masked-contig_5-processed-gene-2.153-mRNA-1	3.01%	27.30%	1.50%
2.36E-02	fgenesh_masked-contig_84-processed-gene-2.87-mRNA-1	6.84%	24.30%	3.40%
3.49E-02	augustus_masked-scaffold_m46-processed-gene-1.151-mRNA-1	4.43%	26.20%	2.20%
3.81E-02	augustus_masked-scaffold_m42-processed-gene-3.173-mRNA-1	6.37%	24.30%	3.20%
7.82E-02	maker-contig_112-fgenesh-gene-1.236-mRNA-1	2.73%	35.00%	1.40%
9.14E-02	genemark-contig_10-processed-gene-1.36-mRNA-1	7.24%	22.60%	3.60%

F)

E Value	Name	Query coverage	Pairwise Identity	Grade
0	augustus_masked-contig_280-processed-gene-0.23-mRNA-1	47.72%	34.90%	48.90%
0	maker-contig_17-augustus-gene-1.203-mRNA-1	97.44%	30.50%	73.70%
0	maker-contig_38-fgenesh-gene-0.269-mRNA-1	52.96%	34.40%	51.50%
0	maker-contig_282-snap-gene-0.161-mRNA-1	55.74%	34.00%	52.90%
0	maker-contig_301-snap-gene-0.98-mRNA-1	48.57%	34.30%	49.30%
0	snap_masked-contig_187-processed-gene-0.130-mRNA-1	40.51%	37.10%	45.30%
2.54E-177	fgenesh_masked-contig_30-processed-gene-1.114-mRNA-1	42.52%	36.50%	46.30%
5.42E-175	augustus_masked-contig_14-processed-gene-0.66-mRNA-1	49.81%	35.70%	49.90%
1.22E-165	augustus_masked-contig_233-processed-gene-0.136-mRNA-1	44.43%	35.20%	47.20%
8.32E-123	genemark-contig_58-processed-gene-0.40-mRNA-1	36.33%	33.10%	43.20%
1.51E-104	maker-contig_60-snap-gene-2.193-mRNA-1	45.46%	28.00%	47.70%
1.08E-99	snap_masked-contig_60-processed-gene-2.105-mRNA-1	16.59%	40.80%	33.30%
8.90E-94	augustus_masked-scaffold_m24-processed-gene-1.219-mRNA-1	38.04%	29.50%	44.00%
1.00E-90	maker-contig_220-fgenesh-gene-0.8-mRNA-1	26.40%	31.40%	38.20%
1.42E-83	maker-scaffold_m46-fgenesh-gene-0.119-mRNA-1	40.81%	27.60%	45.40%
1.54E-81	maker-contig_1-fgenesh-gene-2.140-mRNA-1	24.09%	36.20%	37.00%
5.15E-77	snap_masked-contig_118-processed-gene-3.158-mRNA-1	26.01%	29.70%	38.00%
4.35E-74	maker-contig_187-snap-gene-0.262-mRNA-1	52.58%	23.10%	51.30%
2.95E-73	maker-contig_118-augustus-gene-3.254-mRNA-1	30.87%	31.80%	40.40%
7.97E-39	maker-contig_220-fgenesh-gene-0.9-mRNA-1	8.49%	39.50%	29.20%
1.28E-24	augustus_masked-contig_5-processed-gene-0.137-mRNA-1	14.58%	27.00%	32.30%
2.39E-18	maker-contig_51-augustus-gene-4.195-mRNA-1	13.43%	25.10%	6.70%
3.86E-16	maker-contig_137-fgenesh-gene-2.388-mRNA-1	13.60%	28.30%	6.80%
2.87E-13	fgenesh_masked-contig_27-processed-gene-0.105-mRNA-1	9.38%	32.50%	4.70%
3.46E-13	maker-contig_147-fgenesh-gene-0.136-mRNA-1	8.78%	29.10%	4.40%
6.28E-11	fgenesh_masked-contig_112-processed-gene-1.91-mRNA-1	11.77%	25.20%	5.90%
1.56E-10	maker-scaffold_m17-fgenesh-gene-0.247-mRNA-1	12.11%	23.20%	6.10%
6.61E-10	maker-contig_330-augustus-gene-0.55-mRNA-1	5.63%	28.80%	2.80%
1.71E-09	maker-contig_301-snap-gene-0.99-mRNA-1	3.33%	30.80%	1.70%
6.47E-09	maker-contig_61-snap-gene-2.323-mRNA-1	5.71%	30.40%	2.90%
2.72E-08	maker-scaffold_m24-fgenesh-gene-0.152-mRNA-1	9.34%	26.60%	4.70%
2.78E-08	fgenesh_masked-contig_29-processed-gene-0.97-mRNA-1	12.62%	24.90%	6.30%
1.02E-07	augustus_masked-scaffold_m46-processed-gene-1.151-mRNA-1	4.35%	32.50%	2.20%

F) (Continued)

1.63E-07	maker-contig_38-fgenesh-gene-0.280-mRNA-1	11.26%	25.10%	5.60%
1.80E-07	maker-contig_169-fgenesh-gene-0.301-mRNA-1	6.95%	26.20%	3.50%
2.76E-07	maker-contig_37-fgenesh-gene-5.166-mRNA-1	4.73%	31.30%	2.40%
5.01E-07	maker-contig_37-fgenesh-gene-1.202-mRNA-1	6.57%	27.30%	3.30%
5.10E-07	maker-contig_238-fgenesh-gene-0.34-mRNA-1	10.83%	25.00%	5.40%
5.73E-07	fgenesh_masked-contig_37-processed-gene-6.81-mRNA-1	6.14%	28.10%	3.10%
6.80E-07	augustus_masked-contig_1-processed-gene-3.280-mRNA-1	9.17%	25.80%	4.60%
1.06E-06	augustus_masked-contig_5-processed-gene-2.153-mRNA-1	3.84%	31.90%	1.90%
1.20E-06	genemark-scaffold_m42-processed-gene-2.33-mRNA-1	6.35%	30.50%	3.20%
1.39E-06	snap_masked-contig_134-processed-gene-0.169-mRNA-1	11.43%	24.40%	5.70%
2.60E-06	maker-contig_17-fgenesh-gene-4.199-mRNA-1	6.27%	26.10%	3.10%
3.04E-06	maker-contig_158-fgenesh-gene-0.94-mRNA-1	7.97%	24.40%	4.00%
5.07E-06	augustus_masked-contig_212-processed-gene-0.82-mRNA-1	8.10%	30.70%	4.10%
1.46E-05	augustus_masked-scaffold_m42-processed-gene-3.173-mRNA-1	6.40%	26.40%	3.20%
1.87E-05	maker-contig_192-fgenesh-gene-0.151-mRNA-1	13.48%	22.60%	6.70%
2.84E-05	genemark-contig_17-processed-gene-1.45-mRNA-1	12.62%	24.00%	6.30%
3.06E-05	augustus_masked-contig_37-processed-gene-0.142-mRNA-1	12.88%	23.00%	6.40%
2.58E-04	fgenesh_masked-contig_113-processed-gene-0.81-mRNA-1	6.40%	24.30%	3.20%
3.89E-04	genemark-contig_72-processed-gene-0.13-mRNA-1	9.68%	25.60%	4.80%
5.50E-04	augustus_masked-contig_193-processed-gene-0.126-mRNA-1	7.68%	26.40%	3.80%
8.56E-04	fgenesh_masked-contig_37-processed-gene-1.97-mRNA-1	5.07%	27.10%	2.50%
3.14E-03	maker-contig_141-fgenesh-gene-0.328-mRNA-1	6.23%	21.10%	3.10%
4.12E-03	maker-contig_17-snap-gene-0.195-mRNA-1	6.70%	24.30%	3.30%
4.23E-03	maker-contig_112-snap-gene-1.295-mRNA-1	5.16%	25.20%	2.60%
4.72E-03	maker-contig_10-augustus-gene-1.205-mRNA-1	4.95%	25.80%	2.50%
7.40E-03	maker-contig_183-fgenesh-gene-0.174-mRNA-1	5.03%	25.80%	2.50%
9.77E-03	maker-contig_152-fgenesh-gene-1.285-mRNA-1	5.42%	26.80%	2.70%
1.19E-02	fgenesh_masked-contig_5-processed-gene-2.71-mRNA-1	4.35%	26.50%	2.20%
1.57E-02	augustus_masked-scaffold_m42-processed-gene-1.140-mRNA-1	7.38%	24.70%	3.70%
5.05E-02	maker-scaffold_m29-augustus-gene-0.308-mRNA-1	5.97%	29.30%	3.00%
5.71E-02	maker-contig_55-augustus-gene-3.280-mRNA-1	4.95%	28.00%	2.50%
5.87E-02	maker-contig_1-augustus-gene-2.157-mRNA-1	9.98%	23.70%	5.00%
8.43E-02	fgenesh_masked-contig_264-processed-gene-0.64-mRNA-1	10.53%	22.50%	5.30%

G)

E Value	Name	Query coverage	Pairwise Identity	Grade
0	fgenesh_masked-contig_301-processed-gene-0.34-mRNA-1	94.63%	33.70%	72.30%
0	maker-contig_58-snap-gene-0.220-mRNA-1	86.00%	41.90%	68.00%
0	maker-contig_246-snap-gene-0.414-mRNA-1	95.99%	37.90%	73.00%
2.42E-140	augustus_masked-contig_113-processed-gene-0.134-mRNA-1	63.11%	30.70%	56.60%
1.49E-73	maker-contig_301-fgenesh-gene-0.83-mRNA-1	14.74%	51.90%	33.30%
2.91E-69	fgenesh_masked-contig_246-processed-gene-0.103-mRNA-1	82.11%	24.10%	66.10%
3.19E-61	augustus_masked-contig_51-processed-gene-1.140-mRNA-1	79.21%	23.80%	64.60%
6.91E-61	augustus_masked-contig_166-processed-gene-1.135-mRNA-1	62.37%	25.40%	56.20%
1.46E-57	fgenesh_masked-contig_175-processed-gene-0.41-mRNA-1	59.41%	25.70%	54.70%
1.60E-55	augustus_masked-scaffold_m42-processed-gene-0.88-mRNA-1	78.78%	23.20%	64.40%
4.57E-55	genemark-contig_55-processed-gene-3.77-mRNA-1	48.92%	25.90%	49.50%
1.30E-54	snap_masked-contig_100-processed-gene-0.55-mRNA-1	68.72%	23.30%	59.40%
4.35E-54	maker-contig_134-snap-gene-0.394-mRNA-1	46.21%	27.10%	48.10%
2.62E-50	augustus_masked-contig_163-processed-gene-0.152-mRNA-1	57.00%	24.20%	53.50%
4.37E-45	fgenesh_masked-contig_280-processed-gene-0.11-mRNA-1	32.51%	28.90%	41.30%
2.93E-41	genemark-contig_207-processed-gene-0.9-mRNA-1	29.36%	28.80%	39.70%
1.18E-40	maker-scaffold_m42-snap-gene-0.127-mRNA-1	70.08%	22.90%	60.00%
5.86E-39	augustus_masked-contig_14-processed-gene-0.66-mRNA-1	54.10%	24.30%	52.10%
6.68E-38	snap_masked-contig_100-processed-gene-0.53-mRNA-1	33.07%	27.30%	41.50%
1.01E-37	augustus_masked-contig_20-processed-gene-0.252-mRNA-1	32.14%	28.00%	41.10%
7.67E-37	snap_masked-contig_245-processed-gene-0.164-mRNA-1	28.62%	25.50%	39.30%
1.76E-35	augustus_masked-scaffold_m29-processed-gene-0.249-mRNA-1	31.96%	27.60%	41.00%
6.40E-35	augustus_masked-contig_207-processed-gene-0.46-mRNA-1	38.68%	24.90%	44.30%
3.16E-33	maker-contig_38-fgenesh-gene-0.269-mRNA-1	33.62%	25.30%	41.80%
1.02E-31	fgenesh_masked-contig_84-processed-gene-2.87-mRNA-1	33.25%	27.00%	41.60%
3.52E-31	fgenesh_masked-contig_113-processed-gene-2.65-mRNA-1	24.37%	26.90%	37.20%
1.90E-29	snap_masked-contig_100-processed-gene-0.54-mRNA-1	24.74%	27.90%	37.40%
2.20E-28	fgenesh_masked-contig_37-processed-gene-10.84-mRNA-1	23.07%	24.20%	36.50%
4.02E-26	augustus_masked-contig_245-processed-gene-0.245-mRNA-1	39.73%	22.80%	44.90%
2.06E-16	maker-contig_30-snap-gene-0.203-mRNA-1	20.30%	25.60%	10.10%
9.58E-16	maker-contig_187-fgenesh-gene-0.193-mRNA-1	23.63%	24.40%	11.80%
6.57E-13	maker-scaffold_m42-fgenesh-gene-0.99-mRNA-1	16.41%	27.40%	8.20%
1.77E-11	genemark-contig_117-processed-gene-0.13-mRNA-1	27.39%	22.80%	13.70%

H)

E Value	Name	Query coverage	Pairwise Identity	Grade
0	fgenesh_masked-contig_301-processed-gene-0.34-mRNA-1	87.31%	31.20%	68.70%
0	maker-contig_58-snap-gene-0.220-mRNA-1	61.03%	31.00%	55.50%
1.80E-159	maker-contig_246-snap-gene-0.414-mRNA-1	65.71%	28.40%	57.90%
2.25E-118	fgenesh_masked-contig_246-processed-gene-0.103-mRNA-1	90.44%	26.20%	70.20%
2.01E-108	genemark-contig_55-processed-gene-3.77-mRNA-1	80.52%	25.50%	65.30%
2.97E-98	snap_masked-contig_100-processed-gene-0.55-mRNA-1	89.98%	24.10%	70.00%
2.31E-86	augustus_masked-contig_51-processed-gene-1.140-mRNA-1	82.86%	24.80%	66.40%
9.60E-86	augustus_masked-contig_113-processed-gene-0.134-mRNA-1	36.02%	29.40%	43.00%
5.82E-82	maker-contig_134-snap-gene-0.394-mRNA-1	83.61%	24.40%	66.80%
1.76E-72	fgenesh_masked-contig_175-processed-gene-0.41-mRNA-1	79.25%	23.90%	64.60%
3.50E-62	augustus_masked-contig_166-processed-gene-1.135-mRNA-1	46.18%	26.20%	48.10%
6.56E-52	augustus_masked-contig_163-processed-gene-0.152-mRNA-1	39.25%	25.20%	44.60%
4.17E-51	fgenesh_masked-contig_280-processed-gene-0.11-mRNA-1	46.32%	25.00%	48.20%
1.78E-48	augustus_masked-contig_14-processed-gene-0.66-mRNA-1	40.94%	23.90%	45.50%
2.20E-41	genemark-contig_207-processed-gene-0.9-mRNA-1	18.64%	32.50%	34.30%
4.46E-41	maker-contig_301-fgenesh-gene-0.83-mRNA-1	11.43%	37.30%	30.70%
5.70E-41	maker-contig_38-fgenesh-gene-0.269-mRNA-1	26.18%	25.70%	38.10%
1.81E-40	maker-scaffold_m42-snap-gene-0.127-mRNA-1	38.31%	25.40%	44.20%
7.33E-40	snap_masked-contig_100-processed-gene-0.53-mRNA-1	27.31%	29.00%	38.70%

H) (Continued)

4.02E-39	snap_masked-contig_100-processed-gene-0.54-mRNA-1	22.62%	30.70%	36.30%
8.28E-39	augustus_masked-scaffold_m42-processed-gene-0.88-mRNA-1	42.90%	23.80%	46.50%
1.38E-37	augustus_masked-scaffold_m29-processed-gene-0.249-mRNA-1	29.84%	26.60%	39.90%
1.45E-37	augustus_masked-contig_20-processed-gene-0.252-mRNA-1	24.26%	26.90%	37.10%
2.09E-36	augustus_masked-contig_207-processed-gene-0.46-mRNA-1	30.68%	24.70%	40.30%
1.90E-33	snap_masked-contig_245-processed-gene-0.164-mRNA-1	18.17%	26.80%	34.10%
1.38E-31	fgenesh_masked-contig_113-processed-gene-2.65-mRNA-1	21.64%	26.00%	35.80%
1.45E-31	augustus_masked-contig_245-processed-gene-0.245-mRNA-1	42.76%	24.30%	46.40%
8.00E-31	fgenesh_masked-contig_84-processed-gene-2.87-mRNA-1	27.03%	25.90%	38.50%
6.69E-30	fgenesh_masked-contig_37-processed-gene-10.84-mRNA-1	24.59%	23.10%	37.30%
2.58E-20	maker-contig_30-snap-gene-0.203-mRNA-1	15.32%	27.60%	7.70%
4.72E-20	maker-contig_151-fgenesh-gene-1.190-mRNA-1	20.00%	23.60%	10.00%
1.18E-15	maker-scaffold_m42-fgenesh-gene-5.203-mRNA-1	18.41%	22.40%	9.20%
6.45E-15	maker-scaffold_m42-fgenesh-gene-0.99-mRNA-1	19.86%	25.50%	9.90%
7.50E-14	maker-contig_187-fgenesh-gene-0.193-mRNA-1	16.25%	23.10%	8.10%
8.44E-14	genemark-contig_117-processed-gene-0.13-mRNA-1	17.28%	24.60%	8.60%
1.23E-13	maker-contig_150-fgenesh-gene-0.150-mRNA-1	16.39%	26.40%	8.20%
1.77E-13	maker-contig_13-fgenesh-gene-0.366-mRNA-1	20.84%	22.10%	10.40%
9.49E-13	fgenesh_masked-contig_246-processed-gene-0.159-mRNA-1	18.17%	23.70%	9.10%
2.73E-11	maker-scaffold_m17-fgenesh-gene-0.238-mRNA-1	17.38%	21.60%	8.70%

I)

E Value	Name	Query coverage	Pairwise Identity	Grade
0	maker-contig_134-snap-gene-0.394-mRNA-1	55.99%	27.10%	53.00%
0	maker-scaffold_m42-snap-gene-0.127-mRNA-1	51.56%	40.20%	50.80%
3.79E-176	snap_masked-contig_100-processed-gene-0.55-mRNA-1	68.61%	23.80%	59.30%
9.30E-176	genemark-contig_55-processed-gene-3.77-mRNA-1	67.73%	24.20%	58.90%
7.86E-175	fgenesh_masked-contig_246-processed-gene-0.103-mRNA-1	69.41%	24.10%	59.70%
1.30E-155	augustus_masked-contig_51-processed-gene-1.140-mRNA-1	68.34%	24.00%	59.20%
2.23E-98	fgenesh_masked-contig_175-processed-gene-0.41-mRNA-1	36.68%	25.90%	43.30%
3.72E-98	augustus_masked-scaffold_m42-processed-gene-0.88-mRNA-1	38.19%	26.10%	44.10%
1.28E-74	augustus_masked-contig_166-processed-gene-1.135-mRNA-1	32.69%	24.10%	41.30%
6.01E-64	genemark-contig_207-processed-gene-0.9-mRNA-1	24.61%	24.00%	37.30%
4.81E-63	fgenesh_masked-contig_280-processed-gene-0.11-mRNA-1	27.46%	24.40%	38.70%
1.52E-58	snap_masked-contig_100-processed-gene-0.53-mRNA-1	20.85%	26.60%	35.40%
6.82E-52	fgenesh_masked-contig_301-processed-gene-0.34-mRNA-1	28.66%	24.50%	39.30%
2.43E-51	augustus_masked-contig_163-processed-gene-0.152-mRNA-1	19.95%	25.60%	35.00%
5.82E-48	snap_masked-contig_100-processed-gene-0.54-mRNA-1	10.27%	30.90%	30.10%
4.06E-45	maker-contig_246-snap-gene-0.414-mRNA-1	18.33%	25.50%	34.20%
4.31E-45	augustus_masked-contig_245-processed-gene-0.245-mRNA-1	19.86%	24.50%	34.90%
2.66E-43	augustus_masked-scaffold_m29-processed-gene-0.249-mRNA-1	20.91%	24.00%	35.50%
1.20E-41	maker-contig_58-snap-gene-0.220-mRNA-1	22.25%	22.70%	36.10%
4.76E-41	augustus_masked-contig_20-processed-gene-0.252-mRNA-1	11.48%	29.00%	30.70%
1.95E-40	snap_masked-contig_245-processed-gene-0.164-mRNA-1	10.48%	27.20%	30.20%
7.99E-40	augustus_masked-contig_14-processed-gene-0.66-mRNA-1	20.16%	24.20%	35.10%
2.37E-38	fgenesh_masked-contig_113-processed-gene-2.65-mRNA-1	13.04%	26.80%	31.50%
1.27E-35	augustus_masked-contig_207-processed-gene-0.46-mRNA-1	11.65%	28.70%	30.80%
3.46E-35	maker-contig_38-fgenesh-gene-0.269-mRNA-1	12.51%	27.50%	31.30%
8.85E-26	fgenesh_masked-contig_84-processed-gene-2.87-mRNA-1	12.22%	25.60%	31.10%
6.49E-24	augustus_masked-contig_113-processed-gene-0.134-mRNA-1	7.83%	29.10%	28.90%

J)

E Value	Name	Query coverage	Pairwise Identity	Grade
0	augustus_masked-contig_51-processed-gene-1.140-mRNA-1	63.03%	29.10%	56.50%
0	augustus_masked-scaffold_m42-processed-gene-0.88-mRNA-1	35.03%	29.60%	42.50%
0	fgenesh_masked-contig_175-processed-gene-0.41-mRNA-1	42.68%	27.00%	46.30%
0	fgenesh_masked-contig_246-processed-gene-0.103-mRNA-1	67.59%	29.30%	58.80%
0	genemark-contig_55-processed-gene-3.77-mRNA-1	68.65%	28.70%	59.30%
0	snap_masked-contig_100-processed-gene-0.55-mRNA-1	62.86%	28.90%	56.40%
5.68E-179	augustus_masked-contig_163-processed-gene-0.152-mRNA-1	31.01%	29.30%	40.50%
9.14E-152	augustus_masked-contig_166-processed-gene-1.135-mRNA-1	28.67%	28.20%	39.30%
3.81E-140	genemark-contig_207-processed-gene-0.9-mRNA-1	22.42%	31.40%	36.20%
3.54E-129	fgenesh_masked-contig_280-processed-gene-0.11-mRNA-1	28.27%	26.10%	39.10%
1.02E-115	maker-contig_134-snap-gene-0.394-mRNA-1	42.83%	24.10%	46.40%
1.85E-104	snap_masked-contig_100-processed-gene-0.53-mRNA-1	20.08%	29.00%	35.00%
2.28E-99	snap_masked-contig_100-processed-gene-0.54-mRNA-1	17.57%	29.30%	33.80%
3.70E-94	augustus_masked-contig_207-processed-gene-0.46-mRNA-1	12.38%	32.90%	31.20%
7.91E-90	augustus_masked-contig_245-processed-gene-0.245-mRNA-1	20.53%	27.80%	35.30%
2.80E-80	fgenesh_masked-contig_301-processed-gene-0.34-mRNA-1	32.96%	24.30%	41.50%
5.29E-79	augustus_masked-scaffold_m29-processed-gene-0.249-mRNA-1	20.08%	25.40%	35.00%
1.93E-66	fgenesh_masked-contig_113-processed-gene-2.65-mRNA-1	10.33%	31.90%	30.20%
1.08E-65	maker-scaffold_m42-snap-gene-0.127-mRNA-1	19.07%	26.80%	34.50%
7.17E-61	maker-contig_58-snap-gene-0.220-mRNA-1	21.79%	24.50%	35.90%
1.62E-60	snap_masked-contig_245-processed-gene-0.164-mRNA-1	10.29%	29.30%	30.10%
6.13E-58	maker-contig_246-snap-gene-0.414-mRNA-1	19.22%	23.10%	34.60%
4.52E-48	maker-contig_38-fgenesh-gene-0.269-mRNA-1	21.33%	23.40%	35.70%
9.65E-45	augustus_masked-contig_14-processed-gene-0.66-mRNA-1	19.03%	25.20%	34.50%

Appendix 3: AntiSMASH-based predicted amino acids (AA) selected by adenylation domains of the core genes identified in *R. collo-cygni*.

Rcc core gene	A domain	Predicted AA		
		NRPSPredictor2	Stachelhaus	Minowa
Hps1-2.140	N/A	Hydrophobic-aliphatic	Bht	Ala
Hps14-0.66	N/A	Leu	Trp	Ala
Hps38-0.269	N/A	Asp/Asn/Glu/Gln/Aad	-	Pip / Glu
Nps100	A1	Ala	Hpg	Ala
	A2	Gly/Ala/Val/Leu/Ile/Abu/Iva	-	Leu
	A3	Val/Leu/Ile/Abu/Iva	Bht	Ala
	A4	Ala	Pro	Leu
	A5	Hydrophobic-aliphatic	Pro	Ala
Nps51-1.140	A1	-	-	Ala
	A2	Hydrophobic-aliphatic	Cys	Lys
	A3	Hydrophobic-aliphatic	Pro	Ala
	A4	Leu	Ile	Leu
Nps134-0.394	A1	-	Ala	Ala
	A2	Gly/Ala/Val/Leu/Ile/Abu/Iva	Pro	Ala
	A3	Glu	Gly	Ala
Nps175-0.41	A1	Ala	Gly	Ala
	A2	Hydrophobic-aliphatic	Gly	Ala
	A3	Ala	-	Ala
Npsm42-0.127	A1	Pro	Pro	Ala
	A2	-	Orn	Ala
Nps301-0.34	A1	Hydrophobic-aliphatic	-	Trp
	A2	-	-	Ala
Npsm40-0.149	N/A	*	*	*

Rcc core gene	A domain	Predicted AA		
		NRPSPredictor2	Stachelhaus	Minowa
Nps55-3.77	A1	Gly/Ala/Val/Leu/Ile/Abu/Iva	Lys	Ala
	A2	Gly/Ala	Ser	Ala
	A3	Leu	Ile	Ala
	A4	Hydrophilic	Gly	Ala
Nps280-0.11	A1	Phe/Trp	Met	Ala
	A2	Gly/Ala	Ala	Ala
Nps246-0.103	A1	Val/Leu/Ile/Abu/Iva	Gly	Ala
	A2	Hydrophobic-aliphatic	Pro	Ala
	A3	-	Orn	Ala
	A4	-	Apa	Ala
Npsm42-0.88	A1	Ala	Phe	Ala
	A2	Leu	Arg	Ala
Nps163-0.152	A1	*	*	*
	A2	-	Glu	Ala
Npsm46-0.414	N/A	Hydrophobic-aliphatic	-	Tyr
Nps207-0.9	N/A	Hydrophobic-aliphatic	Glu	Ala
Nps207-0.46	N/A	Hydrophobic-aliphatic	Arg	Ala
Nps58-0.220	N/A	-	-	Phe
Npsm29-0.249	N/A	Hydrophobic-aliphatic	-	Ala
Nps166-1.135	N/A	Val/Leu/Ile/Abu/Iva	Val	Ala
Nps301-0.83	N/A	-	-	Ala
Nps113-0.134	N/A	Gly/Ala/Val/Leu/Ile/Abu/Iva	Ile	Leu
Nps245-0.245	N/A	-	Tyr	Ala
Nps245-0.164	N/A	Pro	Ser	Ala

N/A: non-applicable, *: domain not recognised by AntiSMASH, -: no prediction

Aad: 2-aminoadipic acid, Abu: 2-aminobutyric acid, Bht: beta-hydroxy-tyrosine, Dhpg: 3,5-dihydroxy-phenylglycine, Hpg: 4-hydroxy-phenylglycine, Iva: Isovaline, Orn: ornithine Pip: pipecolic acid, Hydrophobic-aliphatic: Ala, Gly, Val, Leu, Ile, Abu, Iva, Ser, Thr, Hpg, Dhpg, Cys, Pro, Pip, Hydrophilic: Arg, Asp, Glu, His, Asn, Lys, Gln, Orn, Aad

Appendix 4: Unresolved phylogenetic tree of non-ribosomal peptide synthetases of *R. collo-cygni*.

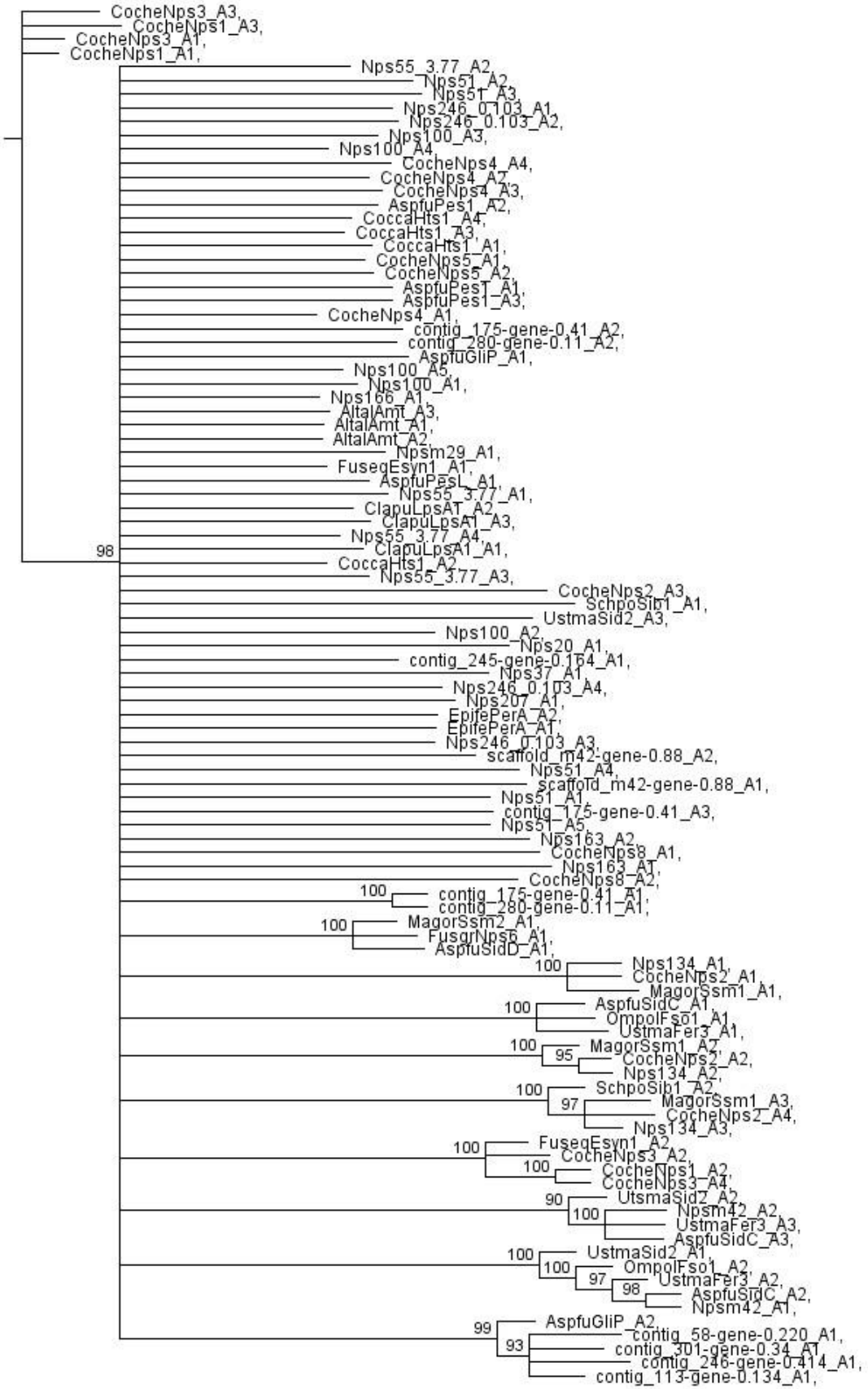

Appendix 5: List of primers used in the expression study of *R. collo-cygni* secondary metabolism-related genes.

Gene	Forward primer	Reverse primer	Amplicon size (bp)
Pks17-1.203	CATTAGCACCGCCAAATCCG	GTCCCTACCTTTGGCGTTGA	144
Pks282-0.161	TGATCGCATGGTCTTTGGCT	ACTCTCCACACGCTCTTTGG	124
Pksm24-1.219	CTGGGAGACACTTGAGCAGG	GCCGGTTGGATCGAAATGTG	87
Pksm46-0.119	AGCAGAAGCCGTTTCCATCA	CCATACCTGCATTTGCGAGC	82
Pks30-1.114	GATCCGGCGACATTTGATGC	CCAAGGCCTCGTATACCGTC	105
Pks118-3.254	CTCGCACAAAACTCACCACG	GTGTTCCGATCACCGTTCCT	140
Pks58-0.40	GTCATGCTAGGTCCACGGAG	ACATTCAACGCCACCAATGC	79
Pks60	TCGTGTAGAAGTTGTCGGGC	AGGCCCAAGTGTGAATCTCG	145
Pks233-0.136	ACCGACGAAGCATCCAACAT	TAGTGCGCGAATGCCTAGAG	70
Hps1.140	ATTGTCTTGATGGAGCCGCA	GACCGACCGCAGTACTTTGA	163
Hps14-0.66	AAGCCAGCAGAAATGTCCGT	TTGAAGTGGGAGCAGGAACC	99
Hps38-0.269	AGTGCTGGATGTGGAGAAGC	CACCAGGCTTGAGAAGGGAG	142
Nps175-0.41	GCACGCCTTTTCAGATCGAC	ATCGCATTCTCCCCGGTAAC	147
Nps55-3.77	GTCTCCCGGCTGTATGAAGG	CCAGGCTTGTGTTGTTGTCG	84
Nps100	ACCCTCTCTCACCACTCCAA	AGACCCCCTTCTCGATGTCA	75
Nps134-0.394	GCAGGTCGATGTGTTGGAGA	AAGGCACAGACTTCCAGACG	118
Nps280-0.11	GATCTCGAAGGTGGTAGGCG	GTCCCAGCCACACATACACA	156
Nps245-0.245	TGCGGACGAAGAAATGACGA	GATGTCTGTGCGTTCCCAGA	97
Nps246-0.414	TTGGACATGGTGGTGACTCG	ACGAGTAGAACAGGCTGCAC	150
Nps246-0.103	CAGAGCTTCCCCTACACAGC	GCTGCCATGCTTCTTGATGG	120
Catalase	TGGCGAATCTGGATCTCACG	TCACGAAGGAAGAACACCGG	119
PacC	CCCCATCTTCCGTATCGTCG	CACTGCCGCTACCAAAACTG	83
LaeA	TTGGCCCCATAGAAAGAGGC	CTTGAGCTCCAGGACTACGG	80
CreA	TGTTGAATTCCCCTGGTCCG	GGGCTGAGATGGTGTTGAGT	103
AreA	ACATCTCAGCAGCAGTTCGT	GTTGGAGGGATCGAGGTGAC	128
VeA	CCTGTGTTGACCGGTACTCC	CTCAGACGGTACTTGCCCTC	115
AflJ	TCGATGGACGCAGCTCATAC	TGGACGATTGGCGGTTGTAA	85
AflR	GGACATGACAGCAGCAGGAT	ATTGTGCCGAAAACGACGTG	77
StcQ	TGGTTGAGGCTGTGGATGAC	ATATAGTGTCGCAGCAGGCC	132
Actin	TGGGCGAATATGACGTCGAG	GAACACCCTGCTGACTCTCC	125
EFα	GAGGTCAAGTCCGTCGAGAT	TTCTTGACGTTGAAGCCGAC	80
α *tubullin*	GTGCACTGGTATGTCGGTGA	GCATTCGTACTCGCCGTCTA	158
GAPDH	GTCTTCACCACCACCGAGAA	GTTGACGCCCATGACGAAC	100

Appendix 6: Data from barley fields naturally infected with Ramularia leaf spot harvested at GS78 and GS83.
A) Ramularia leaf spot levels. B) Green leaf area retention

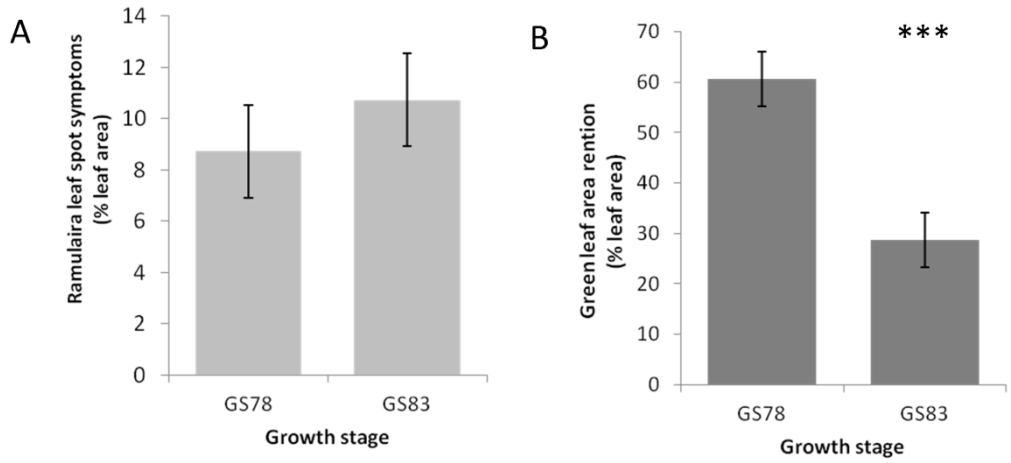

Appendix 7: Rubellin D-induced lesions on *Arabidopsis thaliana* Col-0 observed 24 hours after infiltration with different rubellin D concentrations.